ABC Imagem Cardiovascular

Volume 36 | Number 3

July/August September 2023

Sociedade Brasileira de Cardiologia
ISSN-2675-312X

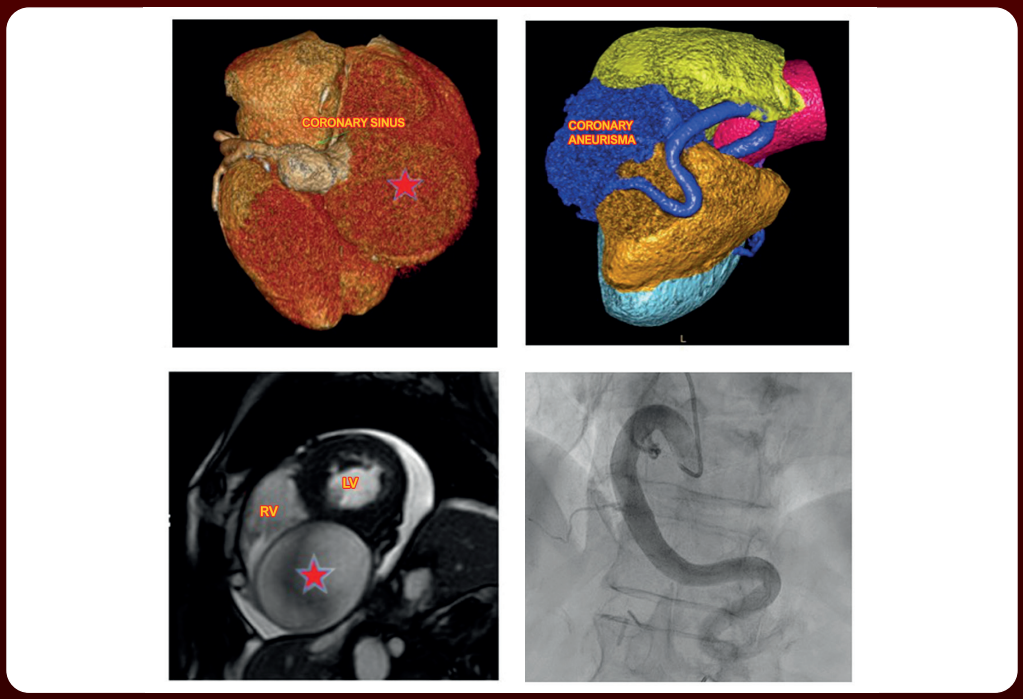

Figures 2, 3, 4 and 5 of the article: Giant Right Coronary Artery Aneurysm with Arteriovenous Fistula

DIC | SBC Sociedade Brasileira de Cardiologia 1943 | ABC Imagem Cardiovascular

Contents

Click on the title to read the article

Case Report

Departament of Cardiovascular Imaging

President
André Luiz Cerqueira de Almeida - BA

Vice President of Echocardiography
Alex dos Santos Félix - RJ

Vice President of Nuclear Cardiology
Simone Cristina Soares Brandão - PE

Vice President of Vascular Echography
José Aldo Ribeiro Teodoro - SP

Vice President of Magnetic Resonance Imaging
Otávio Rizzi Coelho Filho - SP

Vice President of Computed Tomography
Márcio Sommer Bittencourt - SP

Vice President of Congenital Heart Disease and Pediatric Cardiology
Adriana Mello Rodrigues dos Santos - MG

Managing Director
Silvio Henrique Barberato - PR

Financial Director
Mohamed Hassan Saleh - SP

Journal Director
Daniela do Carmo Rassi Frota - GO

Board of Trustees

President
Fábio Villaça Guimarães Filho - SP

Members
Afonso Akio Shiozaki - PR
Bruna Morhy Borges Leal Assunção - SP
David Costa de Souza Le Bihan - SP
Jorge Andion Torreão - BA
José Luiz Barros Pena - MG
José Olimpio Dias Júnior - MG
Rafael Willain Lopes - SP

Scientific Committee

Coordinator
Alex dos Santos Félix - RJ

Members
Simone Cristina Soares Brandão - PE
José Aldo Ribeiro Teodoro - SP
Otávio Rizzi Coelho Filho - SP
Márcio Sommer Bittencourt - SP

Qualification Committee

Coordinator
Andrea de Andrade Vilela - SP
Antonio Tito Paladino Filho - SP

Adult Echo Members
Antônio Amador Calvilho Júnior - SP
Candice Machado Porto - BA
Eliza de Almeida Gripp - RJ
João Carlos Moron Saes Braga - SP
Rafael Modesto Fernandes – BA
Sandra Nívea dos Reis Saraiva Falcão - CE

Congenital Echo Members
Carlos Henrique de Marchi - SP
Daniela Lago Kreuzig - SP
Halsted Alarcão Gomes Pereira da Silva - SP
Márcio Miranda Brito - TO

Seniors
Fábio Villaça Guimarães Filho - SP
Maria Estefânia Bosco Otto - DF
Solange Bernades Tatani - SP

Communication, Information and Internet Committee

Coordinator
José Roberto Matos Souza - SP

Members
Fabio Roston
Issam Shehadeh

Committee of Institutional Relations, Fees and Advocacy

Coordinator
Marcelo Haertel Miglioranza - RS

Members
Wagner Pires de Oliveira Júnior - DF

Committee of Education and Accreditation

Coordinator
Edgar Bezerra de Lira Filho - SP

Intersociety Committee

Coordinator
Marcelo Luiz Campos Vieira - SP

DIC Youth Committee

Coordinator
Eliza de Almeida Gripp - RJ

Positioning and Guidelines Committee

Coordinator
Marcelo Dantas Tavares de Melo - PB

Consultant
José Luiz Barros Pena - MG

Representatives

ASE
José Luiz Barros Pena - MG

EACVI
Alex dos Santos Félix - RJ

SISIAC
Ana Cristina de Almeida Camarozano - PR

Board of Former Presidents
Jorge Eduardo Assef - SP
Arnaldo Rabischoffsky - RJ
Samira Saady Morhy - SP
Marcelo Luiz Campos Vieira - SP
Carlos Eduardo Rochitte -SP

Board of Directors – Year 2023 (Brazilian Society of Cardiology)

North/Northeast
Nivaldo Menezes Filgueiras Filho (BA)
Sérgio Tavares Montenegro (PE)

East
Denilson Campos de Albuquerque (RJ)
Andréa Araujo Brandão (RJ) – Presidente do Conselho Administrativo

State of São Paulo
Celso Amodeo (SP)
João Fernando Monteiro Ferreira (SP)

Center
Carlos Eduardo de Souza Miranda (MG) — Vice-presidente do Conselho Administrativo
Weimar Kunz Sebba Barroso de Souza (GO)

South
Paulo Ricardo Avancini Caramori (RS)
Gerson Luiz Bredt Júnior (PR)

Scientific Committee
Denilson Campos de Albuquerque (RJ)
Ibraim Masciarelli Francisco Pinto (SP)
Weimar Kunz Sebba Barroso de Souza (GO)

National Editorial Board

ABC Imagem Cardiovascular

Volume 36, Nº 3, July/August/September 2023

Indexing: Lilacs (Latin American and Caribbean Health Sciences Literature) and DOAJ (Directory of Open Access Journals)

Address: Av. Marechal Câmara, 160 - 3º andar - Sala 330
20020-907 • Centro • Rio de Janeiro, RJ • Brazil
Phone.: (21) 3478-2700
E-mail: abcimaging@cardiol.br
https://www.abcimaging.org/

Commercial Department
Phone: (11) 3411-5500
E-mail: comercialsp@cardiol.br

Editorial Production
SBC - Scientific Department

Graphic Design and Diagramming
SBC - Scientific Department

Decoding the Diagnostic Dilemmas of Heart Failure with Preserved Ejection Fraction: Applying the Universal Definition for Enhanced Diagnosis Standardization

Renato A. Hortegal[1]
Instituto Dante Pazzanese de Cardiologia,[1] *São Paulo, SP – Brazil*

Heart Failure (HF) is a clinical syndrome in which the heart is unable to meet the metabolic demands of the body at normal level of filling pressures, whether at rest or while exercising.[1] Traditionally, HF is classified based on the left ventricular ejection fraction (LVEF), which measures the percentage of the left ventricular end diastolic volume ejected during each contraction. Whereas a normal LVEF is established as ≥50%, it is worth noting that approximately half of all HF patients display values within this normal range.

HF with Preserved Ejection Fraction (HFpEF) and HF with Reduced Ejection Fraction (HFrEF) are distinct diseases characterized by different underlying mechanisms, diagnostic workup and treatment approaches.[2] Moreover, diagnosing HFpEF in clinical practice is often more challenging due to the lack of standardized criteria in clinical trials and guidelines,[3,4] as well as complexities arising from the heterogeneity of the HFpEF syndrome.[5] In an attempt to standardize the diagnosis of HF, a universal definition and classification of HF were proposed,[6] encompassing the diverse spectrum of HF phenotypes based on LVEF.

According to this guideline, a diagnosis of HF requires the presence of past or current symptoms and/or signs of HF caused by structural/functional cardiac abnormalities and corroborated by at least one of the following: 1) elevated natriuretic peptides (NP); or 2) objective evidence of cardiogenic pulmonary or systemic congestion.[6]

Nevertheless, how can we apply these universal HF criteria to the unique intricacies of diagnosing HFpEF?

Implementing the Universal Definition of HF for HFpEF Diagnosis

The clinical diagnosis of HFpEF is straightforward when a patient presents with typical symptoms and signs of left and/or right congestive HF with LVEF ≥50%, along with echocardiography abnormalities and elevated NP.

However, patients with HFpEF may not display this classical HF presentation. Indeed, a significant proportion of patients (~50%) will only display symptoms during exertion, without current or previous evidence of fluid overload on clinical examination or prior hospitalization for decompensated HF[7] (Figure 1). This exercise-induced left atrial hypertension phenotype makes diagnosis challenging in clinical practice, with the Framingham criteria showing limited sensitivity.[1,6]

Moreover, some HFpEF patients may lack detectable structural abnormalities in imaging studies. For instance, Ho et al.[3] found that in a cohort of 243 patients with an invasive diagnosis of HFpEF, 59% lacked left atrial enlargement, 73% lacked LV hypertrophy, and 29% had no abnormalities in resting echocardiography. Similarly, functional abnormalities may not be evident, leading to low sensitivity of these features for HFpEF diagnosis.

Elevated NP are commonly observed in patients with HFpEF, as demonstrated in the DELIVER trial, where the median NT-proBNP was 1011 pg/mL.[8] However, it is important to note that patients with HFpEF can definitely display normal NP levels, yet they still face a threefold increase in mortality rates compared to patients without HF.[9]

In such cases, the guideline recommends investigating objective evidence of cardiogenic pulmonary or systemic congestion using diagnostic modalities such as chest radiography or elevated filling pressures on echocardiography, or even invasive hemodynamic measurements (e.g., pulmonary artery catheter) at rest or during exercise.

Echocardiographic Assesment of Diastolic Dysfunction to Diagnose HFpEF

Echocardiography is the main diagnostic tool for evaluating patients suspected of having HFpEF. Nonetheless, what the current evidence-based arguments support the predictive capabilities of echocardiographic parameters and its diastolic indexes in assessing cardiac filling pressures or establishing a formal diagnosis of HFpEF?

In 2016, the American Society of Echocardiography (ASE) and the European Association of Cardiovascular Imaging (EACVI) jointly updated their recommendations, combining the best evidence with expert opinions, and endorsed the algorithm "B" for assessing filling pressures. Nevertheless, it is worth noting that, despite this endorsement, at least three significant studies showed conflicting results regarding the performance of the ASE 2016 algorithm to predict filling pressures,[10-13] raising concerns about its external validity.

Initially, HFpEF was described as "diastolic HF," but this terminology is no longer recommended. While echocardiography remains as a key diagnostic tool for assessing HFpEF, it is crucial to recognize that diastolic dysfunction observed

Keywords

Heart Failure, Diastolic; Heart Failure; Heart Function Tests

Mailing Address: Renato A. Hortegal •
Instituto Dante Pazzanese de Cardiologia. Av. Dr. Dante Pazzanese, 500. Postal code: 04012-909. Vila Mariana, São Paulo – SP, Brazil
E-mail: renato.hortegal@dantepazzanese.org.br

DOI: https://doi.org/10.36660/abcimg.20230074i

Contents

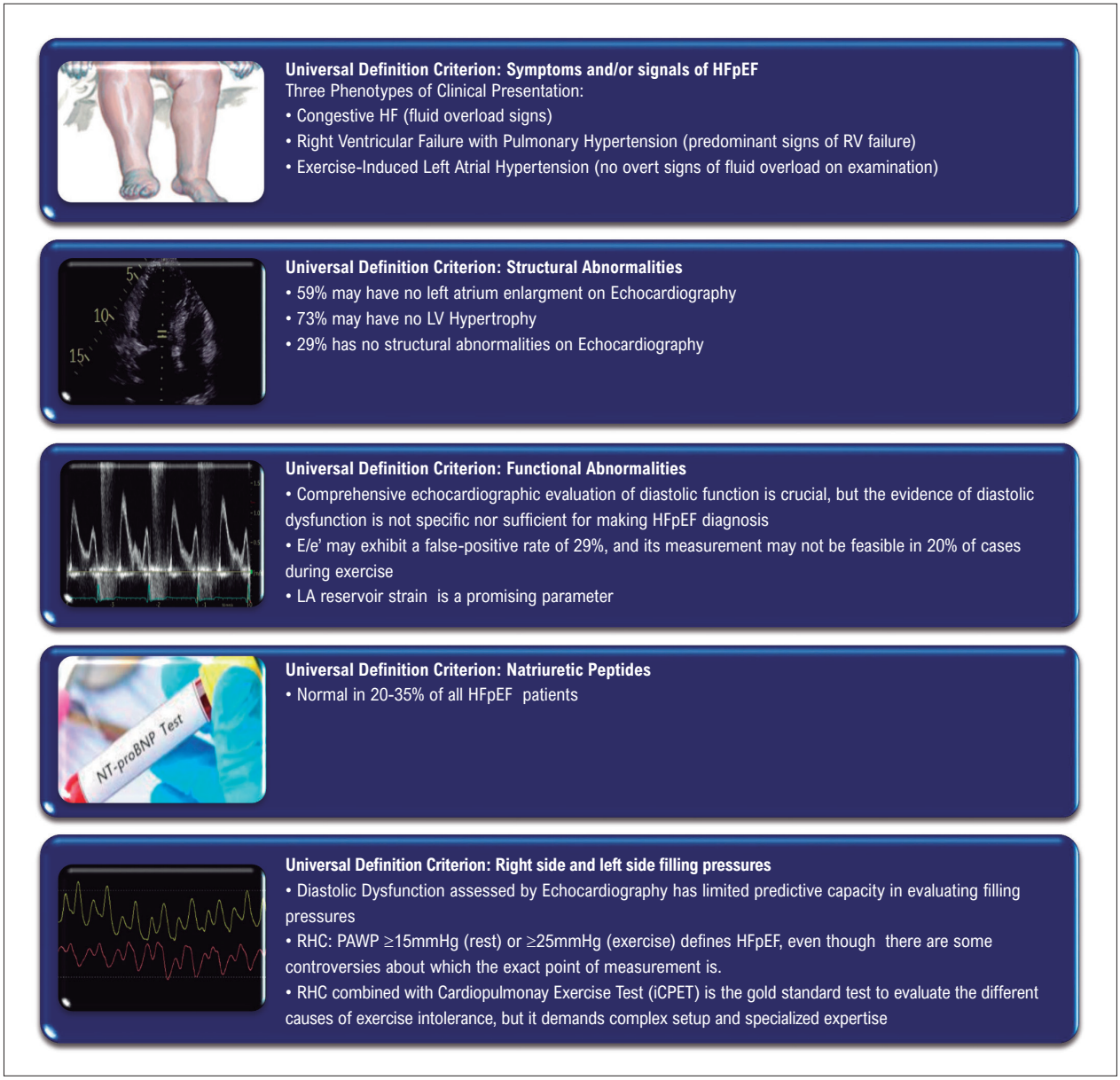

Figure 1 – *Applying the Criteria of Universal Definition of HF for HFpEF diagnosis. HFpEF: HF with Preserved Ejection Fraction; RV: right ventricle; LV: left ventricle; LA: left atrium; RHC: right heart catheterization; PAWP: pulmonary capillary wedge pressure.*

on echocardiography is not specific or sufficient for making an HFpEF diagnosis.[1]

One of the main echocardiography parameters used is the E/e' ratio, which is associated with mean left atrial pressure. Bovenkamp et al.[10] demonstrated that E/e' >9 had sensitivity of 78% and specificity of 59%, whereas a cut of E/e'>14 had lower sensitivity (38%), but higher specificity (89%). However, the reliability of the E/e' ratio may be compromised in various clinical scenarios, including mitral annulus calcification, conduction delay, regional wall motion abnormalities, and high output state.[14,15]

In the diastolic stress test during exercise, the measurement of E/e' may be challenging, with approximately 20% being unfeasible during peak exercise and a false-positive rate at approximately 29%.[16]

Left atrial reservoir strain (LArS) is a promising parameter for HFpEF diagnosis. LArS ≤18% or ≤24% is associated with increased filling pressures.[17] However, this parameter, along with other new parameters derived from speckle tracking[18,19] demand further research to evaluate its performance in less selected populations.

Using the recently proposed H_2FPEF[20] and HFA-PEFF[2] scores for suspected HFpEF can be valuable in balancing clinical, echocardiographic, and NP parameters in the diagnostic workup (Figure 2). The H_2FPEF score, proposed by the Mayo Clinic group in 2018, provides a probability

of HFpEF for individuals with unexplained dyspnea and has been validated using invasive measurements of pulmonary capillary wedge pressure (PAWP). It is important to note that the prevalence of HFpEF in this study population was 64%, which may lead to selection bias.[20]

In 2019, the European Society of Cardiology published a consensus recommendation proposing a stepwise approach to evaluate patients with suspected HFpEF. After excluding other conditions that may mimic HFpEF in the pre-test assessment (Step "P"), they suggested a scoring system (Step "E") to classify patients as having low, intermediate, or high probability of HFpEF.[2] This scoring system was subsequently prospectively validated.[21]

While validation studies generally demonstrate good overall performance for both score systems, some inaccuracies have been identified. For example, false negative rates of 25% (23 out of 91 cases) and 28% (14 out of 50 cases) were reported for patients classified as low probability (score) or 1) by HFAPEFF and H_2FPEF, respectively.[22]

Furthermore, recent data suggest that applying these scores to less selected populations may result in high prevalence of intermediate scores,[23,24] requiring additional tests such as exercise right heart catheterization (RHC).

Exercise RHC for the Diagnosis of HFpEF

Exercise RHC is the gold standard for diagnosing HFpEF as it directly measures PAWP. In reference centers, simultaneous measurement of VO_2 (Invasive CardioPulmonary Test) allows estimation of the kinetics of all components of the Fick equation through the different stages of exercise.

A PAWP ≥15mmHg at rest or ≥25mmHg during exercise defines HFpEF.[25-27] Additionally, the increase in PAWP indexed to change in cardiac output (PAWP slope/Cardiac Output>2) has been proposed as a diagnostic criterion to define HFpEF.[28]

However, conducting RHC requires a complex setup and demands specialized expertise for data acquisition and interpretation. Moreover, there are notable variations in protocols (upright vs. supine) and standardization methods for measuring PAWP, such as the reference point (mid-A wave end of expiration vs. mean during the respiratory cycle).[29]

Despite those limitations, exercise RHC is a highly accurate approach to fulfill the criteria for objective evidence of pulmonary congestion as stipulated by the universal definition of HF. Furthermore, it not only provides insights into the mechanisms underlying exercise limitation, but also enables prognostication of patients diagnosed with HFpEF.

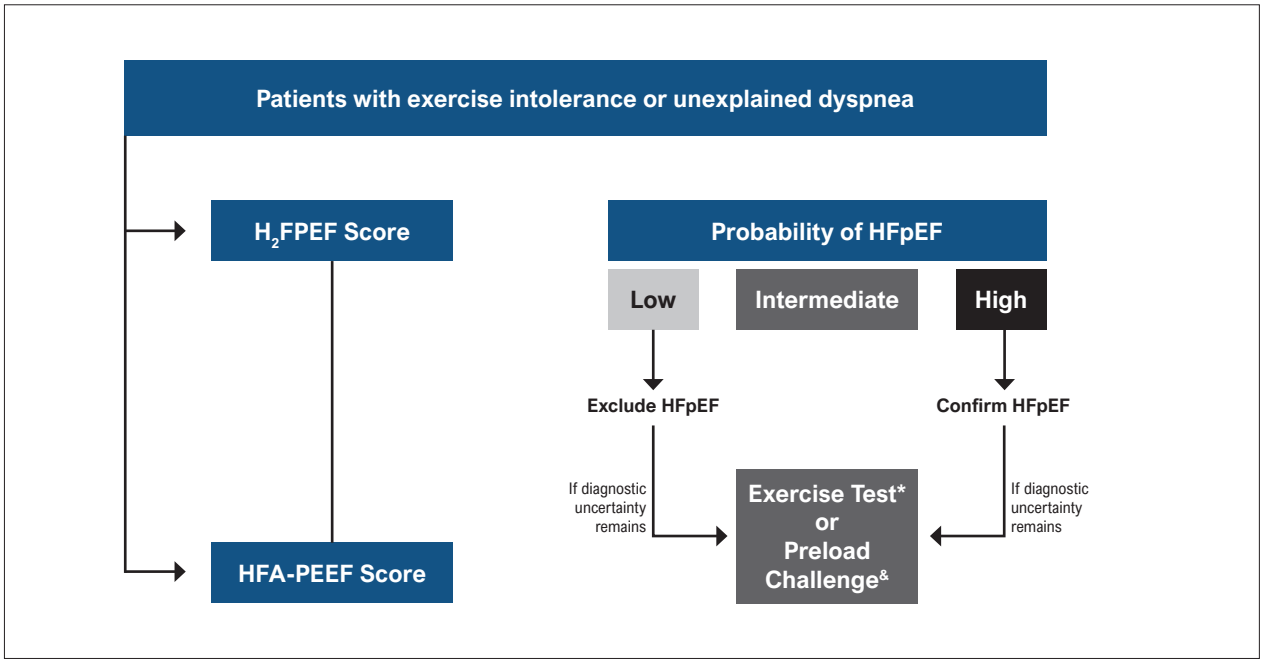

Figure 2 – *Current recommendations for the diagnostic approach of patients with suspected HFpEF. HFpEF: Heart Failure with Preserved Ejection Fraction; *Exercise Test encompasses both Diastolic Stress Echocardiography and Exercise RHC. &Preload Challenge refers either to infusion of normal saline or passive leg raising maneuver during RHC*

References

1. Kittleson MM, Panjrath GS, Amancherla K, Davis LL, Deswal A, Dixon DL, et al. 2023 ACC Expert Consensus Decision Pathway on Management of Heart Failure with Preserved Ejection Fraction: A Report of the American College of Cardiology Solution Set Oversight Committee. J Am Coll Cardiol. 2023;81(18):1835-78. doi: 10.1016/j.jacc.2023.03.393.

2. Pieske B, Tschöpe C, Boer RA, Fraser AG, Anker SD, Donal E, et al. How to Diagnose Heart Failure with Preserved Ejection Fraction: The HFA-PEFF Diagnostic Algorithm: A Consensus Recommendation from the Heart Failure Association (HFA) of the European Society of Cardiology (ESC). Eur Heart J. 2019;40(40):3297-317. doi: 10.1093/eurheartj/ehz641.

3. Ho JE, Zern EK, Wooster L, Bailey CS, Cunningham T, Eisman AS, et al. Differential Clinical Profiles, Exercise Responses, and Outcomes Associated with Existing HFpEF Definitions. Circulation. 2019;140(5):353-65. doi: 10.1161/CIRCULATIONAHA.118.039136.

4. Ho JE, Redfield MM, Lewis GD, Paulus WJ, Lam CSP. Deliberating the Diagnostic Dilemma of Heart Failure with Preserved Ejection Fraction. Circulation. 2020;142(18):1770-80. doi: 10.1161/CIRCULATIONAHA.119.041818.

5. Shah SJ, Borlaug BA, Kitzman DW, McCulloch AD, Blaxall BC, Agarwal R, et al. Research Priorities for Heart Failure with Preserved Ejection Fraction: National Heart, Lung, and Blood Institute Working Group Summary. Circulation. 2020;141(12):1001-26. doi: 10.1161/CIRCULATIONAHA.119.041886.

6. Bozkurt B, Coats AJS, Tsutsui H, Abdelhamid CM, Adamopoulos S, Albert N, et al. Universal Definition and Classification of Heart Failure: A Report of the Heart Failure Society of America, Heart Failure Association of the European Society of Cardiology, Japanese Heart Failure Society and Writing Committee of the Universal Definition of Heart Failure: Endorsed by the Canadian Heart Failure Society, Heart Failure Association of India, Cardiac Society of Australia and New Zealand, and Chinese Heart Failure Association. Eur J Heart Fail. 2021;23(3):352-80. doi: 10.1002/ejhf.2115.

7. Litwin SE, Komtebedde J, Hu M, Burkhoff D, Hasenfuß G, Borlaug BA, et al. Exercise-Induced Left Atrial Hypertension in Heart Failure with Preserved Ejection Fraction. JACC Heart Fail. 2023:S2213-1779(23)00095-1. doi: 10.1016/j.jchf.2023.01.030.

8. Solomon SD, Vaduganathan M, Claggett BL, Boer RA, DeMets D, Hernandez AF, et al. Baseline Characteristics of Patients with HF with Mildly Reduced and Preserved Ejection Fraction: DELIVER Trial. JACC Heart Fail. 2022;10(3):184-97. doi: 10.1016/j.jchf.2021.11.006.

9. Verbrugge FH, Omote K, Reddy YNV, Sorimachi H, Obokata M, Borlaug BA. Heart failure with Preserved Ejection Fraction in Patients with Normal Natriuretic Peptide Levels is Associated with Increased Morbidity and Mortality. Eur Heart J. 2022;43(20):1941-51. doi: 10.1093/eurheartj/ehab911.

10. van de Bovenkamp AA, Enait V, Man FS, Oosterveer FTP, Bogaard HJ, Vonk Noordegraaf A, et al. Validation of the 2016 ASE/EACVI Guideline for Diastolic Dysfunction in Patients With Unexplained Dyspnea and a Preserved Left Ventricular Ejection Fraction. J Am Heart Assoc. 2021;10(18):e021165. doi: 10.1161/JAHA.121.021165.

11. Gillebert TC. Estimating LV Filling Pressures Noninvasively: A Word of Caution. JACC Cardiovasc Imaging. 2022;15(10):1692-5. doi: 10.1016/j.jcmg.2022.05.003.

12. Andersen OS, Smiseth OA, Dokainish H, Abudiab MM, Schutt RC, Kumar A, et al. Estimating Left Ventricular Filling Pressure by Echocardiography. J Am Coll Cardiol. 2017;69(15):1937-48. doi: 10.1016/j.jacc.2017.01.058.

13. Pak M, Kitai T, Kobori A, Sasaki Y, Okada T, Murai R, et al. Diagnostic Accuracy of the 2016 Guideline-Based Echocardiographic Algorithm to Estimate Invasively-Measured Left Atrial Pressure by Direct Atrial Cannulation. JACC Cardiovasc Imaging. 2022;15(10):1683-91. doi: 10.1016/j.jcmg.2022.03.022.

14. Oh JK, Miranda WR, Kane GC. Diagnosis of Heart Failure with Preserved Ejection Fraction Relies on Detection of Increased Diastolic Filling Pressure, But How? J Am Heart Assoc. 2023;12(6):e028867. doi: 10.1161/JAHA.122.028867.

15. Hortegal R AH. Ecocardiografia com Strain para Avaliação de Pacientes com Disfunção Diastólica e Fração de Ejeção Preservada: Estamos Prontos? Arq Bras Cardiol: Imagem Cardiovasc. 2017;30(4):132-9. doi: 10.5935/2318-8219.20170034 .

16. Obokata M, Kane GC, Reddy YN, Olson TP, Melenovsky V, Borlaug BA. Role of Diastolic Stress Testing in the Evaluation for Heart Failure with Preserved Ejection Fraction: A Simultaneous Invasive-Echocardiographic Study. Circulation. 2017;135(9):825-38. doi: 10.1161/CIRCULATIONAHA.116.024822.

17. Inoue K, Khan FH, Remme EW, Ohte N, García-Izquierdo E, Chetrit M, et al. Determinants of Left Atrial Reservoir and Pump Strain and Use of Atrial Strain for Evaluation of Left Ventricular Filling Pressure. Eur Heart J Cardiovasc Imaging. 2021;23(1):61-70. doi: 10.1093/ehjci/jeaa415.

18. Hortegal RA, Hossri C, Giolo L, Cancellier R, Gun C, Assef J, et al. Mechanical Dispersion is a Superior Echocardiographic Feature to Predict Exercise Capacity in Preclinical and Overt Heart Failure with Preserved Ejection Fraction. Int J Cardiovasc Imaging. 2023;39(7):1239-50. doi: 10.1007/s10554-023-02830-0.

19. Hortegal RA, Valeri R, Grizante M, Cancellier R, Uemoto V, Gun C, et al. Afterload Increase Challenge Unmasks Systolic Abnormalities in Heart Failure with Preserved Ejection Fraction. Int J Cardiol. 2023;380:20-7. doi: 10.1016/j.ijcard.2023.03.042.

20. Reddy YNV, Carter RE, Obokata M, Redfield MM, Borlaug BA. A Simple, Evidence-Based Approach to Help Guide Diagnosis of Heart Failure with Preserved Ejection Fraction. Circulation. 2018;138(9):861-70. doi: 10.1161/CIRCULATIONAHA.118.034646.

21. Aizpurua AB, Wijk SS, Rocca HPB, Henkens M, Heymans S, Beussink-Nelson L, et al. Validation of the HFA-PEFF Score for the Diagnosis of Heart Failure with Preserved Ejection Fraction. Eur J Heart Fail. 2020;22(3):413-21. doi: 10.1002/ejhf.1614.

22. Churchill TW, Li SX, Curreri L, Zern EK, Lau ES, Liu EE, et al. Evaluation of 2 Existing Diagnostic Scores for Heart Failure with Preserved Ejection Fraction Against a Comprehensively Phenotyped Cohort. Circulation. 2021;143(3):289-91. doi: 10.1161/CIRCULATIONAHA.120.050757.

23. Tada A, Nagai T, Omote K, Iwano H, Tsujinaga S, Kamiya K, et al. Performance of the H2FPEF and the HFA-PEFF Scores for the Diagnosis of Heart Failure with Preserved Ejection Fraction in Japanese Patients: A Report from the Japanese Multicenter Registry. Int J Cardiol. 2021;342:43-8. doi: 10.1016/j.ijcard.2021.08.001.

24. Amanai S, Harada T, Kagami K, Yoshida K, Kato T, Wada N, et al. The H2FPEF and HFA-PEFF Algorithms for Predicting Exercise Intolerance and Abnormal Hemodynamics in Heart Failure with Preserved Ejection Fraction. Sci Rep. 2022;12(1):13. doi: 10.1038/s41598-021-03974-6.

25. Hsu S, Fang JC, Borlaug BA. Hemodynamics for the Heart Failure Clinician: A State-of-the-Art Review. J Card Fail. 2022;28(1):133-48. doi: 10.1016/j.cardfail.2021.07.012.

26. Borlaug BA, Nishimura RA, Sorajja P, Lam CS, Redfield MM. Exercise Hemodynamics Enhance Diagnosis of Early Heart Failure with Preserved Ejection Fraction. Circ Heart Fail. 2010;3(5):588-95. doi: 10.1161/CIRCHEARTFAILURE.109.930701.

27. Deis T, Wolsk E, Mujkanovic J, Komtebedde J, Burkhoff D, Kaye D, et al. Resting and Exercise Haemodynamic Characteristics of Patients with Advanced Heart Failure and Preserved Ejection Fraction. ESC Heart Fail. 2022;9(1):186-95. doi: 10.1002/ehf2.13697.

28. Eisman AS, Shah RV, Dhakal BP, Pappagianopoulos PP, Wooster L, Bailey C, et al. Pulmonary Capillary Wedge Pressure Patterns During Exercise Predict Exercise Capacity and Incident Heart Failure. Circ Heart Fail. 2018;11(5):e004750. doi: 10.1161/CIRCHEARTFAILURE.117.004750.

29. Pagnamenta A, Azzola A, Beghetti M, Lador F, On Behalf Of The Swiss Society Of Pulmonary Hypertension. Invasive Haemodynamic Evaluation of the Pulmonary Circulation in Pulmonary Hypertension. Swiss Med Wkly. 2017;147:w14445. doi: 10.4414/smw.2017.14445.

ABCDE Protocol in Stress Echocardiography

José Luis de Castro e Silva Pretto,[1] *Clarissa Borguezan Daros*[2]
Hospital São Vicente de Paulo, CD2,[1] *Passo Fundo, RS – Brazil*
Hospital São José,[2] *Criciuma, SC – Brazil*

The clinical evaluation of coronary artery disease (CAD) is an individualized, winding road to be followed every day in cardiology practice. It is based on the need for an appropriate diagnosis, considering the optimization of different conducts, with the primary goal of improving patients' quality of life and, at times, avoiding hard endpoints, such as infarction and death.

An ideal method for this complex purpose is the assumption of not causing damage to the person being assessed in order to extract as much physiological information as possible in a kind manner with the least financial (and, therefore, environmental) impact to allow for a large-scale application, as this is a highly prevalent disease.[1]

Non-invasive functional imaging for myocardial ischemia is recommended as an initial test for diagnosing CAD in symptomatic patients as well as for those subjected to coronary angiotomography, which revealed CAD of uncertain functional significance or non-diagnostic CAD.[2]

Stress echocardiography (SEC) is an established CAD diagnosis and stratification method, and the imbalance caused in the bloodstream, and its repercussion on myocardial contractility is a common basis for all modalities. This classic form of semi-quantitative characterization is subject to such factors as the examiner's experience and subjectivity, and its high point is the specificity of the findings. Non-invasive functional tests are associated with high precision in detecting flow-limiting coronary stenosis, when compared to invasive functional tests — fractional flow reserve (FFR). However, non-ischemic, low-grade coronary atherosclerosis is still poorly detected by the functional test.[3]

This classic form of semi-quantitative characterization is subject to factors such as the examiner's experience and subjectivity, and its high point is the specificity of the findings. Non-invasive functional tests are associated with high precision in detecting flow-limiting coronary stenosis when compared to invasive functional tests (FFR). However, non-ischemic, low-grade coronary atherosclerosis is still poorly detected by the functional test.[3]

In 2017, Picano et al.[1] published a multicenter observation study design to be developed in laboratories with a high volume of SEC tests, including Brazilian laboratories, called Stress Echo 2020. The study was endorsed by the Italian Society of Cardiovascular Echography and organized in 10 subprojects with focus on: contractile reserve for cardiac resynchronization forecast or response to medication therapy; stress B-lines in heart failure; hypertrophic cardiomyopathy; heart failure with preserved ejection fraction; mitral failure after transcatheter or surgical aortic valve replacement; outdoors SEC under extreme physiology; right ventricle contractile reserve in repaired Tetralogy of Fallot; suspected or early pulmonary arterial hypertension; coronary flow velocity, left ventricular elastance reserve and B-lines in known or suspected CAD; identification of subclinical familial disease in genotype-positive, phenotype-negative healthy relatives of inherited disease (such as hypertrophic cardiomyopathy).

Based on the study's results, a new protocol has been proposed for the execution of SEC to increase the test power, and assist in better performing its function in different heart disease scenarios. The coronary artery stenosis-centered model has changed over the past decades, and is now accepted as not the only, nor probably the most important, patient prognostic vulnerability, within and beyond the CAD context. Plaque composition is even more important than its geometry and obstruction level.[4] Pulmonary congestion and diastolic function, left ventricular structure and contractile reserve, coronary microcirculation, and cardiac autonomic balance are equally important risk determinants; however, they are difficult to assess in a non-invasive manner using the methods that are currently available.[5] An international consensus has been reached in recent years concerning the role played in the scenario of non-ischemic, valvular, and pulmonary diseases.[6]

ABCDE SEC constitutes a broad approach, seeking the assessment of other significant prognostic aspects. Leveraging the echocardiography method's versatility and simplicity ("one-stop-shop"),[5] Doppler data and 2D image readings are conceptually increased. Their parameters are conceptually unified, synchronized, and harmonized as the acronym[7] (Figure 1).

A for Asynergy

This is based on the presumable myocardial contractility alteration induced by stress in the presence of flow-limiting coronary stenosis. The substrate supply-demand imbalance leads to a reduction in myocardial radial thickening, a parameter sometimes limited by its semi-quantitative and subjective nature. Operator dependency can be minimized (but not eliminated) by specialized training and the adoption of conservative reading measures, as well as the accreditation and quality control of advanced echocardiography laboratories.

Keywords

Echocardiography; Echocardiography, Stress; Clinical Protocols

Mailing Address: José Luis de Castro e Silva Pretto •
Hospital São Vicente de Paulo, CD2. Rua Teixeira Soares, 808.
Postal Code: 99010-080. Passo Fundo, RS – Brazil
E-mail: jlpretto@cardiol.br

DOI: https://doi.org/10.36660/abcimg.20230070i

Contents

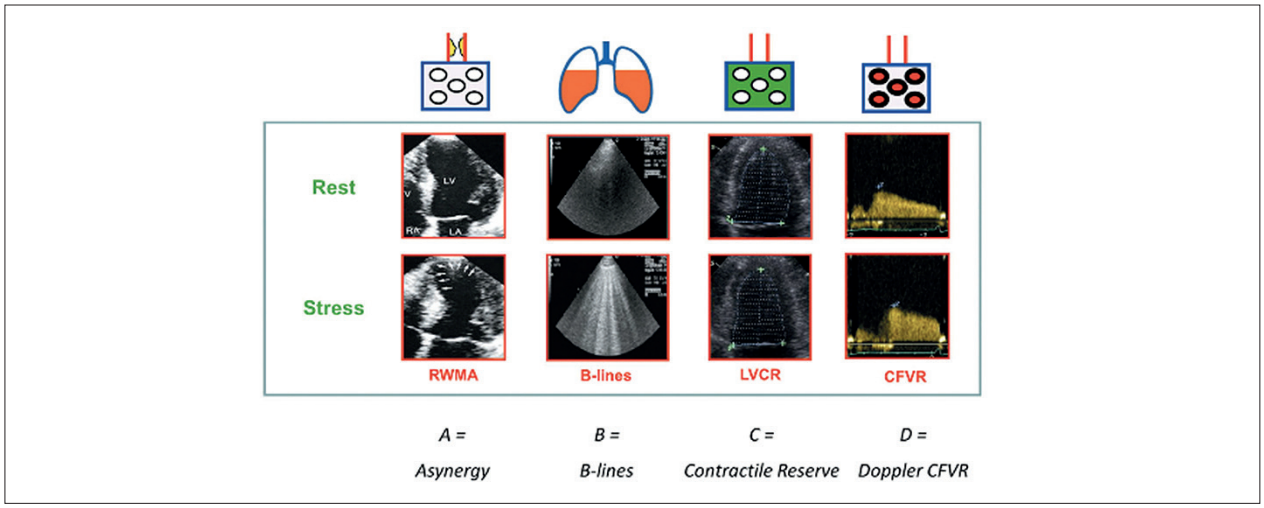

Figure 1 – *The targets of integrated quadruple imaging stress echo. The four pathophysiological targets are epicardial coronary artery stenosis (with RWMA); pulmonary water (with B-lines); myocardial function (with LVCR); coronary microvascular function (with CFVR) [Picano et al. Cardiovascular Ultrasound (2018)].*

The regional motility assessment indicates that the higher the number of affected segments (universally defined), the worse the prognosis. This parameter is viewed as stenosis centered and has its value limited outside the epicardial coronary disease context.[7]

B for B-lines

Increased left atrial pressure forms the basis of a myriad of conditions. Its pathophysiological consequence has the liquid outflow in the pulmonary pericapillary interstitium as hydrostatic substrate. In its acute form, this liquid may be detected by ultrasound in the form of echo lines that reverberate it. During the physical SEC, the induction of physiological processes that potentially provoke the disease homeostasis limit is a parameter that has prognostic significance.[8]

C for Contractility

Contractility is the myocardium's inherent ability to contract regardless of changes in pre- or afterload.

During the SEC, the left ventricle end-systolic volume (ESV) is progressively lower, resulting in higher arterial tension peaks, and increased subsequent afterload. The ratio between arterial pressure (SAP) and ESV predicts the ventricle's ability to empty up to different afterload values.[9]

The left ventricle elastance measures the chamber's contractile reserve by comparing its performance in rest and stress conditions, by dividing the SAP/ESV ratio in stress conditions by the ratio in rest conditions. Physical stress and dobutamine validated values are above 2.0, and with the use of vasodilators, the ratio that indicates appropriate contractility is above 1.1.

D for coronary artery Doppler

The coronary flow may be affected under epicardial stenosis pathological conditions, and muscular dysfunction. In the first scenario, at a given flow measurement point, a limitation with compromised blood intake may occur downstream of the obstruction under stress situations. In the second, several conditions may take place, such as perivascular hypertrophy and ruptured endothelium function caused by inflammation and atherosclerosis, preventing adequate blood flow.

The coronary flow reserve in an echocardiogram is measured, by Doppler, using the velocity ratio at the medial distal section of the anterior descending artery under stress and rest conditions. Normal values are those above 2.0 in any SEC modality.

E for Electrocardiogram

The heart rate variability in response to stress may provide information about the autonomic function of the cardiac conduction system, constituting a status marker for it during the test. This parameter, heart rate reserve, is obtained by dividing the maximum heart rate attained by the value under rest conditions. It is classified as a positive criterion if the ratio is under 1.80, for physical stress and dobutamine, and under 1.22 for vasodilators. Beta blockers reduce heart rate values under rest and stress conditions, with no impact on the ratio for prognostic purposes.[8]

In 2021, Q. Ciampi et al.[10] published the concept that the functional test with SEC may detect other biomarkers, in addition to myocardial ischemia, which could improve the risk stratification for patients with suspected or known CAD. In this multicenter study, the authors prospectively recruited 3,574 patients with suspected or known CAD referred to SEC. All findings were normal for 31% of the patients, and all findings were abnormal for 5% of the patients. Among those with normal SEC who underwent coronary cineangiography, 30% exhibited obstructive CAD, while among those whose SEC findings were all abnormal, 95% exhibited significant CAD. The mortality rate was 0.4% per year for normal SEC, in comparison to 2.7% per year

when all SEC findings were abnormal. These data reinforce the feasibility and improvement of risk stratification information provided by the ABCDE - SEC protocol.

When added to the traditional SEC assessment, these parameters result in a broader spectrum of variables evaluated by the stress protocol. Together, they allow for better risk stratification as well as assist in defining the diagnosis. The application in other scenarios, especially of heart failure in all systolic function spectra, makes this protocol an important complement in these patients' evaluations. Patients with microvascular disease and diastolic dysfunction sometimes have atypical presentations and may benefit from this new protocol, as it broadens the traditional test's diagnostic power.

A new patient recruitment stage was recently launched to evaluate other scenarios, including congenital disease (Tetralogy of Fallot), post-COVID infection, valvular diseases, among others.

The systematic use of SEC reduces test costs, lowers the volumes of myocardial scintigraphy tests, reduces the need for non-invasive and invasive coronary angiography, and poses a substantial barrier, even in medical-legal terms, to a shortcut for anatomy induced coronary revascularization procedures, which are futile and inadequate in terms of prognosis.[7] The ABCDE protocol proposes the full use of this consolidated tool in a simplified and intuitive manner, systematizing the different additional parameters.

References

1. Picano E, Ciampi Q, Citro R, D'Andrea A, Scali MC, Cortigiani L, et al. Stress Echo 2020: The International Stress Echo Study in Ischemic and Non-Ischemic Heart Disease. Cardiovasc Ultrasound. 2017;15(1):3. doi: 10.1186/s12947-016-0092-1.
2. Knuuti J, Wijns W, Saraste A, Capodanno D, Barbato E, Funck-Brentano C, et al. 2019 ESC Guidelines for the Diagnosis and Management of Chronic Coronary Syndromes. Eur Heart J. 2020;41(3):407-77. doi: 10.1093/eurheartj/ehz425.
3. Hoffmann U, Ferencik M, Udelson JE, Picard MH, Truong QA, Patel MR, et al. Prognostic Value of Noninvasive Cardiovascular Testing in Patients with Stable Chest Pain: Insights from the PROMISE Trial (Prospective Multicenter Imaging Study for Evaluation of Chest Pain). Circulation. 2017;135(24):2320-32. doi: 10.1161/CIRCULATIONAHA.116.024360.
4. Marzilli M, Merz CN, Boden WE, Bonow RO, Capozza PG, Chilian WM, et al. Obstructive Coronary Atherosclerosis and Ischemic Heart Disease: An Elusive Link! J Am Coll Cardiol. 2012;60(11):951-6. doi: 10.1016/j.jacc.2012.02.082.
5. Picano E, Ciampi Q, Arbucci R, Cortigiani L, Zagatina A, Celutkiene J, et al. Stress Echo 2030: The New ABCDE Protocol Defining the Future of Cardiac Imaging. Eur Heart J Suppl. 2023;25(Suppl C):C63-C67. doi: 10.1093/eurheartjsupp/suad008.
6. Lancellotti P, Pellikka PA, Budts W, Chaudhry FA, Donal E, Dulgheru R, et al. The Clinical Use of Stress Echocardiography in Non-Ischaemic Heart Disease: Recommendations from the European Association of Cardiovascular Imaging and the American Society of Echocardiography. Eur Heart J Cardiovasc Imaging. 2016;17(11):1191-229. doi: 10.1093/ehjci/jew190.
7. Picano E, Ciampi Q, Wierzbowska-Drabik K, Urluescu ML, Morrone D, Carpeggiani C. The New Clinical Standard of Integrated Quadruple Stress Echocardiography with ABCD Protocol. Cardiovasc Ultrasound. 2018;16(1):22. doi: 10.1186/s12947-018-0141-z.
8. Scali MC, Zagatina A, Ciampi Q, Cortigiani L, D'Andrea A, Daros CB, et al. Lung Ultrasound and Pulmonary Congestion During Stress Echocardiography. JACC Cardiovasc Imaging. 2020;13(10):2085-95. doi: 10.1016/j.jcmg.2020.04.020.
9. Bombardini T. Myocardial Contractility in the Echo Lab: Molecular, Cellular and Pathophysiological Basis. Cardiovasc Ultrasound. 2005;3:27. doi: 10.1186/1476-7120-3-27.
10. Ciampi Q, Zagatina A, Cortigiani L, Wierzbowska-Drabik K, Kasprzak JD, Haberka M, et al. Prognostic Value of Stress Echocardiography Assessed by the ABCDE Protocol. Eur Heart J. 2021;42(37):3869-78. doi: 10.1093/eurheartj/ehab493.

Role of Strain Echocardiography in the Evaluation of Patients with Chagas Disease

Vinicius Tostes Carvalho,[1] *Luís Henrique Coelho Pinto,*[1,2] *Maria Carmo Pereira Nunes*[1,2]

Hospital das Clinicas da Universidade Federal de Minas Gerais,[1] *Belo Horizonte, MG – Brazil*

Programa de Pós-Graduação em Ciências da Saúde Infectologia e Medicina, Tropical da UFMG,[2] *Belo Horizonte, MG – Brazil*

Chagas disease continues to be a significant public health challenge, affecting approximately six million people worldwide.[1] With increasing globalization, *Trypanosoma cruzi* has already been detected in regions that were not previously considered endemic for the transmission vector, thus becoming one of the main neglected parasites.[1] Although a percentage of infected individuals remain asymptomatic in the chronic indeterminate form of the disease, it is estimated that 2% to 3% of all patients annually progress to the cardiac form. Chagas heart disease was the most severe manifestation of Chagas disease, clinically appearing with heart failure, ventricular and supraventricular arrhythmias, conduction disorders, and embolic events.[2]

The echocardiogram is an important propaedeutic method in the evaluation of patients with Chagas disease, especially in the presence of Chagas heart disease. In general, the echocardiogram investigates parameters related to the analysis of segmental contractility and global systolic function,[2] which is essential for the treatment and prognosis of the disease. However, even well-established variables in the literature, such as ejection fraction, face challenges in simulating all the pathological aspects of Chagas disease.[3]

The echocardiogram with speckle-tracking strain (STE) or two-dimensional strain has been increasingly studied in Chagas disease, due to its ability to identify changes in the early stages of cardiac involvement.[4] As well as in cardioncology, in relation to the cardiotoxicity caused by chemotherapy, it is possible that changes in STE values in patients with Chagas disease may well identify the risk of progression to heart disease.

In the context of Chagas disease, the literature shows that STE has an important clinical application, especially in asymptomatic individuals and with no evidence of cardiac involvement by conventional methods (Figure 1). The early detection of changes in segmental contractility can identify patients with the potential for the evolution of the disease, with an impact on clinical management and medical-labor practices. However, as this is a relatively new technique, available only in some equipment, few studies have analyzed STE in Chagas disease.

A previous study by Barbosa et al. evaluated STE in 78 asymptomatic individuals with Chagas disease, who presented normal chest X-rays and electrocardiograms, and compared them with 38 healthy controls, matched by gender and age. Although there was no difference in ejection fraction and diastolic function between groups, a reduction in STE values was observed in different segments of the left ventricle in patients when compared to controls.[5] In another study comparing patients with cardiomyopathies of different etiologies, including 81 patients with Chagas cardiomyopathy and 31 with idiopathic cardiomyopathy, STE proved to be a predictor of adverse events in both groups, adding prognostic value in addition to ejection fraction.[6]

In an analysis of a cohort consisting of 408 individuals with Chagas disease, which underwent follow-up for a mean period of 6.5 ± 2.7 years, Saraiva et al. identified that circumferential and radial two-dimensional strains were independent predictors of mortality. In addition, they observed that the strain, especially the radial strain, was an independent predictor of progression from the indeterminate form to Chagas cardiomyopathy.[7]

In another study conducted by Romano et al., using STE to compare 25 individuals with the indeterminate form, 20 individuals with Chagas cardiomyopathy, and 20 controls, differences in strain values were identified in four specific segments of the left ventricle: basal-inferior, basal-inferoseptal, mid-inferoseptal and mid-inferolateral. Most interestingly, these abnormalities in segmental strain values were detected even in the absence of myocardial fibrosis assessed by magnetic resonance imaging, highlighting the relevance of the method in the early stages of Chagas disease.[8]

In the SaMi-Trop study, which follows a significant number of patients with Chagas disease in an endemic area with 21 municipalities in the northern region of Minas Gerais, Santos-Junior et al. conducted an assessment of a global longitudinal strain in 1,387 patients (14% with ejection fraction < 50%). Surprisingly, the authors identified that STE was altered in 59% of these individuals. When analyzing the independent factors associated with the reduction of STE, they found electrocardiographic abnormalities, such as changes in both the ST segment and the T wave, as well as in the duration of the QRS. Moreover, the left ventricular ejection fraction and the E/e' ratio were also related to the decrease in STE. It is important to note that STE had already showed changes in a significant number of patients, even when the ejection fraction was within the normal range. The study also highlighted the remarkable finding that, in the subgroup with electrocardiographic alterations, but with an ejection fraction that was still normal, STE was already altered.[9]

A recent meta-analysis, which included several studies on the value of STE in Chagas disease with 1,222

Keywords

Chagas Disease; Trypanosoma cruzi; Cardiomyopathies

Mailing Address: Maria Carmo Nunes •
Universidade Federal de Minas Gerais, Departamento de Clinica Medica. Rua Professor Alfredo Balena, 190. Postal Code: 30130-100. Santa Efigênia, Belo Horizonte, MG – Brazil
E-mail: mcarmo@waymail.com.br

DOI: https://doi.org/10.36660/abcimg.20230075i

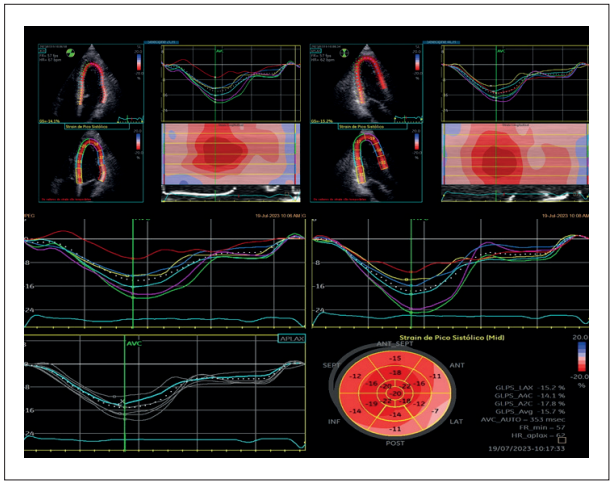

Figure 1 – *Left ventricular longitudinal strain images obtained in apical 4- and 3-chamber views with parametric (color-coded) display of strain in systole and peak values of systolic strain. The colored strain-time curves of each segment are shown at the bottom of the figure with the "bull's eye" image in the lower right quadrant, showing the reduced strain values, especially in the basal segment of the inferolateral wall. SEPT: left ventricular septal segment; ANT-SEPT:left ventricular septal segment; ANT: left ventricular anterior segment; LAT: left ventricular lateral segment; POST: left ventricular posterior segment; INF: left ventricular inferior segment; GLPS: Global longitudinal peak systolic strain; AVC: aortic valve close; FR-MIN: frame rate; HR_aplax: heart rate.*

participants, revealed that STE values were significantly worse in patients with Chagas cardiomyopathy when compared to those with the indeterminate form. However, no significant difference was observed when comparing individuals with the indeterminate form and normal controls without Chagas disease.[10] These results suggest that STE can be a valuable tool in identifying early and subclinical changes in patients with Chagas heart disease, but it may not be as sensitive in detecting changes in the early stages of the disease.

In conclusion, STE represents a promising echocardiographic technique, duly validated for the analysis of myocardial function and with a vast potential for clinical application. Its use is expanding, with several indications in several cardiovascular diseases. The main advantage of the method is the early detection of changes in ventricular contractility, which are not identified in conventional echocardiography. Currently, most devices have this technology, representing a notable contribution to advances in echocardiography, especially because it is a non-invasive, low-cost, angle-independent methodology in relation to Doppler and rarely influenced by load conditions. However, it is important to highlight that there are challenges in using STE in isolation due to the lack of standardization between the reference values of different manufacturers, the diversity of capture and analysis methodologies, among other factors, including the presence of arrhythmias and changes in the STE related to age, sex, and quality of the echocardiographic window. These shortcomings call for caution when considering STE as the sole criterion in clinical decision-making. Therefore, in the context of Chagas disease, further studies are needed to investigate the value of STE in the diagnosis and progression of heart disease in order to establish its main indications.

References

1. Pan American Health Organization. Neglected Infectious Diseases in the Americas: Success Stories and Innovation to Reach the Neediest. Washington: PAHO; 2016.
2. Nunes MCP, Buss LF, Silva JLP, Martins LNA, Oliveira CDL, Cardoso CS, et al. Incidence and Predictors of Progression to Chagas Cardiomyopathy: Long-Term Follow-Up of Trypanosoma cruzi-Seropositive Individuals. Circulation. 2021;144(19):1553-6. doi: 10.1161/CIRCULATIONAHA.121.055112.
3. Rassi DC, Vieira ML, Arruda AL, Hotta VT, Furtado RG, Rassi DT, et al. Echocardiographic Parameters and Survival in Chagas Heart Disease with Severe Systolic Dysfunction. Arq Bras Cardiol. 2014;102(3):245-52. doi: 10.5935/abc.20140003.
4. Liu W, Li W, Li H, Li Z, Zhao P, Guo Z, et al. Two-Dimensional Speckle Tracking Echocardiography Help Identify Breast Cancer Therapeutics-Related Cardiac Dysfunction. BMC Cardiovasc Disord. 2022;22(1):548. doi: 10.1186/s12872-022-03007-8.
5. Barbosa MM, Rocha MOC, Vidigal DF, Carneiro RCB, Araújo RD, Palma MC, et al. Early Detection of Left Ventricular Contractility Abnormalities by Two-Dimensional Speckle Tracking Strain in Chagas' Disease. Echocardiography. 2014;31(5):623-30. doi: 10.1111/echo.12426.
6. Santos OR Jr, Rocha MOC, Almeida FR, Cunha PFS, Souza SCS, Saad GP, et al. Speckle Tracking Echocardiographic Deformation Indices in Chagas and Idiopathic Dilated Cardiomyopathy: Incremental Prognostic Value of Longitudinal Strain. PLoS One. 2019;14(8):e0221028. doi: 10.1371/journal.pone.0221028.
7. Saraiva RM, Mediano MFF, Quintana MSB, Silva GMS, Costa AR, Sousa AS, et al. Two-Dimensional Strain Derived Parameters Provide Independent Predictors of Progression to Chagas Cardiomyopathy and Mortality in Patients with Chagas Disease. Int J Cardiol Heart Vasc. 2022;38:100955. doi: 10.1016/j.ijcha.2022.100955.
8. Romano MMD, Moreira HT, Marin-Neto JA, Baccelli PE, Alenezi F, Klem I, et al. Early Impairment of Myocardial Deformation Assessed by Regional Speckle-Tracking Echocardiography in the Indeterminate Form of Chagas Disease without Fibrosis Detected by Cardiac Magnetic Resonance. PLoS Negl Trop Dis. 2020;14(11):e0008795. doi: 10.1371/journal.pntd.0008795.
9. Santos OR Jr, Sabino EC, Carvalho VT, Brito BOF, Oliveira LC, Ferreira AM, et al. Prevalence and Factors Associated with Impaired Left Ventricular Global Longitudinal Strain in Patients with Chagas Disease: SaMi-Trop Cohort Study. Int J Cardiovasc Imaging. 2022;38(11):2353-62. doi: 10.1007/s10554-022-02640-w.
10. Gómez-Ochoa SA, Rojas LZ, Hernández-Vargas JA, Largo J, Muka T, Echeverría LE. Longitudinal Speckle Tracking Strain Abnormalities in Chagas Disease: A Systematic Review and Meta-Analysis. J Clin Med. 2022;11(3):769. doi: 10.3390/jcm11030769.

Editorial

Is Echocardiographic Assessment of Strain Essential In Daily Routine?

Carlos Eduardo Suaide Silva[1]
Dasa,[1] Barueri, SP – Brazil

The assessment of myocardial fiber deformation (myocardial strain) during the cardiac cycle is a direct measurement of muscle function, which can be obtained by conventional imaging tests such as echocardiography and magnetic resonance.

Strain measurement can identify abnormalities in global and regional myocardial function, in addition to making the differential diagnosis of some cardiomyopathies. Furthermore, it is an earlier marker of ventricular dysfunction than ejection fraction and may predict adverse cardiovascular events.

The most used parameter to assess the global ventricular function is the ejection fraction, and the choice of diagnostic method depends on the patient's clinical situation. Magnetic resonance imaging has been considered the gold standard, but the ideal method would be minimally invasive, low-cost, reproducible with little interobserver variation, without irradiation or use of contrasts, and repeatable as many times as necessary. Magnetic resonance imaging is highly accurate, and it is able to assess both anatomy and ventricular function; however, it is expensive, more time-consuming, and not widely available. Contrast allergy is also a relatively limiting factor to its use. This makes echocardiography the most widely available and least uncomfortable method for patients in order to assess cardiac physiology.

Strain is a dimensionless measurement that expresses the deformation of a myocardial segment as a percentage and, therefore, provides information on the contractile function of that segment.[1] We can assess longitudinal, circumferential, and radial contractile function. The most widely used method is longitudinal strain, in part because most of the initial studies used this parameter, in part because the equipment does not calculate the radial or circumferential strain, except with specialized software, and, finally, because of the absence of well-defined normal values for age, sex, and race. Only recently have world societies established these values through the World Alliance Societies of Echocardiography Study.[2]

Keywords

Cardíac Imaging Techniques; Ventricular Function; Echocardiography

Mailing Address: Carlos Eduardo Suaide Silva •
Diagnósticos da America AS, Cardiologia. Av. Jurua 434. Postal code: 06455-010. Barueri, SP – Brazil.
E-mail: csuaide@cardiol.br
Editor responsible for the review: Daniela do Carmo Rassi Frota

DOI: https://doi.org/10.36660/abcimg.20230063i

Cardiac muscle fibers are arranged in different directions according to their subendocardial, middle, and subepicardial layers, causing the myocardium to shorten longitudinally and circumferentially and to thicken radially during systole.

Strain quantification by echocardiography was initially performed using the tissue Doppler technique. By measuring the speed of movement of two points of the myocardium and dividing by the distance between them, we can quantify the deformation of a given segment. As it was a technique based on the Doppler effect, it was influenced by the angle of incidence of the ultrasound, which limited its use. mainly in the apical segments, where the direction of the muscle movement vector is practically perpendicular to that of the ultrasound beam, making it extremely unfavorable for speed calculation and demanding great expertise on the part of the operator. In addition, there was reasonable interobserver variation. Strain measurement by Doppler was soon replaced by the speckle-tracking technique based on two-dimensional echocardiography.[3] Software designed to follow the positions of the speckles (bright dots on the ultrasound image) frame by frame made it possible to quantify the myocardial deformation more accurately, eliminating angle dependence, with a more satisfactory signal-to-noise ratio, making it possible to measure strain in two dimensions (rather than just in the direction of the Doppler beam).[4] This is the universally used technique for measuring strain to this day.

Global longitudinal strain (GLS) values are more reliable and more relevant than ejection fraction in the early detection of ventricular dysfunction.[5] The prediction of cardiovascular events is more reliable using GLS than ejection fraction.[6] Although it does not replace ejection fraction, this information alone would be a good reason to include GLS among the parameters routinely displayed on echocardiography.

Myocardial deformation is influenced by both preload (the strain value increases with the increase in the size of the ventricular cavity) and afterload (strain decreases with the increase in arterial pressure).

A major clinical contribution of strain is the fact that it can detect myocardial dysfunction early, even before the ejection fraction begins to decrease. This applies to many clinical situations. In ischemia, for example, myocardial impairment begins in the subendocardial layer, predominantly composed of longitudinal fibers, which facilitates assessment by echocardiography through the measurement of longitudinal strain in apical views. This impairment may be subclinical, without any decrease in

ejection fraction, but the longitudinal shortening of the fibers may already be altered by ischemia and affect the strain curve. The identification of post-systolic contraction can also alert us to the presence of ischemia, even before any more evident contractile alteration appears on the two-dimensional test. In addition to diagnosis, this technique has great prognostic value and is an excellent tool for the follow-up of these patients. Figure 1 shows the 13-year follow-up of a patient who had his first infarction in 2010, which slightly altered the GLS, and a second one in 2014, which compromised the apex. Nine years later, a worsening could be observed in the affected area. Strain maps give us a perfect idea of the evolution of myocardial damage.

In athletes, strain measurement is very important in assessing both systolic and diastolic function.[7] It can help make the differential diagnosis between physiological and pathological hypertrophy and help detect early ventricular dysfunction in users of anabolic steroids, which are, unfortunately, becoming more and more frequent in our setting.

In valve diseases, strain serves as an important prognostic tool and, in situations bordering on surgical indication, reduced strain can be the missing piece of information for clinical decision making.

In cardio-oncology, the role of strain in the early detection of cardiotoxicity has been amply defined. Numerous studies have shown a reduction in strain values before the drop in ejection fraction occurs. According to the consensus of the American Society of Echocardiography and the European Association of Cardiovascular Imaging,[8] a drop of 15 percentage points in the GLS value is highly suggestive of cardiotoxicity. It is fundamental to perform strain echocardiography before initiating chemotherapy to compare with future sequential echocardiograms and observe whether there is a drop in GLS.

In cardiomyopathies, the presence of specific patterns on the polar map may even suggest the etiology of the disease. When contraction is preserved in the apical region and decreased in the middle and basal segments (apical sparing), it is highly suggestive of amyloidosis (Figure 2). A decrease in strain values in the septal region alone, even without a large increase in myocardial thickness, leads us to suspect hypertrophic cardiomyopathy (Figure 3).

In our opinion, the quantification of myocardial strain is indeed essential in daily routine. As previously set forth, in almost all heart diseases, strain assessment always has something to add, whether to diagnosis, prognosis, or therapeutic follow-up. Only patients who are known to be normal, who come to us for routine evaluations, perhaps do not need to undergo strain echocardiography. Even so, from time to time, there are some surprises. Given that we carry out routine tests in our service, occasionally, young people who practice physical activities, with absolutely normal echocardiograms, present a reduction in the GLS and, with a more focused anamnesis, we discover that they use or have used anabolic steroids, which is very important information for the requesting physician. In other cases, a decrease in strain in a slightly thickened localized segment may suggest the presence of hypertrophic cardiomyopathy that could have gone unnoticed; however, it alerts us to continue the investigation. Another situation that we have observed with a certain frequency is the decrease in strain in some segments, without any other echocardiographic alteration, in post-COVID patients. When they are referred for magnetic resonance imaging, myocarditis is detected.

In conclusion, whenever possible (if there is appropriate equipment and the routine permits), we believe that the few extra minutes to perform the procedure are rewarded by the enormous gain in diagnostic quality that this method has to offer.

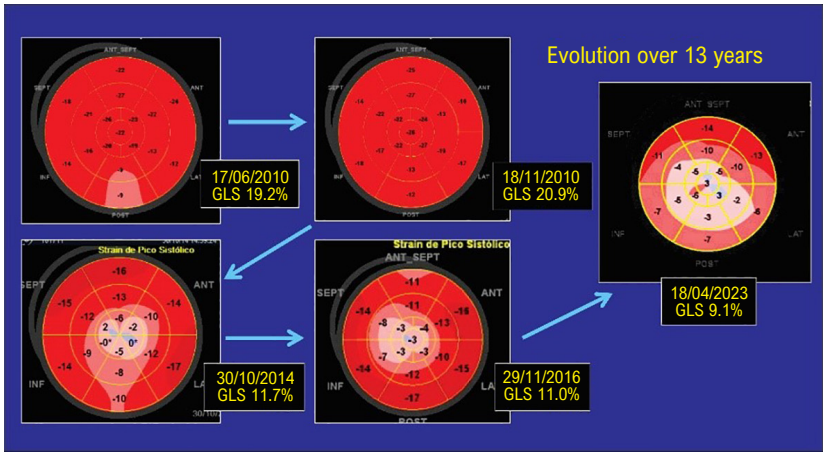

Figure 1 – *Strain maps for follow-up of the evolution of a patient with coronary disease who had a first infarction in 2010 and a second one in 2014. GLS: Global longitudinal strain*

Editorial

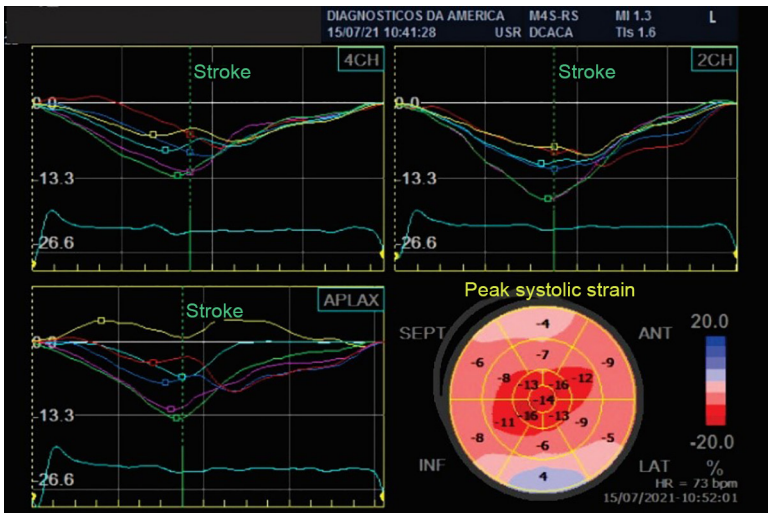

Figure 2 – *Apical sparing in a patient with amyloidosis AVC: Acidente Vascular Cerebral.*

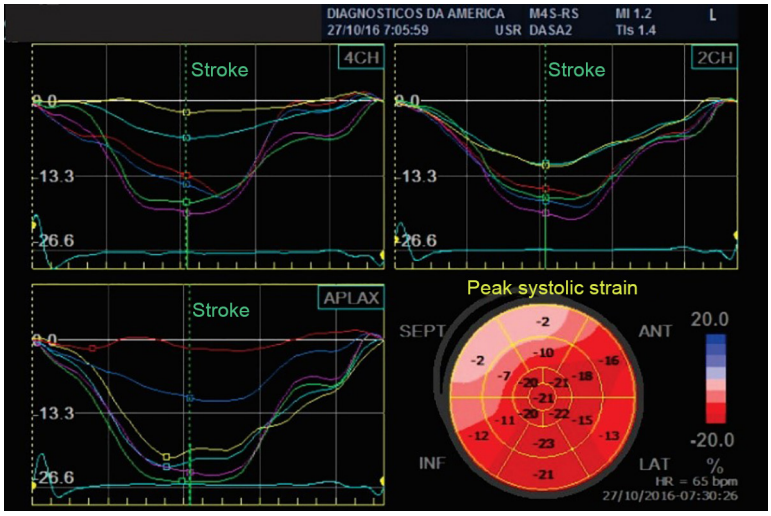

Figure 3 – *Decreased strain in the septal region of a patient with hypertrophic cardiomyopathy*

References

1. Mirsky I, Parmley WW. Assessment of Passive Elastic Stiffness for Isolated Heart Muscle and the Intact Heart. Circ Res. 1973;33(2):233-43. doi: 10.1161/01.res.33.2.233.
2. Singulane CC, Miyoshi T, Mor-Avi V, Cotella JI, Schreckenberg M, Blankenhagen M, et al. Age-, Sex-, and Race-Based Normal Values for Left Ventricular Circumferential Strain from the World Alliance Societies of Echocardiography Study. J Am Soc Echocardiogr. 2023;36(6):581-590.e1. doi: 10.1016/j.echo.2022.12.018.
3. Marwick TH. Measurement of Strain and Strain Rate by Echocardiography: Ready for Prime Time? J Am Coll Cardiol. 2006;47(7):1313-27. doi: 10.1016/j.jacc.2005.11.063.
4. Heimdal A, Støylen A, Torp H, Skjaerpe T. Real-Time Strain Rate Imaging of the Left Ventricle by Ultrasound. J Am Soc Echocardiogr. 1998;11(11):1013-9. doi: 10.1016/s0894-7317(98)70151-8.
5. Venneri L, Khattar RS. Cancer and Myocardial Dysfunction: Is There a Link? Expert Rev Cardiovasc Ther. 2016;14(11):1207-9. doi: 10.1080/14779072.2016.1226129.
6. Luis SA, Chan J, Pellikka PA. Echocardiographic Assessment of Left Ventricular Systolic Function: An Overview of Contemporary Techniques, Including Speckle-Tracking Echocardiography. Mayo Clin Proc. 2019;94(1):125-38. doi: 10.1016/j.mayocp.2018.07.017.

7. Silva CES. Appropriate Use of Diastolic Function Guideline When Evaluating Athletes: It is not Always what it Seems to Be. Arq Bras Cardiol. 2020;115(1):134-8. doi: 10.36660/abc.20190689.

8. Plana JC, Galderisi M, Barac A, Ewer MS, Ky B, Scherrer-Crosbie M, et al. Expert Consensus for Multimodality Imaging Evaluation of Adult Patients During and after Cancer Therapy: A Report from the American Society of Echocardiography and the European Association of Cardiovascular Imaging. J Am Soc Echocardiogr. 2014;27(9):911-39. doi: 10.1016/j.echo.2014.07.012.

Women in the DIC: What Motivates Us?

Samira Saady Morhy[1]

Hospital Israelita Albert Einstein,[1] *São Paulo, SP – Brazil*

During the period from November 2022 to March 2023, a survey was made available on the website of the Department of Cardiovascular Imaging (DIC) of the Brazilian Society of Cardiology (SBC), aimed at female members of the DIC-SBC, with the objective of better understanding the challenges faced by women during their training and professional exercise.

We obtained 131 responses, and the results are displayed in Figures 1 to 6.

We observed that the majority of the respondents were young (41.2% were between 30 and 40 years old; Figure 1), had graduated from medical school between 10 and 20 years ago (37.4%; Figure 2), and had put off starting a family due to their profession (71.8%; Figure 3).

Regarding the situations they had aleady experienced while exercising their profession, 72.5% of the respondents cited lack of motivation, 41.2% impostor syndrome, and 40.5% depression. (Figure 4).

When asked about pay, slightly more than half (61.1%) answered that they receive the same amount as their male colleagues (Figure 5).

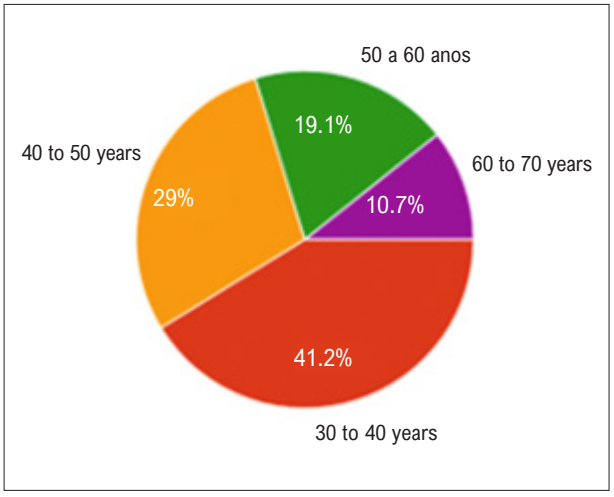

Figure 1 – *Age of survey respondents (131 respondents)*

Keywords

Mulheres; Diagnóstico por Imagem; Medicina.

Correspondência: Samira Saady Morhy •
Hospital Israelita Albert Einstein. Av. Albert Einstein, 627/701. CEP: 05652-900. Morumbi, São Paulo, SP – Brasil
E-mail: samira.morhy@einstein.br

DOI: https://doi.org/10.36660/abcimg.20230079i

In relation to their job opportunities compared to men, opinions were very close: 51% thought they had equal opportunities (Figure 6).

Our challenges are not very different from those reported by women physicians in other countries. The Women's Taskforce of the European Association of Cardiovascular Imaging (EAVCI) conducted a survey of women in cardiovascular imaging worldwide: 60% of them reported lack of motivation, 54% imposter syndrome, and 70% anxiety.[1] Regarding pay, 45% answered that they received similar amounts to male physicians; 10% received less than their male colleagues, and 45% answered that they did not know, or that there was no transparency about this.[1]

During the Twelfth DIC Congress, held from August 18 to 20, this year, in Brasilia, I participated in the second meeting of Women in Cardiovascular Imaging with the physicians Adenalva Beck, Daniela Rassi Frota, Márcia Barberato, and Marly Uellendahl.

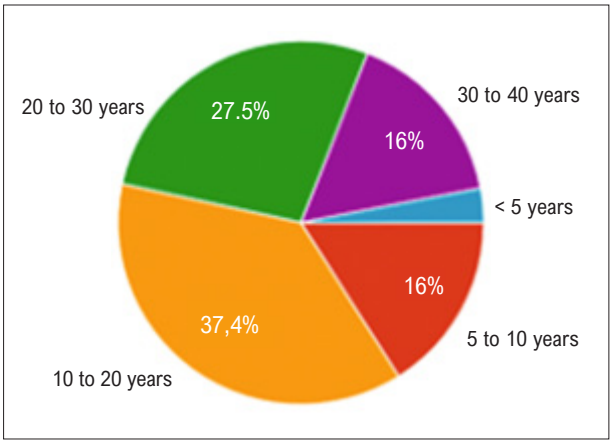

Figure 2 – *Time since graduating from medical school (131 respondents)*

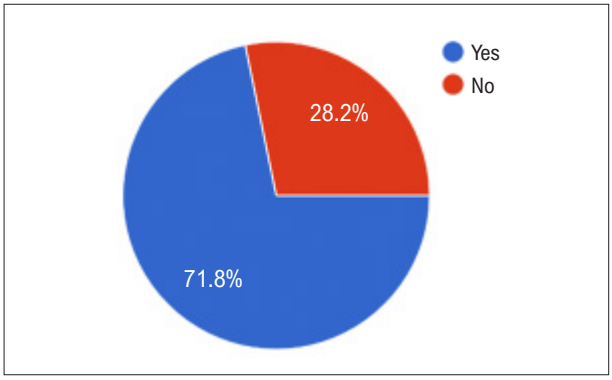

Figure 3 – *Answers to the question: "Do you feel that you put off starting a family or having children due to your medical studies or your profession?" (131 respondents)*

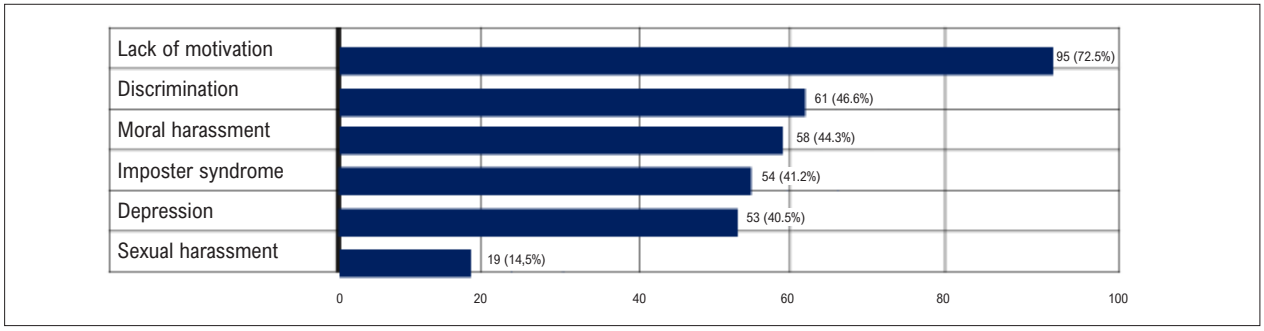

Figure 4 – *Answers to the question: "Have you ever felt that you were in any of the following situations during your professional practice?" (131 respondents)*

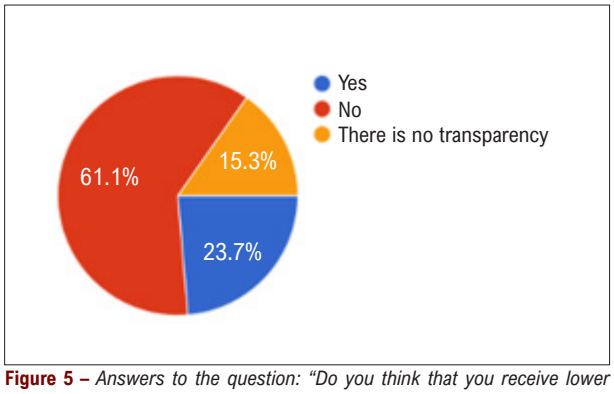

Figure 5 – *Answers to the question: "Do you think that you receive lower pay than your male colleagues working in the same professional position?" (131 respondents)*

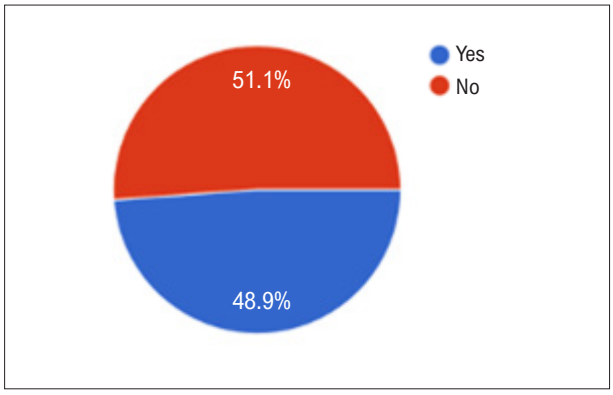

Figure 6 – *Answers to the question: "Do you feel that you have had fewer opportunities than your male colleagues?" (131 respondents)*

On this occasion, we were able to discuss the results of the survey about Women in the DIC, and ask the women colleagues at the table and the audience what motivates them, and it was very moving to hear their responses, including: "the example of their mothers, the purpose of helping people (patients), loving and 'liking' the profession, family (children and husbands), among others."

At this meeting, as well as at the first meeting of Women in the DIC, held at the Eleventh DIC Congress in São Paulo,[2] we left with the conviction that, in addition to discussions about women's participation on the boards of medical societies and health institutions, we must help each other to face the challenges that we still encounter in the exercise of our profession, such as equity of opportunities, balance between family and work, and respect.

References

1. Joshi SS, Kadavath S, Mandoli GE, Gimelli A, Gulati M, Thamman R, et al. Women in Cardiovascular Imaging: A Call for Action to Address Ongoing Challenges. Eur Heart J Cardiovasc Imaging. 2023;jead158. doi: 10.1093/ehjci/jead158.
2. Morhy SS, Uellendahl M. DIC-SBC Women's Group. Arq Bras Cardiol: Imagem Cardiovasc. 2022;35(4):1-3. doi: 10.47593/2675-312X/20223504eed_33i.

Incremental Determinants of The Combined Supine-Prone Protocol for Myocardial Perfusion Scintigraphy

Tiago Oliveira Costa,[1,2] *Mário de Seixas Rocha,*[1,2] *Gilson Feitosa Soares Filho,*[1] *Raphael Abegão de Camargo,*[3] *Cristiano Ricardo Bastos de Macedo*[4]

Escola Bahiana de Medicina e Saúde Pública, Pós-Graduação em Medicina e Saúde Humana,[1] *Salvador, BA – Brazil*
Grupo de Medicina Nuclear (GMN), Grupo CAM, Oncoclínicas,[2] *Salvador, BA – Brazil*
Hospital Português, Nuclear Medicine,[3] *Salvador, BA – Brazil*
Hospital Universitário Professor Edgard Santos,[4] *Cardiologia, Salvador, BA – Brazil*

Abstract

Background: **Myocardial perfusion scintigraphy is an important non-invasive method for diagnosing coronary artery disease, but it is not free from artifacts. Performing the combined supine-prone protocol can bring benefits to images with artifacts from the standard protocol in the supine position. The lack of unanimity in the implementation of the combined protocol may be related to the lack of objective data for the prior selection of patients.**

Objective: **To evaluate which anthropometric profiles may be associated with a greater benefit in excluding artifacts for the optimized performance of the combined protocol.**

Methods: **A cross-sectional and analytical study was carried out with 370 patients at the Nuclear Medicine Group Clinic between April and August 2022. The estimated level of statistical significance was 5%. Statistical analysis using binary logistic regression was used to evaluate the association between anthropometric data and the change in the initial test result after carrying out the combined protocol.**

Results: **The combined protocol promoted a 19.7% increase in the normality ratio of the standard protocol. The variables weight, for both genders [OR = 1.02 (95% CI, 1.0002 – 1.04; p = 0.047)], and bust in women [OR = 1.06 (95% CI, 1. 01 – 1.11; p = 0.014)] represented incremental determinants with statistical significance. Weight greater than 76.5kg for both genders (S: 58.5%; E: 61.5%) and bust greater than 100.0 cm in women (S: 73.9%; E: 53.4%) were the best cutoff points in the receiver operating characteristic (ROC) curve.**

Conclusion: **The optimized implementation of the combined protocol using the described weight and bust measurement criteria can promote greater efficiency in image acquisition.**

Keywords: **Radionuclide Imaging; Myocardial Perfusion Imaging; Prone Position; Anthropometry; Coronary disease.**

Introduction

Myocardial perfusion scintigraphy represents an important non-invasive method in the diagnosis of coronary artery disease (CAD), with sensitivity and specificity of 88 and 74%, respectively.[1] The standard protocol of the exam comprises the acquisition of images with the patient in dorsal decubitus (supine position) after intravenous injection of the radiotracer, obtaining scintigraphic images at rest and post-stress.

Mailing Address: Tiago Oliveira Costa •
Escola Bahiana de Medicina e Saúde Pública, Pós-Graduação em Medicina e Saúde Humana. Rua Santa Isabela, 100, apto 2901 A. Postal code: 40221-225. Salvador, BA – Brazil
E-mail: tiago_oliveirac@hotmail.com
Manuscript received June 23,2023; revised August 31, 2023; accepted September 4, 2023
Editor responsible for the review: Rafael Lopes

DOI: https://doi.org/10.36660/abcimg.20230060i

However, myocardial perfusion scintigraphy is a diagnostic tool subject to interference by artifacts, which can be caused by the attenuation of gamma radiation photons by soft tissues interposed between the myocyte and the gamma-camera detector, as well as artifacts resulting from the movement of the patient, among others that degrade the image quality, decreasing the specificity and the percentage of normality (normalcy rate) of the test. Results of exams with artifacts can greatly influence clinical decision-making, sometimes with continuation of the investigation of CAD through unnecessary invasive diagnostic methods, costly to the health system and not free of complications for the patient.[2]

Some techniques were then developed to minimize the impact of potential attenuation artifacts on myocardial perfusion scintigraphy. Among them, there is the combined protocol of supine-prone images, with benefits reported by previous scientific studies in different scenarios.[3-7] The technique consists of positioning patients in prone position on the examination table and performing the acquisition of additional images after the standard image acquisition in supine position in post-stress images. This positioning promotes caudal displacement of the diaphragm and subphrenic organs, potential interference factors

Contents

Central Illustration: Incremental Determinants Of The Combined Supine-Prone Protocol For Myocardial Perfusion Scintigraphy

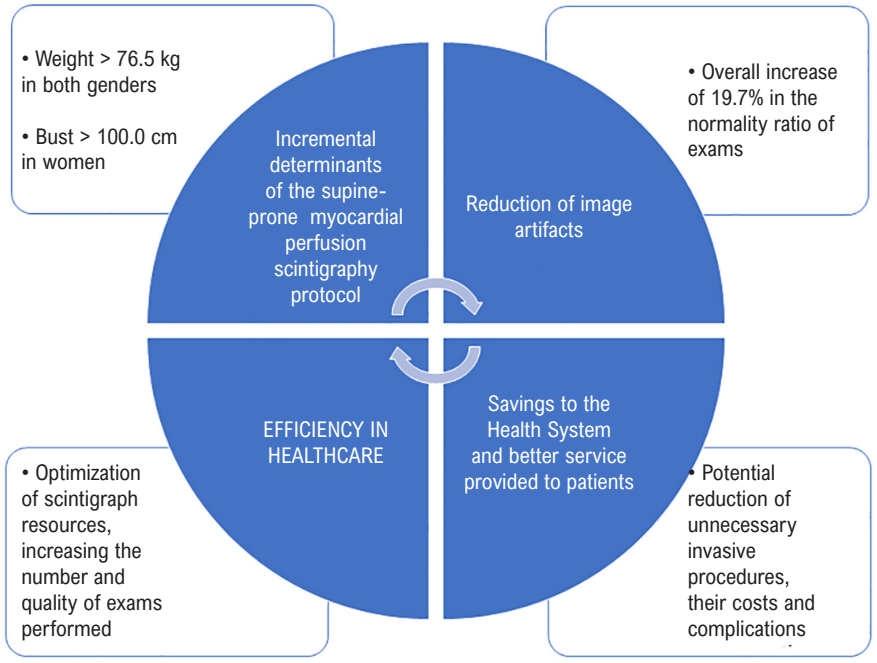

Arq Bras Cardiol: Imagem cardiovasc. 2023;36(3):e20230060

Health efficiency through the incremental determinants of the combined supine-prone imaging protocol of myocardial perfusion scintigraphy.

by attenuating photons emitted by the inferior wall of the left ventricle, thus enabling better detection of them by the gamma camera (Figure 1).

Changing the patients' position and compressing the soft parts of the chest (breasts, adipose tissue) in the prone position can also, sometimes, promote a better assessment of the anterior wall of the left ventricle (Figure 2), especially in cases of breast attenuation in women.

However, performing additional images in the prone position can affect the logistics of the exams due to the additional time spent. In services with a high volume of exams, it may be difficult to perform the combined protocol in all patients. Furthermore, its implementation in some patients would be unnecessary when there are no attenuation artifacts on images in the supine position. To our knowledge, there are no studies that evaluate anthropometric variables as criteria for the selective identification of patients with greater benefit in obtaining the image in the prone position, representing, therefore, a gap in the Literature that we intend to fill.

Methods

Study design

A cross-sectional and analytical study was carried out. Data were collected prospectively from spontaneous demand patients who sought the Service of the Nuclear Medicine Group (*Grupo de Medicina Nuclear* – GMN), Grupo CAM/Oncoclínicas, Salvador–Bahia, Brazil, in order to investigate CAD through myocardial perfusion scintigraphy, in the period between April and August 2022.

Patients of both genders were selected for the study, complying with the following inclusion criteria: absence of known previous coronary disease; minimum age of 18 years, with no upper age limit; prior indication of a myocardial perfusion scintigraphy exam to check for CAD by the attending physician. Exclusion criteria were: previous myocardial infarction or myocardial revascularization; non-ischemic cardiomyopathy or significant heart valve disease; pacemaker wearers; patients with left bundle branch block; inability to remain in prone position due to orthopedic or other limitations; poor technical quality of the exam performed (e.g. low image statistics, significant patient movement during the exam, significant interposition of extracardiac radioactive activity); non-signing of the Informed Consent.

Eligible patients who agreed to participate in the research protocol were previously assessed before the exam by trained nursing professionals to measure weight (kg), height (m), and waist circumference (cm) for both genders, in addition to measurements of the bust at nipple height (cm), chest circumference (cm), and delta between the bust and chest circumference (cm) for women, and then subjected to a combined supine-prone imaging protocol.

To acquire radionuclide images, a GE Medical Systems dual head gamma camera, model Ventri, was used, with all necessary calibrations and equipment quality controls performed. The technique used to acquire the images was single photon emission computed tomography (SPECT), with low energy high-resolution (LEHR) collimators and an energy window of 15% at 140 Kev, 64x64 matrix, using he radiotracer ^{99m}Tc-sestamibi. Male patients weighing more than 100 kg and female patients weighing more than 90 kg, who underwent the protocol for acquiring the rest and stress stages on different days (2-day protocol), while the others performed the stages of rest and stress on the same day (1-day protocol). The radiotracer dose used was 10 to 14 mCi at rest and 30 to 42 mCi in the stress stage in the 1-day protocol, with image acquisition lasting approximately 10 to 15 minutes in the rest stage and 7 to 9 minutes in the stress stage. In the 2-day protocol, the radiotracer dose injected was 15 to 20 mCi in each step, with a corresponding image acquisition time of 10 to 20 minutes. The images in the prone position were taken immediately after the acquisition of the stress images in the supine position, without the need for a new injection of the radiotracer, with an approximate duration of 7 minutes.

The images acquired were then analyzed by a specialist physician, without knowledge of the anthropometric data and identification of the patients, initially only with the analysis of the images of the standard protocol in the supine position and description of the scintigraphic findings of the exam and, later, a new evaluation with the addition of post-stress images in the prone position. Statistical analysis using binary logistic regression was used to assess the association between anthropometric data and the change in the initial result of the test after performing the combined protocol. This study was approved by the Research Ethics Committee of the School of Medicine and Public Health of Bahia (*Escola Bahiana de Medicina e Saúde Pública*) on March 19th, 2022, under registration CAAE 55279921.6.0000.5544, with all participants signing the Informed Consent, in accordance with resolution 466/2012.

Statistical analysis

Based on the premise of an incremental gain of 15% in the ratio of normality of the exams after the execution of the supine-prone protocol and the percentage of normality of approximately 65% in the exams in the supine position in our Service, a sample size calculation of 370 patients was performed

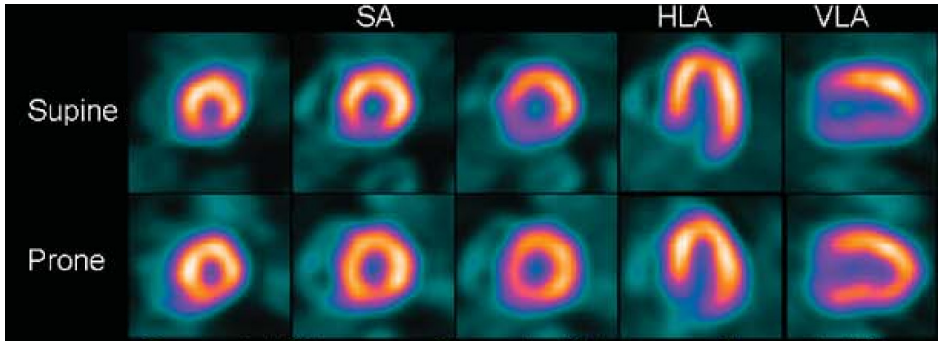

Figure 1 – *Example of diaphragmatic attenuation artifact with reduced uptake on the inferior wall in the post-stress image in the supine position (upper line), corrected in the post-stress image in the prone position (bottom line). Images displayed in 3 axes: short (SA), horizontal long (HLA), and vertical long (VLA). Adapted from Nishina et al, 2006.*[8]

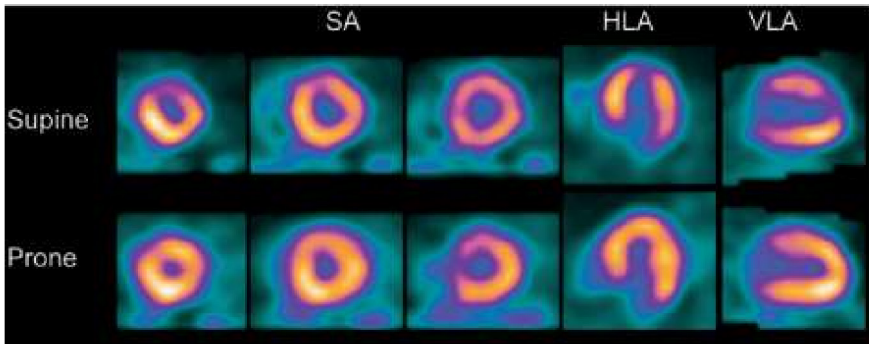

Figure 2 – *Example of artifact due to breast attenuation with reduced uptake in the anterior wall in the post-stress image in the supine position (upper line), corrected in the post-stress image in the prone position (bottom line). Images displayed in 3 axes: short (SA), horizontal long (HLA), and vertical long (VLA). Adapted from Slomka et al, 2007.*[5]

through the WinPepi program, version 11.65. The estimated statistical significance level was 5%.

Initially, descriptive statistics of the collected data were elaborated, in which the categorical variables were expressed in relative frequency and percentages. Numerical variables in our study were evaluated using the Kolmogorov-Smirnov test with Lilliefors correction and showed normal distribution, being expressed as mean and standard deviation.

Then, univariate statistical analyzes were performed using the unpaired Student's *t*-test to identify whether there was a statistically significant difference between the compared groups in relation to each numerical predictor variable with $p < 0.20$ and, thus, be eligible to enter the multiple model with the other numeric predictor variables. Therefore, statistical analysis was performed using binary logistic regression to assess the association between numerical predictor variables and the categorical outcome with or without modification of the result of the examination of the standard protocol of images in supine position after performing the combined supine-prone protocol. The Backward LR procedure was used for binary logistic regression analysis, which included all variables eligible for univariate analysis and, then, step by step, possible combinations of variables were made until arriving at the one(s) that best discriminated as independent predictor(s), with $p < 0.05$, for incremental gain with exclusion of artifacts through the combined supine-prone imaging protocol. 10% of the sample (37 exams) were selected for reanalysis and the Kappa test was used to evaluate interobserver agreement at two moments regarding the outcome variable. ROC curve analysis was used in order to identify the best cutoff point for anthropometric variables to discriminate the group of patients with the highest incremental gain through the combined protocol of supine-prone images.

SPSS software, version 26.0, for Windows was used as an auxiliary tool in the set of analyses previously described.

Results

From April to August/2022, 370 participants were included in the study analysis. Table 1 presents the characteristics of the sample studied in relation to gender, presence and type of comorbidities, as well as the type of stress and protocol performed in the exams.

Next, in Table 2, the specific age and anthropometric characteristics of the study sample can be verified.

In the initial analysis of the standard protocol with only images in the supine position, it was observed that most of the exams in the sample showed preserved perfusion in the left ventricular walls (63.5%). Among the exams that showed some type of myocardial hypoperfusion (persistent or transient), it was noted that the majority had mild hypoperfusion (125 exams) and only 10 exams in the sample showed moderate hypoperfusion (Graphic 1). No exams with severe hypoperfusion were observed in the studied sample.

After the inclusion of images in the prone position, the analysis of the combined protocol of supine-prone images led to changes in the exam results in 74 patients (20% of the total sample), the majority of individuals represented by the male gender (70.3 %), with pharmacological stress with dipyridamole (52.7%) and the study protocol with rest and stress stages carried out on the same day (85.1%), being the most frequent modalities. There was an overall increase of 19.7% in the proportion of normal exams, a finding that reflects the role of the combined protocol in the exclusion of artifacts. In 0.3% of the total sample, there was no complete normalization of the exam, as in the study that was initially considered as a mixed perfusion disorder on images in the supine position (persistent hypoperfusion with associated ischemia) and, after the combined protocol, was considered only as persistent hypoperfusion – the ischemic component in this case was attributed to attenuation artifact. When analyzing separately the subset of patients who initially had a perfusion deficit on images in the supine position ($n = 135$), this change in the result in 74 patients represents more than half of them after performing the combined protocol of supine-prone images. The kappa test applied after reanalysis of 10% of the total sample showed significant interobserver reliability ($k = 0.983$; $p < 0.001$; agreement = 99.5%).

The inferior wall was the region of the left ventricle that represented the highest absolute number of exams with modified results after analyzing the combined supine-prone imaging protocol. The anterior wall and apex occupied the second position. The other walls were also represented in Graphic 2.

The logistic binary regression analysis between anthropometric data for both genders (weight, height, and abdominal circumference) and the modification of the results of the standard protocol examination, after carrying out the combined supine-prone protocol, highlighted the weight variables at the end of the model [OR = 1.018 (95% CI, 1.0002 – 1.0370; $p = 0.047$)] and male gender [OR = 4.445 (95% CI, 2.4951 – 7.9199; $p < 0.001$)] as potential incremental determinants for the combined protocol. The ROC curve illustrated in Graphic 3 shows the criterion of weight greater than 76.5 kg as the best cutoff point for incremental gain with the supine-prone protocol in both genders – Sensitivity (S): 58,5%; Specificity (E): 61,5%.

Figure 3 shows the radionuclide images of myocardial perfusion of a study participant with significant diaphragmatic attenuation in the inferior wall of the left ventricle, with their respective anthropometric data, and the significant improvement in capture after taking the images in the prone position.

By separately performing the logistic regression analysis between anthropometric data in women (weight, height, abdominal circumference, bust, chest circumference, delta between the bust and chest circumference) and the modification of the initial examination result after the combined supine-prone protocol, the bust variable was at the end of the model that represented a possible incremental determinant for the supine-prone protocol [OR = 1.057 (95% CI, 1.011 – 1.106; $p = 0.014$)]. In Graphic 4, the criterion of a bust greater than 100.0 cm can be seen in the ROC curve as the best cutoff point for incremental gain with the supine-prone protocol (S: 73.9%; E: 53.4%).

Figure 4 below illustrates the radionuclide images of myocardial perfusion of a study participant with breast attenuation in the anterior wall of the left ventricle, with their

Table 1 – Characteristics of the categorical sample

Characteristics	n=370	%
Gender		
Female	226	61.1
Comorbidities		
Yes	292	80.0
High blood pressure	260	70.8
Dyslipidemia	144	41.6
Diabetes mellitus	134	36.5
Stress method		
Pharmacological-dipyridamole	220	59.8
Ergometric	148	40.2
Protocol		
1 day	338	91.4
2 days	32	8.6

Source: the author.

Table 2 – Specific characteristics of the studied sample

Characteristics	Mean	Standard deviation
Age (years)[1]	61.5	11.2
Weight (kg)[1]	74.7	15.2
Height (m)[1]	1.63	0.09
Abdominal circumference (cm)[1]	97.3	0.09
Male	98.7	11.7
Female	96.4	10.9
Bust (cm)[2]	99.8	9.9
Chest circumference (cm)[2]	88.9	9.9
Bust-Chest circumference (cm)[2]	9.9	3.5

[1]Both genders. [2]Only females. Source: the author.

respective anthropometric data, and the improvement in uptake after taking the images in the prone position.

Discussion

The combined protocol of supine-prone images of myocardial perfusion scintigraphy represents an important method for excluding artifacts and increasing the percentage of normality of the exams. In the present case series, an overall percentage increase of 19.7% in the number of normal exams was observed when compared to images from the standard protocol, only in the supine position. Other studies in the literature had already shown an increase in the percentage of normality through the combined protocol, although with analyses in subgroups (men, women or obese), one of the strengths of this work being the considerable global increase in the percentage of normality when analyzing the entire population studied.

The inferior, anterior, and apex walls were the regions of the left ventricle with the highest frequency of changes after the inclusion of the combined protocol, findings related to the presence of diaphragmatic attenuation artifacts in the inferior wall and attenuation by soft tissues, adipose tissue, and breasts in the anterior and apex walls.

The impact of changing exam results with the combined protocol becomes even more evident when analyzing separately the subset of patients who initially presented perfusion deficits on images only in the supine position (n = 135). In this group of study participants, 74 of them showed a change in the exam results after performing the combined supine-prone imaging protocol. In other words, more than half of the patients (54.8%) had their test results modified by the combined protocol. This number of patients could have been unnecessarily taken to other invasive diagnostic procedures that are not free from complications, such as coronary angiography, if images in the prone position had not been added to the analysis. The combined protocol images do not expose the patient to additional doses of radiation, as they are acquired with the same radiotracer material as the previously performed injection, with only a change in position on the examination table. Furthermore, there is no need for additional costs when purchasing expensive software to correct image attenuation. In addition to the direct benefit to patients, there is also the savings generated for the healthcare system by avoiding expenses related to unnecessary invasive procedures.

Despite the benefits reported in excluding artifacts and increasing the number of normal exams through the combined supine-prone imaging protocol, reported by several authors and corroborated by the present study, there is no universalization of its use in all nuclear medicine services. The additional time spent performing the step in the prone position, in the context of services with a high volume of exams and the associated pressure for high productivity, may explain this heterogeneity in the application of the combined protocol. When considering exams that already present preserved perfusion in the images of the standard protocol in the supine position, the prone position of the combined protocol would not add value and would waste unnecessary additional time in acquiring images of the same patient, while the myocardial perfusion scintigraphy equipment could be used to assist other patients, increasing the total number of exams performed. The lack of objective criteria in the literature that could guide prior screening of patients with a greater chance of benefiting from the combined supine-prone protocol, based on the evaluation of anthropometric data most associated with attenuation artifacts, endorses the importance of this work in the search for its incremental determinants.

The weight variable represented an incremental determinant in a statistically valid way for both genders in the combined supine-prone protocol in the present study. The attenuation promoted by adipose tissue can be considered one of the pillars of this association. The criterion of weight above 76.5 kg was the best cutoff point for the ROC curve in this scenario. In parallel to the data found in the literature, the work of Hidetaka Nishina et al.,[8] showed an increase in the normality ratio of exams by around 17% in the subgroup of obese patients after carrying out the supine-prone protocol. However, it did not identify what would be the anthropometric determinant associated

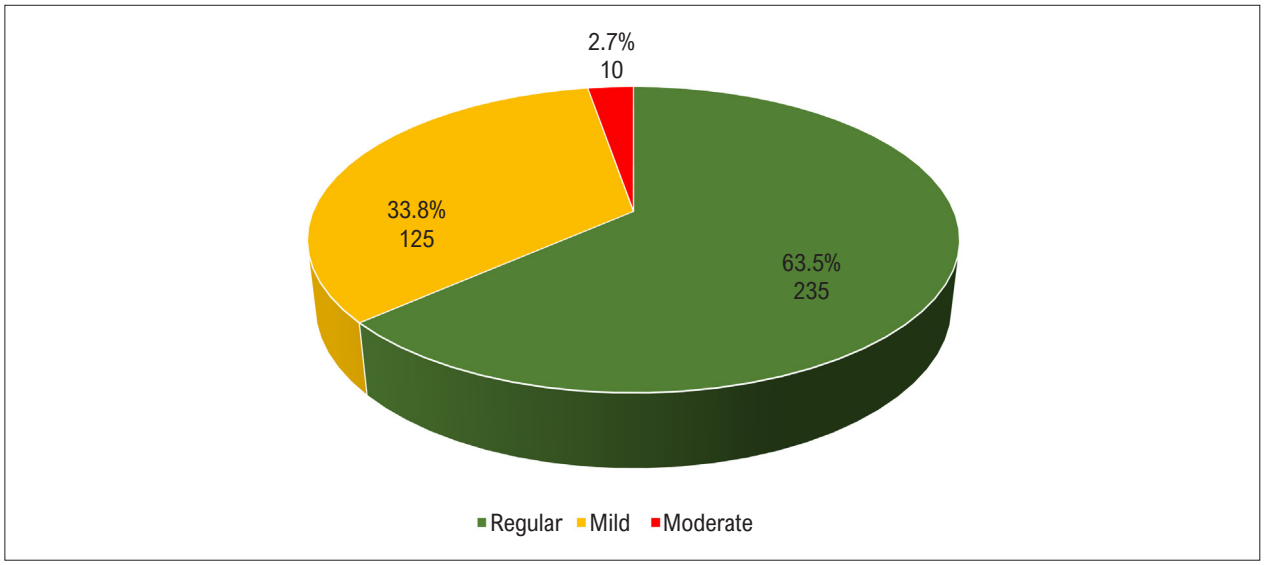

Graphic 1 – *Standard protocol (supine): percentage of normal and hypoperfused exams.*

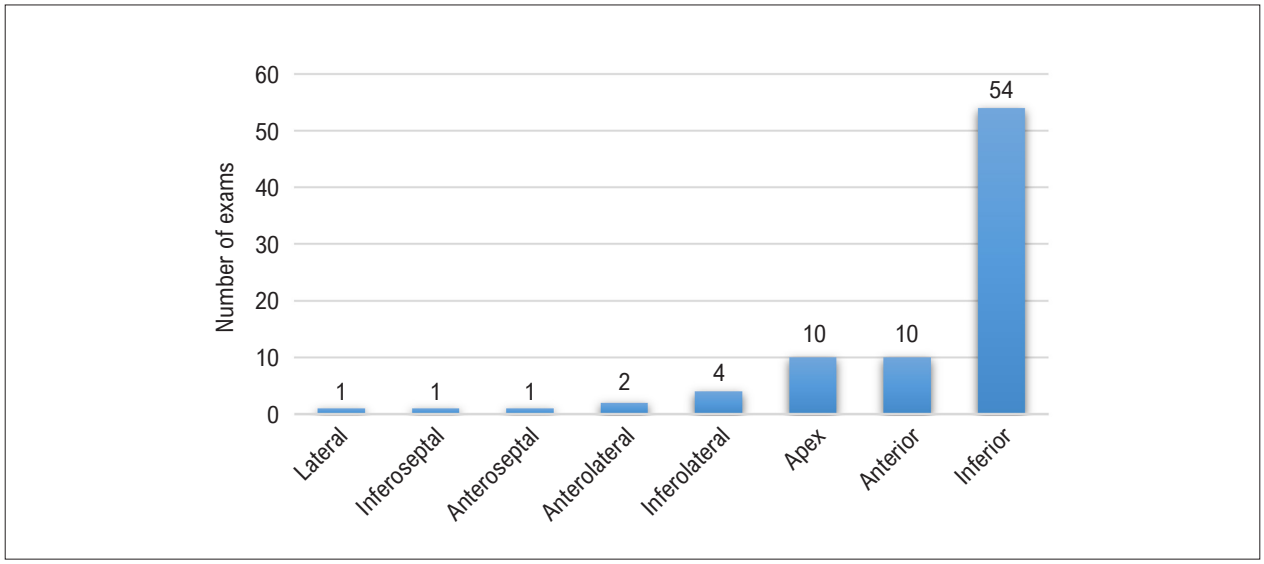

Graphic 2 – *Frequency of myocardial walls that improved uptake with the combined supine-prone protocol.*

with incremental gain nor its best cutoff point for performing the technique, data found in our series.

The present study showed an association between males and a 4.44 times greater chance of benefit from the combined supine-prone protocol compared to females, most likely due to the greater prevalence of diaphragmatic attenuation artifacts and abdominal fat concentration (android pattern). In the same direction, the article by Vicente Taasan et al.,[4] concluded that the supine-prone protocol promotes increased diagnostic certainty and improves the accuracy of the test in detecting coronary disease in men with related risk factors, especially in obese ones, when compared to the standard protocol in the supine position only. However, as it was an exclusive study on men, it did not show a greater chance of improvement through the combined protocol in men when compared to women, a finding added by this work.

When analyzing females separately, the bust variable was a statistically valid incremental determinant. The measurement of the bust at nipple height with a value greater than 100.0 cm was configured as the criterion for the best cut-off point in the ROC curve. Breast attenuation, added to that of other soft tissues in the thoracic region, may represent a generator of artifacts in myocardial perfusion scintigraphy exams in women. A previous study by Slomka et al.,[5] had demonstrated, after carrying out the supine-prone protocol, an increase of 7 to 12% in the normality ratio of exams in women when compared to the standard protocol in the supine position. However, the objective of this study was not to identify the best cutoff point

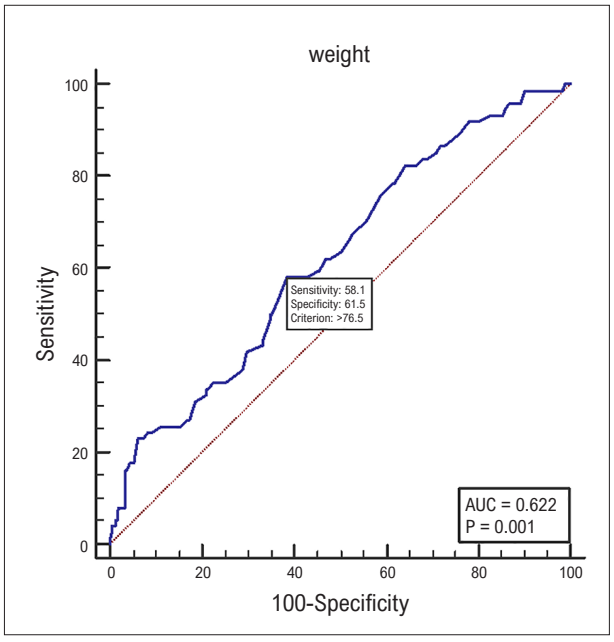

Graphic 3 – *ROC curve weight x change with the combined supine-prone protocol.*

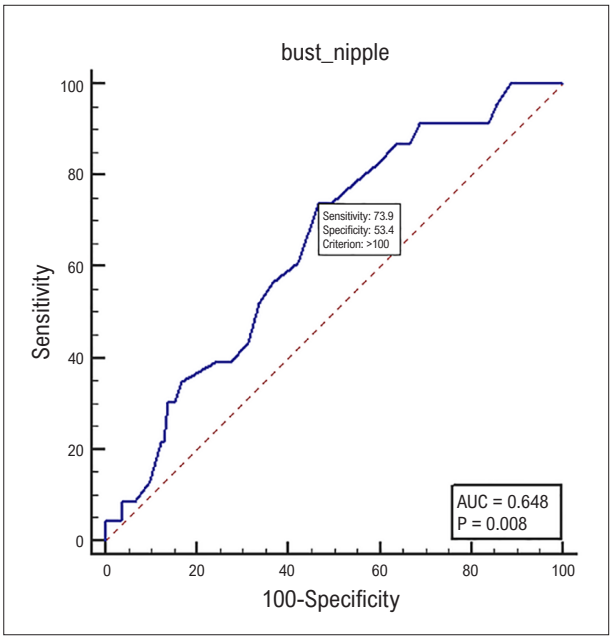

Graphic 4 – *ROC curve of bust measurement in women x change with the combined supine-prone protocol.*

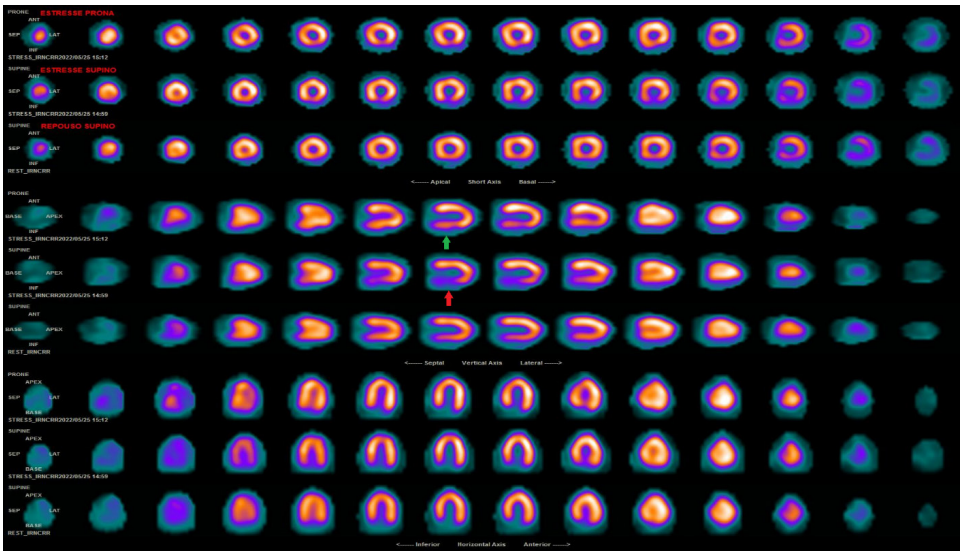

Figure 3 – *Male, 67 years old, 110.0 kg, 1.67 m, abdominal circumference of 122.0 cm, with diaphragmatic attenuation artifact in the lower wall in the post-stress image of the supine position (red arrow), corrected in post-stress image of the prone position (green arrow). Images displayed on 3 axes: short (top lines), vertical long (middle lines), and horizontal long (bottom lines).*

for the incremental determinant for the acquisition of the supine-prone protocol.

The body distribution pattern of adipose tissue, not covered by the isolated weight analysis, may represent a limitation to the external validity of this work. The biotypes of patients in other populations, sometimes different from those found in patients in our Nuclear Medicine Service, could impact the results found as criteria for the incremental determinants of the combined supine-prone protocol. Specific studies in other populations may be necessary.

The contribution of the present work to scientific knowledge is based on highlighting the importance of the combined supine-prone protocol, already described in other studies, and adding potential criteria for better selection and management of patients with greater benefit from carrying out this protocol. In this scenario, patients

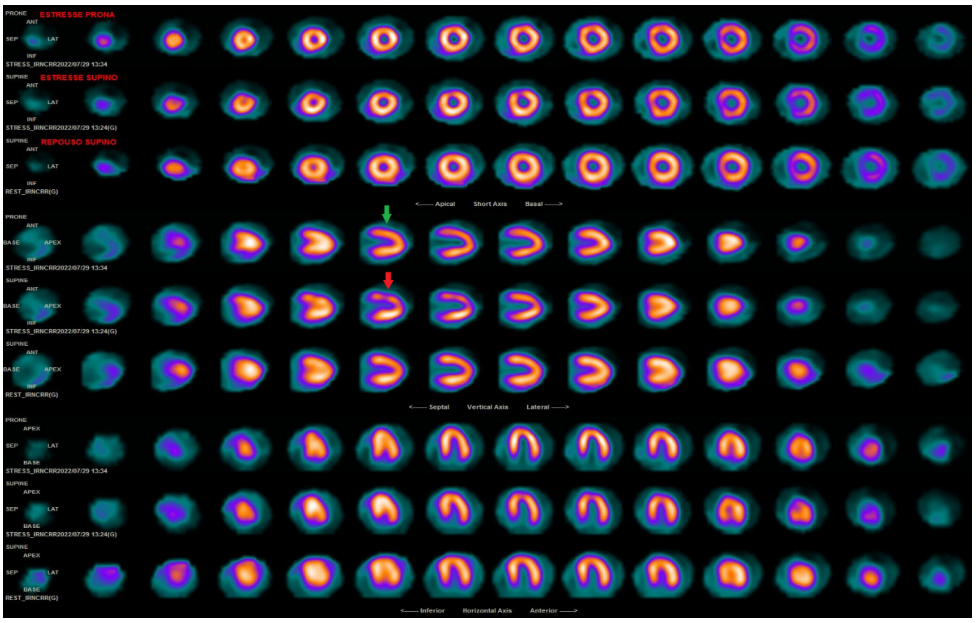

Figure 4 – *Female, 60 years old, 68.0 kg, 1.60 m, abdominal circumference of 97.0 cm, bust measurement of 104.0 cm, with breast attenuation artifact on the anterior wall in the post-stress image of the supine position (red arrow), corrected in post-stress image of the prone position (green arrow). Images displayed on 3 axes: short (upper lines), vertical long (middle lines), and horizontal long (bottom lines).*

of both genders weighing more than 76.5 kg and women with a bust measurement greater than 100.0 cm will have a progressive incremental gain with the combined supine-prone protocol.

Conclusions

It is of utmost importance that Nuclear Medicine Services encourage the use of a combined supine-prone imaging protocol in myocardial perfusion scintigraphy exams. The benefits brought by this technique, notably avoiding unnecessary invasive examinations due to false-positive results of the standard protocol, are extremely valuable.

The identification of specific anthropometric predictors of weight in both genders and bust measurement in women may represent an interesting strategy in better patient management for the combined supine-prone protocol. The selective inclusion of this protocol makes it possible to obtain more efficient images, as it allows the optimization of the gamma camera's resources. In this way, it is possible to select and include patients with the greatest benefit from prone imaging, improving both the quality of the images and enabling the equipment to be used to serve a greater number of patients. Efficiency in the use of resources in the Health Sector, increasingly essential to our population, therefore, constitutes an important paradigm to be constructed by all agents involved.

The work was financed by the authors themselves.

Acknowlegments

To Clínica GMN/Grupo CAM/Oncoclínicas.

Author Contributions

Conception and design of the research, acquisition of data, analysis and interpretation of the data, statistical analysis, writing of the manuscript, critical revision of the manuscript for intellectual content: Costa TO, Rocha MS, Feitosa Filho G, Camargo RA, Macedo C.

Potential Conflict of Interest

No potential conflict of interest relevant to this article was reported.

Sources of Funding

There were no external funding sources for this study.

Study Association

This article is part of the thesis of master submitted by Tiago Oliveira Costa, from Escola Bahiana de Medicina e Saúde Pública.

Ethics Approval and Consent to Participate

This study was approved by the Ethics Committee of the Escola Bahiana de Medicina e Saúde Pública under the protocol number 55279921.6.0000.5544. All the procedures in this study were in accordance with the 1975 Helsinki Declaration, updated in 2013. Informed consent was obtained from all participants included in the study.

References

1. Klocke FJ, Baird MG, Lorell BH, Bateman TM, Messer JV, Berman DS, et al. ACC/AHA/ASNC Guidelines for the Clinical use of Cardiac Radionuclide Imaging--Executive Summary: A Report of the American College of Cardiology/American Heart Association Task Force on Practice Guidelines (ACC/AHA/ASNC Committee to Revise the 1995 Guidelines for the Clinical Use of Cardiac Radionuclide Imaging). Circulation. 2003;108(11):1404-18. doi: 10.1161/01.CIR.0000080946.42225.4D.

2. Dorbala S, Ananthasubramaniam K, Armstrong IS, Chareonthaitawee P, DePuey EG, Einstein AJ, et al. Single Photon Emission Computed Tomography (SPECT) Myocardial Perfusion Imaging Guidelines: Instrumentation, Acquisition, Processing, and Interpretation. J Nucl Cardiol. 2018;25(5):1784-846. doi: 10.1007/s12350-018-1283-y.

3. Stathaki M, Koukouraki S, Papadaki E, Tsaroucha A, Karkavitsas N. The Benefits of Prone SPECT Myocardial Perfusion Imaging in Reducing Both Artifact Defects and Patient Radiation Exposure. Arq Bras Cardiol. 2015;105(4):345-52. doi: 10.5935/abc.20150122.

4. Taasan V, Wokhlu A, Taasan MV, Dusaj RS, Mehta A, Kraft S, et al. Comparative Accuracy of Supine-Only and Combined Supine-Prone Myocardial Perfusion Imaging in Men. J Nucl Cardiol. 2016;23(6):1470-6. doi: 10.1007/s12350-015-0358-2.

5. Slomka PJ, Nishina H, Abidov A, Hayes SW, Friedman JD, Berman DS, et al. Combined Quantitative Supine-Prone Myocardial Perfusion SPECT Improves Detection of Coronary Artery Disease and Normalcy Rates in Women. J Nucl Cardiol. 2007;14(1):44-52. doi: 10.1016/j.nuclcard.2006.10.021.

6. Arsanjani R, Hayes SW, Fish M, Shalev A, Nakanishi R, Thomson LE, et al. Two-Position Supine/Prone Myocardial Perfusion SPECT (MPS) Imaging Improves Visual Inter-Observer Correlation and Agreement. J Nucl Cardiol. 2014;21(4):703-11. doi: 10.1007/s12350-014-9895-3.

7. Hayes SW, De Lorenzo A, Hachamovitch R, Dhar SC, Hsu P, Cohen I, et al. Prognostic Implications of Combined Prone and Supine Acquisitions in Patients with Equivocal or Abnormal Supine Myocardial Perfusion SPECT. J Nucl Med. 2003;44(10):1633-40.

8. Nishina H, Slomka PJ, Abidov A, Yoda S, Akincioglu C, Kang X, et al. Combined Supine and Prone Quantitative Myocardial Perfusion SPECT: Method Development and Clinical Validation in Patients with no Known Coronary Artery Disease. J Nucl Med. 2006;47(1):51-8.

Original Article

Diagnostic Accuracy of the Coronary Calcium Score Acquired with Reduced Radiation Dose and Iterative Reconstruction

Daniela Rodrigues Carnaval,[1] Adriano Liebl,[2] Miguel Morita Fernandes Silva,[3] Bruno Marques Sartori,[2] Caio Nogara de Menezes Couto,[2] Gabriel Bergonse Garaluz da Silva,[2] Ítalo Gabriel Beltrame Vazzoler,[2] Vinícius Maksoud Medeiros,[2] Rodrigo Julio Cerci[3]

Hospital Santa Casa de Misericórdia de Curitiba,[1] Curitiba, PR – Brazil
Pontifícia Universidade Católica do Paraná,[2] Curitiba, PR – Brazil
Clínica Quanta Diagnóstico e Terapia,[3] Curitiba, PR – Brazil

Abstract

Background: The calcium score is an imaging test used to evaluate cardiovascular risk by detecting coronary artery calcification (CAC). However, exposure to ionizing radiation during computed tomography (CT) has been a concern.

Objective: The objective of this study was to evaluate radiation dose and the diagnostic quality of the calcium score using reduced tube voltage and iterative image reconstruction.

Methods: This was a cross-sectional, observational study with patients over 18 years of age. Patients with previous coronary artery disease and patients who declined to participate were excluded. We acquired calcium score twice (120 kV and 100 kV) with different iterative reconstruction techniques. Two professionals interpreted the exams.

Results: We evaluated 153 patients, and the reduction in radiation dose between acquisitions with 120 kV and 100 kV was 43%. The agreement of the degree of CAC between the different acquisitions was high, ranging from 93.9% to 96.2%. In Bland-Altman analysis, we observed a slight overestimation of the results in the acquisition with 100 kV compared to the acquisition with 120 kV.

Conclusion: Calcium score acquired at 100 kV using Iterative Model Reconstruction (IMR) iterative reconstruction resulted in a significant reduction in radiation dose. Furthermore, agreement with acquisition at 120 kV was high, indicating that this approach may be a viable alternative to decrease radiation exposure during calcium score testing. However, it is important to underscore the slight overestimation of the results in the acquisition with 100 kV, which must be considered in the clinical interpretation.

Keywords: Vascular Calcification; Coronary Artery Disease; Radiation Dosage; Tomography.

Introduction

Cardiovascular diseases represent one of the leading causes of mortality worldwide, with approximately 17.3 million deaths per year; of these deaths, 7.3 million are associated with coronary atherosclerotic disease.[1]

The use of diagnostic imaging methods for earlier detection of coronary atherosclerotic disease has intensified in recent years. Some of these methods use ionizing radiation, raising concerns regarding their possible side effects. Ionizing radiation can cause biological damage to those who are exposed to it. The damage is classified into 2 categories: stochastic and deterministic effects. The stochastic effects occur proportionally to the radiation dose received, without the existence of a threshold, and they are related to the development of cancer and genetic mutations, being the main cause of health risks resulting from radiation. Deterministic effects are caused by the total radiation that a patient receives during a procedure, so that tissue damage is caused at the focus of radiation that is not compensated by cellular repair, which generates damage, such as skin lesions.[2,3] Accordingly, means of reducing the effective radiation dose in these exams have become the focus of research by professionals in the fields of cardiology and radiology worldwide.[4]

The calcium score is a cardiovascular diagnostic imaging test that uses ionizing radiation in its acquisition. It is indicated for cardiovascular risk stratification, detecting the degree of coronary artery calcification (CAC), a pathognomonic sign of coronary atherosclerotic disease, by means of cardiac computed tomography (CT).[5,6] The radiation dose used to obtain the calcium score is usually low, around 0.9 to 1.3 millisieverts, but it may pose a risk to the health of patients if it is used more widely as a screening tool for cardiovascular disease.[4]

Mailing Address: Adriano Liebl •
Pontifícia Universidade Católica do Paraná. R. Imaculada Conceição, 1155. Postal code: 80215-901. Prado Velho, Curitiba, PR – Brazil
E-mail: adriano_liebl@hotmail.com
Manuscript received August 15, 2023; revised August 29, 2023; accepted September 4, 2023
Editor responsible for the review: Tiago Senra

DOI: https://doi.org/10.36660/abcimg.20230069i

Contents

Central Illustration: Diagnostic Accuracy of the Coronary Calcium Score Acquired with Reduced Radiation Dose and Iterative Reconstruction

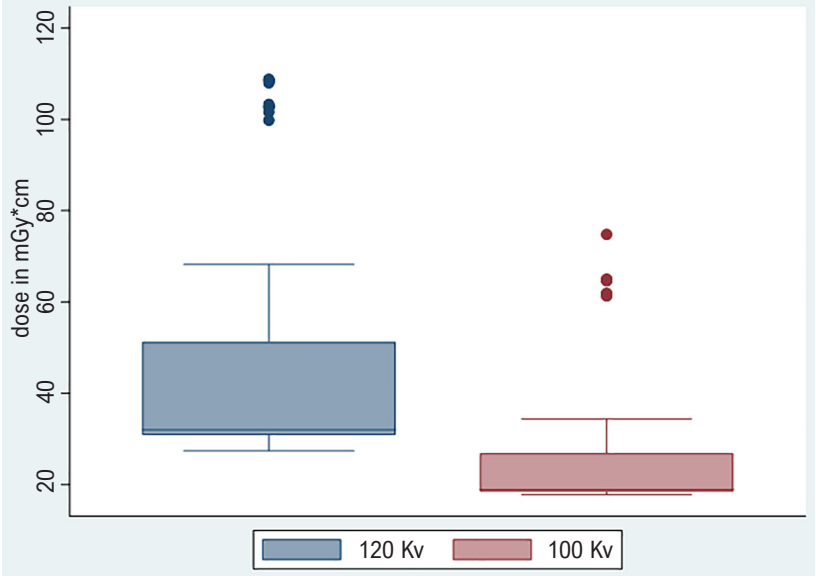

Arq Bras Cardiol: Imagem cardiovasc. 2023;36(3):e20230069

Image quality and radiation dose are positively related. Reducing the dose leads to a decrease in image quality, so that excessively zealous efforts to obtain low doses can produce poor quality images.[2] Reduced radiation dose increases image noise, and the current method of reconstruction with filtered back-projection (FBP) is not able to consistently generate diagnostic quality images at reduced x-ray tube currents (mA).[7] Thus, the iterative reconstruction method is an excellent alternative to improve the quality of images obtained, as it manages to reduce the amount of image noise and artifacts that are normally associated with FBP, so that the worsened image quality resulting from the decrease in tube voltage is compensated by the iterative image reconstruction.[8]

In this study, our objective was to compare the effective dose of radiation in the acquisition of the calcium score with tube voltage of 120 kV and 100 kV, using different forms of reconstruction, and their impacts on the diagnostic accuracy of the exam.

Methods

Study population

We included 156 patients who underwent calcium score testing at an imaging clinic in the city of Curitiba, Paraná, Brazil from October 2019 to February 2020. The inclusion criteria were as follows: patients over 18 years old referred to the clinic by medical specialists to undergo coronary calcium score testing. Patients already diagnosed with coronary heart diseases and/or patients who declined to participate in the study were excluded. All patients referred to the imaging clinic filled out a questionnaire before the test, providing the following data: sex, age, weight, height, history of systemic arterial hypertension, diabetes, dyslipidemia, smoking, family history of heart disease, acute myocardial infarction, percutaneous revascularization, and surgical revascularization. This information was recorded in the clinic's database. Three patients were excluded from the analysis because they had a history of previous acute myocardial infarction (2) or percutaneous revascularization (1), leaving 153 participants for analysis. All participants provided consent prior to the test. The study was submitted to the institution's ethics committee, and it received approval under opinion number 3.623.828.

Study type

This was a cross-sectional, observational study.

Image acquisition protocol

The calcium score was acquired by means of transverse sections, up to 3 millimeters thick, of the heart on CT synchronized with an electrocardiogram, without the use of intravenous contrast. In this study, patients were submitted to 2 consecutive cardiac CT scans to obtain the calcium score. The first with a tube voltage of 120 kV (gold standard) and the other with a voltage of 100 kV. Both were performed with a 256-slice CT scanner (Brilliance, Philips,

Healthcare, The Netherlands), and patients remained in the same position during both acquisitions, with the current adjusted by the body mass index (BMI), which was the same in both acquisitions (BMI < 30: 30 mAs, BMI between 30 and 35: 50 mAs, and BMI > 35: 100 mAs).

In the images obtained with 120 kV, FBP image reconstruction was performed, constituting the gold standard for obtaining the calcium score. On the other hand, on images acquired at 100 kV, FBP reconstruction and iterative reconstructions were performed with 2 pieces of technology: iDose 6 (Philips, Healthcare, The Netherlands) and IMR 1 (Philips, Healthcare, The Netherlands). Both tests obtained were sent, blindly, to 2 specialist doctors to determine the calcium score, using dedicated software (Heartbeat CS, Philips, Healthcare, The Netherlands). Hyperattenuating images with more than 130 Hounsfield units and an area ≥ 3 adjacent pixels were highlighted by the software, and those confined in the coronary tree were selected by the physician. The software then calculated the sum of these points according to the Agatston method and determined a final score.[6,9] Furthermore, we categorized the calcium score result as follows: equal to 0, between 1 and 99, between 100 and 399, and above 399, in the different combinations of voltage and reconstruction.

Radiation dose

The radiation dose was calculated automatically after each acquisition. The standard used was the dose length product (DLP), which is automatically calculated by the CT acquisition software (iPatient Philips, Healthcare, The Netherlands) and presented in a report at the end of the exam. The DLPs of the 120 kV and 100 kV acquisitions for each patient were recorded in a Microsoft Excel spreadsheet for analysis.

Statistical analysis

Data were collected and stored in a Microsoft Excel spreadsheet. The results were expressed as means, medians, minimum values, maximum values, and standard deviations (quantitative variables) or as frequencies and percentages (qualitative variables). Data analysis was performed using the STATA computer program. The radiation dose used in the acquisitions at 120 kV and 100 kV was compared using the Wilcoxon rank-sum (Mann-Whitney) test, and the correlation of values of the degree of CAC was analyzed using kappa tests. Bland-Altman curves were also used to evaluate the agreement between the scores obtained in the study. P values < 0.05 were considered to indicate statistical difference.

To facilitate the clinical interpretation of the results, we considered clinically significant changes in the calcium score categories between the different acquisitions and reconstructions, those that would lead to a change in clinical management according to the guidelines, namely: change from calcium score of 0 to any positive result (1 to 99, 100 to 399, or above 399) or change from a calcium score below 100 (1 to 99) to greater than 100 (100 to 399 or above 399), given that a score above 100 is considered an aggravating cardiovascular risk factor, and a score above 0 represents the presence of calcified coronary atherosclerosis.

Results

Demographics of the study population

The exams of 153 patients were analyzed, showing a mean calcium score of 221.9 Agatston units.

The mean age of the study population was 58.9 ± 13.1 with a mean BMI of 27.8 ± 4.42. Risk factors for cardiovascular disease were present in research sample participants as follows: systemic arterial hypertension in 65 patients (43.3%), diabetes mellitus in 24 (16%), dyslipidemia in 57 (38%), and tobacco use in 17 (11.3%). The main characteristics of the study population are displayed in Table 1.

Radiation dose

There was a 43% reduction in radiation dose between the 120 kV and 100 kV acquisitions (p < 0.0001). For the 120 kV voltage, the average DLP was 41 (± 19.3) mGy*cm ,while it was 23.8 (± 11.4) mGy*cm for the voltage of 100 kV (Central Figure).

Diagnostic accuracy

There was a good correlation between the calcium score calculated by the observers in all forms of acquisition and reconstruction. For 120 kV with FBP, the interobserver correlation coefficient was 0.99. For 100 kV with FBP, the correlation was 0.99. For 100 kV with iDose 6, it was 0.99, and for 100 kV with IMR 1, it was 0.99, considering interclass correlation coefficient between 0.75 and 1 as excellent values.

Agreement of the calcium score in the Agatston classification using the kappa test between 120 kV with FBP and 100 kV with IMR was 94.2% with kappa index

Table 1 – Characteristics of the study population

Variables	N = 156
Age, mean (SD)	58.97 (± 13.13)
BMI, mean (SD)	27.82 (± 4.42)
Female sex, N (%)	65 (41.6 %)
SAH, N (%)	65 (43.8%)
Diabetes, N (%)	24 (16%)
Dyslipidemia, N (%)	57 (38%)
Current tobacco use, N (%)	17 (11.3%)
Family history, N (%)	34 (22.7%)
AMI, N (%)	2 (1.3%)
Percutaneous revascularization, N (%)	1 (0.7%)
Calcium score, mean (SD)	221.95 (± 563.76)

AMI: previous acute myocardial infarction; BMI: body mass index; SAH: systemic arterial hypertension; SD: standard deviation.

of 0.9. For 120 kV with FBP and 100 kV with FBP, it was 93.8% with kappa index of 0.9. For 120 kV with FBP and 100 kV with iDose 6, it was 96.2% with kappa 0.93 ($p < 0.001$). When we stratified agreement using the kappa index in patients with BMI less than or equal to 25 versus greater than 25, we observed a drop in agreement in the most obese patients, as shown in Table 2.

The comparison of the results in the Bland-Altman analysis at the voltage of 120 kV with FBP versus 100 kV with IMR showed the following data: 95% limit of agreement with scores −162.6 to 139.6 and mean difference of −11.5 (confidence interval [CI]: −23.5 to 0.5), as shown in Figure 1. For voltage of 120 kV with FBP versus 100 kV with iDose 6, the 95% limits of agreement were −226.6 to 164.8, with mean difference of −30.8 (CI −46.5 to −15.2; n = 153; p = 0.0001), as shown in Figure 2. For the voltage of 120 kV with FBP compared to the dosage of 100 kV with FBP, the 95% limits of agreement were −366.9 to 252.7 with mean difference of −57 (CI −81.8 to −32.3; p = 0.0001), as shown in Figure 3. For the reconstruction with IMR 1, there was a lower dispersion value with a mean difference of −11.5. We observed an overestimation of the value for IMR 1; thus, for higher calcium score values, the mean difference increased. Using iDose 6 reconstruction, for calcium score of 130 Hounsfield units, the dispersion was −30. Using 100 kV with FBP, for calcium score of 157 Hounsfield units, the dispersion was −57.

When we considered clinically significant changes in the calcium score category between acquisition at 100 kV with IMR compared to the gold standard acquisition (120 kV with FBP), we observed a total of 5 (3.2%) changes, 2 (1.3 %) changes from category 0 to the category 1 to 99 and 3 (1.9%) changes from the category 1 to 99 to the category 100 to 399.

Discussion

In any procedure that involves exposing an individual to radiation for diagnostic purposes, the technique applied must provide maximum visual information using the minimum dose; in other words, the benefit to the patient undergoing radiological diagnostic examination must be associated with optimized practices that guarantee image quality at the lowest dose.[3,10] Iterative reconstruction algorithms can be applied to cardiac CT data, and they can reduce image noise to allow for improved image quality and/or reduced radiation dose.[11,12]

Table 2 – Kappa index of agreement stratified by patients with BMI less than or equal to 25 and above 25.

Kappa index	Agreement for BMI ≤ 25	Agreement for BMI > 25
120 kV FBP vs 100 kV FBP	95.2% (kappa 0.92)	88.2% (kappa 0.83)
120 kV FBP vs 100 kV iDose 6	98.8% (kappa 0.97)	90.8% (kappa 0.86)
120 kV FBP vs 100 kV IMR	94.9% (kappa 0.91)	93.1% (kappa 0.89)

BMI: body mass index; FBP: filtered back projection.

In the reconstruction process of CT images, attenuation data from a large number of projections are mathematically processed to create an image of the volume examined. FBP is the established method, resulting from a quick mathematical procedure. Before reconstruction, the data are filtered to achieve adequate balance between spatial resolution and noise. The limitations of FBP are revealed in low radiation dose acquisitions, where image quality can be compromised by high levels of noise and artifacts.[13] In recent years, these limitations have been circumvented by the introduction of iterative reconstruction methods,[7,3] which can remove noise from low-dose images using a variety of mathematical models.[14-16] Martin J. Willemink et al. performed a systematic literature review of 380 articles, observing that iterative reconstruction reduced noise and artifacts, and improved subjective and objective image quality compared to FBP at the same dose.[7,17]

International studies have shown that it is possible to reduce the effective radiation dose by up to 74% in determined CT scanners, maintaining the diagnostic accuracy of the calcium score. This reduction in radiation dose occurs by decreasing the tube voltage from 120 kV to 100 kV so that the quality of the CT image is maintained with the use of a new reconstruction method.[18,19]

In our study, we compared FBP with 2 methods of iterative reconstruction (iDose and IMR), and we observed that it is possible to perform the calcium score with a lower radiation dose, using modern reconstruction techniques. There was a 43% reduction in radiation dose between acquisitions from the voltage of 120 kV to 100 kV.

In relation to diagnostic quality, there was high agreement (kappa test above 0.9) between the CAC values obtained by the traditional method (120 kV with FBP) and the values obtained by the tested method, both for 100 kV with iDose 6 and for 100 kV with IMR 1, demonstrating the maintenance of clinical applicability of CAC, even when acquired with lower radiation doses.

The Bland-Altman plots demonstrated that, in general, there is an overestimation of the value of CAC when calculated using acquisitions of 100 kV. The difference between the means was smaller when IMR 1 reconstruction was used, ranging from −11.5 (120 kV with IMR 1) to −57.1 (120 kV with FBP). Furthermore, we observed that, in all comparisons, the lower the CAC, the smaller the difference; and the higher the CAC, the greater the dispersion. Therefore, acquisition with 100 kV and IMR reconstruction proved to be the most suitable for clinical application.

A limitation of the study was the occurrence of the COVID-19 pandemic during the inclusion of individuals, which limited the sample size. Studies carried out with a larger sample can help confirm these results.

Conclusion

Acquiring the calcium score with a voltage of 100 kV significantly reduced the radiation dose. When using the IMR 1 iterative reconstruction in the acquisition with 100 kV, it maintained high agreement and slight overestimation of

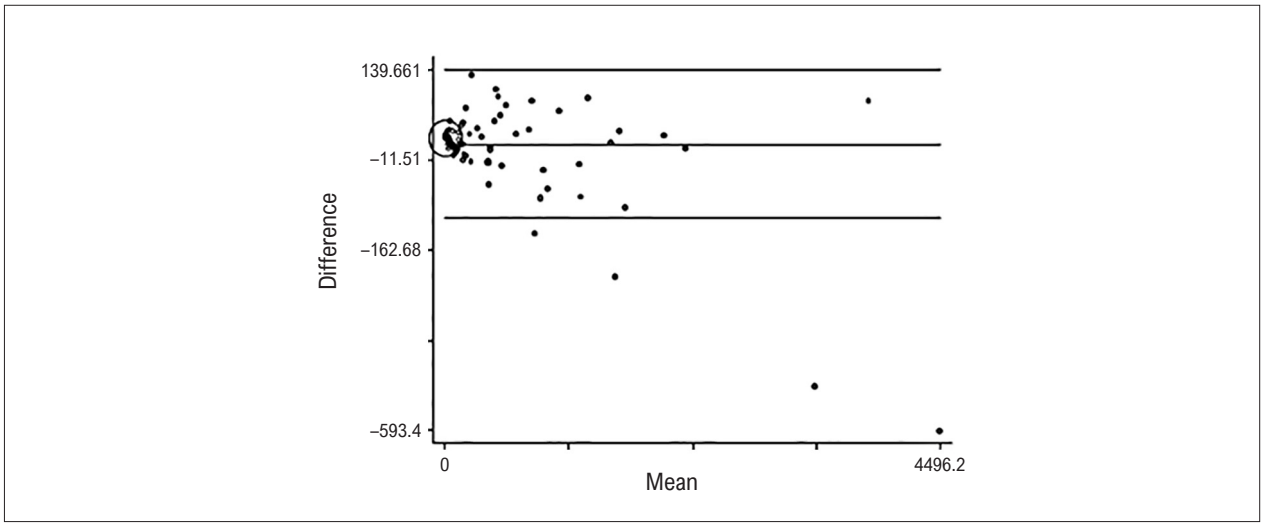

Figure 1 – *Bland-Altman plot comparing calcium scores obtained with 120 kV and FBP reconstruction versus 100 kV and IMR 1 reconstruction*

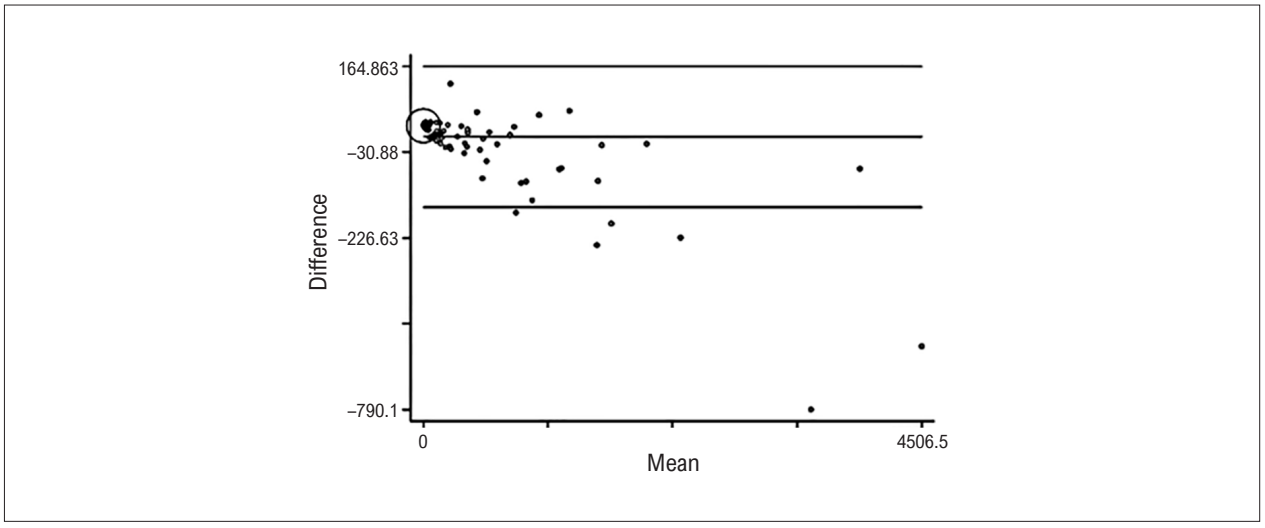

Figure 2 – *Bland-Altman plot comparing calcium scores obtained with 120 kV and FBP reconstruction versus 100 kV and iDose 6 reconstruction*

the results when compared to the acquisition with 120 kV and traditional FBP reconstruction.

Author Contributions

Conception and design of the research, Statistical analysis, Analysis and interpretation of the data, Critical revision of the manuscript for intellectual content: Carnaval DR, Silva MMF, Cerci RJ; obtenção de dados: Liebl A, Sartori BM, Couto CNM, Silva GBG, Vazzoler IGB, Medeiros VM; writing of the manuscript: Liebl A, Sartori BM, Couto CNM, Carnaval DR, Silva GBG, Vazzoler IGB, Cerci RJ, Medeiros VM.

Potential Conflict of Interest

No potential conflict of interest relevant to this article was reported.

Sources of Funding

There were no external funding sources for this study.

Study Association

This study is not associated with any thesis or dissertation work.

Ethics Approval and Consent to Participate

This study was approved by the Ethics Committee of the Hospital de Clínicas da Universidade Federal do Paraná under the protocol number 20501119.5.0000.0096. All the procedures in this study were in accordance with the 1975 Helsinki Declaration, updated in 2013. Informed consent was obtained from all participants included in the study.

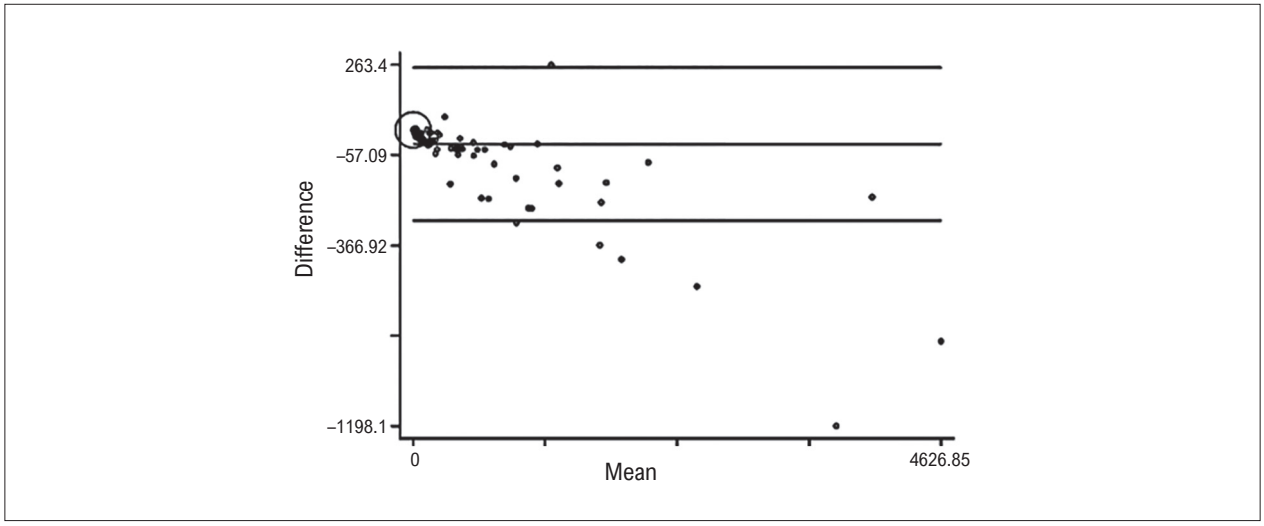

Figure 3 – *Bland-Altman plot comparing calcium scores obtained with 120 kV and FBP reconstruction versus 100 kV and FBP reconstruction*

References

1. Azevedo CF, Rochitte CE, Lima JA. Coronary Artery Calcium Score and Coronary Computed Tomographic Angiography for Cardiovascular Risk Stratification. Arq Bras Cardiol. 2012;98(6):559-68. doi: 10.1590/s0066-782x2012000600012.
2. Leyton F, Canevaro L, Dourado A, Castello H, Bacelar A, Navarro MT, et al. Riscos da radiação X e a Importância da proteção Radiológica na Cardiologia Intervencionista: Uma Revisão Sistemática. Rev Bras Cardiol Invasiva. 2014;22(1):87-98. doi: 10.1590/0104-1843000000015.
3. Abbara S. SCCT Guidelines on Radiation Dose and Dose-Optimization Strategies in Cardiovascular CT. Yearb Diagnostic Radiol. 2012;2012:233. doi: 10.1016/j.yrad.2012.03.023.
4. Sara L, Szarf G, Tachibana A, Shiozaki AA, Villa AV, Oliveira AC, et al. II Guidelines on Cardiovascular Magnetic Resonance and Computed Tomography of the Brazilian Society of Cardiology and the Brazilian College of Radiology. Arq Bras Cardiol. 2014;103(6 Suppl 3):1-86. doi: 10.5935/abc.2014S006.
5. Schoenhagen P, Tuzcu EM. Métodos por Imagem da Aterosclerose em Estudos de Progressão/Regressão: Marcador Substituto ou Janela Direta para o Processor Patológico da Aterosclerose? Arq Bras Cardiol. 2008;91(6):385-398. doi: 10.1590/S0066-782X2008001800010.
6. Neves P, Andrade J, Monção H. Escore de Cálcio Coronariano: Estado Atual. Radiol Bras. 2017;50(3):182-9. doi: 10.1590/0100-3984.2015.0235.
7. Willemink MJ, Leiner T, de Jong PA, de Heer LM, Nievelstein RA, Schilham AM, et al. Iterative Reconstruction Techniques for Computed Tomography Part 2: Initial Results in Dose Reduction and Image Quality. Eur Radiol. 2013;23(6):1632-42. doi: 10.1007/s00330-012-2764-z.
8. Renker M, Ramachandra A, Schoepf UJ, Raupach R, Apfaltrer P, Rowe GW, et al. Iterative Image Reconstruction Techniques: Applications for Cardiac CT. J Cardiovasc Comput Tomogr. 2011;5(4):225-30. doi: 10.1016/j.jcct.2011.05.002.
9. Barros MVL, Rabelo DR, Nunes MCP, Silva EC, Villamagna AR, Cardoso JMB, et al. Escore de Cálcio na Predição de Eventos Adversos em Pacientes com Suspeita de Doença Coronariana. Arq Bras Cardiol - Imagem Cardiovascular. 2014;27(3):191-6. doi: 0.5935/2318-8219.20140021.
10. Saint'Yves TLA, Travassos PCB, Gonçalves EAS, Mecca FA, Silveira TB. Otimização da Relação Dose x Ruído na Imagem em Protocolos de Tomografia Computadorizada de Crânio Pediátrico. Rev Bras Física Médica. 2010;4(1):11-4. doi: 10.29384/rbfm.2010.v4.n1.p11-14.
11. Rodrigues MA, Williams MC, Fitzgerald T, Connell M, Weir NW, Newby DE, et al. Iterative Reconstruction Can Permit the Use of Lower X-Ray Tube Current in CT Coronary Artery Calcium Scoring. Br J Radiol. 2016;89(1064):20150780. doi: 10.1259/bjr.20150780.
12. Maxfield MW, Schuster KM, McGillicuddy EA, Young CJ, Ghita M, Bokhari SA, et al. Impact of Adaptive Statistical Iterative Reconstruction on Radiation Dose in Evaluation of Trauma Patients. J Trauma Acute Care Surg. 2012;73(6):1406-11. doi: 10.1097/TA.0b013e318270d2fb.
13. Lança L. Potencial de Redução de Dose em Tomografia Computorizada com Técnicas de Reconstrução Iterativa. Proceedings of the 5th Congresso Nacional e 2nd Intercâmbio Internacional dos Profissionais das Técnicas Radiológicas. 2015 Oct 30-Nov 1. Brasília: Conter; 2015.
14. Juri H, Matsuki M, Itou Y, Inada Y, Nakai G, Azuma H, et al. Initial Experience with Adaptive Iterative Dose Reduction 3D to Reduce Radiation Dose in Computed Tomographic Urography. J Comput Assist Tomogr. 2013;37(1):52-7. doi: 10.1097/RCT.0b013e3182742c0e.
15. Chen MY, Steigner ML, Leung SW, Kumamaru KK, Schultz K, Mather RT, et al. Simulated 50 % Radiation Dose Reduction in Coronary CT Angiography Using Adaptive Iterative Dose Reduction in Three-Dimensions (AIDR3D). Int J Cardiovasc Imaging. 2013;29(5):1167-75. doi: 10.1007/s10554-013-0190-1.
16. Kurata A, Dharampal A, Dedic A, de Feyter PJ, Krestin GP, Dijkshoorn ML, et al. Impact of Iterative Reconstruction on CT Coronary Calcium Quantification. Eur Radiol. 2013;23(12):3246-52. doi: 10.1007/s00330-013-3022-8.
17. Dalmazo J, Elias J Jr, Brocchi MAC, Costa PR, Azevedo-Marques PM. Otimização da Dose em Exames de Rotina em Tomografia Computadorizada: Estudo de Viabilidade em um Hospital Universitário. Radiol Bras. 2010;43(4):241-8. doi: 10.1590/S0100-39842010000400008.
18. Tatsugami F, Higaki T, Fukumoto W, Kaichi Y, Fujioka C, Kiguchi M, et al. Radiation Dose Reduction for Coronary Artery Calcium Scoring at 320-Detector CT with Adaptive Iterative Dose Reduction 3D. Int J Cardiovasc Imaging. 2015;31(5):1045-52. doi: 10.1007/s10554-015-0637-7.
19. Choi AD, Leifer ES, Yu J, Shanbhag SM, Bronson K, Arai AE, et al. Prospective Evaluation of the Influence of Iterative Reconstruction on the Reproducibility of Coronary Calcium Quantification in Reduced Radiation Dose 320 Detector Row CT. J Cardiovasc Comput Tomogr. 2016;10(5):359-63. doi: 10.1016/j.jcct.2016.07.016.

My Approach to Myocardial Work: Why and for Whom?

Rodolfo de Paula Lustosa,[1,2,3] *Arnaldo Rabischoffsky,*[2,4] *Eliza de Almeida Gripp*[4,5]

Hospital Copastar,[1] *Rio de Janeiro, RJ – Brazil*
Hospital Américas Medical City,[2] *Rio de Janeiro, RJ – Brazil*
Hospital Quinta D'Or,[3] *Rio de Janeiro, RJ – Brazil*
Hospital Pró-Cardíaco,[4] *Rio de Janeiro, RJ – Brazil*
Hospital Universitário Antônio Pedro (UFF),[5] *Rio de Janeiro, RJ – Brazil*

Central Illustration: My Approach to Myocardial Work: Why and for Whom?

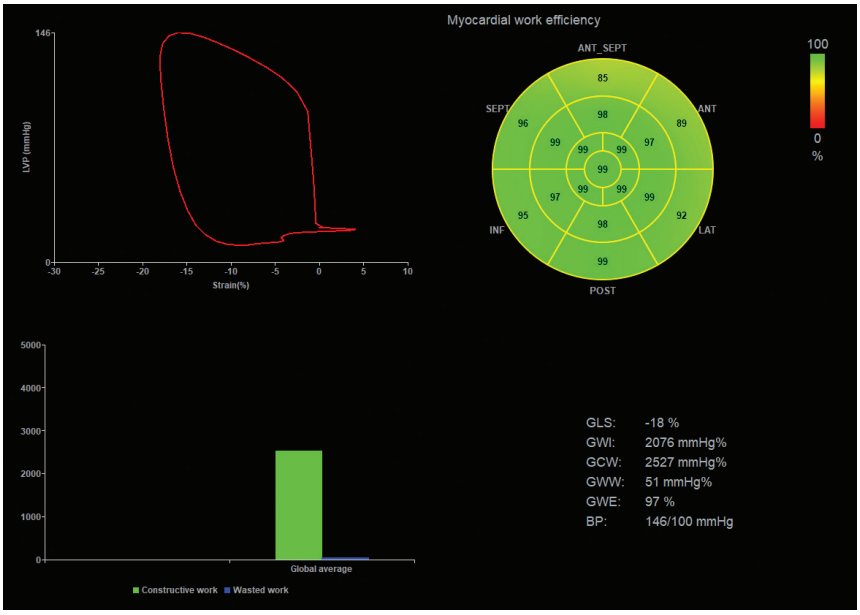

Arq Bras Cardiol: Imagem cardiovasc. 2023;36(3):e20230052

Calculation of left ventricular GWE, in a 17-segment model showing GWE segmental values. Preserved segmental GWE values are shown in green and expressed in %. The patient's GWI, GCW, GWW, GWE, and blood pressure values are shown in white. GCW: global constructive work; GWE: global work efficiency; GWI: global work index; GWW: global wasted work (Source: Author).

Abstract

The emergence of a new noninvasive tool known as myocardial work (MW) for assessing ventricular function, which is independent of load conditions, has been fundamental in advancing current imaging methods, such as myocardial strain. Strain is considered a sensitive technique in the detection of subclinical dysfunction, even though it is still dependent on load conditions, making it impossible to differentiate contractile alteration from interference caused by increased afterload alone. This new technology incorporated into myocardial strain will increase the sensitivity of the method.

Introduction

The concept of pressure-volume curves has been widely used in cardiovascular physiology and assessment of cardiac function.[1-3] Experimental studies have demonstrated that it is possible to assess the global performance of the ventricles by means of a contractility index that is independent of load conditions. This concept has not yet become the "gold standard" in clinical practice and research, because invasive techniques are still required to determine these curves. However, studies have shown that the noninvasive estimation

Mailing Address: Rodolfo de Paula Lustosa •
Américas Medical City, Ecocardiografia. Av Jorge Curi, 550. Postal code: 22275-001. Rio de Janeiro, RJ - Brazil
E-mail: rodolfolustosarj@gmail.com
Manuscript received June 2, 2023; revised manuscript June 2, 2023; accepted June 2, 2023
Editor responsible for the review: Daniela do Carmo Rassi Frota

DOI: https://doi.org/10.36660/abcimg.20230052i

Contents

of these curves is a strong predictor of events regardless of left ventricular ejection fraction (LVEF), as demonstrated in the study by Spevack et al.[4]

My approach

According to the same principle as pressure-volume curves, the concept of noninvasive evaluation of myocardial work (MW) was published by Russell et al. in 2012.[5] According to the authors, the determination of pressure-strain loop area by means of Doppler echocardiography would reflect MW and oxygen consumption. Currently, the calculation of MW by Doppler echocardiography is performed using commercially available software (EchoPac, GE Medical Systems). MW indices are estimated by combining noninvasive estimation of peak left ventricular (LV) pressure using blood pressure measurements with a sphygmomanometer (in which peak LV systolic pressure is assumed to be equal to systolic arterial pressure) associated with echocardiographic data from strain curves.

After calculating the strain and inserting the blood pressure values obtained by sphygmomanometer, the opening and closing times of the aortic and mitral valves are identified by echocardiogram in the apical 3-chamber view. A LV pressure-strain curve is then constructed with strain data from the entire cardiac cycle, according to the duration of relaxation and isovolumetric contraction, the ejection and filling phases defined by the opening and closing times of the aortic and mitral valves, and blood pressure values.[6]

LV work is calculated as a product of the segmental shortening rate and the instantaneous LV pressure. The following indices are derived from measurements of cardiac work by echocardiography (Central Figure):

Global work index (GWI): total work calculated from mitral valve closure to mitral valve opening, representing the area of the loop provided by the software (expressed in mmHg%);

Global constructive work (GCW): work performed by a segment during systolic shortening added to work performed during diastolic lengthening, representing the work that contributes to myocardial contractility (expressed in mmHg%);

Global wasted work (GWW): negative work performed by a segment during lengthening in systole added to the work performed during shortening in diastole, which represents the work that does not contribute to myocardial contractility (expressed in mmHg%);

Global work efficiency (GWE): GCW divided by the sum of GCW and GWW, representing the measure of LV performance (expressed in %).

The mean reported normal values[7] for GWI and GCW are 2010 mmHg% (95% confidence interval [CI]: 1907 to 2113 mmHg%) and 2278 mmHg% (95% CI: 2186 to 2369 mmHg%), respectively. The mean for GWW is 80 mmHg% (95% CI: 73 to 87 mmHg%), and for GWE it is 96% (95% CI: 96% to 96%). The differences between men and women significantly contribute to the normal ranges for GWI, GWW and GWE.

Applicability

Ischemic heart disease

The use of MW in coronary artery disease can be divided into the context of acute coronary syndromes and chronic coronary artery disease. Moreover, global values are relevant, as are regional values derived from the software. In patients with acute ST-segment elevation myocardial infarction (STEMI), the study by El Mahdiui et al.[8] provided evidence that GWE was reduced in patients with heart failure with reduced ejection fraction (HFrEF) after STEMI, compared to healthy individuals and those with risk factors for cardiovascular disease. A study by Lustosa et al.[9] demonstrated, in a cohort of 600 patients after STEMI, that cardiac work indices were reduced 3 months after the index event in patients who had ventricular remodeling. The same author demonstrated that reduced GWE values (< 86%) measured by transthoracic Doppler echocardiography in the first 48 hours of STEMI admission would be associated with worse prognosis.[10] The study by Meimoun et al.[11] demonstrated that, in patients with STEMI previously treated with percutaneous coronary intervention, GCW was an independent factor for global and segmental LV recovery, and it was significantly reduced in patients who had in-hospital complications.

In the context of regional assessment of MW, the study by Boe et al.[12] demonstrated that the presence of reduced regional GWI values could identify coronary occlusion in patients with acute non-ST-segment elevation myocardial infarction (NSTEMI). A study by Lustosa et al.,[13] using regional GWI values, demonstrated that reduced regional GWI values in the territory of the culprit artery were independently associated with early cardiac remodeling.

MW has also been studied in chronic coronary artery disease. A study by Edwards et al.[14] evaluated 115 patients with normal LVEF referred for coronary angiography due to different indications and demonstrated that GWI values less than 1810 mmHg% were predictive of significant coronary artery disease (defined by stenosis above 70%), with a sensitivity of 92% and specificity of 51%. A study by Borrie et al.[15] demonstrated that MW indices can be used in stress echocardiography to identify myocardial ischemia.

Cardiomyopathies

The main role of MW analysis in clinical practice for evaluating patients with cardiomyopathies focuses on patients with dilated cardiomyopathy (DCM), hypertrophic cardiomyopathy (HCM), and cardiac amyloidosis. The study by Chan et al.[16] observed the difference between MW indices in patients with hypertension and DCM (19 non-ischemic and 10 ischemic). The authors reported that GWI, GCW, and GWE were significantly reduced, and GWW was significantly increased in patients with DCM compared to the control group. A study by Schrub et al.[17] investigated the relationship between MW analysis and exercise tolerance in 51 patients with DCM who underwent a cardiopulmonary exercise test to assess exercise performance and reported that, in patients with DCM and intraventricular dyssynchrony, septal work efficiency was the only predictor of exercise capacity in the

multivariate analysis (β = 0.68, p = 0.03). A study by Cui et al.[18] compared MW indices in 30 patients with DCM and 30 healthy patients, finding significantly reduced values of MW indices in the DCM group compared to the control group (p < 0.05).

In 2019, Galli et al.[19] studied 82 patients with non-obstructive HCM who underwent MW assessment. Patients also underwent cardiac magnetic resonance imaging to estimate LV fibrosis with delayed gadolinium enhancement. The authors reported that GCW is significantly reduced in patients with HCM and normal LVEF, and a cutoff value of 1623 mmHg% demonstrated a sensitivity of 82% and specificity of 67% to predict LV fibrosis in this population (area under the curve [AUC] 0.80, 95% CI: 0.66 to 0.93, p < 0.001). A study by Hiemstra et al.[20] reported the prognostic role of MW analysis in 110 patients with non-obstructive HCM. Patients with GCW > 1730 mmHg% had better survival compared to those with GCW < 1730 mmHg% (log-rank 11.2, p = 0.001).

The value of the clinical application of MW indices in patients with cardiac amyloidosis has been reported by Clemmensen et al.[21] The authors' objective was to characterize resting and peak MW during exercise in patients with cardiac amyloidosis. They observed that patients with cardiac amyloidosis showed significantly reduced MW index values, and this difference was more evident during exercise compared to healthy subjects. In another study, the prognostic implications of MW analysis were demonstrated in 100 patients with cardiac amyloidosis.[22] Patients with GWI < 1043 mmHg% had a higher number of events than patients with GWI > 1043 mmHg% (hazard ratio [HR] 2.3, 95% CI: 1.2 to 4.3, p = 0.01). Furthermore, patients with GWI < 1039 mmHg% had a higher risk of all-cause mortality than patients with GWI > 1039 mmHg% (HR 2.6, 95% CI: 1.2 to 5.5, p < 0.05).

HFrEF and response to cardiac resynchronization therapy (CRT)

The first reports in clinical practice on the application of MW in patients with HFrEF were published in 2013. In an experimental study, Russell et al.[23] evaluated the WW ratio (WWR) in 6 anesthetized dogs with left bundle branch block (LBBB) and 28 patients with cardiomyopathy, including patients with LBBB and CRT. The study demonstrated a strong correlation between invasively and noninvasively estimated WWR in dogs (r = 0.94) and patients (r = 0.96), with higher global WWR values in patients with LBBB. The study by Galli et al.[24] estimated GCW and GWW in 97 patients before CRT and at 6-month follow-up. The authors showed that the addition of GCW > 1057 mmHg% and GWW > 384 mmHg% to a baseline model significantly increased the model's power to identify CRT responders. The authors reported good specificity (100%) and positive predictive value (100%), but low sensitivity (22%), negative predictive value (41%), and accuracy (49%). In another study,[25] the authors also showed, in 97 patients undergoing CRT implantation, that GCW > 1057 mmHg% (odds ratio [OR] 14.69, p = 0.005) and septal flash (OR 8.05, p = 0.004) were the only predictors of response to CRT. The study by Cvijic et al.[26] calculated segmental MW in 26 patients with sinus rhythm and non-ischemic cardiomyopathy. Before CRT, work was unevenly distributed with reduced work in the septal and anteroseptal walls and increased work in the lateral and posterior walls (p < 0.001). The authors showed that, after CRT, the segmental distribution of work was uniform. MW asymmetry between the septal segments and the lateral wall was also observed in a prospective multicenter study with 200 patients.[27] The authors showed that the lateral wall-septum work difference predicted the CRT response with an AUC of 0.77 (95% CI: 0.70 to 0.84); when combined with assessment of septal viability by cardiac magnetic resonance, the AUC increased to 0.88 (95% CI: 0.81 to 0.95). The prognostic importance of calculating MW in patients with heart failure was demonstrated by Van der Bijl et al.[28] in a cohort of patients with class I indications for CRT. The authors demonstrated that patients with lower energy efficiency (GWE < 75%) before CRT demonstrated a lower rate of events than patients with higher energy efficiency (GWE > 75%). Bouali et al.[29] investigated the effects of treatment with sacubitril/valsartan on MW indices in 79 patients with HFrEF and reported that the treatment significantly increased GCW (1023 ± 449 mmHg% to 1424 ± 484 mmHg%, p < 0.001) and GWE (87% [78% to 90%] to 90% [86% to 95%], p < 0.001). GCW was the only predictor of major adverse cardiovascular events (HR 0.99, 95% CI: 0.99 to 1.00, p = 0.04). Furthermore, GCW < 910 mmHg% was related to a high risk of major adverse cardiovascular events (HR 11.09, 95% CI: 1.45 to 98.94, p = 0.002, log-rank test p < 0.001). Another study by Wang et al.[30] investigated a cohort of 508 patients (62.9 ± 15.8 years, 29.1% women) with LVEF ≤ 40%. The authors showed that GWI < 750 mmHg% was associated with significantly higher mortality and heart failure hospitalization and significantly higher all-cause death (HR 3.33, 95% CI: 2.31 to 4.80) than in patients with GWI ≥ 750 mmHg%. Regarding observations from these studies, MW analysis in patients with HFrEF may be valuable to identify CRT responders and provide prognostic information in this population.

The assessment of MW indices in heart failure with preserved ejection fraction (HFpEF) was reported in 2019 by Przewlocka-Kosmala et al.[31] In the STRUCTURE (Spironolactone in Myocardial Dysfunction with Reduced Exercise Capacity) study, with 57 patients randomized to spironolactone and 57 to placebo, the authors measured MW indices at rest and immediately after exercise at baseline and at 6-month follow-up and reported GCW as a better determinant of exercise capacity than strain in HFpEF.

Valve disease

Previous studies have also explored the clinical application of MW analysis in valve disease. Hubert et al.[32] studied LV mechanics using MW analysis in 37 patients with heart failure and important functional mitral regurgitation who underwent percutaneous mitral valve repair, compared with 19 patients with functional mitral regurgitation in optimal clinical treatment. The authors reported that GCW significantly improved in both groups and demonstrated that GWI identifies patients with worse evolution (AUC = 0.882, p = 0.009), mainly patients with GWI < 482 mmHg%. Papadopoulos et al.[33] investigated echocardiographic predictors of clinical

response and LV reverse remodeling in 86 patients with severe functional mitral regurgitation and high surgical risk, including MW indices. The authors reported that baseline GWI and GCW were associated with a reduction in LV end-diastolic volume 1 year after the MitraClip intervention, and GCW was the only variable associated with a reduction in LV end-systolic volume. The MitraClip procedure was associated with significant improvement in GWI ($p = 0.045$) and GCW ($p < 0.001$). Yedidya et al.[34] evaluated the prognostic impact of MW indices in functional mitral regurgitation. In 143 patients with functional mitral regurgitation, worse GWI and GCW values and better GWW and GWE values independently reflected worse prognosis in this population.

Jain et al.[35] explored the relationship between severe aortic stenosis and MW analysis in a cohort of 35 patients undergoing transcatheter aortic valve replacement (TAVR). The authors evaluated MW indices in severe aortic stenosis with the addition of the mean aortic gradient to noninvasive systolic blood pressure. Based on this method, which showed a high correlation ($r = 0.92$), the authors demonstrated that GWI reduced between the pre-TAVR and post-TAVR periods (1856.2 mmHg% ± 704.6 versus 1534.8 mmHg% ± 385). The study by Fortuni et al.[36] used the same calculation of MW indices in severe aortic stenosis that were shown to be independently associated with symptoms of heart failure. D'Andrea et al.[37] recruited 115 asymptomatic patients with severe aortic insufficiency and 55 controls. GWE was significantly reduced in patients with aortic insufficiency compared to controls (87.1% ± 3.3% versus 94.4% ± 4.1%, $p < 0.01$), and strain and GWE were strong independent predictors of contractile reserve, suggesting early subclinical damage in this population. In a recent review by Muthukumar et al.[38] on the association between malignant mitral valve prolapse and sudden cardiac death, the authors reported that patients with mitral valve prolapse and mitral annulus disjunction had higher MW regional index values in the posterolateral region of LV segments, suggesting the hypothesis that more work due to repeated traction causes greater energy demand and stress in these segments.

Limitations and future directions

As with any new technology, MW needs to be disseminated for widespread knowledge of the protocol, with a learning curve and improved expertise. New software that has come to replace the invasive gold-standard method is the objective that researchers always seek to reduce the complications inherent to invasive methods, in this case, cardiac catheterization. For the time being, there is only one software product available from a single company.

The technical limitations are mostly related to the classic limitations of strain. For example, it requires an adequate acoustic window and frame rate, absence of tachycardia, and regular rhythm. Regarding blood pressure measurements, they need to be taken correctly, and patients with aortic stenosis or fixed LV outflow tract obstruction should be excluded, as noninvasively measured systolic pressure is not equivalent to invasive measurement. Blood pressure measurement needs to be adequate.

Moreover, MW is not useful for evaluating cases with important cardiac remodeling. It is a promising technique still under development.

Conclusion

The development of new software associated with strain that presents good sensitivity and specificity, inserting only blood pressure measurements in a noninvasive manner will be important in the assessment of subclinical alterations that ejection fraction is not able to detect, assisting in the early treatment of several diseases that affect the myocardium, such as infiltrative, valvular, and ischemic diseases, thus changing their prognosis.

Author Contributions

Conception and design of the research, writing of the manuscript and critical revision of the manuscript for intellectual content: Lustosa RP, Rabischoffsky A, Gripp EA.

Potential Conflict of Interest

No potential conflict of interest relevant to this article was reported.

Sources of Funding

There were no external funding sources for this study.

Study Association

This study is not associated with any thesis or dissertation work.

Ethics Approval and Consent to Participate

This article does not contain any studies with human participants or animals performed by any of the authors.

Referências

1. Suga H, Sagawa K, Kostiuk DP. Controls of Ventricular Contractility Assessed by Pressure-Volume Ration, Emax. Cardiovasc Res. 1976;10(5):582-92. doi: 10.1093/cvr/10.5.582.
2. Sagawa K, Suga H, Shoukas AA, Bakalar KM. End-Systolic Pressure/Volume Ratio: A New Index of Ventricular Contractility. Am J Cardiol. 1977;40(5):748-53. doi: 10.1016/0002-9149(77)90192-8.
3. Suga H, Sagawa K, Shoukas AA. Load Independence of the Instantaneous Pressure-Volume Ratio of the Canine Left Ventricle and Effects of Epinephrine and Heart Rate on the Ratio. Circ Res. 1973;32(3):314-22. doi: 10.1161/01.res.32.3.314.
4. Spevack DM, Karl J, Yedlapati N, Goldberg Y, Garcia MJ. Echocardiographic Left Ventricular End-Diastolic Pressure Volume Loop Estimate Predicts

Survival in Congestive Heart Failure. J Card Fail. 2013;19(4):251-9. doi: 10.1016/j.cardfail.2013.02.003.

5. Russell K, Eriksen M, Aaberge L, Wilhelmsen N, Skulstad H, Remme EW, et al. A Novel Clinical Method for Quantification of Regional Left Ventricular Pressure-Strain Loop Area: A Non-Invasive Index of Myocardial Work. Eur Heart J. 2012;33(6):724-33. doi: 10.1093/eurheartj/ehs016.

6. van der Bijl P, Kostyukevich M, El Mahdiui M, Hansen G, Samset E, Marsan NA, et al. A Roadmap to Assess Myocardial Work: From Theory to Clinical Practice. JACC Cardiovasc Imaging. 2019;12(12):2549-54. doi: 10.1016/j.jcmg.2019.05.028.

7. Truong VT, Vo HQ, Ngo TNM, Mazur J, Nguyen TTH, Pham TTM, et al. Normal Ranges of Global Left Ventricular Myocardial Work Indices in Adults: A Meta-Analysis. J Am Soc Echocardiogr. 2022;35(4):369-377.e8. doi: 10.1016/j.echo.2021.11.010.

8. El Mahdiui M, van der Bijl P, Abou R, Marsan NA, Delgado V, Bax JJ. Global Left Ventricular Myocardial Work Efficiency in Healthy Individuals and Patients with Cardiovascular Disease. J Am Soc Echocardiogr. 2019;32(9):1120-27. doi: 10.1016/j.echo.2019.05.002.

9. Lustosa RP, van der Bijl P, El Mahdiui M, Montero-Cabezas JM, Kostyukevich MV, Marsan NA, et al. Noninvasive Myocardial Work Indices 3 Months after ST-Segment Elevation Myocardial Infarction: Prevalence and Characteristics of Patients with Postinfarction Cardiac Remodeling. J Am Soc Echocardiogr. 2020;33(10):1172-79. doi: 10.1016/j.echo.2020.05.001.

10. Lustosa RP, Butcher SC, van der Bijl P, El Mahdiui M, Montero-Cabezas JM, Kostyukevich MV, et al. Global Left Ventricular Myocardial Work Efficiency and Long-Term Prognosis in Patients after ST-Segment-Elevation Myocardial Infarction. Circ Cardiovasc Imaging. 2021;14(3):e012072. doi: 10.1161/CIRCIMAGING.120.012072.

11. Meimoun P, Abdani S, Stracchi V, Elmkies F, Boulanger J, Botoro T, et al. Usefulness of Noninvasive Myocardial Work to Predict Left Ventricular Recovery and Acute Complications after Acute Anterior Myocardial Infarction Treated by Percutaneous Coronary Intervention. J Am Soc Echocardiogr. 2020;33(10):1180-90. doi: 10.1016/j.echo.2020.07.008.

12. Boe E, Russell K, Eek C, Eriksen M, Remme EW, Smiseth OA, et al. Non-Invasive Myocardial Work Index Identifies Acute Coronary Occlusion in Patients with Non-ST-Segment Elevation-Acute Coronary Syndrome. Eur Heart J Cardiovasc Imaging. 2015;16(11):1247-55. doi: 10.1093/ehjci/jev078.

13. Lustosa RP, Fortuni F, van der Bijl P, Goedemans L, El Mahdiui M, Montero-Cabezas JM, et al. Left Ventricular Myocardial Work in the Culprit Vessel Territory and Impact on Left Ventricular Remodelling in Patients with ST-Segment Elevation Myocardial Infarction after Primary Percutaneous Coronary Intervention. Eur Heart J Cardiovasc Imaging. 2021;22(3):339-47. doi: 10.1093/ehjci/jeaa175.

14. Edwards NFA, Scalia GM, Shiino K, Sabapathy S, Anderson B, Chamberlain R, et al. Global Myocardial Work Is Superior to Global Longitudinal Strain to Predict Significant Coronary Artery Disease in Patients with Normal Left Ventricular Function and Wall Motion. J Am Soc Echocardiogr. 2019;32(8):947-57. doi: 10.1016/j.echo.2019.02.014.

15. Borrie A, Goggin C, Ershad S, Robinson W, Sasse A. Noninvasive Myocardial Work Index: Characterizing the Normal and Ischemic Response to Exercise. J Am Soc Echocardiogr. 2020;33(10):1191-200. doi: 10.1016/j.echo.2020.05.003.

16. Chan J, Edwards NFA, Khandheria BK, Shiino K, Sabapathy S, Anderson B, et al. A New Approach to Assess Myocardial Work by Non-Invasive Left Ventricular Pressure-Strain Relations in Hypertension and Dilated Cardiomyopathy. Eur Heart J Cardiovasc Imaging. 2019;20(1):31-9. doi: 10.1093/ehjci/jey131.

17. Schrub F, Schnell F, Donal E, Galli E. Myocardial Work is a Predictor of Exercise Tolerance in Patients with Dilated Cardiomyopathy and Left Ventricular Dyssynchrony. Int J Cardiovasc Imaging. 2020;36(1):45-53. doi: 10.1007/s10554-019-01689-4.

18. Cui C, Liu L, Li Y, Liu Y, Huang D, Hu Y, et al. Left Ventricular Pressure-Strain Loop-Based Quantitative Examination of the Global and Regional Myocardial Work of Patients with Dilated Cardiomyopathy. Ultrasound Med Biol. 2020;46(10):2834-45. doi: 10.1016/j.ultrasmedbio.2020.06.008.

19. Galli E, Vitel E, Schnell F, Le Rolle V, Hubert A, Lederlin M, et al. Myocardial Constructive Work is Impaired in Hypertrophic Cardiomyopathy and Predicts Left Ventricular Fibrosis. Echocardiography. 2019;36(1):74-82. doi: 10.1111/echo.14210.

20. Hiemstra YL, van der Bijl P, El Mahdiui M, Bax JJ, Delgado V, Marsan NA. Myocardial Work in Nonobstructive Hypertrophic Cardiomyopathy: Implications for Outcome. J Am Soc Echocardiogr. 2020;33(10):1201-8. doi: 10.1016/j.echo.2020.05.010.

21. Clemmensen TS, Eiskjær H, Mikkelsen F, Granstam SO, Flachskampf FA, Sørensen J, et al. Left Ventricular Pressure-Strain-Derived Myocardial Work at Rest and during Exercise in Patients with Cardiac Amyloidosis. J Am Soc Echocardiogr. 2020;33(5):573-82. doi: 10.1016/j.echo.2019.11.018.

22. Clemmensen TS, Eiskjær H, Ladefoged B, Mikkelsen F, Sørensen J, Granstam SO, et al. Prognostic Implications of Left Ventricular Myocardial Work Indices in Cardiac Amyloidosis. Eur Heart J Cardiovasc Imaging. 2021;22(6):695-704. doi: 10.1093/ehjci/jeaa097.

23. Russell K, Eriksen M, Aaberge L, Wilhelmsen N, Skulstad H, Gjesdal O, et al. Assessment of Wasted Myocardial Work: A Novel Method to Quantify Energy Loss Due To Uncoordinated Left Ventricular Contractions. Am J Physiol Heart Circ Physiol. 2013;305(7):H996-1003. doi: 10.1152/ajpheart.00191.2013.

24. Galli E, Leclercq C, Fournet M, Hubert A, Bernard A, Smiseth OA, et al. Value of Myocardial Work Estimation in the Prediction of Response to Cardiac Resynchronization Therapy. J Am Soc Echocardiogr. 2018;31(2):220-30. doi: 10.1016/j.echo.2017.10.009.

25. Galli E, Leclercq C, Hubert A, Bernard A, Smiseth OA, Mabo P, et al. Role of Myocardial Constructive Work in the Identification of Responders to CRT. Eur Heart J Cardiovasc Imaging. 2018;19(9):1010-18. doi: 10.1093/ehjci/jex191.

26. Cvijic M, Duchenne J, Ünlü S, Michalski B, Aarones M, Winter S, et al. Timing of Myocardial Shortening Determines Left Ventricular Regional Myocardial Work and Regional Remodelling in Hearts with Conduction Delays. Eur Heart J Cardiovasc Imaging. 2018;19(8):941-49. doi: 10.1093/ehjci/jex325.

27. Aalen JM, Donal E, Larsen CK, Duchenne J, Lederlin M, Cvijic M, et al. Imaging Predictors of Response to Cardiac Resynchronization Therapy: Left Ventricular Work Asymmetry by Echocardiography and Septal Viability by Cardiac Magnetic Resonance. Eur Heart J. 2020;41(39):3813-23. doi: 10.1093/eurheartj/ehaa603.

28. van der Bijl P, Vo NM, Kostyukevich MV, Mertens B, Marsan NA, Delgado V, Bax JJ. Prognostic Implications of Global, Left Ventricular Myocardial Work Efficiency Before Cardiac Resynchronization Therapy. Eur Heart J Cardiovasc Imaging. 2019;20(12):1388-94. doi: 10.1093/ehjci/jez095.

29. Bouali Y, Donal E, Gallard A, Laurin C, Hubert A, Bidaut A, et al. Prognostic Usefulness of Myocardial Work in Patients with Heart Failure and Reduced Ejection Fraction Treated by Sacubitril/Valsartan. Am J Cardiol. 2020;125(12):1856-62. doi: 10.1016/j.amjcard.2020.03.031.

30. Wang CL, Chan YH, Wu VC, Lee HF, Hsiao FC, Chu PH. Incremental Prognostic Value of Global Myocardial Work Over Ejection Fraction and Global Longitudinal Strain in Patients with Heart Failure and Reduced Ejection Fraction. Eur Heart J Cardiovasc Imaging. 2021;22(3):348-56. doi: 10.1093/ehjci/jeaa162.

31. Przewlocka-Kosmala M, Marwick TH, Mysiak A, Kosowski W, Kosmala W. Usefulness of Myocardial Work Measurement in the Assessment of Left Ventricular Systolic Reserve Response to Spironolactone in Heart Failure with Preserved Ejection Fraction. Eur Heart J Cardiovasc Imaging. 2019;20(10):1138-46. doi: 10.1093/ehjci/jez027.

32. Hubert A, Galli E, Leurent G, Corbineau H, Auriane B, Guillaume L, et al. Left Ventricular Function after Correction of Mitral Regurgitation: Impact of the Clipping Approach. Echocardiography. 2019;36(11):2010-8. doi: 10.1111/echo.14523.

33. Papadopoulos K, Ikonomidis I, Chrissoheris M, Chalapas A, Kourkoveli P, Parissis J, et al. MitraClip and Left Ventricular Reverse Remodelling: A Strain Imaging Study. ESC Heart Fail. 2020;7(4):1409-18. doi: 10.1002/ehf2.12750.

34. Yedidya I, Lustosa RP, Fortuni F, van der Bijl P, Namazi F, Vo NM, et al. Prognostic Implications of Left Ventricular Myocardial Work Indices in Patients with Secondary Mitral Regurgitation. Circ Cardiovasc Imaging. 2021;14(9):e012142. doi: 10.1161/CIRCIMAGING.120.012142.

35. Jain R, Bajwa T, Roemer S, Huisheree H, Allaqaband SQ, Kroboth S, et al. Myocardial Work Assessment in Severe Aortic Stenosis Undergoing Transcatheter Aortic Valve Replacement. Eur Heart J Cardiovasc Imaging. 2021;22(6):715-21. doi: 10.1093/ehjci/jeaa257.

36. Fortuni F, Butcher SC, van der Kley F, Lustosa RP, Karalis I, de Weger A, et al. Left Ventricular Myocardial Work in Patients with Severe Aortic Stenosis. J Am Soc Echocardiogr. 2021;34(3):257-66. doi: 10.1016/j.echo.2020.10.014.

37. D'Andrea A, Sperlongano S, Formisano T, Tocci G, Cameli M, Tusa M, et al. Stress Echocardiography and Strain in Aortic Regurgitation (SESAR protocol): Left Ventricular Contractile Reserve and Myocardial Work in Asymptomatic Patients with Severe Aortic Regurgitation. Echocardiography. 2020;37(8):1213-21. doi: 10.1111/echo.14804.

38. Muthukumar L, Jahangir A, Jan MF, Moreno ACP, Khandheria BK, Tajik AJ. Association between Malignant Mitral Valve Prolapse and Sudden Cardiac Death: A Review. JAMA Cardiol. 2020;5(9):1053-61. doi: 10.1001/jamacardio.2020.1412.

Review Article

What do Cardiologists Expect from Imaging For Ischemic Heart Disease in Women

Maria Cristina Costa de Almeida,[1] Claudia Maria Vilas Freire,[2] Larissa Neto Espíndola,[3] Gláucia Maria Moraes de Oliveira[4]

Centro Universitário de Belo Horizonte (UNIBH),[1] Belo Horizonte, MG – Brazil

Universidade Federal de Minas Gerais,[2] Belo Horizonte, MG – Brazil

Hospital Municipal de Salvador,[3] Salvador, BA – Brazil

Universidade Federal do Rio de Janeiro,[4] Rio de Janeiro, RJ – Brazil

Abstract

Ischemic heart disease (IHD) is an important cause of morbidity and mortality in women and men. This paper emphasizes the differences of IHD in women, focusing on the diagnostic investigation in its stable phase.

The higher prevalence of atypical symptoms, anatomical differences, and adverse psychosocial aspects, in addition to the association of specific risk factors regarding obstetrical history, requires an accurate clinical assessment and a targeted diagnostic investigation that consider the limitations, as well as the positive and negative predictive values of the methods. Because of breast exposure, tests involving radiation should be reconsidered in selected cases.

It is worth emphasizing that non-cardiological tests often performed in women, such as mammography, provide an opportunity to assess CVR at early ages or even in patients with few traditional risk factors.

Complementary tests for microcirculation assessment should be used in cases of proven ischemia in the absence of obstructive coronary artery disease, which is known to be more frequent in women.

Introduction

Despite the worldwide reduction in mortality from cardiovascular diseases (CVDs) in women and men in the past ten years, unfavorable outcomes, such as higher in-hospital mortality rates from ischemic heart disease (IHD) following percutaneous and surgical interventions, are more frequent among women.

Anatomical and pathophysiological differences, such as smaller epicardial coronary arteries adjusted for body surface, lower coronary vasomotor tonus with functional changes even in the absence of obstructive coronary artery disease, and higher microcirculation dysfunction, could explain the different IHD phenotypes in women.[1,2] Figure 1 shows the relevant differences of IHD between women and men.

The IHD clinical manifestations and characteristics of the complementary diagnostic methods are different in women, with false-negative or false-positive results, misinterpretations, and, consequently, inappropriate women's IHD management and treatment.[2,3] It is essential to consider the peculiarities of noninvasive imaging tests related to the female sex, assessing the advantages and disadvantages of each diagnostic modality to increase the accuracy of the tests that will impact on the IHD treatment and prognosis.[1]

Cardiovascular risk (CVR) stratification

CVD remains the major cause of death in adults, thus, the development of new strategies is required to mitigate CVR, mainly in women.

The difference in clinical presentation of IHD in women, whose symptoms are triggered by emotional or mental stress, the higher prevalence of symptoms other than chest pain, as well as the presence of nonclassical risk factors not considered in usual risk scores make CVR stratification a challenge in the female sex.

A growing body of evidence suggests that traditional cardiovascular risk factors (CVRFs), such as hypertension, diabetes, dyslipidemia, and obesity, pose a differential risk to women as compared to men. For example, diabetes poses a 40% higher risk of IHD to women as compared to men. Premenopausal women have a lower risk of CVD than men at the same age, but women lose that advantage in the menopausal transition.

For younger adults, CVDs account for 10.3% and 20.9% of the deaths in the age ranges of 25-44 years and 45-64 years, respectively. In young women, recognition of adverse pregnancy outcomes (APOs) as a women-specific CVRF is critical for CVR stratification. Women with history of pregnancies complicated by hypertension, gestational diabetes, premature delivery, low birth weight, and fetal growth restriction are at a higher risk for short- and long-term cardiovascular complications. Women with history of APOs can have increased risk for CVD even after achieving normoglycemia and standard control of postpartum blood pressure.[1] In addition, sex-specific or predominantly sexual risk markers, such as early menopause, polycystic ovary

Keywords

Women; Myocardial Ischemia; Multimodal Imaging; Risk

Mailing address: Gláucia Maria Moraes de Oliveira •
Universidade Federal do Rio de Janeiro. R. Prof. Rodolpho P. Rocco, 255, 8°. Andar, Sala 6. Postal code: 21941-913. Rio de Janeiro, RJ – Brazil.
E-mail: glauciamoraesoliveira@gmail.com

Manuscript received June 23, 2023; revised July 24, 2023; accepted July 24, 2023
Editor responsible for the review: Daniela do Carmo Rassi Frota

DOI: https://doi.org/10.36660/abcimg.20230071i

Central Illustration: Imaging For Ischemic Heart Disease in Women: What Cardiologists Expect

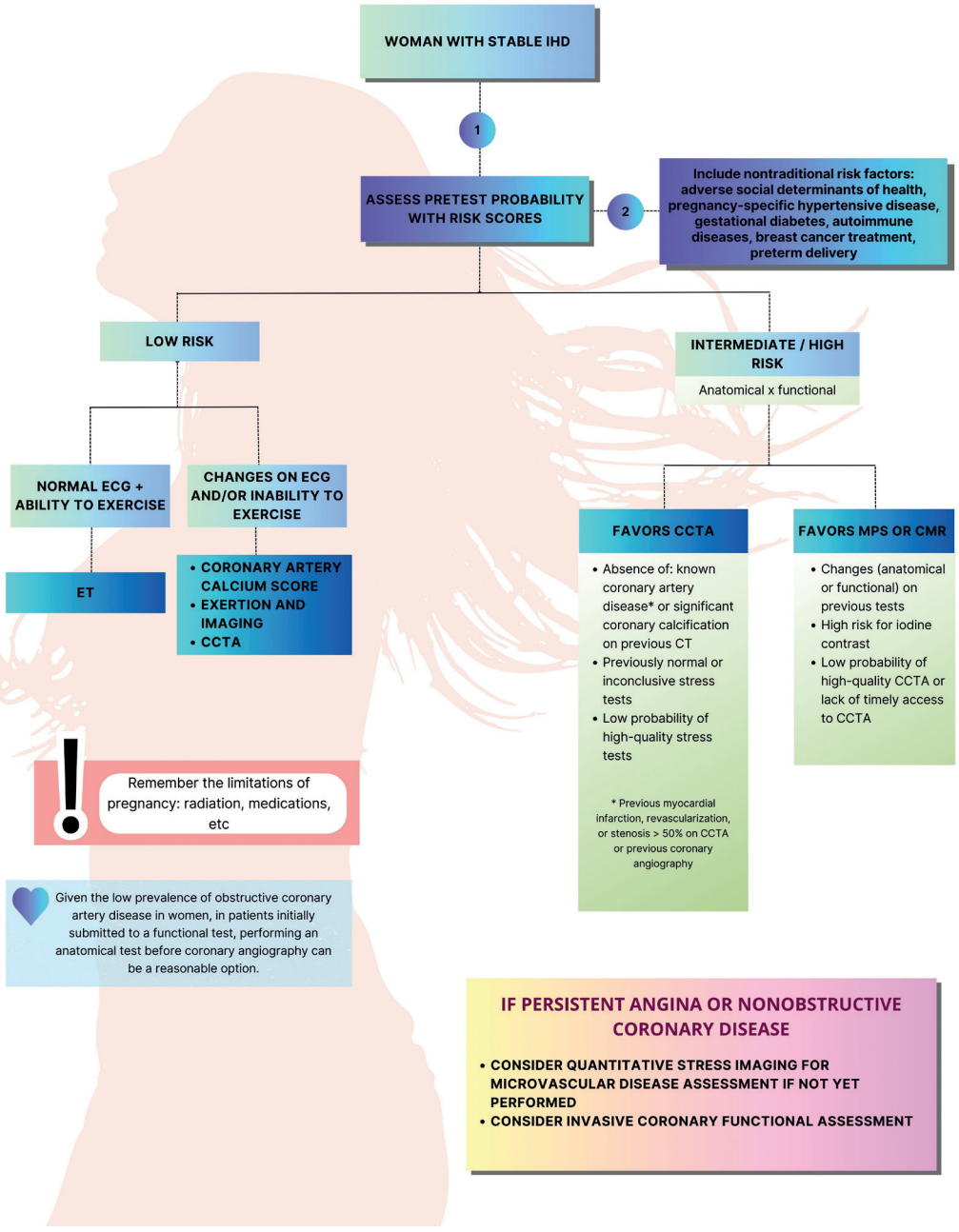

Arq Bras Cardiol: Imagem cardiovasc. 2023;36(3):e20230071

Proposal of a diagnostic algorithm for women with suspected stable IHD. CCTA: coronary computed tomography angiography; MPS: myocardial perfusion scintigraphy; ECG: electrocardiogram; CMR: cardiac magnetic resonance; CT: computed tomography; ET: exercise test; IHD: Ischemic heart disease; CCTA: Coronary computed tomography angiography.

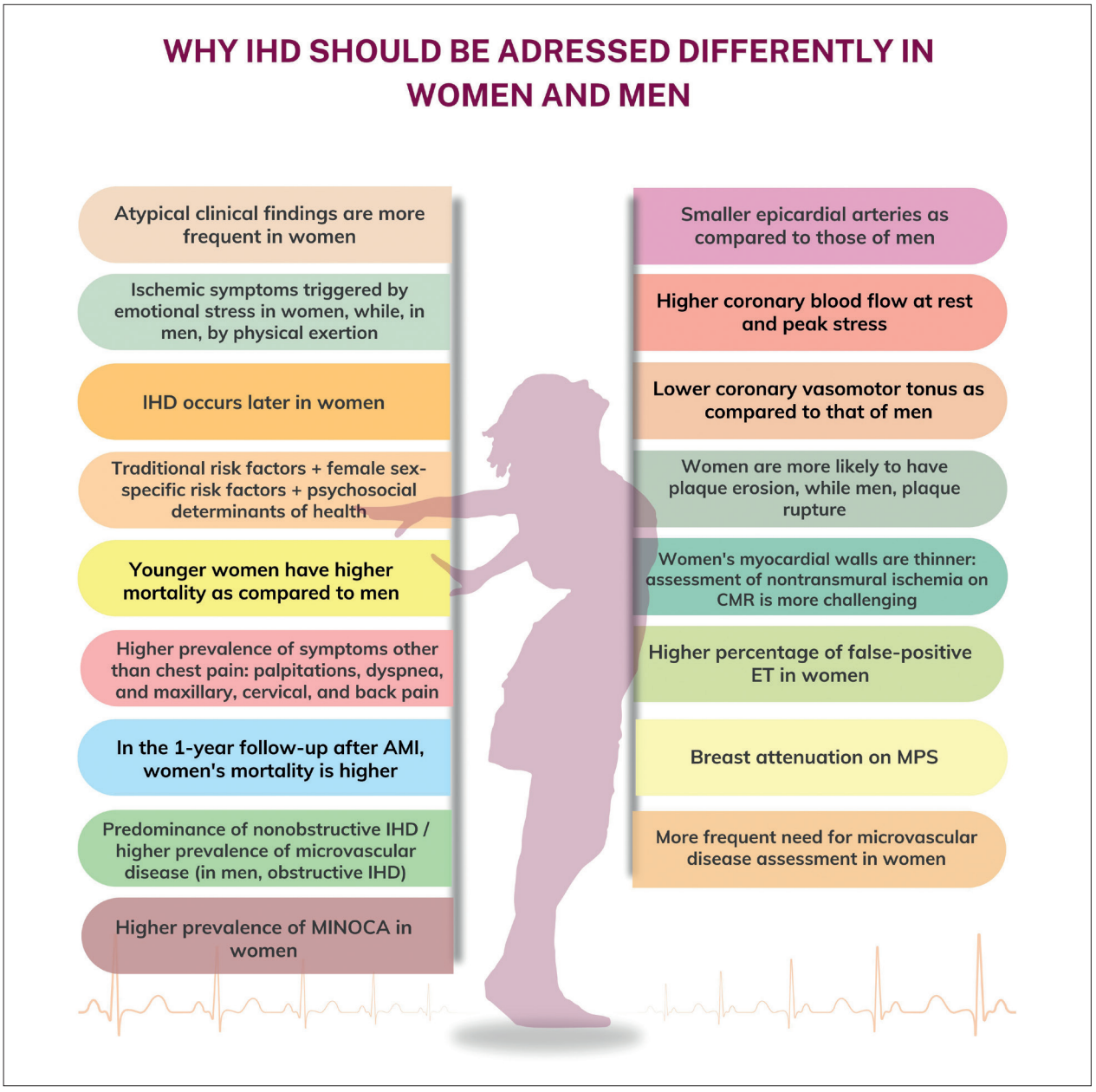

Figure 1 – *Relevant differences of IHD between women and men. IHD: ischemic heart disease; AMI: acute myocardial infarction; MINOCA: myocardial infarction with non-obstructive coronary arteries; ET: exercise test; MPS: myocardial perfusion scintigraphy; CMR: cardiac magnetic resonance.*

syndrome, rheumatological disorders, APOs, and presence of depression and adverse socioeconomic factors, are called enhancers of the traditional CVRFs, and pregnancy works as a "physical and metabolic exercise test (ET)" specific to women.[1]

At rest, coronary blood flow is maintained by autoregulation up to the development of critical stenosis, defined as the capacity to preserve blood flow during perfusion pressure changes, with constant metabolic needs. When an atherosclerotic plaque occludes more than 70% of the luminal cross-section, with a 50% reduction in the coronary diameter, it significantly increases proximal resistance and decreases distal coronary perfusion pressure. In that situation, autoregulation can maintain baseline coronary blood flow, but coronary reserve is impaired. Thus, at rest, the condition is asymptomatic, but, at high metabolic demands during physical exercise, the coronary flow is insufficient.

A large percentage of women with IHD has minimal or no epicardial coronary artery disease. Coronary microvascular disease, however, plays an important role in the etiology of IHD in the female sex, regulating blood flow and oxygen delivery and energetic substrates in the microcirculation-myocardium interaction. Myocardial ischemia is directly

dependent on a balance between myocardial energy *status* and coronary blood flow.[1-3] These changes are shown in Figure 2.[4]

Figure 3 describes the role of complementary tests for IHD stratification and diagnosis in women.

IHD diagnostic tests in women

A. ET

The ET is an accessible, safe, reproducible, low-cost, radiation-free functional test that provides information to support IHD diagnosis, CVR stratification, therapeutic assessment, and physical exercise prescription. It is recommended as the initial method to assess symptomatic women at low/intermediate CVR for IHD who have normal electrocardiogram (ECG) at rest and who can exercise.[1] The factors that contribute to reduce ET accuracy in women are as follows: lower prevalence of multivessel disease; less severe coronary lesions; women's ET performance below ideal (inappropriate physical capacity, shorter exercise duration, and lower achieved heart rate). The ET has sensitivity and specificity of 62% and 68%, respectively, with a positive predictive value of only 47%.[1,5]

B. Transthoracic echocardiography at rest and under stress

In addition to assessing segmental contractility abnormalities, transthoracic echocardiography is a valuable tool to screen for cardiomyopathies, such as hypertensive, hypertrophic, and Takotsubo cardiomyopathies, and other causes of chest pain.[2,3] Combined with exercise, more physiological, or pharmacological stress, it can be used for the IHD diagnosis and prognosis in symptomatic women at intermediate/high CVR. In abnormal stress echocardiography (SEC), the extension and severity of

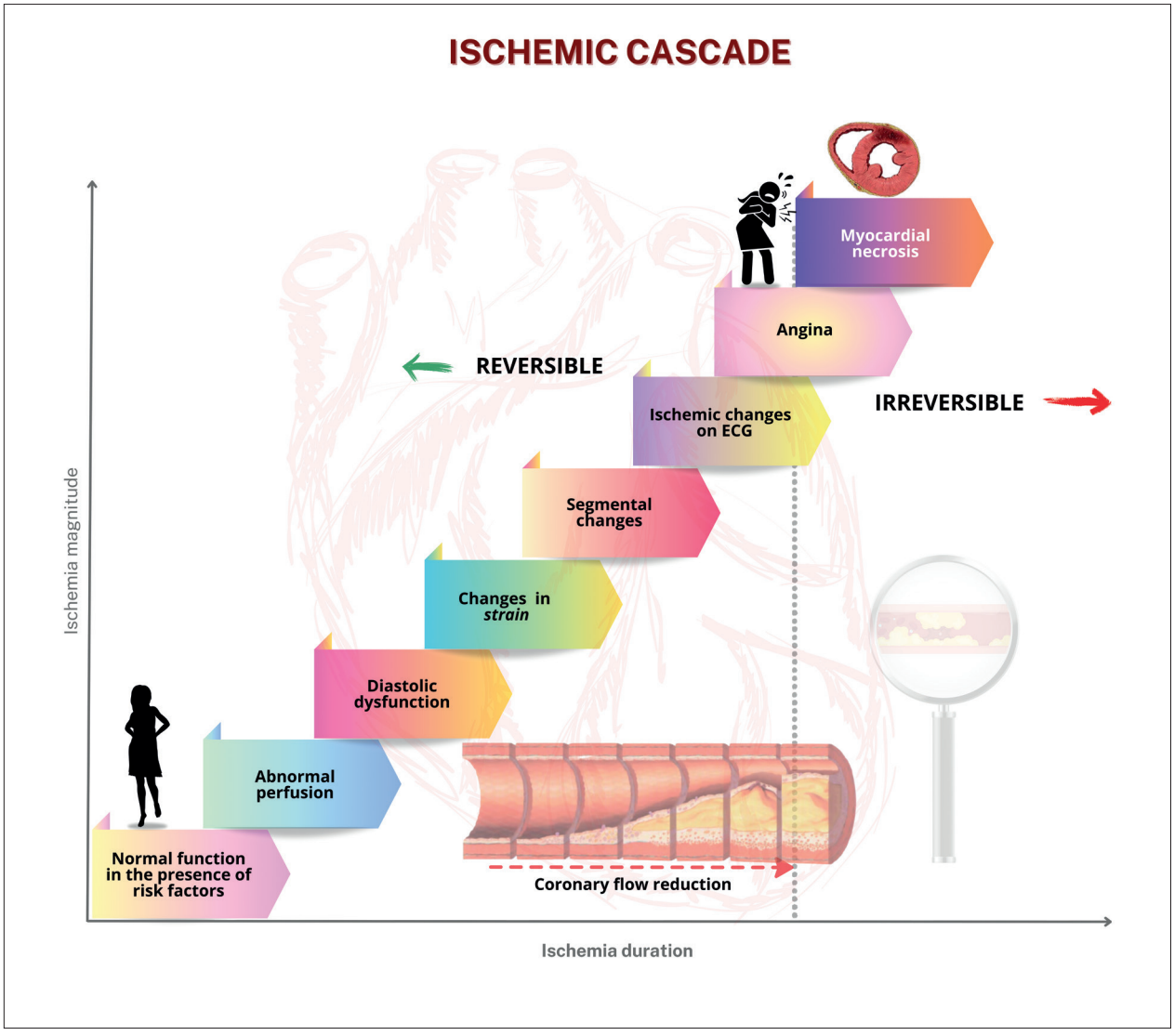

Figure 2 – *Ischemic cascade related to coronary flow reduction to detect IHD. ECG: electrocardiogram.*

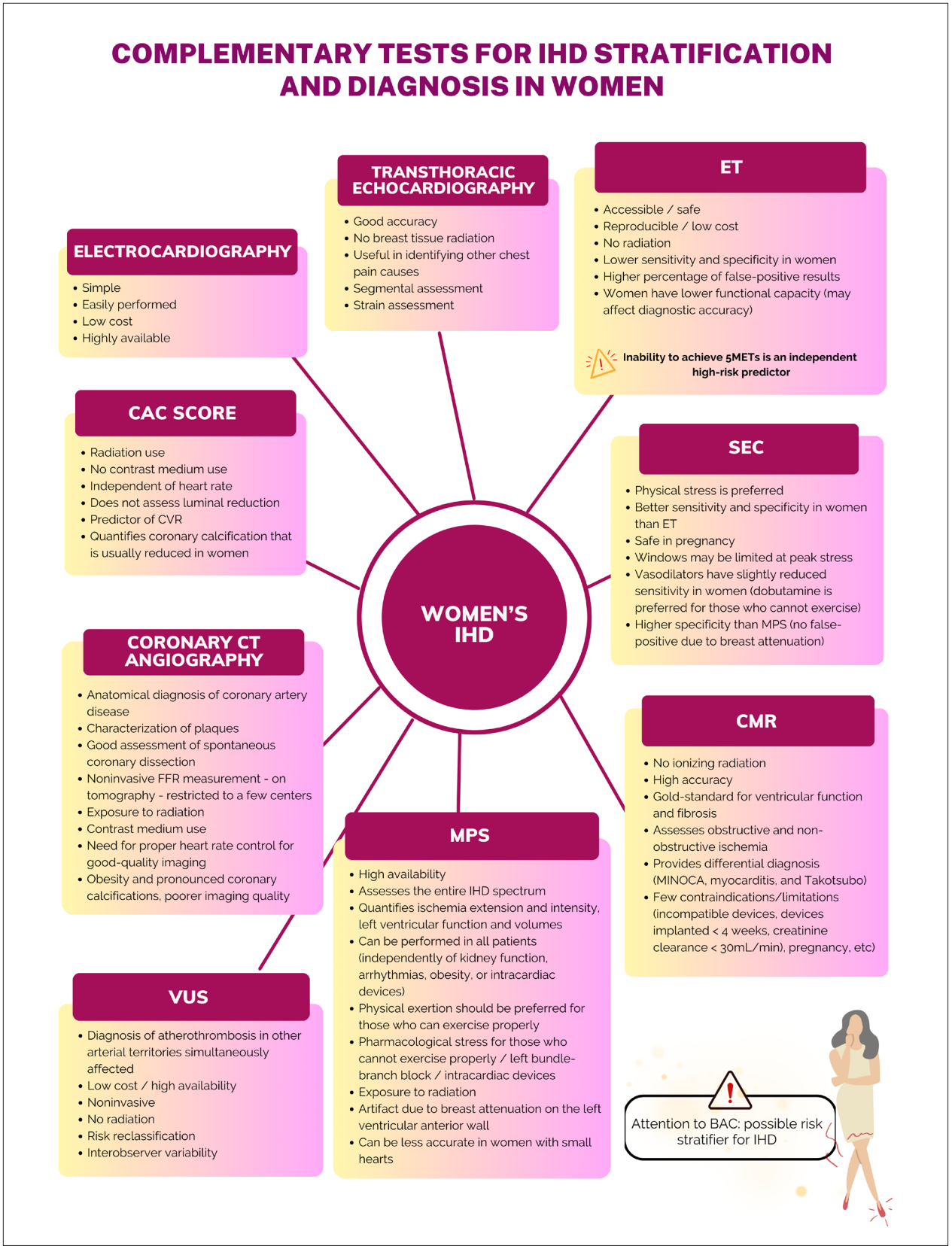

Figure 3 – *Complementary tests to assess IHD in women, with advantages and limitations. CVR: cardiovascular risk; IHD: ischemic heart disease; MINOCA: myocardial infarction with non-obstructive coronary arteries; FFR: fractional flow reserve; ET: exercise test; SEC: stress echocardiography; VUS: vascular ultrasound; MPS: myocardial perfusion scintigraphy; CT: computed tomography; CMR: cardiac magnetic resonance; BAC: breast arterial calcification; CAC: coronary artery calcium.*

contractility changes are associated with higher rates of cardiac events, even in the absence of obstructive IHD on invasive coronary angiography.[2,3] The markers of high CVR on SEC in women are: left ventricular ejection fraction (LVEF) at rest ≤ 40%; extensive wall contractility abnormalities at rest or extensive ischemia (≥ 4–5 left ventricular segments); right ventricular ischemia; increased left ventricular end-systolic diameter in the stress phase; and LVEF reduction with stress.[2,3]

The wall contractility abnormalities detected on echocardiography appear later in the ischemic cascade, being preceded by perfusion abnormalities detected on SPECT (Figure 2). Both techniques have comparable diagnostic accuracy and similar prognostic value. Thus, the local experience and equipment availability are crucial to select the imaging modality.[2,3]

C. Vascular ultrasound (VUS)

The investigation of atherothrombosis of the carotid system and femoral arteries with VUS has an excellent cost-benefit ratio for CVR stratification, because it is a noninvasive, widely available, and easily performed test.[5] The carotid VUS can detect subclinical atherosclerosis by measuring the intima-media thickness (IMT) of the common carotid artery and identify the presence of an atherosclerotic plaque (characteristics, quantification, and assessment of atherosclerotic burden).[6] A cohort study with a North American population[7] has shown a significant increase of IMT with age; however, the presence of atherosclerotic plaque is an aggravating factor in patients at intermediate CVR.[8,9] The ELSA study (Longitudinal Study of Adult Health) has shown that the IMT measure differed with sex, ethnicity, and age ranges in Brazilians, being important in CVR stratification in special subgroups.[10] The IMT measure or identification of a carotid plaque on VUS helps the CVR reclassification of women with at least two risk factors not considered in the usual risk scores or at intermediate risk.[11]

The carotid and femoral atherosclerosis assessment has been recently suggested to improve the early detection of the disease, and the presence of a femoral plaque in women is more indicative of IHD than that of a carotid plaque.[1]

D. Nuclear medicine tests

The myocardial perfusion tests SPECT and PET play an important role in the assessment of women with symptoms suggestive of IHD and at intermediate/high CVR,[1] mainly because of low radiation exposure (9-12mSv on SPECT). Regarding radiation exposure, the benefit-risk ratio favors benefit in IHD detection, as long as the indication is appropriate.

Stress myocardial perfusion scintigraphy (MPS) provides information on the perfusion deficit extension and severity, ischemic burden, and myocardium at risk, as well as the LVEF and wall motility at rest and under stress. For women at intermediate risk with ECG changes at rest or those who cannot exercise, MPS can be the first test requested. Technetium-99m is the radionuclide of choice because it involves less radiation exposure for the patient.

In the assessment of IHD in women, the MPS has shown sensitivity ranging from 78% to 88%, specificity, from 64% to 91%, and lower accuracy as compared to that in men.[12,13] Women have a smaller heart, and MPS has lower sensitivity to detect obstructive IHD because of the low resolution of conventional gamma cameras, in addition to breast attenuation that can result in false-positive tests, mainly in the anterior wall. Regarding breast attenuation, techniques of correction and pronation should be considered to improve the MPS SPECT specificity.[12,13] In women, LVEF can be overestimated with that technique, because of the methodology used for calculation in smaller and/or hypertrophic ventricular cavities.[12,13]

The MPS with pharmacological stress with vasodilators (dipyridamole, adenosine, regadenoson) is the best option for women who cannot exercise, with sensitivity of 91% and specificity of 86%.[3] The use of MPS could reclassify 36% of the patients, which was superior to the clinical and SEC results. The combination of MPS and PET has better resolution than SPECT and increases diagnostic accuracy by 20% in women (88% *versus* 67%), improving the detection of severe multivessel obstructive IHD.[14] A normal test result or of low risk (<5% of abnormal myocardium or equivalent to added stress score <4) is associated with an annual risk of death from IHD or nonfatal infarction < 1%[1,3] (Figure 4).

Women have a higher prevalence of microvascular disease and lower prevalence of obstructive coronary disease than men, and, for that analysis, complementary tests other than luminography are required. The combination of MPS and PET is a technique appropriate to assess coronary flow reserve (CFR), but it is not widely available. Evidence of reduced CFR (defined as <1.9–2.0) suggests underlying vascular dysfunction and can help detect microvascular IHD. Abnormal CFR is associated with diastolic dysfunction and can play a role in the assessment of heart failure with preserved ejection fraction (HFpEF), more prevalent in women. A study with 64.7% of women without obstructive IHD has shown an independent association of CFR reduction and diastolic dysfunction. Imaging protocols with hybrid equipment (PET/CT or SPECT/CT) add the assessment of anatomical changes to the coronary artery calcium score (CAC) quantification, thus increasing the sensitivity for the diagnosis of IHD in a single test.[1,12]

E. Coronary computed tomography (CT)

Symptomatic women with positive functional tests are often submitted to invasive methods, such as coronary angiography, that evidence no atherosclerotic plaque, which, when present, is not severe (stenosis < 50%).[2] Coronary CT is a noninvasive method that assesses the CAC in the presence of atheromatosis. Coronary computed tomography angiography (CCTA), despite its disadvantages, such as radiation emission and cost, provides the quantification and assessment of the characteristics and extension of atherosclerotic plaques, with an excellent accuracy when compared to coronary angiography for IHD

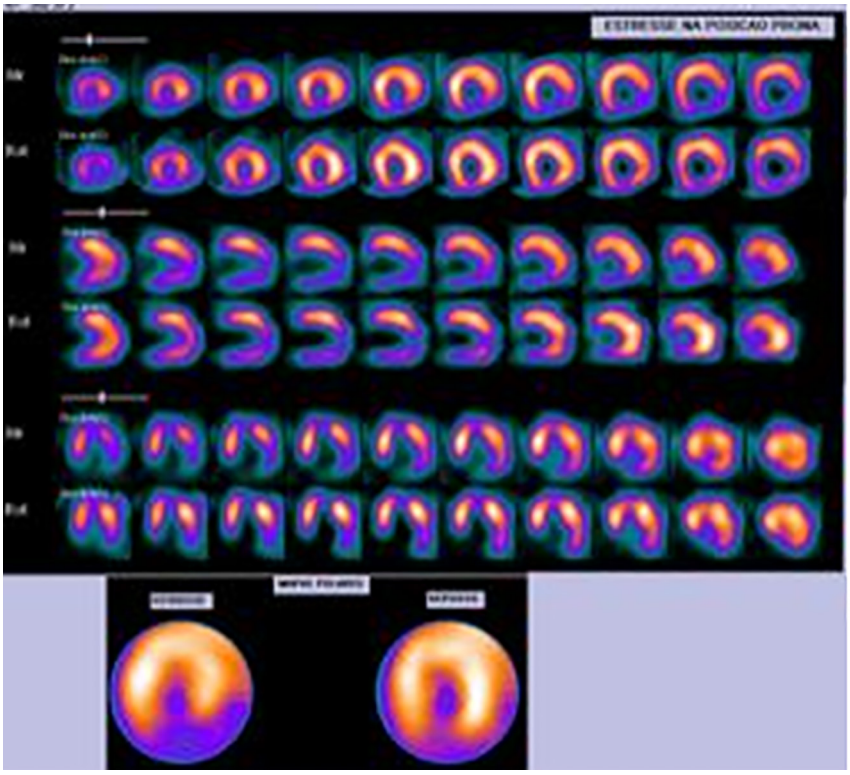

Figure 4 – *Abnormal MPS with a clear transient perfusion deficit in a patient with normal coronary angiography. Images provided by Dr. Viviane Parisotto Marino.*

diagnosis and treatment. Advanced diagnostic centers count on software that can noninvasively quantify CFR on CCTA, which has a good correlation with coronary angiography.[1,2]

The CAC plays an important role in CVR stratification, mainly in asymptomatic patients at low/intermediate risk. In symptomatic women, its role is controversial, because women's have fewer calcified vessels and/or plaques and lower coronary calcium volume. A CAC of 0 practically excludes obstructive IHD, with negative predictive value > 96.5% for lesions ≥ 50% (CONFIRM registry), in addition to indicating low CVR in both sexes (< 1%).[15] Mortality increases with the increase in CAC (0.8% and 9.8% with CAC of 0 and 400, respectively).[2] Although a CAC of 0 indicates low risk for cardiovascular events in women and men, women with any detectable CAC have a 1.3 higher relative risk of mortality from CVD as compared to men.[3]

CCTA has high diagnostic accuracy for obstructive IHD, even after sex-specific analysis. Sensitivity, specificity, and positive and negative predictive values increase with the increase in the stenosis degree. Because women's epicardial coronary arteries are thinner than those of men, the CCTA accuracy is lower (70% x 90%; p < 0.05), mainly in distal coronary arteries and branches.[3] However, in women, CCTA has higher accuracy to detect atherosclerotic disease as compared to stress tests. The CONFIRM study has shown an association of obstructive IHD, mortality, and major cardiovascular events (MACE), with odds ratio of 2.16 and 2.56 for women and men, respectively. In women, the presence of major coronary lesions and higher CAC increases the risk of mortality from CVD by 2.2 times as compared to men.[16]

In addition to detecting the presence of plaque, CCTA provides the assessment of calcium volume and load, presence of remodeling, and plaque vulnerability. Women have lower volumes of calcified or noncalcified plaques, regardless of age. The PROMISE study (n = 5007; 51% women) has compared anatomical and functional tests in patients with chest pain and low/intermediate risk, showing that, in women, positive *versus* negative CCTA was more strongly associated with subsequent clinical events (HR 5.9; 95% CI 3.3-10.4) than a positive *versus* negative stress test (HR 2.3; 95% CI 1.2-4.3). Because CT can detect nonobstructive IHD, its efficacy to predict events is better than that of the functional test, CT (CAC / CCTA) being more sensitive, while the functional test is more specific.[17]

Regarding the characteristics of atherosclerotic plaques, those with higher risk for MACE in women have low attenuation, positive remodeling, punctate calcification, and napkin-ring sign (suggesting a thin fibrous cap) (adjusted OR: 2.41; 95% CI 1.25-4.64).[3]

F. Cardiac magnetic resonance (CMR)

CMR plays an important role in the assessment of women with suspected or known IHD because it is noninvasive and involves neither ionizing radiation nor nephrotoxic contrast

media. In addition, it has high spatial resolution, wide visual field, excellent reproducibility, and provides the assessment of cardiac and vascular anatomy, ventricular function, ischemia, viability, and tissue characterization with high accuracy. CMR has been increasingly used in the assessment of suspected IHD in symptomatic women or those at intermediate/high risk.[18-19]

The CMR with stress has good accuracy for IHD diagnosis, risk stratification, and prognosis.[3,19] The CEMARC study (*Clinical Evaluation of Magnetic Resonance Imaging in Coronary Heart Disease*), with 5-year follow-up, has shown that women with false-positive MPS and negative CMR with dobutamine had low probability of MACE. In addition, that study has shown that the SPECT accuracy was significantly worse in women than in men, while CMR with stress was better than SPECT in women (AUC 0.90 x 0.67) and in men (AUC 0.89 x 0.74).[19]

CMR is an important strategy in suspected MINOCA (myocardial infarction with non-obstructive coronary artery), providing the location of inflammation, edema, and myocardial fibrosis, differentiating ischemic from nonischemic etiologies, identifying the underlying etiology in up to 87% of the cases, and providing the CVR stratification and management definition in women.[3,19] Subendocardial perfusion abnormalities have been described in patients with syndrome X and microvascular dysfunction confirmed by coronary reactivity testing (Figures 5, 6 and 7).[19]

One of the great advantages of CMR is its ability to overcome the technical limitations of other conventional stress imaging modalities, such as breast tissue, obesity, pulmonary disease, and low exercise capacity of the patients.[19]

G. Breast arterial calcifications (BACs)

Mammography can identify BACs or arteriosclerosis by showing radiopaque structures involving the entire circumference of the artery (Figures 8 and 9).

The estimated prevalence of BAC ranges from 8.2% to 12% in women aged over 50 years. There is an association between the presence of BAC and kidney disease, stroke, peripheral vascular disease, carotid artery disease, and IHD. The finding of BAC on mammographies of women under the age of 59 years has been reported to be an additional risk factor for CVD, mainly in women with diabetes, even asymptomatic.[20]

A retrospective cohort study of women assessed for breast cancer in a 23-year follow-up has estimated that those with BAC had higher relative risks as follows: 1.66 (95% CI 1.31–2.10) for cardiovascular events; 3.25 (95% CI 1.53–6.90) for IHD; 2.85 (95% CI 1.59–5.09) for hypertensive heart disease; 2.06 (95% CI 1.19–3.56) for congestive heart failure; 2.8 (95% CI 1.42–5.52) for peripheral vascular disease; 1.83 (95% CI 1.09–3.08) for atrial fibrillation; and 2.23 (95% CI 1.21–4.09) for lacunar infarction. Cox multivariate analysis, considering also the classical CVRFs, has shown a significant and independent association of BAC with both cardiovascular-event-free and specific survivals (1.94 - 95% CI 1.38–2.73).[20]

Another study has assessed 292 women by use of digital mammography and CCTA, and BAC and CAC were quantitatively assessed (0 to 12), correlated with each other and with the Framingham risk score. The sensitivity, specificity, positive and negative predictive values, and accuracy of BAC > 0 for CAC > 0 were 63%, 76%, 70%, 69%, and 70%, respectively. BAC > 0 had an area under the curve of 0.73 for the identification of women with CAC > 0. There was a strong quantitative association between BAC and CAC, and BAC was superior to the traditional CVRFs regarding CAC accuracy. The incorporation of BAC for the CVR assessment of peri- and postmenopausal women is premature, but BAC is an opportunity to identify women at high risk by using routine mammography analysis in breast cancer screening.[21]

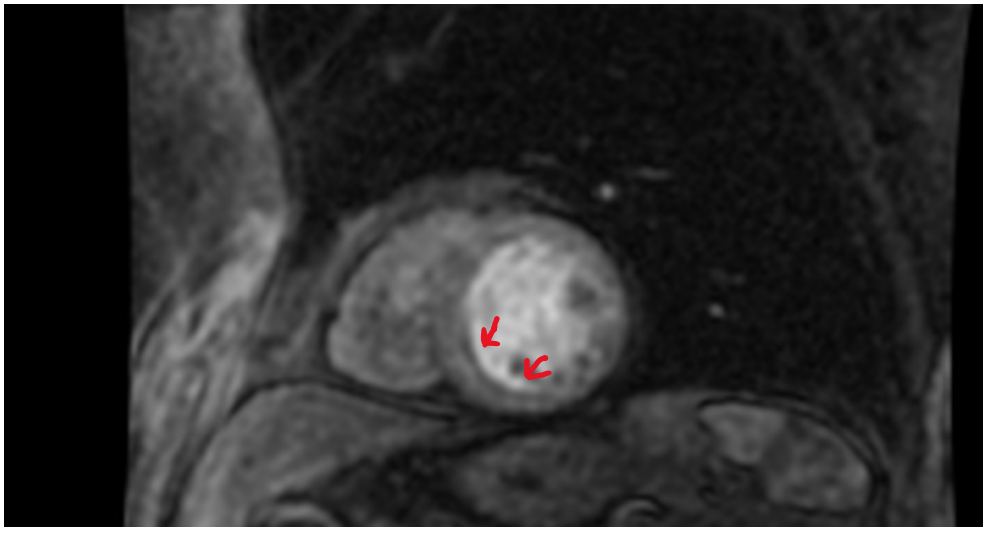

Figure 5 – *CMR imaging showing positive inferior subendocardial perfusion (red arrows). Images provided by Dr. Eduardo Belizário Falchetto.*

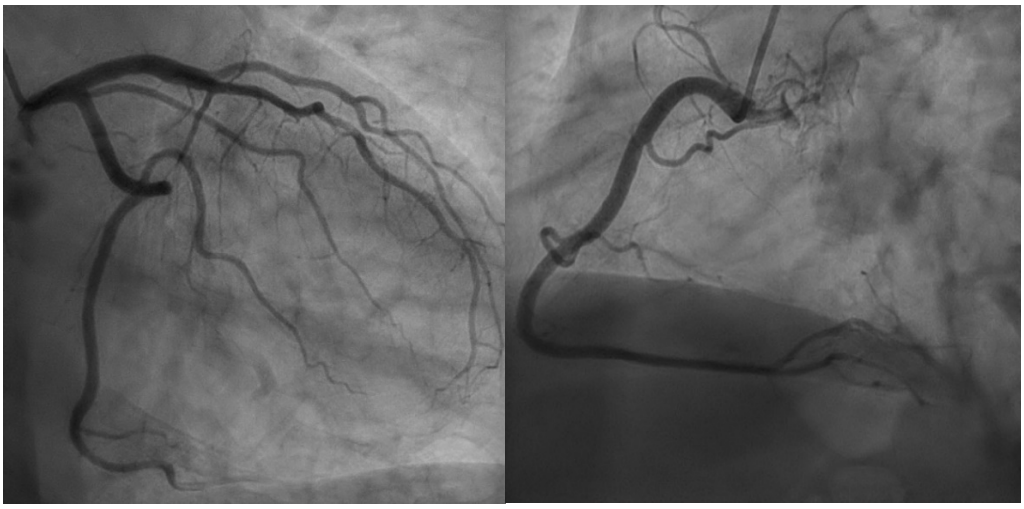

Figure 6 and 7 – *Normal coronary angiography of the left and right coronary arteries from a patient with changes on CMR imaging.*

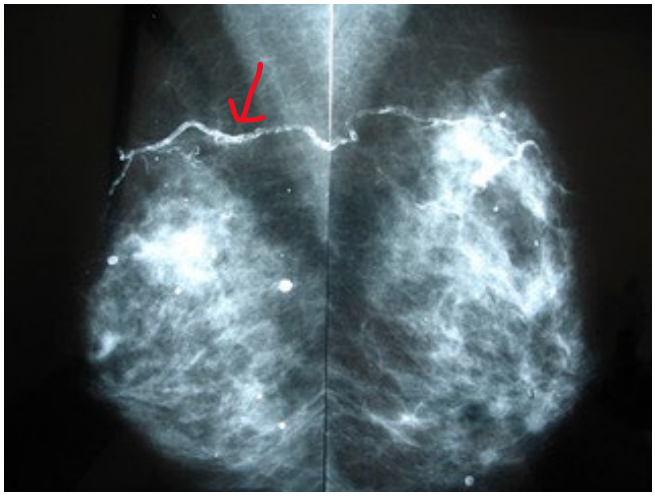

Figure 8 – *Calcified vascularization on the mammography of a 67-year-old woman (red arrow).*

Conclusion

IHD is an important cause of morbidity and mortality in women and men. This paper emphasizes the differences of IHD in women, focusing on the diagnostic investigation in its stable phase.

The higher prevalence of atypical symptoms, anatomical differences, and adverse psychosocial aspects, in addition to the association of specific risk factors regarding obstetrical history, requires an accurate clinical assessment and a targeted diagnostic investigation that consider the limitations, as well as the positive and negative predictive values of the methods. Because of breast exposure, tests involving radiation should be reconsidered in selected cases.

In addition, we emphasize that non-cardiological tests often performed in women, such as mammography, provide an opportunity to assess CVR at early ages or even in patients with few traditional risk factors.

There is no specific algorithm for risk assessment that considers such differences. Thus, this study presents the advantages and limitations of each complementary test (Figure 3) and provides an investigative suggestion, as briefly shown in the Central Illustration.

Complementary tests that assess the microcirculation should be used in cases of proven ischemia in the absence of obstructive coronary artery disease, which is known to be more frequent in women.

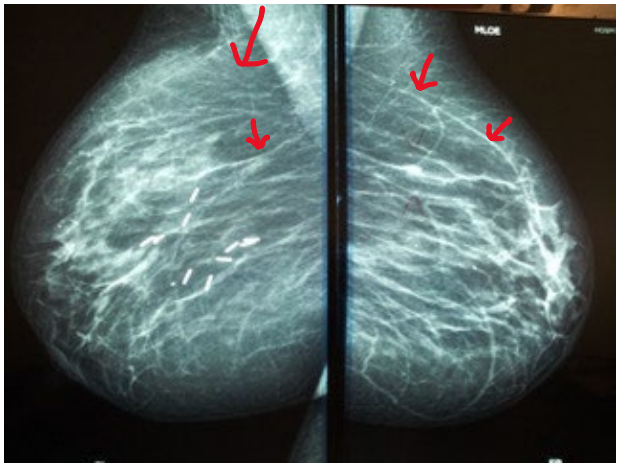

Figure 9 – *55-year-old patient with BACs (red arrows). Images provided by Prof. Washington Cançado Amorim.*

Author Contributions

Conception and design of the research; acquisition of data; analysis and interpretation of the data; writing of the manuscript and critical revision of the manuscript for intellectual content: Almeida MCC, Freire CMV, Espíndola LN, Oliveira GMM.

Potential Conflict of Interest

No potential conflict of interest relevant to this article was reported.

Sources of Funding

There were no external funding sources for this study.

Study Association

This study is not associated with any thesis or dissertation work.

Ethics Approval and Consent to Participate

This article does not contain any studies with human participants or animals performed by any of the authors.

References

1. Oliveira GMM, Almeida MCC, Rassi DDC, Bragança ÉOV, Moura LZ, Arrais M, et al. Position Statement on Ischemic Heart Disease - Women-Centered Health Care - 2023. Arq Bras Cardiol. 2023;120(7):e20230303. doi: 10.36660/abc.20230303.
2. Baldassarre LA, Raman SV, Min JK, Mieres JH, Gulati M, Wenger NK, et al. Noninvasive Imaging to Evaluate Women with Stable Ischemic Heart Disease. JACC Cardiovasc Imaging. 2016;9(4):421-35. doi: 10.1016/j.jcmg.2016.01.004.
3. Lozano PFR, Kaso ER, Bourque JM, Morsy M, Taylor AM, Villines TC, et al. Cardiovascular Imaging for Ischemic Heart Disease in Women: Time for a Paradigm Shift. JACC Cardiovasc Imaging. 2022;15(8):1488-1501. doi: 10.1016/j.jcmg.2022.01.006.
4. Stillman AE, Oudkerk M, Bluemke DA, Boer MJ, Bremerich J, Garcia EV, et al. Imaging the Myocardial Ischemic Cascade. Int J Cardiovasc Imaging. 2018;34(8):1249-63. doi: 10.1007/s10554-018-1330-4.
5. Del Giorno R, Reveilhac M, Stauffer I, Berthoud M, Mazzolai L, Depairon M, et al. A New Score for Improving Cardiovascular Risk Prediction and Prevention. Nutr Metab Cardiovasc Dis. 2023;33(8):1546-55. doi: 10.1016/j.numecd.2023.04.019.
6. Johri AM, Nambi V, Naqvi TZ, Feinstein SB, Kim ESH, Park MM, et al. Recommendations for the Assessment of Carotid Arterial Plaque by Ultrasound for the Characterization of Atherosclerosis and Evaluation of Cardiovascular Risk: From the American Society of Echocardiography. J Am Soc Echocardiogr. 2020;33(8):917-33. doi: 10.1016/j.echo.2020.04.021.
7. Boulos NM, Gardin JM, Malik S, Postley J, Wong ND. Carotid Plaque Characterization, Stenosis, and Intima-Media Thickness According to Age and Gender in a Large Registry Cohort. Am J Cardiol. 2016;117(7):1185-91. doi: 10.1016/j.amjcard.2015.12.062.
8. Freire CMV, Alcântara ML, Santos SN, Amaral SI, Veloso O, Porto CLL, et al. Recomendação para a Quantificação pelo Ultrassom da Doença Aterosclerótica das Artérias Carótidas e Vertebrais: Grupo de Trabalho do Departamento de Imagem Cardiovascular da Sociedade Brasileira de Cardiologia – DIC - SBC. Arq Bras Cardiol. 2015;28:1-64. doi: 10.5935/2318-8219.20150018.
9. Précoma DB, Oliveira GMM, Simão AF, Dutra OP, Coelho OR, Izar MCO, et al. Updated Cardiovascular Prevention Guideline of the Brazilian Society of Cardiology - 2019. Arq Bras Cardiol. 2019;113(4):787-891. doi: 10.5935/abc.20190204.
10. Santos IS, Bittencourt MS, Oliveira IR, Souza AG, Meireles DP, Rundek T, et al. Carotid Intima-Media Thickness Value Distributions in the Brazilian Longitudinal Study of Adult Health (ELSA-Brasil). Atherosclerosis. 2014;237(1):227-35. doi: 10.1016/j.atherosclerosis.2014.09.004.
11. Oliveira GMM, Almeida MCC, Marques-Santos C, Costa MENC, Carvalho RCM, et al. Position Statement on Women's Cardiovascular Health - 2022. Arq Bras Cardiol. 2022;119(5):815-82. doi: 10.36660/abc.20220734.
12. Mieres JH, Gulati M, Merz NB, Berman DS, Gerber TC, Hayes SN, et al. Role of Noninvasive Testing in the Clinical Evaluation of Women with Suspected Ischemic Heart Disease: A Consensus Statement from the American Heart Association. Circulation. 2014;130(4):350-79. doi: 10.1161/CIR.0000000000000061.

13. Mastrocola LE, Amorim BJ, Vitola JV, Brandão SCS, Grossman GB, Lima RSL, et al. Update of the Brazilian Guideline on Nuclear Cardiology - 2020. Arq Bras Cardiol. 2020;114(2):325-429. doi: 10.36660/abc.20200087.

14. Shaw LJ, Wilson PW, Hachamovitch R, Hendel RC, Borges-Neto S, Berman DS. Improved Near-Term Coronary Artery Disease Risk Classification with Gated Stress Myocardial Perfusion SPECT. JACC Cardiovasc Imaging. 2010;3(11):1139-48. doi: 10.1016/j.jcmg.2010.09.008.

15. Villines TC, Hulten EA, Shaw LJ, Goyal M, Dunning A, Achenbach S, et al. Prevalence and Severity of Coronary Artery Disease and Adverse Events among Symptomatic Patients with Coronary Artery Calcification Scores of Zero Undergoing Coronary Computed Tomography Angiography: Results from the CONFIRM (Coronary CT Angiography Evaluation for Clinical Outcomes: An International Multicenter) registry. J Am Coll Cardiol. 2011;58(24):2533-40. doi: 10.1016/j.jacc.2011.10.851.

16. Shaw LJ, Min JK, Nasir K, Xie JX, Berman DS, Miedema MD, et al. Sex Differences in Calcified Plaque and Long-Term Cardiovascular Mortality: Observations from the CAC Consortium. Eur Heart J. 2018;39(41):3727-35. doi: 10.1093/eurheartj/ehy534.

17. Bittner DO, Mayrhofer T, Budoff M, Szilveszter B, Foldyna B, Hallett TR, et al. Prognostic Value of Coronary CTA in Stable Chest Pain: CAD-RADS, CAC, and Cardiovascular Events in PROMISE. JACC Cardiovasc Imaging. 2020;13(7):1534-45. doi: 10.1016/j.jcmg.2019.09.012.

18. International Atomic Energy Agency Health Series. Imaging of Ischemic Heart Disease in Women: A Critical Review of the Literature. Vienna: IAEA; 2022.

19. Bucciarelli-Ducci C, Ostenfeld E, Baldassarre LA, Ferreira VM, Frank L, Kallianos K, et al. Cardiovascular Disease in Women: Insights from Magnetic Resonance Imaging. J Cardiovasc Magn Reson. 2020;22(1):71. doi: 10.1186/s12968-020-00666-4.

20. Galiano NG, Eiro N, Martín A, Fernández-Guinea O, Martínez CDB, Vizoso FJ. Relationship between Arterial Calcifications on Mammograms and Cardiovascular Events: A Twenty-Three Year Follow-Up Retrospective Cohort Study. Biomedicines. 2022;10(12):3227. doi: 10.3390/biomedicines10123227.

21. Margolies L, Salvatore M, Hecht HS, Kotkin S, Yip R, Baber U, et al. Digital Mammography and Screening for Coronary Artery Disease. JACC Cardiovasc Imaging. 2016;9(4):350-60. doi: 10.1016/j.jcmg.2015.10.022.

Review Article

Echocardiographic Characteristics of PRKAG2 Syndrome: An Integrative Review

José Luiz Barros Pena,[1,2] *Igor de Souza Neto,*[1] *Alice Pinheiro Barbosa,*[1] *Dinamar Amador dos Santos Neto*[1]
Faculdade de Ciências Médicas de Minas Gerais,[1] *Belo Horizonte, MG – Brazil*
Hospital Felício Rocho, Ecocardiografia,[2] *Belo Horizonte, MG – Brazil*

Central Illustration: Echocardiographic Characteristics of PRKAG2 Syndrome: An Integrative Review

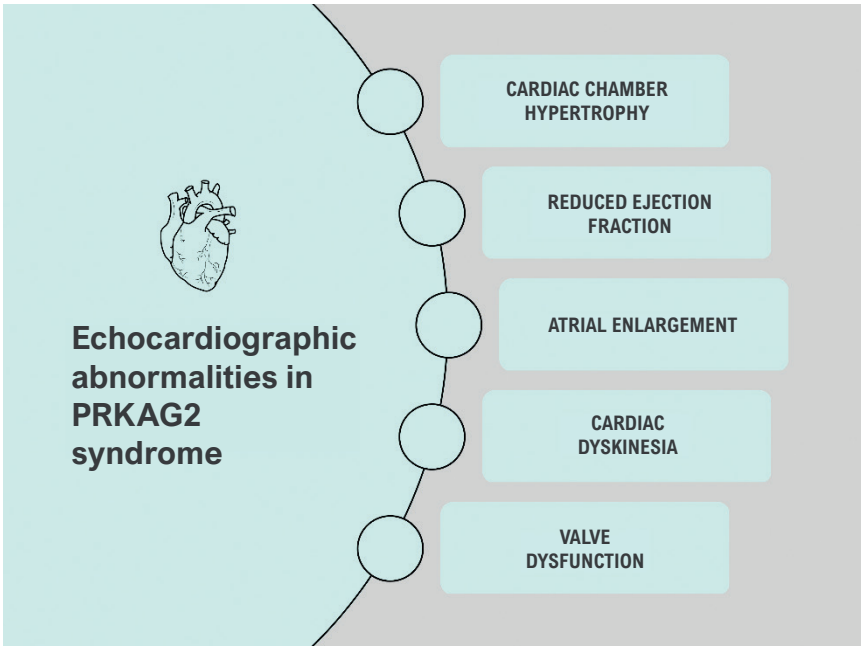

Arq Bras Cardiol: Imagem cardiovasc. 2023;36(3):e20230047

Abstract

PRKAG2 syndrome is a rare, early-onset, autosomal dominant, inherited lysosomal glycogen storage disease that develops with ventricular preexcitation syndrome, supraventricular arrhythmias, and cardiac hypertrophy. The disease is caused by mutations in the gene encoding the adenosine monophosphate-activated protein kinase (AMPK) protein, leading to glycogen accumulation in cardiomyocytes. Echocardiography is a noninvasive, widely available, and highly effective technique for identifying and quantifying left ventricular hypertrophy (LVH). Therefore, this review focuses mainly on echocardiographic patterns, describing the main alterations in patients with PRKAG2 syndrome.

O objective of this paper is to conduct an integrative review of the echocardiographic features presented by patients with PRKAG2 syndrome.

We conducted an integrative review of echocardiographic features in PRKAG2 syndrome by searching PubMed, SciELO, IBECS, and LILACS electronic databases using the following keywords: "PRKAG2 syndrome" and "PRKAG2."

The predominant echocardiographic finding in patients with PRKAG2 syndrome was cardiac chamber hypertrophy, particularly affecting the left ventricle. In addition, other findings included abnormal ejection fraction, changes in strain patterns, and heart valve abnormalities.

Keywords

Glycogen Storage Disease; Echocardiography; Cardiomyopathy, Hypertrophic

Mailing Address: José Luiz Barros Pena. •
Alameda Ezequiel Dias, 275. Postal Code: 30130-110. Belo Horizonte, MG – Brazil
E-mail: jose.pena@cienciasmedicasmg.edu.br.
Manuscript received May 3, 2023; revised May 22, 2023; accepted May 22, 2023
Editor responsible for the review: Daniela do Carmo Rassi Frota

DOI: https://doi.org/10.36660/abcimg.20230047i

Contents

Cardiac chamber hypertrophy was demonstrated in most studies, with a predominance of LVH. Reduced ejection fraction was also described, both in the left and right ventricles. Other features reported included atrial enlargement, cardiac dyskinesia, and valve dysfunction. However, the findings varied widely, highlighting the phenotypic variability of this syndrome.

Introduction

PRKAG2 syndrome is a rare, early-onset, autosomal dominant, inherited lysosomal glycogen storage disease that develops with ventricular preexcitation syndrome, supraventricular arrhythmias, and cardiac hypertrophy. The disease is caused by mutations in the gene encoding adenosine monophosphate-activated protein kinase (AMPK) in the gamma 2 subunit. The mutation causes anomalous AMPK activity, leading to glycogen accumulation in cardiomyocytes that causes their progressive increase. PRKAG2 syndrome can be expressed in different ways, both by left ventricular hypertrophy (LVH) and by arrhythmic features, ranging from an asymptomatic condition, Wolff-Parkinson-White syndrome, and progression of atrioventricular block requiring pacemaker (PM) implantation to sudden cardiac death (SCD).[1]

Regarding clinical parameters, the onset of symptoms usually occurs in the first 3 decades of life and is often characterized by tachycardia and bradyarrhythmias; less often, heart failure or SCD may be the first manifestations of the disease. Prolonged dynamic electrocardiogram monitoring and exercise stress testing are useful tools in patients with syncope, palpitations, or with a family history of SCD.[2]

Regarding echocardiographic patterns, echocardiography is a noninvasive, widely available, and highly effective technique for identifying and quantifying ventricular hypertrophy, assisting in the evaluation and monitoring of the disease and allowing early follow-up.[3] Increasing access to genetic testing to diagnose this syndrome, associated with the description of echocardiographic parameters, has made it possible to distinguish and assess disease progression. Since the pathogenesis and natural history of this syndrome differ from other arrhythmogenic cardiomyopathies, a differentiated diagnostic approach and follow-up are required.[4] Therefore, this review focuses mainly on echocardiographic parameters, describing the main alterations in patients with PRKAG2 syndrome.

This review is justified by the fact that there are few published studies that have provided evidence of echocardiographic findings in PRKAG2 syndrome. Therefore, describing these parameters will have practical implications for the diagnosis and follow-up of patients with this condition. The echocardiographic findings are illustrated in the Central Figure.

Objectives

To conduct an integrative review of the echocardiographic features presented by patients with PRKAG2 syndrome, with the following guiding question: "What are the echocardiographic features presented by patients with PRKAG2 syndrome?". Thus, we aim to show which short-term and long-term cardiac abnormalities are found in this condition.

Methods

We conducted an integrative review of echocardiographic features in PRKAG2 syndrome. Studies were identified by searching the following electronic databases from inception to April 24, 2023: PubMed, SciELO, IBECS, and LILACS. A simple search was performed in all database fields (title, abstract, text word, etc.) using the following keywords: "PRKAG2 syndrome" and "PRKAG2," using the Boolean operator "OR." Studies eligible for inclusion in this review were published in English up to the date the last search was run and answered the guiding question, that is, addressed echocardiographic findings in PRKAG2 syndrome. Studies providing a systematization of data, such as integrative or systematic reviews, were excluded. Two reviewers independently screened titles and abstracts, and then screened candidate full-text articles for selection on the basis of our eligibility criteria. For studies meeting eligibility, data were extracted using a standardized table, with a specific column for each information to be collected, as follows: author/year, article title, study design, sample, and results.

Results

The database searches resulted in a total of 98 articles. Of these, 80 were excluded for the following reasons: 13 integrative or systematic reviews, 3 duplicates, 1 editorial about another article, and 63 studies that did not answer the guiding question. Therefore, 18 studies were included in this review. The flow diagram of study selection is shown in Figure 1. Table 1 summarizes the included studies, which are presented in ascending order of year of publication, according to the database from which the article was retrieved.

Discussion

Cardiac chamber hypertrophy

According to Lipshultz et al.,[4] hypertrophic cardiomyopathy (HCM) has a reported incidence of 0.24-0.47 per 100,000 children and is a leading cause of SCD in young people. It is characterized by abnormal thickening of the heart muscle, especially of the left ventricle (LV) and the interventricular septum. In this context, cardiac hypertrophy is one of the main manifestations of the PRKAG2 syndrome, being a finding in all of the 18 studies analyzed in this review.

There is still no consensus on when this abnormality begins, but some studies indicate that it may be present during intrauterine development. In the case reported by Gorla et al.,[16] cardiac hypertrophy was observed as early as 28 weeks of gestation, demonstrating a severe form of HCM with involvement of both ventricles, the interventricular septum, and the right atrial wall. Torok et al.[13] reported 2 cases of *PRKAG2* mutation carriers, with presentation of this condition in infancy. One of the patients presented with hypertrophy of the interventricular septum at birth, which, however, was no longer observed at age 3 months, whereas the other patient presented with severe biventricular hypertrophy at birth. Also, regarding manifestations in the pediatric population, Aggarwal et al.[11] reported the case of an adolescent female

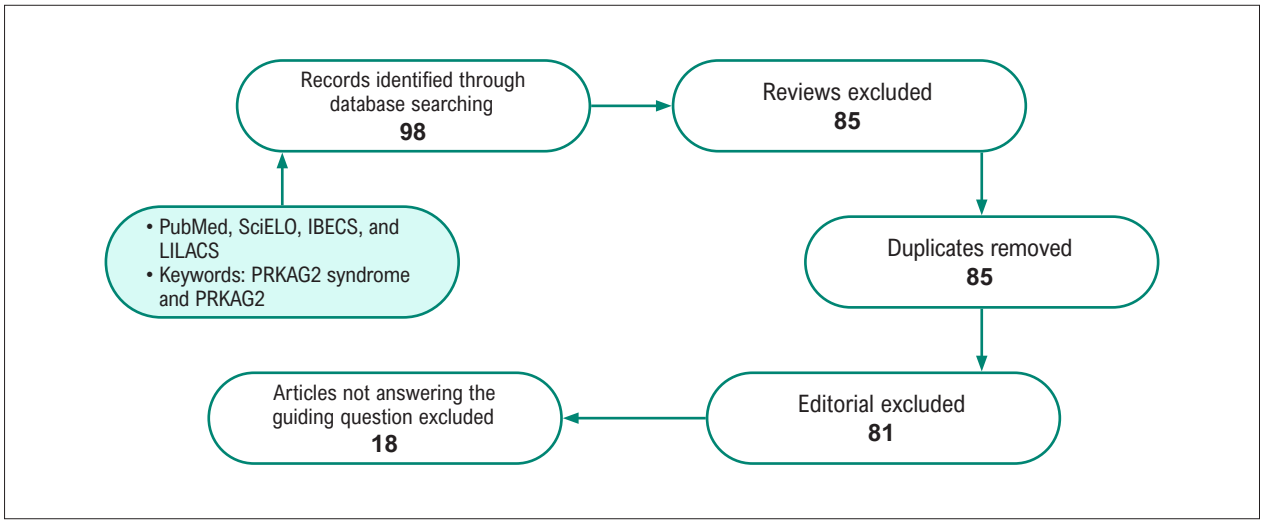

Figure 1 – *Flow diagram of study selection. Source: Designed by the authors.*

affected by *PRKAG2* gene mutation and found that she had concentric LVH.

Tan et al.,[7] in the first published study on *PRKAG2* mutations, although without a focus on echocardiographic abnormalities in *PRKAG2* mutation carriers, reported that, of the 17 retrospectively studied patients, 8 had undergone echocardiography and 7 of them had cardiac hypertrophy. An interesting finding of the study was the histopathological confirmation of this diagnosis. Later, in the comparative study by Sternick et al.,[8] 30% of patients with *PRKAG2* mutation (n = 10) had LVH, whereas control patients (n = 9), without the mutation, had no structural heart disease.

Fabris et al.[9] reported the case of a 17-year-old individual with echocardiography showing mild asymmetric LVH with posterolateral distribution and maximum wall thickness (MWT) of 13 mm. Sternick et al.[10] reported the case of an 18-year-old patient with severe LVH associated with acute myocardial infarction, with an LV septal thickness of 44 mm. In the case of a 40-year-old patient reported by Müllertz and Jensen,[12] LVH was initially misinterpreted as hypertensive heart disease, highlighting the importance of considering rare causes of HCM in patients presenting with tachycardia, preexcitation, and atrioventricular block. Van Der Steld et al.[14] observed that, in 60 patients who were members of a Brazilian family with PRKAG2 syndrome, the predominant pattern was generalized and diffuse LVH, which predominated in the apical and medial portions later in life. Epicoco et al.[15] reported the case of a 30-year-old patient identified with *PRKAG2* gene mutation whose echocardiogram showed marked and symmetric HCM without outflow obstruction, with an MWT of 28 mm.

Regarding the remaining studies analyzed in this review, the most recent ones, published in the last 3 years, also reported the patterns found in the previously mentioned studies. Ahamed et al.,[17] for example, observed that 19 individuals (86%), from a cohort of 22 individuals with a mean age of 39.5 ± 18.1 years, had evidence of diffuse and concentric LVH, with right ventricular (RV) hypertrophy being observed in 19 patients with LVH (19/22; 86%). Hu et al.[18] reported that 4 patients (80%) had LVH; in 3 of them, the analysis showed diffuse asymmetric hypertrophy, with a pattern of LV middle-anterior-lateral-inferior hypertrophy and especially interventricular septal hypertrophy. In contrast, 1 patient showed symmetric hypertrophy. The study also brought to light a new finding at that time, atrial enlargement, which was present in half of the patients, with or without hypertrophy, suggesting that this phenomenon might precede hypertrophy in the early stages. Furthermore, the youngest patient, aged 9 years, presented with mild symmetric hypertrophy, speculating that this is also a finding that might occur in the early stages. Lopez-Sainz et al.[19] reported that patients with PRKAG2 syndrome, with a mean age of 37 years, had LVH with an MWT of 19 ± 7 mm. Pena et al.[20] analyzed 30 individuals with PRKAG2 syndrome, with a mean age of 39.1 ± 15.4 years, and found LVH in different degrees in 25 patients (86%), with a mean LV septal thickness of 14.1 ± 4.2 mm. The relative wall thickness (RWT) was increased (0.56 ± 0.18), characterizing concentric hypertrophy, and RV hypertrophy occurred in 90% of patients. Furthermore, regarding sex differences, men had higher myocardial mass than women. Regarding age, no correlation was found between age and hypertrophy-related variables. In the study conducted by Magalhães et al.,[5] of 16 individuals with a mean age of 40 ± 11 years, 7 (54%) had LVH on echocardiography.

In the past year, 2 studies have made significant contributions to the understanding of the disease – the first, conducted by Tang et al.,[22] by comparing *PRKAG2* mutation carriers with a group of healthy individuals, and the second, conducted by Pena et al.,[21] by describing a feature little explored in this syndrome, the involvement of the RV. The cross-sectional study by Tang et al.,[22] including 9 patients with *PRKAG2* mutation and mean age of 40.22 ± 14.01 years, showed that these individuals had increased LV wall asymmetry compared with the group of 202 healthy individuals (1.42 ± 0.52 vs 0 .14 ± 0.14 mm, p = 0.001), with asymmetric septal hypertrophy. Furthermore, RWT was higher in the PRKAG2 group than in the healthy group (0.48 ± 0.15 vs 0.39 ± 0.07, p = 0.002),

Table 1 – Summary of evidence of echocardiographic findings in PRKAG2 syndrome

Author/year	Article title	Study design	Sample – what was t he study population?	Results
			LILACS	
Magalhães LP et al. (2022)[5]	Long-Term Cardiac Complications of *PRKAG2* Syndrome	Ambispective observational cohort study	n =16 Members of a single family carrying the Arg302Gln mutation in the *PRKAG2* gene.	Seven patients (54%) had LVH (defined as interventricular septum or posterior wall thickness ≥13 mm, with no apparent cause) on echocardiography.
			PUBMED	
Charron P et al. (2007)[6]	A familial form of conduction defect related to a mutation in the *PRKAG2* gene	Case report	n = 4 Members of the same family with a mutation in the *PRKAG2* gene.	The study describes a family with a mutation in the *PRKAG2* gene and a particular phenotype characterized by the absence of echocardiographic hypertrophy.
Tan HL et al. (2008)[7]	Nodoventricular Accessory Pathways in *PRKAG2*-Dependent Familial Preexcitation Syndrome Reveal a Disorder in Cardiac Development	Retrospective observational cohort study	n = 17 Medical records, collected between 1955 and 2007, of 17 members of a 5-generation Dutch family.	Among the patients studied, 8 underwent echocardiography and 7 had cardiac hypertrophy.
Sternick EB et al. (2011)[8]	Clinical, electrocardiographic, and electrophysiologic characteristics of patients with a fasciculoventricular pathway: the role of *PRKAG2* mutation	Retrospective observational cohort study	n = 19 Two groups of patients: group A consisted of 10 patients with *PRKAG2* mutation (Arg302Gln); and group B consisted of 9 patients without the mutation.	In group A, 30% of patients had LVH and none had an additional accessory pathway. Patients in group B had no structural heart disease.
Fabris E et al. (2013)[9]	Cardiac hypertrophy, accessory pathway, and conduction system disease in an adolescent: the *PRKAG2* cardiac syndrome.	Case report	n = 1 A 17-year-old asymptomatic patient was referred for family screening because of his father's unexplained LVH.	Echocardiography showed mild asymmetric LVH with posterolateral distribution. Cardiac magnetic resonance imaging confirmed asymmetric LVH (MWT of 13 mm).
Sternick EB et al. (2014)[10]	Myocardial infarction in a teenager	Case report	n = 1 An 18-year-old man was diagnosed with an AMI of the interventricular septum, and genetic analysis identified a mutation in the *PRKAG2* gene.	An echocardiogram showed massive LVH. The LV septal thickness was 44 mm. The authors speculated that the septal AMI resulted from a demand-supply mismatch of a severely hypertrophied septum.
Aggarwal V et al. (2015)[11]	*PRKAG2* mutation: An easily missed cardiac specific non-lysosomal glycogenosis	Case report	n = 1 An adolescent female affected by a mutation in the PRKAG2 gene.	The patient had concentric LVH.

Müllertz KM et al. (2016)[12]	Variable primary phenotypic manifestations in a rare familial form of Wolff-Parkinson-White syndrome and HCM	Case report	n = 3 Different primary phenotypic manifestations of *PRKAG2*-gene heart disease in a 3-generation family were described. The proband presented with atrial fibrillation, her daughter with Wolff-Parkinson-White syndrome, and her mother with atrioventricular block.	Echocardiographic examination of the index patient's mother revealed marked LVH, initially misinterpreted as hypertensive heart disease. Several years later, LVH also developed in the index patient and her daughter, and PRKAG2-gene heart disease became evident.
Torok RD et al. (2017)[13]	*PRKAG2* mutations presenting in infancy	Case report	n = 3 Report of 3 cases of *PRKAG2* mutation carriers.	Patient in case 1 presented with hypertrophy of the interventricular septum at birth, but at age 3 months this abnormality was no longer observed. The mitral valve was thickened and tethered by shortened chordae. There was moderate mitral regurgitation and subsequent LV dilation. Patient in case 2 presented with severe biventricular hypertrophy, severe mitral regurgitation, and moderate tricuspid regurgitation. Patient in case 3 did not undergo echocardiography.
Van Der Steld LP et al. (2017)[14]	Wolff-Parkinson-White Syndrome with Ventricular Hypertrophy in a Brazilian Family	Case series	n = 60 Sixty patients from 84 members of a Brazilian family with *PRKAG2* syndrome.	The predominant pattern was generalized and diffuse LVH and mitral valve insufficiency. Hypertrophy predominated in the apical and medial portions later in life. The prevalence of mitral regurgitation occurred in the second and third decades of life.
Epicoco G et al. (2018)[15]	An Unusual Pattern of Ventricular Pre-Excitation: Electrophysiological and Genetic Substrate	Case report	n = 1 A 30-year-old man known for ventricular preexcitation and recurrent episodes of typical atrial flutter.	Twelve-lead electrocardiogram showed ventricular preexcitation during sinus rhythm and common atrial flutter. Echocardiography and cardiac magnetic resonance imaging revealed marked and HCM without outflow obstruction (MWT = 28 mm).
Gorla SR et al. (2018)[16]	Infantile Onset HCM Secondary to *PRKAG2* Gene Mutation is Associated with Poor Prognosis	Case report	n = 1 A premature infant delivered at 36 weeks due to fetal hydrops secondary to severe HCM.	A fetal echocardiogram performed at 28 weeks of gestation was significant for a severe form of HCM with involvement of both ventricles, the interventricular septum, and the right atrial wall. Serial postnatal echocardiograms demonstrated hyperdynamic ventricular function (shortening fraction of 49%), diastolic dysfunction, decreased end-diastolic LV volumes (z score of -6), and dynamic LV outflow tract obstruction (peak instantaneous systolic gradient of 58-88 mm Hg) with near complete obliteration of the LV cavity in end systole.
Ahamed H et al. (2020)[17]	Phenotypic expression and clinical outcomes in a South Asian *PRKAG2* cardiomyopathy cohort	Ambispective observational cohort study	n = 50 Twenty-two patients with PRKAG2 cardiomyopathy belonging to 3 unrelated families from Ernakulam and Trichur district in central Kerala, India. The remaining 28 individuals did not exhibit the clinical phenotype of the disease.	The mean LV MWT (n = 19) was 25.3 ± 6.5 mm (range 13-33 mm). The mean LV MWT for the entire 22 patient cohort was 22.9 ± 8.7 mm. Right ventricular hypertrophy was observed in 19 patients with LVH (19/22; 86%), with a mean RV free wall thickness of 7.5 ± 1.3 mm (range 6-11 mm). The mean LV ejection fraction (EF) of all 22 patients was 53.4% ± 6.6% (40%-65%). None of the 22 patients had LV outflow tract obstruction > 30 mm Hg or evidence of systolic anterior movement of the mitral valve.
Hu J et al. PE (2020)[18]	Familial Atrial Enlargement, Conduction Disorder and Symmetric Cardiac Hypertrophy Are Early Signs of *PRKAG2* R302Q	Estudo observacional coorte retrospectivo	n = 10 Ten members of a Chinese family with HCM, 5 of whom were diagnosed with the *PRKAG2* R302Q mutation.	Four (80%) of the patients diagnosed with *PRKAG2* R302Q mutation had LVH. The analysis showed diffuse asymmetric hypertrophy in 3 patients, with a pattern of LV middle-anterior-lateral-inferior wall hypertrophy and especially interventricular septal hypertrophy. One patient showed symmetric hypertrophy, with a thickness of the LV wall and the interventricular septal wall of 1.2 cm (normal value: 0.8-1.0 cm). All patients had atrial enlargement.
Lopez-Sainz A et al. (2020)[19]	Clinical Features and Natural History of *PRKAG2* Variant Cardiac Glycogenosis	Retrospective observational cohort study	n = 90 Patients with PRKAG2 genetic variants recruited from 27 European cardiomyopathy centers.	At the last evaluation in the entire cohort, individuals with PRKAG2 syndrome (68%-75.6%) had LVH (maximum LV thickness ≥ 13 mm) with an MWT of 19 ± 7 mm. In this group, mean LVEF was 57% ± 13%, and 10 patients had LVEF < 50%.

Pena JLB et al. (2021)[20]	Glycogen storage cardiomyopathy (*PRKAG2*): diagnostic findings of standard and advanced echocardiography techniques	Estudo observacional transversal	n = 30 Thirty patients with genetically proven *PRKAG2* syndrome belonging to 5 families with *PRKAG2* gene mutation.	Mean patient age was 39.1 ± 15.4 years. LVH was found in varying degrees in 25 patients (86%), with a mean LV septal thickness of 14.1 ± 4.2 mm. Myocardial mass on M-mode, in g/m² and 4D, was above normal limits in these 25 patients. There was no statistically significant difference between patients with and without a PM. The mean RWT was increased for all hypertrophic patients (0.56 ± 0.18), characterizing concentric hypertrophy. The LAVI was increased in 70% of patients, with a mean value of 38.41 ± 14.9, and patients with PM had a significantly increased LAVI. The mean EF measured by the 3D technique was 55.7% ± 11.2%, but in 7 patients (24%) the EF was below normal limits. Patients with PM had lower fractional shortening and 4D EF, fractional shortening, and global circumferential strain values than patients without PM. No statistically significant difference was detected when comparing other echocardiographic parameters. Men had higher myocardial mass (p = 0.01) and indexed mass values (p = 0.05) than women. No correlation was found between age and hypertrophy-related variables. RV hypertrophy occurred in 90% of patients, and the mean RV lateral wall thickness was 7.9 ± 2.9 mm. Regarding LV diastolic dysfunction, 26% of patients had normal diastolic function, whereas the remaining patients had varying degrees of dysfunction, with a predominance of Grade I and III (according to ASE/EACVI guidelines).
Pena JLB et al. (2022)[21]	Right Ventricle Involvement by Glycogen Storage Cardiomyopathy (*PRKAG2*): Standard and Advanced Echocardiography Analyses	Observational cross-sectional study	n = 30 Thirty patients from 5 families with *PRKAG2* gene mutation (28 with Arg302Gln and 2 with His401Gln).	The median RV lateral wall thickness was 7.0 mm (range 6.0-9.0 mm). In 3 patients, the RV 4-chamber longitudinal strain (RV4LS) was significantly reduced, demonstrating RV wall dyskinesia. The RV was affected in most patients, and RV hypertrophy occurred in 90% of patients, with a regular pattern that involved all portions of the chamber. RVEF was below normal limits (≥ 45%) in 56.7% of patients, and in 7 patients, RVEF was < 35%. RV4LS and RV free wall longitudinal strain (RVFWLS) were below normal reference limits even in asymptomatic patients. A positive correlation was confirmed between RVFWLS and RVEF, indicating that such strain indices are a fast and widely available method to detect dysfunction. Tricuspid regurgitation was detected in half of the patients, but only 4 had pulmonary artery systolic pressure above normal limits.
Tang L et al. (2022)[22]	Echocardiographic characteristics of *PRKAG2* syndrome: a research using three-dimensional speckle tracking echocardiography compared with sarcomeric HCM	Retrospective cross-sectional study	n = 252 Nine patients with *PRKAG2* syndrome, 41 with sarcomere gene mutations and 202 healthy volunteers.	Patients with PRKAG2 syndrome had significantly higher LV wall asymmetry than healthy volunteers (1.42 ± 0.52 vs 0.14 ± 0.14 mm, p = 0.001), with asymmetric septal hypertrophy. RWT was higher in the PRKAG2 group than in the healthy group (0.48 ± 0.15 vs 0.39 ± 0.07, p = 0.002), reaching a pattern of concentric hypertrophy (RWT > 0.42). The LV end-systolic diameter was significantly larger in the PRKAG2 group than in the healthy group (p < 0.05). Patients with PRKAG2 syndrome demonstrated impaired LV diastolic function parameters, including A, e', and E/e', but their LVEF remained normal (PRKAG2 group 62.67% ± 8.56% vs healthy group 65.79% ± 6.88%, p = 0.189). As a limitation of the study, the sample consisted of patients with PRKAG2 syndrome with LVH, but some patients did not have LVH, in addition to the small sample size (n = 9).

Source: Designed by the authors.
n: number of individuals; LVH: left ventricular hypertrophy; PM: pacemaker; MWT: maximum wall thickness; RWT: relative wall thickness; AMI: acute myocardial infarction; HCM: hypertrophic cardiomyopathy; LV: left ventricle; RV: right ventricle; LVEF: left ventricular ejection fraction; EF: ejection fraction. RVFWLS: RV free wall longitudinal strain; LAVI: left atrial volume index

reaching a pattern of concentric hypertrophy. Pena et al.,[21] unlike the previous studies analyzed, brought the perspective of RV involvement in PRKAG2 syndrome by analyzing 30 patients with genetically proven PRKAG2 syndrome. The results showed that the RV was affected in most patients, and RV hypertrophy occurred in 90% of patients, with a regular pattern that involved all portions of the chamber, with a median RV lateral wall thickness of 7.0 mm (range 6.0-9.0 mm). This feature is consistent with the findings of Ahamed et al.[17]

In one of the included studies, Charron et al.,[6] in contrast to the pattern shown by the other studies, described 4 members of the same family with an atypical phenotype of *PRKAG2* gene mutation, characterized by the absence of echocardiographic hypertrophy.

Ejection fraction

In the case reported by Gorla et al.,[16] serial postnatal echocardiograms demonstrated hyperdynamic ventricular function (shortening fraction of 49%), diastolic dysfunction, decreased end-diastolic LV volumes, and dynamic LV outflow tract obstruction (peak instantaneous systolic gradient of 58-88 mm Hg) with near complete obliteration of the LV cavity in end systole.

According to Ahamed et al.,[17] the mean LV ejection fraction (EF) of all 22 patients was 53.4% ± 6.6% (40%–65%), and none of the 22 patients had LV outflow tract obstruction > 30 mm Hg. In the retrospective cohort study by Lopez-Sainz et al.,[19] LVEF was 57% ± 13%, and 10 patients (11.1%) had LVEF < 50%. Pena et al.[20] also found abnormal EF in individuals with PRKAG2 syndrome, with a prevalence of 7 patients (24%) with EF below normal limits, although the mean EF was 55.7% ± 11.2% among the 30 participants. Data from the study conducted by Pena et al.[21] showed that in 56.7% of the 30 study participants with mutations in the PRKAG2 gene, RVEF was below normal limits (≥ 45%), and in 7 patients, this value was < 35%. In the analysis performed by Tang et al.,[22] LVEF remained normal (PRKAG2 group 62.67% ± 8.56% vs healthy group 65.79% ± 6.88%, p = 0.189).

Strain patterns

Pena et al.[20] showed that the left atrial volume index (LAVI) was increased in 70% of patients, with a mean value of 38.41 ± 14.9 mL/m^2, and patients with PM had a significantly increased LAVI. Therefore, there is a change in atrial volume in PRKAG2 syndrome, and patients with PM seem to be more affected. Also, regarding LV diastolic dysfunction, 26% of patients had normal diastolic function, and the remaining patients had varying degrees of dysfunction, with a predominance of Grade I and III (according to ASE/EACVI guidelines).

Tang et al.[22] reported that the LV end-systolic diameter was significantly larger in the PRKAG2 group than in the healthy group ($p < 0.05$), and that the PRKAG2 group also had impaired LV diastolic function parameters.

Using the strain method, a measure of cardiac deformation, Pena et al.[21] found that the RV 4-chamber longitudinal strain (RV4LS) and the RV free wall longitudinal strain (RVFWLS) were below normal reference limits, even in asymptomatic patients. In 3 patients (10%), the RV4LS was significantly reduced, demonstrating RV wall dyskinesia. Furthermore, the authors confirmed a positive correlation between RVFWLS and RVEF, indicating that such strain indices are a fast and widely available method to detect dysfunction.

Heart valve abnormalities

Among the included studies, the first one to report heart valve abnormalities was that of Van der Steld et al.,[14] who observed that the predominant pattern was mitral valve insufficiency, with its prevalence occurring in the second and third decades of life. Later, Torok et al.[13] reported that, of 2 children followed up, one had thickened mitral valve leaflets with shortened chordae, in addition to moderate mitral regurgitation and subsequent LV dilation, whereas the other child was identified with severe mitral regurgitation and moderate tricuspid regurgitation. In the study conducted by Pena et al.,[21] tricuspid regurgitation was detected in half of the patients (n = 15), but only 4 had pulmonary artery systolic pressure above normal limits.

In the article published by Ahamed et al.,[17] none of the 22 patients with PRKAG2 cardiomyopathy had evidence of systolic anterior movement of the mitral valve, an abnormality commonly observed in HCMs secondary to significant septal enlargement.

Limitations

The main limitation is that the evidence included in this review is mostly derived from observational studies, more specifically: 8 case reports; 3 ambispective studies; 2 cross-sectional studies; 4 retrospective cohorts; and 1 case series. Therefore, the evidence is considered to be of low quality, where the main limitations include inadequate patient selection and inclusion, lack of blinding, failure to adequately control for confounding factors, and incomplete patient follow-up.[23] An important factor to be mentioned is the non-standardization of the echocardiographic data, such as the parameters observed during examination (wall thicknesses, strain pattern, EF, etc.), with discrepancies between the studies in the analyzed variables. In addition, some studies have not reported the reference values used to characterize their findings, thus interfering with the conclusions. Furthermore, because PRKAG2 syndrome is rare and probably underdiagnosed, the sample size of the included studies should also be considered a major limitation.

Conclusion

Familial ventricular hypertrophy, associated with other abnormalities, such as ventricular preexcitation and atrial tachyarrhythmias, is one of the signs that should raise the suspicion of PRKAG2 syndrome, and echocardiographic parameters are essential for this diagnosis. Cardiac chamber hypertrophy was demonstrated in most of the included studies, with variations in the location of this hypertrophy and thickness. LVH was the predominant finding, but some studies also reported RV involvement. It is worth noting

that one of the studies detected no cardiac hypertrophy in the patients. Additionally, in the included studies, patients presented with quite different echocardiographic abnormalities and clinical courses, supporting the notion of wide phenotypic variability in patients with *PRKAG2* mutations. Another finding was EF changes in the heart chambers, with reduced LVEF and RVEF. As in the case of hypertrophy, one study also showed conflicting results, where patients with PRKAG2 syndrome had normal LVEF compared with controls, highlighting the instability of the phenotypic expression. Other findings included atrial enlargement and changes in the heart strain pattern, with the presence of wall dyskinesia. Finally, heart valve abnormalities were also described, with reports of the presence of mitral valve insufficiency and thickened mitral valve leaflets, as well as mitral and tricuspid regurgitation.

Acknowledgments

To the Undergraduate Research Scholarship Program of Faculdade de Ciências Médicas de Minas Gerais (FCMMG) in partnership with Hospital Felício Rocho (HFR).

Author Contributions

Conception and design of the research, acquisition of data, analysis and interpretation of the data, statistical analysis, writing of the manuscript and critical revision of the manuscript for intellectual content: Pena JLB, Souza Neto I, Barbosa AP, Santos Neto DA.

Potential Conflict of Interest

No potential conflict of interest relevant to this article was reported.

Sources of Funding

There were no external funding sources for this study.

Study Association

This study is not associated with any thesis or dissertation work.

Ethics Approval and Consent to Participate

This article does not contain any studies with human participants or animals performed by any of the authors.

References

1. Sedaghat-Hamedani F, Kayvanpour E, Tugrul OF, Lai A, Amr A, Haas J, et al. Clinical Outcomes Associated with Sarcomere Mutations in Hypertrophic Cardiomyopathy: A Meta-Analysis on 7675 Individuals. Clin Res Cardiol. 2018;107(1):30-41. doi: 10.1007/s00392-017-1155-5.
2. Porto AG, Brun F, Severini GM, Losurdo P, Fabris E, Taylor MRG, et al. Clinical Spectrum of PRKAG2 Syndrome. Circ Arrhythm Electrophysiol. 2016;9(1):e003121. doi: 10.1161/CIRCEP.115.003121.
3. Marwick TH, Gillebert TC, Aurigemma G, Chirinos J, Derumeaux G, Galderisi M, et al. Recommendations on the Use of Echocardiography in Adult Hypertension: A Report from the European Association of Cardiovascular Imaging (EACVI) and the American Society of Echocardiography (ASE)†. Eur Heart J Cardiovasc Imaging. 2015;16(6):577-605. doi: 10.1093/ehjci/jev076.
4. Lipshultz SE, Sleeper LA, Towbin JA, Lowe AM, Orav EJ, Cox GF, et al. The Incidence of Pediatric Cardiomyopathy in Two Regions of the United States. N Engl J Med. 2003;348(17):1647-55. doi: 10.1056/NEJMoa021715.
5. Magalhães LP, Magalhães EFS, Pinheiro JO, Guabiru AT, Reis FJFBD, Aras R. Long-Term Cardiac Complications of PRKAG2 Syndrome. Arq Bras Cardiol. 2022;118(1):106-9. doi: 10.36660/abc.20210062.
6. Charron P, Genest M, Richard P, Komajda M, Pochmalicki G. A Familial form of Conduction Defect Related to a Mutation in the PRKAG2 Gene. Europace. 2007;9(8):597-600. doi: 10.1093/europace/eum071.
7. Tan HL, van der Wal AC, Campian ME, Kruyswijk HH, ten Hove Jansen B, van Doorn DJ, et al. Nodoventricular Accessory Pathways in PRKAG2-Dependent Familial Preexcitation Syndrome Reveal a Disorder in Cardiac Development. Circ Arrhythm Electrophysiol. 2008;1(4):276-81. doi: 10.1161/CIRCEP.108.782862.
8. Sternick EB, Oliva A, Gerken LM, Magalhães L, Scarpelli R, Correia FS, et al. Clinical, Electrocardiographic, and Electrophysiologic Characteristics of Patients with a Fasciculoventricular Pathway: The Role of PRKAG2 Mutation. Heart Rhythm. 2011;8(1):58-64. doi: 10.1016/j.hrthm.2010.09.081.
9. Fabris E, Brun F, Porto AG, Losurdo P, Serdoz LV, Zecchin M, et al. Cardiac Hypertrophy, Accessory Pathway, and Conduction System Disease in an Adolescent: The PRKAG2 Cardiac Syndrome. J Am Coll Cardiol. 2013;62(9):e17. doi: 10.1016/j.jacc.2013.02.099.
10. Sternick EB, Araújo SA, Rocha C, Gollob M. Myocardial Infarction in a Teenager. Eur Heart J. 2014;35(23):1558. doi: 10.1093/eurheartj/ehu015.
11. Aggarwal V, Dobrolet N, Fishberger S, Zablah J, Jayakar P, Ammous Z. PRKAG2 Mutation: An Easily Missed Cardiac Specific Non-Lysosomal Glycogenosis. Ann Pediatr Cardiol. 2015;8(2):153-6. doi: 10.4103/0974-2069.154149.
12. Müllertz KM, Jensen HK. Variable Primary Phenotypic Manifestations in a Rare Familial form of Wolff-Parkinson-White Syndrome and Hypertrophic Cardiomyopathy. Europace. 2016;18(3):397. doi: 10.1093/europace/euv221.
13. Torok RD, Austin SL, Phornphutkul C, Rotondo KM, Bali D, Tatum GH, et al. PRKAG2 Mutations Presenting in Infancy. J Inherit Metab Dis. 2017;40(6):823-30. doi: 10.1007/s10545-017-0072-0.
14. van der Steld LP, Campuzano O, Pérez-Serra A, Zamorano MMB, Matos SS, Brugada R. Wolff-Parkinson-White Syndrome with Ventricular Hypertrophy in a Brazilian Family. Am J Case Rep. 2017;18:766-776. doi: 10.12659/ajcr.904613.
15. Epicoco G, Ali H, Lupo P, Cappato R. An Unusual Pattern of Ventricular Pre-Excitation: Electrophysiological and Genetic Substrate. JACC Clin Electrophysiol. 2018;4(10):1377-8. doi: 10.1016/j.jacep.2018.05.021.
16. Gorla SR, Raja KR, Garg A, Barbouth DS, Rusconi PG. Infantile Onset Hypertrophic Cardiomyopathy Secondary to PRKAG2 Gene Mutation is Associated with Poor Prognosis. J Pediatr Genet. 2018;7(4):180-4. doi: 10.1055/s-0038-1657763.
17. Ahamed H, Balegadde AV, Menon S, Menon R, Ramachandran A, Mathew N, et al. Phenotypic Expression and Clinical Outcomes in a South Asian PRKAG2 Cardiomyopathy Cohort. Sci Rep. 2020;10(1):20610. doi: 10.1038/s41598-020-77124-9.
18. Hu J, Tang B, Wang J, Huang K, Wang Y, Lu S, et al. Familial Atrial Enlargement, Conduction Disorder and Symmetric Cardiac Hypertrophy Are Early Signs of PRKAG2 R302Q. Curr Med Sci. 2020;40(3):486-92. doi: 10.1007/s11596-020-2207-z.
19. Lopez-Sainz A, Dominguez F, Lopes LR, Ochoa JP, Barriales-Villa R, Climent V, et al. Clinical Features and Natural History of PRKAG2 Variant Cardiac Glycogenosis. J Am Coll Cardiol. 2020;76(2):186-97. doi: 10.1016/j.jacc.2020.05.029.

20. Pena JLB, Santos WC, Siqueira MHA, Sampaio IH, Moura ICG, Sternick EB. Glycogen Storage Cardiomyopathy (PRKAG2): Diagnostic Findings of Standard and Advanced Echocardiography Techniques. Eur Heart J Cardiovasc Imaging. 2021;22(7):800-7. doi: 10.1093/ehjci/jeaa176.

21. Pena JLB, Melo FJ, Santos WC, Moura ICG, Nakashima GP, Freitas NC, et al. Right Ventricle Involvement by Glycogen Storage Cardiomyopathy (PRKAG2): Standard and Advanced Echocardiography Analyses. Arq Bras Cardiol. 2022;119(6):902-9. doi: 10.36660/abc.20210801.

22. Tang L, Li X, Zhou N, Jiang Y, Pan C, Shu X. Echocardiographic Characteristics of PRKAG2 Syndrome: A Research Using Three-Dimensional Speckle Tracking Echocardiography Compared with Sarcomeric Hypertrophic Cardiomyopathy. Cardiovasc Ultrasound. 2022;20(1):14. doi: 10.1186/s12947-022-00284-3.

23. Brasil. Ministério da Saúde. Secretaria de Ciência, Tecnologia e Insumos Estratégicos, Departamento de Ciência e Tecnologia. Diretrizes Metodológicas: Sistema GRADE – Manual de Graduação da Qualidade da Evidência e Força de Recomendação para Tomada de Decisão em Saúde. Brasília: Ministério da Saúde; 2014.

Uhl's Anomaly: Case Report and Differential Diagnosis in an Adult

Isaura Elaine Goncalves Moreira Rocha,[1,2] Paulo Henrique Benevides Siqueira,[1] Beatriz Gonçalves Rocha,[3] Bruno Farias Oliveira,[1] George Elias Luna Martins,[1] Simone Cristina Soares Brandão[2]

Universidade Federal do Cariri,[1] Juazeiro do Norte, CE – Brazil
Universidade Federal de Pernambuco,[2] Recife, PE – Brazil
UNINASSAU, Faculdade de Medicina,[3] Recife, PE – Brazil

Introduction

Uhl's anomaly (UA) is a disorder exclusive to the right ventricle (RV) characterized by the absence of total or partial myocardium, in such a way that the ventricular wall is comprised of the overlapping of the endocardium and the epicardium, with no fatty tissue, or inflammatory or infiltrative process. The muscles of the atria, the interventricular septum and the left ventricle (LV) are not involved in the process.[1,2]

The clinical manifestations are due to right ventricular failure (RVF). Forms with partial involvement may be mildly symptomatic and remain undiagnosed for long periods, and may be confused with other more frequent pathologies that affect the right heart in adult life.[3,4]

This study presents a case of a middle-aged patient with previously undiagnosed UA, with a discussion of complementary exams and differential diagnoses with pathologies that evolve with the dilation of the right chambers and RVF.

Case report

A 60-year-old female patient, with no comorbidities for 5 years, began progressive RVF, progressing to idiopathic pulmonary arterial hypertension. In the initial investigation, at our health service, a computed tomography (CT) scan was performed, which showed discrete bronchiectasis in both lung bases and preserved vascular structures. The echocardiogram showed a marked dilation of the right chambers, diffuse hypokinesia, and a significant thinning of the RV wall, with few trabeculations, massive tricuspid regurgitation, and a pulmonary artery (PA) with normal dimensions. The left chambers were normal and the LV ejection fraction (LVEF) was preserved (videos 1, 2, and 3). The coronary arteries did not exhibit significant obstructive lesions on cardiac catheterization, and the pulmonary vasoreactivity test with nitric oxide showed normal pressure in the AP, with equalized pressures in the right chambers. The findings were complemented with cardiac magnetic resonance (CMR), which showed a marked increase in the right atrium (volume of 121 ml/m², reference value: 27ml/m²), dilated and hypocontractile RV — RV end-diastolic volume (RVDV): 118ml/m²; RV end-systolic volume (RVSV): 90ml/m²; and ejection fraction (EF): 24% —, with thinning of the entire free wall, suggesting an absence of myocardium, with a reduction in its trabeculation. No myocardial contrast uptake was observed following delayed enhancement, compatible with the absence of myocardial fibrosis. The left chambers were normal, as were the AP diameters (Figures 1 and 2).

The patient developed advanced signs of RVF, progressive and refractory ascites, in addition to syncope due to advanced atrioventricular conduction disorders, with pauses of up to 5.8 seconds on a 24-hour Holter monitoring, and with pacemaker implantation (Figure. 3). However, the condition was progressive and refractory, and the patient was referred for palliative care, with a fatal outcome within a few months.

Discussion

UA is classified as a congenital heart disease and was described in 1952 by pathologist Henry Stephen M Uhl.[5,6] Considered a rare disease, with greater occurrence in the pediatric age group, it has fascinated cardiologists around the world due to its great instructive value in relation to other heart conditions. In recent years, it has become more reported beyond the pediatric age group; however, as of 2021, only 15 cases had been described in adult patients.[7-13]

Understanding RV maladaptation in insults of any etiology is based on the concept of the hemodynamic importance of the supraventricular crest. As long as this muscular structure remains intact, RV systole and tricuspid valve function will remain preserved, even when the other walls are damaged by a given process. Therefore, a possible explanation for UA remaining silent for long periods of life, as in the case described, would be a selective involvement of the muscles, in which the supraventricular crest remained functional, ensuring the maintenance of right cardiac output.[8,9]

Pathophysiological hypotheses for UA are derived from individual case studies. Genetic substrate as a determining factor in the process is corroborated by the occurrence in family patterns, including those among twins.[5] Defects

Keywords

Cardiovascular Abnormalities; Heart Ventricles; Diagnosis, Differential

Mailing Address: Isaura Elaine Goncalves Moreira Rocha •
Universidade Federal do Cariri. Rua Tenente Raimundo Rocha, 1635. Postal Code: 63048-080. Juazeiro do Norte, CE – Brazil
E-mail: elaine.goncalves@ufca.edu.br
Manuscript received April 14, 2023; revised August 9, 2023; accepted August 22, 2023
Editor responsible for the review: Tiago Senra

DOI: https://doi.org/10.36660/abcimg.20230039i

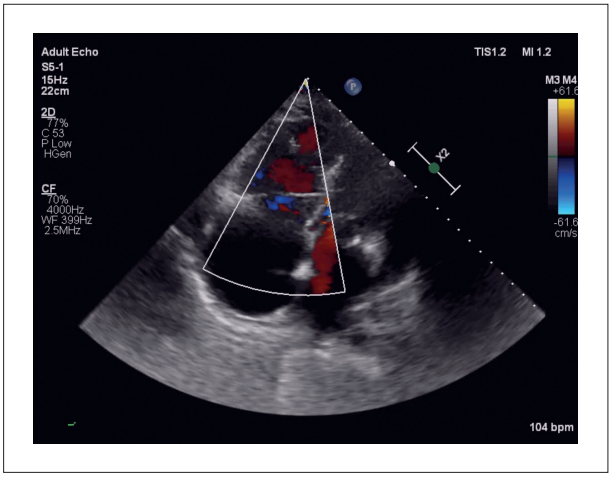

Video 1 – *Link: http://abcimaging.org/supplementary-material/2023/3603/2023-0039_RC_video1_quatro_camaras.mp4*

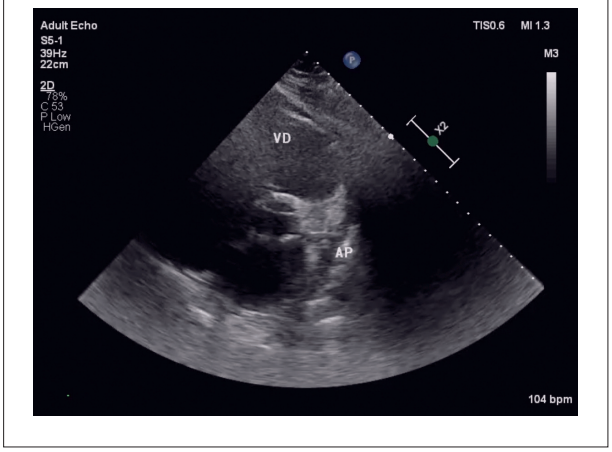

Video 2 – *Link: http://abcimaging.org/supplementary-material/2023/3603/2023-0039_RC_video2_eixo_curto.mp4*

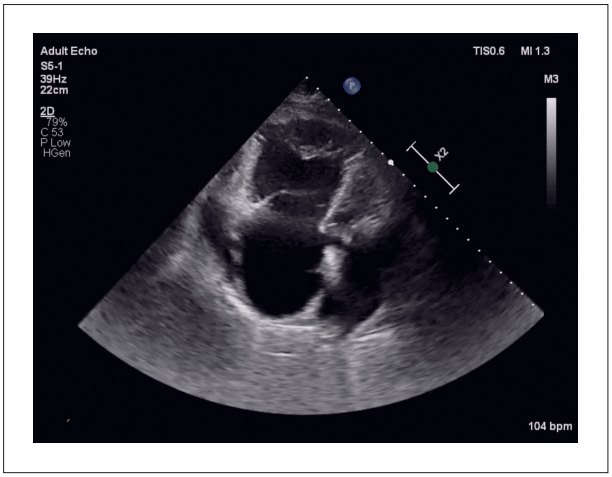

Video 3 – *Link: http://abcimaging.org/supplementary-material/2023/3603/2023-0039_RC_video3_quatro_camaras.mp4*

in the initial stages of embryogenesis, with failure in the development of the right cardiogenic fold due to an unidentified process, can lead to the congenital absence of myocardium restricted to the RV.[4] Selective and uncontrolled apoptotic processes after the myocardium has been formed are corroborated by descriptions of serial fetal echocardiograms, in which progressive thinning of the RV anterior wall, inlet tract and apex, and loss of trabeculations during fetal life are detected,[9,10,11] although electron microscopy and CMR studies have not documented any degree of subsequent myocardial fibrotic degeneration.[12]

The diagnosis must be made based on the clinical picture, associated with imaging methods. In adulthood, treatment-refractory RVF, liver cirrhosis with portal hypertension, sarcopenia, RV aneurysms, arrhythmias, and thromboembolic phenomena are typically observed. Cyanosis can be observed if there is a right-to-left shunt through a patent foramen ovale.[3,11,13,14] Baseline complementary exams include an electrocardiogram and chest X-ray. The ECG shows nonspecific and varied changes, with low voltage QRS complexes; intraventricular conduction disturbances, generally with right bundle branch block; fragmented ventricular depolarization, corresponding to very slow conduction in the RV; atrioventricular conduction blocks; and ventricular tachycardias and paroxysmal supraventricular attacks, in addition to atrial fibrillation as a very common finding. Chest X-rays commonly show cardiomegaly due to the dilation of the right chambers and the dilation of the vena cava.[15,16]

The 24-hour Holter and cardiopulmonary test can be part of the evaluation according to the table presented below. There are no reports on the use of nuclear medicine in UA, but the method could be useful in understanding the pathophysiological mechanism of the destruction of the right ventricular myocardium, through the investigation of inflammation, apoptosis, necrosis, cardiac sympathetic activity, and even fibroblast activation. Hence, several mechanisms of muscle destruction can be studied early and non-invasively through molecular imaging.[17,18]

The echocardiogram usually provides the diagnosis and rules out other possibilities. Characteristically, the left cavities are of normal size, with preserved wall thickness and LVEF. The right atrium is usually markedly dilated, the RV exhibits great dilation and global systolic hypokinesia, and there may be posterior displacement of the interventricular septum during diastole, indicating RV volume overload. The RV wall is markedly thin in circumference, with sparse rudimentary apical trabeculations. The tricuspid ring is quite dilated, with normal insertion, and the leaflets may present mild dysplasia, with restricted movement and complete absence of coaptation, which causes torrential regurgitation and, in more advanced stages, equalization of pressures between the right atrium and the RV. Thrombus formation and slow flow can be observed within the right cavities, in addition to dilation and engorgement of the inferior vena cava and suprahepatic veins, and there may be reverse systolic flow observed on Doppler.[11,13,15]

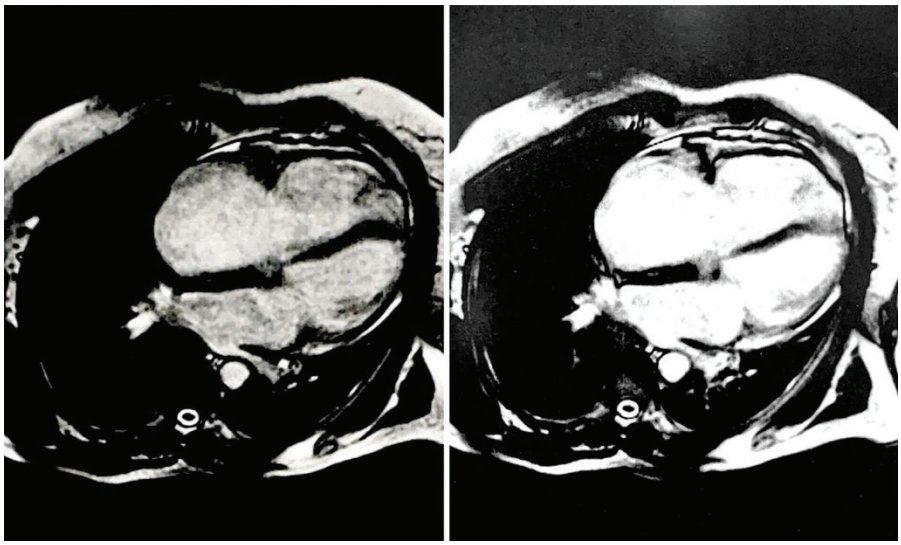

Figure 1 – *Cine-RMC 1A and 1B. Horizontal, long-axis, four-chamber image demonstrating absence of myocardium in the RV. Note the straightened interventricular septum and rejected left ventricular cavity. 1B, images acquired late after the administration of gadolinium, without the presence of contrast uptake (absence of late enhancement).*

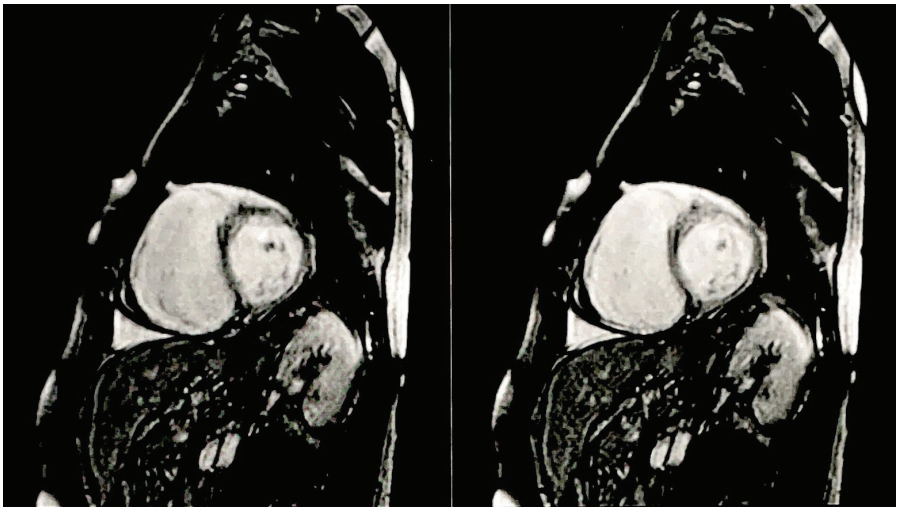

Figure 2 – *Cine – CMR section on the sagittal axis weighted in post-contrast T1, with diffuse enlargement of the RV and thinning of the entire free wall due to the absence of myocardium and reduction of trabeculations.*

CMR, given its high spatial and temporal resolution, in addition to its three-dimensional nature, has excellent accuracy and reproducibility, and is especially useful in the longitudinal monitoring of patients. The examination demonstrates typical RV dilation, with extremely thin walls due to partial or complete absence of the myocardium, a finding described in anatomical specimens as a "parchment" appearance. There is a shortage of apical trabeculations and the contractile function is severely compromised. The delayed enhancement technique typically shows no myocardial contrast uptake, indicating the absence of fibrosis, and there are no fatty infiltrations.[13,16,12] The findings of dilation of the right atrium, normal insertion of the tricuspid valve, deviation to the left of the interventricular septum, and a normal LV can also be seen, similar to what is seen on the echocardiogram.

The less extensive forms of the disease, with partial involvement of the right ventricular cavity, allow for a long asymptomatic phase, with high tolerability of symptoms for decades and late diagnosis,[10,15,18] with a possible

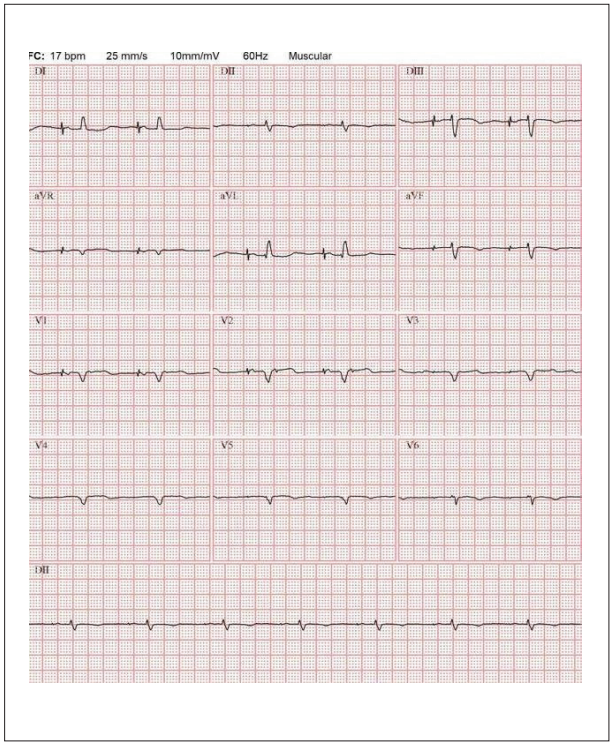

Figure 3 – *Electrocardiogram: rhythm controlled by a pacemaker, with low diffuse voltage in the QRS complexes and absence of R waves in the precordial leads.*

indication of inadequate treatments due to confusion with pathologies that more frequently affect the right heart in adult life. UA can also be found associated with other cardiac malformations, such as dysplasia and agenesis of the tricuspid and pulmonary valves.[19]

Differential diagnosis is made with pathological conditions that result in the dilation of the right heart cavities.[8,9,20] Idiopathic pulmonary arterial hypertension with RVF can lead to diagnostic confusion, due to the relatively high frequency of the disease in the adult population. Arrhythmogenic RV cardiomyopathy, a rare hereditary disease of the heart muscle that causes sudden death due to arrhythmic events resulting from fibrofatty replacement of the RV myocardium and dilation, is an important differential diagnosis, even from the point of view of pathogenesis.[3,20] Ebstein's anomaly, a congenital malformation of the tricuspid valve due to the failure of delamination of the septal cusp, also evolves with RV myopathy and arrhythmias.[21] All of these conditions occur much more frequently than UA and should be considered as a differential diagnosis. both in childhood and in adult life. It is also of interest to differentiate, from a morphological point of view, these forms of serious and potentially lethal involvements of the right heart.

Figure 4 schematically shows the main anatomical characteristics found in the four entities that can establish the differences between them.

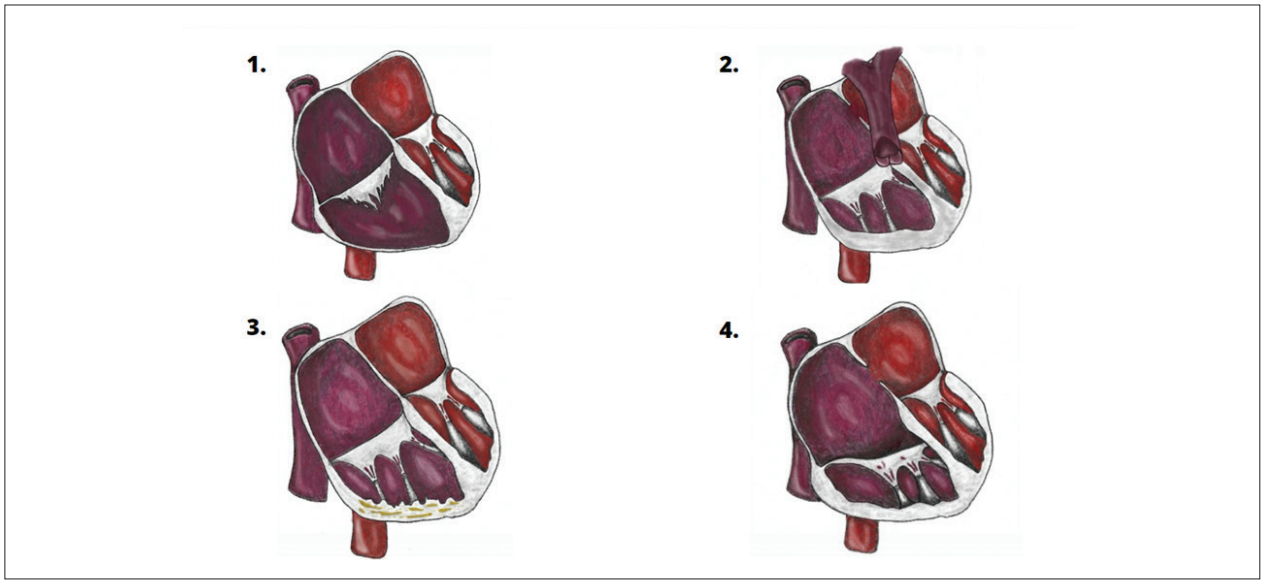

Figure 4 – *Schematic drawing illustrating the main anatomical features found in the right heart chambers in UA, pulmonary arterial hypertension, arrhythmogenic RV cardiomyopathy, and Ebstein's anomaly.*

4.1. UA: *Marked enlargement of the right chambers, thin RV wall, due to absence of the myocardium and few trabeculations, tricuspid valve with normal insertion in the plane of the valve ring.*

4.2. Pulmonary arterial hypertension with RVF: *enlargement of the right chambers, RV with normal thickness, preserved trabeculations, morphologically normal tricuspid valve, interatrial and interventricular septa with bulges toward the left cavities, dilation of the AP, and inferior vena cava.*

4.3. Arrhythmogenic RV cardiomyopathy: *enlargement of the right chambers, hypertrabeculation in the apical region, fatty infiltration in the muscles, and normal tricuspid valve.*

4.4. Ebstein's anomaly: *severe dilation of the right chambers due to "atrialization" of the RV, failure of delamination of the septal leaflet of the tricuspid valve, with apical descent of its orifice, abnormal fenestrations of the anterior leaflet in a "boat sail", and dilation of the right atrioventricular junction.*

Conclusion

Advances in complementary imaging methods with the recognition of this rare cardiac anomaly have made diagnosis possible in adult patients. Reporting this case will help disseminate knowledge to professionals involved in the diagnosis and care for these patients, including radiologists, ultrasonographers, neonatologists, pulmonologists, cardiologists, and cardiac surgeons. Recognition, especially in the early stages of asymptomatic forms, may enable more appropriate management and avoid errors in conduct. Screening first-degree relatives enables the identification of asymptomatic carriers and preventive monitoring.

Differential diagnosis with the most common causes of dilation of the right heart chambers is essential in order to avoid errors in conduct, prevent sudden death, indicate surgical treatment when possible, recommend heart transplantation, provide prenatal counseling, and offer palliative care.

Author Contributions

Conception and design of the research: Rocha IEGM; acquisition of data, writing of the manuscript: Rocha IEGM, Siqueira PHB, Rocha BG, Oliveira BF, Martins GEL; analysis and interpretation of the data: Rocha IEGM, Siqueira PHB, Brandão SCS, Rocha BG, Oliveira BF, Martins GEL; critical revision of the manuscript for intellectual content: Brandão SCS

Potential Conflict of Interest

No potential conflict of interest relevant to this article was reported.

Sources of Funding

There were no external funding sources for this study.

Study Association

This study is not associated with any thesis or dissertation work.

Ethics Approval and Consent to Participate

This study was approved by the Ethics Committee of the Universidade Regional do Cariri (URCA) under the protocol number 65814522.5.0000.5055. All the procedures in this study were in accordance with the 1975 Helsinki Declaration, updated in 2013. Informed consent was obtained from all participants included in the study.

References

1. van der Palen RL, van der Wal AC, Robles de Medina PG, Blom NA, Clur SA. Uhl's Anomaly: Clinical Spectrum and Pathophysiology. Int J Cardiol. 2016;209:118-21. doi: 10.1016/j.ijcard.2016.02.048.
2. Kumar P, Chaturvedi H, Khatri P, Khatri S. Uhl's Anomaly: Rare but Does Exist. Asian Cardiovasc Thorac Ann. 2018;26(7):563-5. doi: 10.1177/0218492316674859.
3. Gerlis LM, Schmidt-Ott SC, Ho SY, Anderson RH. Dysplastic Conditions of the Right Ventricular Myocardium: Uhl's Anomaly vs Arrhythmogenic Right Ventricular Dysplasia. Br Heart J. 1993;69(2):142-50. doi: 10.1136/hrt.69.2.142.
4. Karadas U, Bakiler AR, Eliaçik K, Çavusoglui D, Ulger Z. Uhl´s Anomaly: A Rara Cause of Cardiomegaly. Paediatrics Today. 2014;10(2):154-8. doi: 10.5457/p2005-114.101.
5. Uhl HS. A Previously Undescribed Congenital Malformation of the Heart: Almost Total Absence of the Myocardium of the Right Ventricle. Bull Johns Hopkins Hosp. 1952;91(3):197-209.
6. Uhl HS. Uhl's Anomaly Revisited. Circulation. 1996;93(8):1483-4. doi: 10.1161/01.cir.93.8.1483.
7. Diggelmann U, Baur HR. Familial Uhl's Anomaly in the Adult. Am J Cardiol. 1984;53(9):1402-3. doi: 10.1016/0002-9149(84)90102-4.
8. James TN. Anatomy of the Crista Supraventricularis: Its Importance for Understanding Right Ventricular Function, Right Ventricular Infarction and Related Conditions. J Am Coll Cardiol. 1985;6(5):1083-95. doi: 10.1016/s0735-1097(85)80313-2.
9. Sanz J, Sánchez-Quintana D, Bossone E, Bogaard HJ, Naeije R. Anatomy, Function, and Dysfunction of the Right Ventricle: JACC State-of-the-Art Review. J Am Coll Cardiol. 2019;73(12):1463-82. doi: 10.1016/j.jacc.2018.12.076.
10. Dixon DB, Mackey-Bojack SM, Sivanandam S. Uhl's Anomaly: Perspective of Fetal Echocardiography and Histopathological Correlation. Cardiol Young. 2017;27(2):388-90. doi: 10.1017/S1047951116001232.
11. Mihos CG, Larrauri-Reyes M, Yucel E, Santana O. Clinical Presentation and Echocardiographic Characteristics of Uhl's Anomaly. Echocardiography. 2017;34(2):299-302. doi: 10.1111/echo.13430.
12. Greer ML, MacDonald C, Adatia I. MRI of Uhl's Anomaly. Circulation. 2000;101(24):E230-2. doi: 10.1161/01.cir.101.24.e230.
13. Caruso S, Cannataci C, Romano G. Case 288: Uhl Anomaly. Radiology. 2021;299(1):237-41. doi: 10.1148/radiol.2021192475.
14. Ikari NM, Azeka E, Aiello VD, Atik E, Barbero-Marcial M, Ebaid M. Uhl's Anomaly. Differential Diagnosis and Indication for Cardiac Transplantation in an Infant. Arq Bras Cardiol. 2001;77(1):69-76. doi: 10.1590/s0066-782x2001000700008.
15. James TN, Nichols MM, Sapire DW, DiPatre PL, Lopez SM. Complete Heart Block and Fatal Right Ventricular Failure in an Infant. Circulation. 1996;93(8):1588-600. doi: 10.1161/01.cir.93.8.1588.
16. Otmani A, Leborgne L, Renard C, Bakkour H, Quenum S, Tribouilloy C, et al. Images in Cardiovascular Medicine. Electrocardiogram, Echocardiography, and Magnetic Resonance Imaging Characteristics in Uhl's Disease. Circulation. 2007;115(2):e11-2. doi: 10.1161/CIRCULATIONAHA.106.630061.
17. Wang L, Wang Y, Wang J, Xiao M, Xi XY, Chen BX, et al. Myocardial Activity at 18F-FAPI PET/CT and Risk for Sudden Cardiac Death in Hypertrophic Cardiomyopathy. Radiology. 2023;306(2):e221052. doi: 10.1148/radiol.221052.
18. Martineau P, Grégoire J, Harel F, Pelletier-Galarneau M. Assessing Cardiovascular Infection and Inflammation with FDG-PET. Am J Nucl Med Mol Imaging. 2021 Feb 15;11(1):46-58.

19. Kim T, Ko H, Byun JH, Lee HD, Kim H, Choi K, et al. A Case of Prenatally Diagnosed Uhl's Anomaly with Absent Pulmonary Valve Leaflets and Dysplastic Tricuspid Valve. Children (Basel). 2021;8(3):190. doi: 10.3390/children8030190.

20. Basso C, Corrado D, Marcus FI, Nava A, Thiene G. Arrhythmogenic Right Ventricular Cardiomyopathy. Lancet. 2009;373(9671):1289-300. doi: 10.1016/S0140-6736(09)60256-7.

21. Holst KA, Connolly HM, Dearani JA. Ebstein's Anomaly. Methodist Debakey Cardiovasc J. 2019;15(2):138-44. doi: 10.14797/mdcj-15-2-138.

Cardiac Tamponade: Initial Clinical Presentation of Fibrosing Mediastinitis

Aluísio José de O. Monteiro Neto,[1] *Vitor Medeiros Delgado,*[1] *Filipe Melo A. Leite,*[1] *Álvaro Braga Dutra,*[1] *Marcelo Dantas Tavares de Melo*[1]

Universidade Federal da Paraíba,[1] *João Pessoa, PB – Brazil*

Introduction

Fibrosing mediastinitis (FM) is a rare condition characterized by the proliferation of fibrotic tissue in the mediastinum, presenting as a concentrated mass or diffuse infiltration.[1,2] Clinical conditions can range from benignity to obstruction of critical mediastinal structures, such as vessels, airways, and the esophagus.[3] Common complaints are cough, dyspnea, recurrent pulmonary infection, hemoptysis, and pleuritic pain.[2] Pericardial involvement is not frequently reported in the literature. In this article, we describe a rare case of major pericardial effusion with cardiac tamponade as an initial presentation of FM in a patient with cancer.

Description

A 64-year-old female patient with hormone receptor-positive and human epidermal growth factor receptor 2-positive breast cancer of the invasive ductal carcinoma subtype underwent a mastectomy in 2018 and received adjuvant treatment with paclitaxel and trastuzumab, followed by anastrozole. During routine oncology follow-up, a chest radiograph revealed enlargement of the cardiac area. Additional investigation with echocardiography showed significant pericardial effusion with hemodynamic repercussions (Figure 1, Video 1) requiring urgent pericardial drainage. Pericardial fluid analysis and histology did not indicate neoplastic involvement but showed inflammatory findings. Pericardial fluid cultures were performed and were negative. Following the surgical procedure, the echocardiogram revealed a significant increase in thickness in the right atrium and atrioventricular groove. Computed tomography (CT) of the chest revealed significant evidence of FM, with extensive involvement of the middle and posterior mediastinum, including the arch and descending aorta, and extension into both pleural spaces (Figure 2). One year later, the patient continues to receive treatment with anastrozole and colchicine and remains asymptomatic.

Keywords

Mediastinitis; Breast Neoplasms; Cardiac Tamponade

Mailing Address: Marcelo Dantas Tavares de Melo •
Universidade Federal da Paraíba. Av. Maria Rosa, 441. Postal code: 58051-900; João Pessoa, PB – Brazil
E-mail: marcelot@alumni.usp.br
Manuscript received April 6, 2023; revised July 19, 2023; accepted August 23, 2023
Editor responsible for the review: Alexandre Souza

DOI: https://doi.org/10.36660/abcimg.20230038i

Discussion

FM is a rare disorder resulting from excessive fibrotic proliferation in the mediastinum.[1] Although the pathogenesis of this condition is not fully understood, the most probable cause is an immunological trigger for the proliferation of fibroblast cells.[4] FM can be idiopathic or secondary to other conditions such as infections and malignancies. Infectious causes include tuberculosis, aspergillosis, cryptococcosis, and histoplasmosis, the latter being the most common one, especially in endemic regions. Other conditions associated with FM are radiation therapy, malignancies (especially lymphoma and mesothelioma), sarcoidosis, and medications.[5] In addition to these, some chemotherapy drugs such as paclitaxel, cyclophosphamide, bleomycin, busulfan, carmustine, and gemcitabine are associated with pulmonary fibrosis and may be related to FM.[6]

After left mastectomy, the patient received adjuvant chemotherapy treatment with paclitaxel and trastuzumab, followed by anastrozole, without exposure to other known risk factors for FM. Due to the paucity of publications about FM, epidemiological data are still insufficient.[5]

Cardiac tamponade, on the other hand, is caused by the accumulation of fluid in the pericardial sac, hindering the physiological functioning of the heart. The most common symptoms are tachypnea, tachycardia, and hemodynamic instability, in addition to an increase in systemic venous pressure. The occurrence of tamponade due to compression of the cardiac chambers by a mass, such as the FM described, is uncommon.[7] Considering the aforementioned, to the best of our knowledge, this is the first report in the literature of FM initially presenting as cardiac tamponade.

Most patients with FM present with signs or symptoms related to obstruction or compression of critical mediastinal structures, such as the central airways, superior vena cava, pulmonary veins, pulmonary arteries, and the esophagus. The heart, pericardium, coronary arteries, aorta, and aortic branch vessels are much less frequently involved.[8] Interestingly, our patient only presented mild complaints related to large pericardial effusion and the extensive involvement of the mediastinum and retroperitoneum.

Clinical and laboratory findings in FM are nonspecific.[9] Imaging tests such as chest radiography, contrast-enhanced chest CT, positron emission tomography (PET), and chest magnetic resonance imaging (MRI) are important to

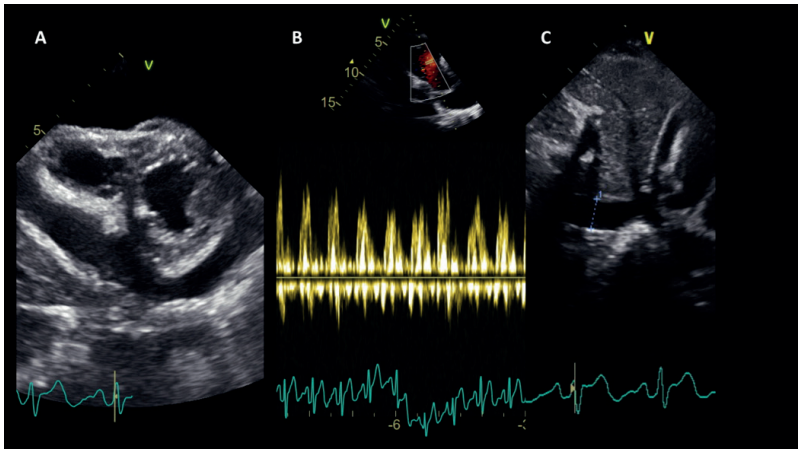

Figure 1 – *Transthoracic echocardiogram showing a large pericardial effusion (A), respiratory variation in tricuspid valve higher than 40% (B), and subxiphoid view of the dilated inferior vena cava greater than 2.1 cm (C).*

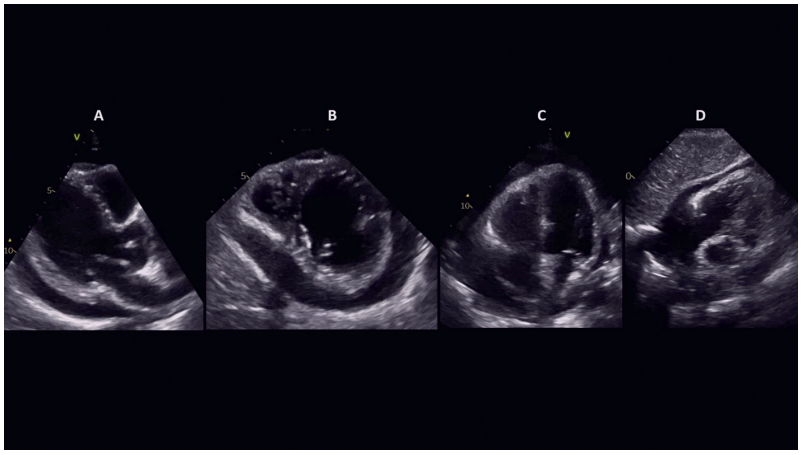

Video 1 – *Two-dimensional echocardiogram showing significant anechoic pericardial effusion with signs of hemodynamic repercussion. Parasternal long-axis view (A); Parasternal short-axis view (B); Apical four-chamber view (C); Subcostal view (D).*
Link: http://abcimaging.org/supplementary-material/2023/3603/2023-0038_RC_video_1.mp4

assess the extent of fibrosis and to guide and monitor therapeutic interventions.[10] However, they do not confirm the diagnosis—they only suggest it. Confirmation is only possible through histopathological evaluation performed after thoracotomy, as ultrasound- or CT-guided biopsy does not obtain enough fragments for the differential diagnosis.[9,10]

Chest radiography has low sensitivity and specificity for FM. Its findings include mediastinal enlargement, presence of pulmonary infiltrates, and a mediastinal or hilar mass that may or may not contain calcifications, airway narrowing, or septum enlargement.[9,10] In the present case, the only change in the chest radiograph was an increase in the cardiac area due to pericardial effusion. Contrast-enhanced chest CT is the imaging method of choice for diagnosis, although it does not differentiate between malignant and benign conditions in the absence of clear signs of metastasis.[10] CT may have a focal or diffuse FM pattern. The focal pattern, marked by the presence of a localized, often calcified mediastinal mass of soft-tissue attenuation in the right paratracheal or subcarinal region, is associated with histoplasmosis. On the other hand, the diffuse pattern is marked by a diffusely infiltrating, often noncalcified mass affecting multiple mediastinal compartments and that may extend into the retroperitoneum.[8,10] PET-CT also does not allow the differentiation between malignant and benign causes, but may assist in the diagnosis and determination of target sites for biopsy, in addition to providing information on response to therapeutic interventions.[10] MRI is similar to CT in determining the extension and involvement of adjacent structures in FM, but it does not consistently demonstrate calcifications.[9] Unfortunately,

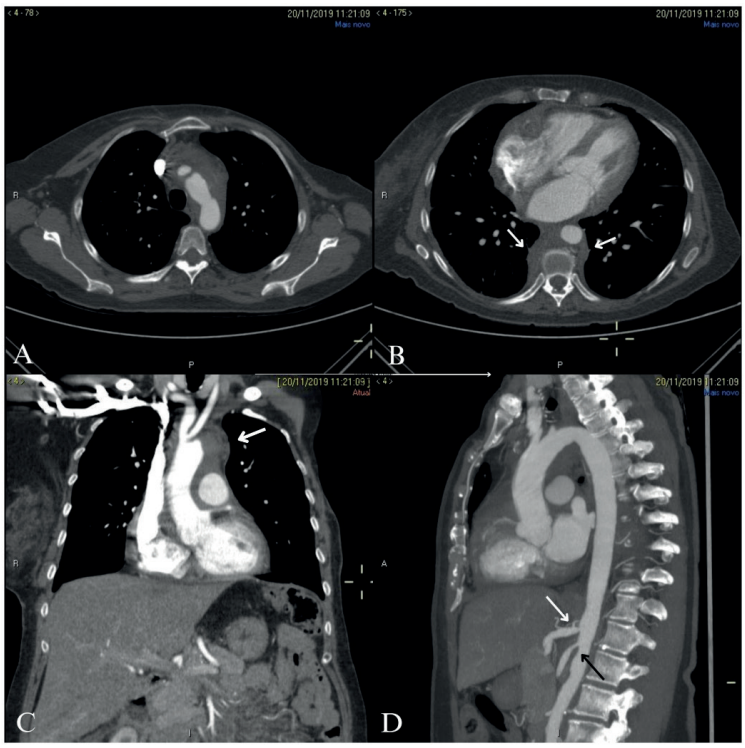

Figure 2 – *CECT (mediastinal window). A-C: axial plane, shows a soft-tissue attenuation mass diffusely infiltrating the middle and posterior mediastinum, involving the arch (A) and descending (B) aorta and extending into both pleural spaces (arrows in B). Coronal plane highlighting enlargement and signs of fibrosis in the mediastinal region (C). Maximum intensity projection (MIP) (D), the periaortic mass continued into the upper abdomen encasing and narrowing the origin of celiac trunk (white arrow) and superior mesenteric artery (black arrow).*

echocardiographic evaluation of the mediastinum is challenging. However, some findings, such as pericardial effusion, constrictive pericarditis, and thickening of cardiac structures surrounding the heart, may be present in FM.

FM usually has an unpredictable course, with spontaneous remission or symptom exacerbation. The most common causes of death are recurrent infection, hemoptysis, or cor pulmonale. The mortality rate of patients with bilateral subcarinal or mediastinal involvement is higher than that of patients with more localized mediastinal or hilar fibrosis.[8] Awareness of this condition is low, and it is often suspected only in the presence of clear signs. Although the prognosis tends to be severe, as the diagnosis is often delayed and most patients die due to compression of critical structures within the mediastinum, our patient no longer presents pericardial effusion, and all symptoms have resolved.[4]

Conclusion

FM is a rare and severe disease whose diagnosis is challenging and often delayed. The importance of multimodal imaging, particularly in the oncologic setting, cannot be understated, as it plays a crucial role in the early detection and management of this condition. In terms of prognosis, FM is often associated with a poor outcome, as patients frequently experience compression of critical structures within the mediastinum, resulting in life-threatening complications. Further research and awareness are needed to achieve timely diagnosis and optimize treatment strategies for FM.

Author Contributions

Conception and design of the research, writing of the manuscript, critical revision of the manuscript for intellectual content: Monteiro Neto AJO, Delgado VM, Leite FMA, Dutra AB, Melo MDT; acquisition of data, analysis and interpretation of the data: Melo MDT.

Potential Conflict of Interest

No potential conflict of interest relevant to this article was reported.

Sources of Funding

There were no external funding sources for this study.

Study Association

This study is not associated with any thesis or dissertation work.

References

1. Lima TC, Marchiori E, Capone D, Barreto MM, Rodrigues RS, Zanetti G. Mediastinite Fibrosante: Relato de caso. Radiol Bras. 2009;42(5):337-9.
2. Rodríguez E, Soler R, Pombo F, Requejo I, Montero C. Fibrosing Mediastinitis: CT and MR Findings. Clin Radiol. 1998;53(12):907-10. doi: 10.1016/s0009-9260(98)80218-3.
3. Wu Z, Jarvis H, Howard LS, Wright C, Kon OM. Post-Tuberculous Fibrosing Mediastinitis: A Review of the Literature. BMJ Open Respir Res. 2017;4(1):e000174. doi: 10.1136/bmjresp-2016-000174.
4. Chatterjee D, Bal A, Singhal M, Vijayvergiya R, Das A. Fibrosing Mediastinitis Due to Aspergillus with Dominant Cardiac Involvement: Report of Two Autopsy Cases with Review of Literature. Cardiovasc Pathol. 2014;23(6):354-7. doi: 10.1016/j.carpath.2014.05.005.
5. Rossi GM, Emmi G, Corradi D, Urban ML, Maritati F, Landini F, et al. Idiopathic Mediastinal Fibrosis: A Systemic Immune-Mediated Disorder. A Case Series and a Review of the Literature. Clin Rev Allergy Immunol. 2017;52(3):446-59. doi: 10.1007/s12016-016-8584-1.
6. Co MLF, Patel HN, Agdamag AC, Okwuosa TM. Fibrosing Mediastinitis-Related Pulmonary Artery and Vein Stenosis-Limiting Chemotherapy. BMJ Case Rep. 2018;2018:bcr2017221905. doi: 10.1136/bcr-2017-221905.
7. Appleton C, Gillam L, Koulogiannis K. Cardiac Tamponade. Cardiol Clin. 2017;35(4):525-37. doi: 10.1016/j.ccl.2017.07.006.
8. Rossi SE, McAdams HP, Rosado-de-Christenson ML, Franks TJ, Galvin JR. Fibrosing mediastinitis. Radiographics. 2001;21(3):737-57. doi: 10.1148/radiographics.21.3.g01ma17737.
9. Atasoy C, Fitoz S, Erguvan B, Akyar S. Tuberculous Fibrosing Mediastinitis: CT and MRI Findings. J Thorac Imaging. 2001;16(3):191-3. doi: 10.1097/00005382-200107000-00011.
10. Kim J, Hwang JH, Nam BD, Park YW, Jeen YM. Mediastinal and Retroperitoneal Fibrosis as a Manifestation of Breast Cancer Metastasis: A Case Report and Literature Review. Medicine (Baltimore). 2018;97(32):e11842. doi: 10.1097/MD.0000000000011842.

Case Report

Prosthetic Aortic Valve Endocarditis With Extensive Para-Aortic Abscess: The Relevance of Multimodal Imaging

Bernardo Boccalon,[1] André Barcellos Amon,[1] Thiago Ferreira Serafini,[1] Álvaro Schmidt Albrecht,[2] Murilo Foppa,[1,2] Angela Barreto Santiago Santos[1,2]

Programa de Pós-Graduação em Cardiologia e Ciências Cardiovasculares, Faculdade de Medicina da Universidade Federal do Rio Grande do Sul (UFRGS),[1] Porto Alegre, RS – Brazil

Hospital de Clínicas de Porto Alegre (HCPA),[2] Porto Alegre – Brazil

Introduction

Infectious endocarditis (IE) is defined as the infection of the endocardium or prosthetic material in the heart, whose pathogenesis is bacterial adherence to the vulnerable endocardium or implanted prosthetic material during a bacteremia.[1] Its clinical presentation is highly variable, depending on the micro-organism that causes it, underlying heart conditions and preexisting comorbidities.[2] The annual estimated incidence of IE is up to 10/100,000 in western countries, and mortality of up to 30% in 30 days.[3]

Description

A 64-year-old woman searched for outpatient care due to cervical pain for three weeks, night sweats, shivering and myalgia. Besides, she complained of precordial pain, intensity 4/10, with a squeezing feeling. Her medical history showed a surgery to replace the aortic valve due to severe aortic stenosis (bicuspid aortic valve), carried out in August, 2018, with an implant of a Mosaic Ultra porcine biologic prosthesis n. 21 (Medtronic). The patient denied having had dental treatments or other invasive procedures in the past ten months.

At physical examination, the patient presented with 94 bmp heart rate (HR), blood pressure (BP) of 150/86 mmHg, with regular rhythm at heart auscultation and rude systolic murmur in the aortic focus, with 3/6+ intensity. As to the other systems, there was no neurological deficit, she was lucid and conscious, without skin changes suggestive of vascular/immunological phenomena, normal kidney function, as well as qualitative urine test.

The choice was to perform an ambulatory investigation of her clinical condition by collecting laboratory examinations, including peripheral blood culture and transthoracic echocardiogram (TTE) due to the hypothesis of IE. Laboratory examinations showed leukocytosis (total leukocyte count – 15,150 μg/L), with prevalence of neutrophils (11,910 μg/L) and increased C-reactive protein (CRP – 20.8 mg/L). Hemoglobin, electrolytes, creatinine and urea were within normal limits. There was increased *Streptococcus anginosus* in one of the blood culture samples, and TTE showed images that suggested vegetations in the aortic valve prosthesis. Therefore, the patient was admitted to a secondary health care institution and was started on intravenous antibiotic therapy with oxacillin, gentamicin and ceftriaxone, solving the initially presented clinic.

Transfer to a tertiary hospital

The patient remained hospitalized for ten days until being transferred to a tertiary hospital to continue with evaluation and treatment. At arrival, the patient was hemodynamically stable, with no fever nor complaints about pain or dyspnea. At physical examination, she remained with systolic murmur in aortic focus, rude, 3/6+. There were no changes in other systems.

Laboratory examinations showed discreet leukocytosis (total leukocyte count – 11,580 μg/L), with prevalence of neutrophils (8,740 μg/L), besides high CRP (140 mg/L), but without increase in micro-organisms in the three pairs of collected blood cultures. The electrocardiogram showed sinus rhythm with normal PR interval, axis in -30º and without changes in ventricular repolarization. Chest x-ray with sternal suture wires, with no other changes.

The TTE performed at admission showed left ventricle with normal dimensions and parietal thickness, and preserved ejection fraction (66% through the Teichholz method). The biological aortic prosthesis presented images with independent mobility in its ventricular wall, suggestive of vegetations, besides mild transvalvular and minimum paravalvular regurgitation, with suspected structural obstructive dysfunction of the biological prosthesis (peak velocity of 3.8 m/s; maximum/medium gradients = 57/38 mmHg and velocity–time integral ratio (VTI) of 0.45; opening time = 112 ms).

The choice was for the maintenance of the antimicrobial treatment with ceftriaxone and gentamicin, with progressive reduction of CRP and normalization of the leukogram, remaining without fever until the 18th day of treatment, when the patient began presenting a subfebrile curve (37.6º) and changes in cardiac rhythm, alternating periods of bigeminy ventricular extrasystole, sinus rhythm and atrial fibrillation with high ventricular response.

Keywords

Endocarditis; Heart Valve Prosthesis Implantation; Diagnostic Imaging

Mailing Address: Bernardo Boccalon •
Hospital de Clínicas de Porto Alegre. R. Ramiro Barcelos, 2350, Sala 2061. Postal code: 90035-903. Santa Cecília, Porto Alegre, RS – Brazil
E-mail: boccalonbernardo@gmail.com
Manuscript received July 9, 2023; revised manuscript August 1, 2023; accepted August 7, 2023
Editor responsible for the review: Daniela do Carmo Rassi Frota

DOI: https://doi.org/10.36660/abcimg.20230068i

For the evaluation of complications related to IE, a transesophageal echocardiogram (TEE) was performed and confirmed the hyperechogenic image adhered to the anatomic correspondent of the left coronary leaflet, moveable, with maximum diameter of 11 mm, suggestive of vegetation, and minimum paravalvular regurgitation. Besides, there was a posterior paraortic hyperechogenic structure involving the ascending aorta, with no flow in its interior, and maximum diameter of 24 mm, suggestive of abscess (Figure 1).

CTs with contrast were conducted for the accurate evaluation of the paraortic image. The changes that were found were suggestive of infectious collection in the aortic root and the left atrium wall, measuring 53x33 mm in the larger axis (Figure 2). There were images suggestive of abscesses in the upper third of the right kidney and the right upper lobe of the lung.

The patient was referred to emergency surgery, which identified a large abscess involving the aortic root, from the left coronary ostium to the right coronary, with disjunction of the aortic prosthesis and the left ventricular outflow tract (LVOT) in 90% of its circumference. Besides, there was presence of pannus in the subvalvular region, determining stenosis of the LVOT (Figure 3).

An aortic prosthesis resection was performed, with debridement of the paravalvular abscess, circumferential reconstruction of the LVOT from the muscle to the subcoronary plan, with a bovine pericardial patch and implant of biological aortic prosthesis n. 19.

The post-operative Evolution required the implantation of a definitive dual-chamber pacemaker due to a total persistent atrioventricular block. In spite of that, recovery was more satisfactory, and laboratory examinations showed no changes suggestive of ongoing infectious processes, normal functioning aortic prosthesis in TTE and hospital discharge after the antimicrobial therapy

Discussion

The diagnosis of IE is challenging, because the early symptoms can be unspecific and variable. Signs such as persistent fever, night sweats, fatigue, weight loss and joint pain can indicate the condition. Medical history of the patient, including the presence of predisposing conditions, such as prosthetic heart valves or previous heart disease, increase the changes of diagnosis.[4]

The early collection of examinations, such as blood culture, aiming at the identification of the micro-organism that causes IE, is extremely important for the clinical

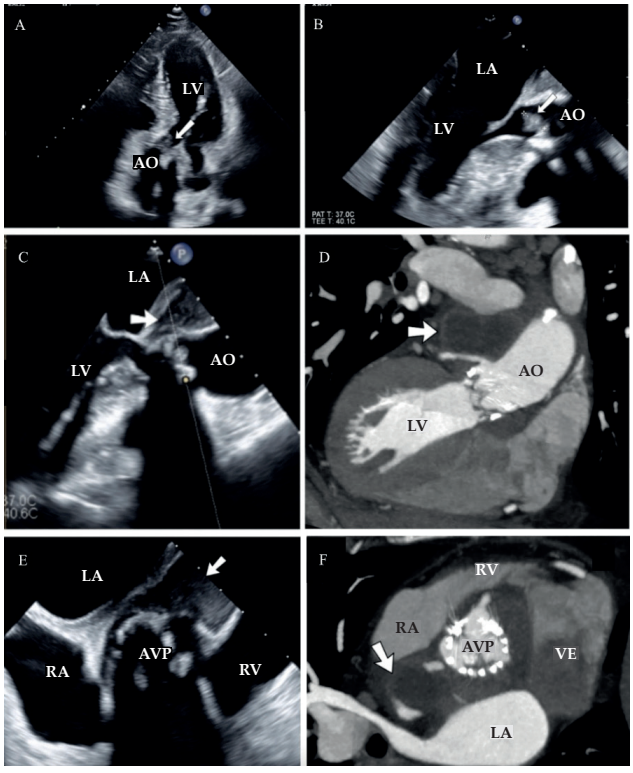

Figure 1 – *A) arrow indicating vegetation in the left ventricular outflow; B) visualized in the TTE and ETE; C e E) abscess between the anterior aortic wall and the left atrium visualized in the TEE; D e F) abscess between the anterior aortic wall and the left atrium visualized in computed tomography. AO: Aorta; LA: left atrium; RA: right atrium; LV: left ventricle; RV: right ventricle; AVP: aortic valve prosthesis.*

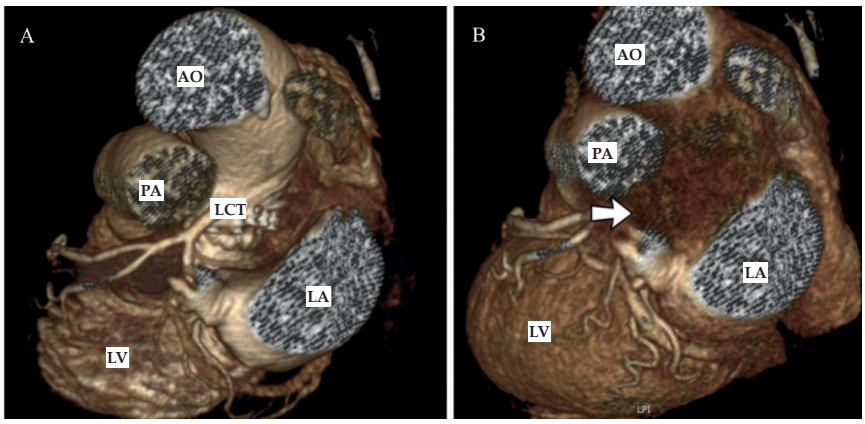

Figure 2 – *A) 3D renderization with superior view showing the aortic root and the origin of the left coronary artery; B) renderization showing the abscess (arrow) involving the aortic ring and the origin of the left coronary. LA: left atrium; LV: left ventricle; PA: pulmonary artery; AO: Aorta; LCT: left coronary trunk.*

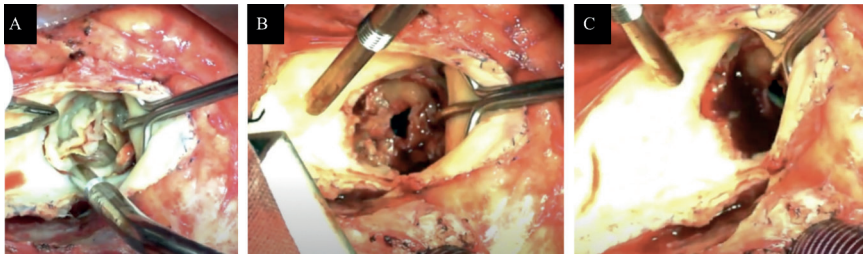

Figure 3 – *Vision by oblique aortotomy. A) Previous aortic prosthesis; B) Abscess, pus and subvalvular pannus after exeresis of the infected prosthesis; C) pus drainage from left infra-coronary abscess with fistulous tract towards the atrial roof (pseudoaneurysm).*

management of this condition, allowing an adequate antimicrobial treatment, which results in better outcomes for the patient. Even if IE caused by *Streptococcus anginosus* is relatively rare, when it occurs there are higher chances of the formation of perivalvular abscesses and higher mortality rates. These germs are uniformly susceptible to beta-lactam antibiotics, recommending the treatment with an antimicrobial of that class (in the case reported above, ceftriaxone was used), associated with gentamicin in the two first weeks of treatment.[5]

The imaging examinations are part of the diagnosis and follow-up, and echocardiogram is the examination of choice. However, it is important to recognize that endocarditis may present variations in clinical manifestation, which may affect the sensitivity of imaging examinations. Currently, the sensitivity for the diagnosis of vegetations in native and prosthetic valves is estimated in 70% and 50%, respectively, for TTE; and 96% and 92%, respectively, for TEE. The sensitivity of TTE for the diagnosis of abscesses is about 50%, in comparison to 90% of the TEE.[5] Other imaging modalities may be necessary, such as CT and cardiac magnetic resonance, especially in the evaluation of complications (abscess/pseudoaneurysm), as in the presented case, in which there is an increase in the accuracy of the anatomic details of these structures.[6,7] Patients with heart prostheses have higher chances of IE and of developing complications related to endocarditis, since the micro-organisms interfere in the perivalvular tissue when invading the prosthetic ring, which increases the risk of abscess, pseudoaneurysm, formation of fistula and valve dehiscence.[8] The mechanical complications of IE need to be considered in case of hemodynamic deterioration and/or absence of clinical improvement with the adequate antimicrobial treatment, or the onset of changes in cardiac rhythm in cases of aortic prosthesis, which should be treated at a reference center.[2]

The complications of IE are frequent causes of early surgical intervention before the conclusion of the antibiotic therapy, for being associated with higher mortality rates, embolic events and recurrence of IE in the first five years after the initial infection. Heart surgery aims at removing infected tissues, repairing or replacing non-functional valves and correcting abnormalities to restore the adequate heart function.[9]

Therefore, it is essential to pay attention to factors such as the presence of heart prosthesis, intracardiac complications and specific clinical conditions of the patient

to guarantee a comprehensive and assertive diagnostic approach of this condition. The judicious integration of clinical findings with the interpretation of imaging examinations allows a better assessment and therapeutic conduction for patients with suspected endocarditis.

Author Contributions

Conception and design of the research: Boccalon B, Foppa M; acquisition of data: Boccalon B, Amon AB, Serafini T, Albrecht A, Foppa M, Santos ABS; a nalysis and interpretation of the data: Boccalon B, Amon AB, Foppa M; writing of the manuscript: Boccalon B, Serafini T; critical revision of the manuscript for intellectual content: Amon AB, Albrecht A, Foppa M, Santos ABS.

Potential Conflict of Interest

No potential conflict of interest relevant to this article was reported.

Sources of Funding

There were no external funding sources for this study.

Study Association

This study is not associated with any thesis or dissertation work.

Ethics Approval and Consent to Participate

This article does not contain any studies with human participants or animals performed by any of the authors.

References

1. Østergaard L, Valeur N, Tuxen CD, Bundgaard H, Iversen K, Moser C, et al. Infective Endocarditis. Ugeskr Laeger. 2022;184(12):V10210751.
2. Rajani R, Klein JL. Infective Endocarditis: A Contemporary Update. Clin Med. 2020;20(1):31-5. doi: 10.7861/clinmed.cme.20.1.1.
3. Mostaghim AS, Lo HYA, Khardori N. A Retrospective Epidemiologic Study to Define Risk Factors, Microbiology, and Clinical Outcomes of Infective Endocarditis in a Large Tertiary-Care Teaching Hospital. SAGE Open Med. 2017;5:2050312117741772. doi: 10.1177/2050312117741772.
4. Larry MB, Anavekar NS, Crestanello JA, Wilson WR. Infectious Endocarditis and Infections of Indwelling Devices. In: Libby P, editor. Braunwald's Heart Disease: A Textbook of Cardiovascular Medicine. New York: Elsevier; 2022. p. 1505-30.
5. Habib G, Lancellotti P, Antunes MJ, Bongiorni MG, Casalta JP, Del Zotti F, et al. 2015 ESC Guidelines for the Management of Infective Endocarditis: The Task Force for the Management of Infective Endocarditis of the European Society of Cardiology (ESC). Endorsed by: European Association for Cardio-Thoracic Surgery (EACTS), the European Association of Nuclear Medicine (EANM). Eur Heart J. 2015;36(44):3075-128. doi: 10.1093/eurheartj/ehv319.
6. Feuchtner GM, Stolzmann P, Dichtl W, Schertler T, Bonatti J, Scheffel H, et al. Multislice Computed Tomography in Infective Endocarditis: Comparison with Transesophageal Echocardiography and Intraoperative Findings. J Am Coll Cardiol. 2009;53(5):436-44. doi: 10.1016/j.jacc.2008.01.077.
7. Hryniewiecki T, Zatorska K, Abramczuk E, Zakrzewski D, Szyma□ski P, Ku□mierczyk M, et al. The Usefulness of Cardiac CT in the Diagnosis of Perivalvular Complications in Patients with Infective Endocarditis. Eur Radiol. 2019;29(8):4368-76. doi: 10.1007/s00330-018-5965-2.
8. Ivanovic B, Trifunovic D, Matic S, Petrovic J, Sacic D, Tadic M. Prosthetic Valve Endocarditis - A Trouble or a Challenge? J Cardiol. 2019;73(2):126-33. doi: 10.1016/j.jjcc.2018.08.007.
9. Otto CM, Nishimura RA, Bonow RO, Carabello BA, Erwin JP 3rd, Gentile F, et al. 2020 ACC/AHA Guideline for the Management of Patients with Valvular Heart Disease: A Report of the American College of Cardiology/American Heart Association Joint Committee on Clinical Practice Guidelines. Circulation. 2021;143(5):e72-e227. doi: 10.1161/CIR.0000000000000923.

Incidental Finding of Arrhythmogenic Right Ventricular Cardiomyopathy in a 72-Year-Old Man Admitted With Acute Coronary Syndrome

Rafael Modesto Fernandes,[1,2,3] *Luciana Cunha Weber,*[1,3] *Vitor Queiroz de Castro Souza,*[2] *Mariana Baptista Guedes,*[1,3] *Diogo Freitas Cardoso de Azevedo,*[1,2,3] *Marcia Maria Nova Rabelo*[1,2,3]

Hospital Aliança Rede D'Or,[1] *Salvador, BA – Brazil*
Escola Bahiana de Medicina e Saúde Pública,[2] *Salvador, BA – Brazil*
Instituto D'Or de Pesquisa e Ensino,[3] *Salvador, BA – Brazil*

Introduction

Arrhythmogenic right ventricular cardiomyopathy (ARVC) – also known as arrhythmogenic right ventricular (RV) dysplasia – is a genetic disorder characterized by progressive loss of RV cardiomyocytes, which are replaced with fibrofatty tissue. This replacement may delay intraventricular conduction and contribute to ventricular arrhythmias through a fibrosis-related macro-reentry mechanism. Thus, ARVC is one of the main causes of arrhythmic cardiac arrest in young people and athletes.[1]

Although initially designated as dysplasia, ARVC is not a congenital defect in the myocardium development. It is caused by mutations in the genes that encode desmosomal proteins, which are responsible for cell-to-cell adhesion. This discovery led to the disease being recognized as cardiomyopathy and included in the classification of cardiomyopathies by the American Heart Association.[1,2]

Diagnosis is complex due to the diverse clinical presentations, intra and interfamilial variations of expressiveness and incomplete penetration. Since the original report by Fontaine and Marcus in 1982, there have been substantial advances in understanding its pathogenesis, clinical manifestations, and long-term prognosis. However, this condition is still understudied and becomes a challenge when outside the most prevalent aspect.[1] A case report and literature review are presented, focusing on the current understanding of its pathogenesis, diagnostic evaluation with new imaging methods, and approach to risk stratification and therapy.

Case Report

A 72-year-old male was admitted to the emergency room with antacid-resistant epigastric pain. During the interview, he denied having chest pain, dyspnea or palpitations. Furthermore, he revealed a history of chest pain on exertion, unspecified arrhythmia, hypertension and dyslipidemia. He denied any previous infarction episodes and/or alterations in previous cardiological exams. Upon physical examination, no relevant alterations were found. The diagnosis of non-ST-elevation myocardial infarction (NSTEMI) was established based on the electrocardiogram, which showed inverted T waves in inferior and anterior leads (Figure 1A), in addition to changes in ultrasensitive troponin, with typical infarction behavior. No electrocardiographic changes suggestive of RV infarction were observed.

An early invasive stratification was performed, where a subocclusive lesion was found in the middle third of the right coronary artery (Figure 1B), requiring percutaneous angioplasty and successful drug-eluting stent implantation. A transthoracic echocardiogram (TTE) was performed, showing preserved left ventricular ejection fraction and no changes in contractility, but severe RV involvement (akinesia and segmental dyskinesia, increased trabeculations, reduced strain, lateral wall microaneurysms and a significant ejection fraction reduction by 3D echocardiography; see Figure 2). Given these RV alterations and their disagreement with the angiographic (obstruction of the right coronary artery in the middle third, after the acute marginal branch origin) and clinical findings, primary RV disease was considered. Cardiac magnetic resonance imaging was performed, which corroborated the echocardiogram findings and showed alterations suggestive of ARVC, in addition to RV diffuse transmural enhancement that suggested it was secondary to fibrofatty infiltration (Figure 3). Upon gathering the findings of the evaluation with multimodality of cardiovascular imaging, the diagnosis of ARVC was established based on the Task Force criteria (Table 1).[3]

The 24-hour Holter identified frequent ventricular extrasystoles without complex arrhythmias. After discussion with the Heart Team and genetic disease specialists, the patient was classified at low risk for sudden death, therefore, without indication for implantable cardioverter defibrillator (ICD) at that time. Family members were instructed to perform additional screening. The patient was discharged from the hospital on dual antiplatelet therapy, statins, beta-blockers and angiotensin-converting enzyme inhibitors. He is currently under outpatient follow-up with no evidence of arrhythmic events.

Keywords

Echocardiography, Three-Dimensional; Global Longitudinal Strain; Arrhythmogenic Right Ventricular Dysplasia

Mailing Address: Rafael Modesto Fernandes •
Hospital Aliança Rede D´Or. Av. Juracy Magalhaes. Postal Code: 40295-560. Salvador, BA – Brazil
E-mail: rafaelmodesto@cardiol.br
Manuscript received May 1, 2023; revised June 3, 2023; accepted July 3, 2023
Editor responsible for the review: Daniela do Carmo Rassi Frotata

DOI: https://doi.org/10.36660/abcimg.20230046i

Contents

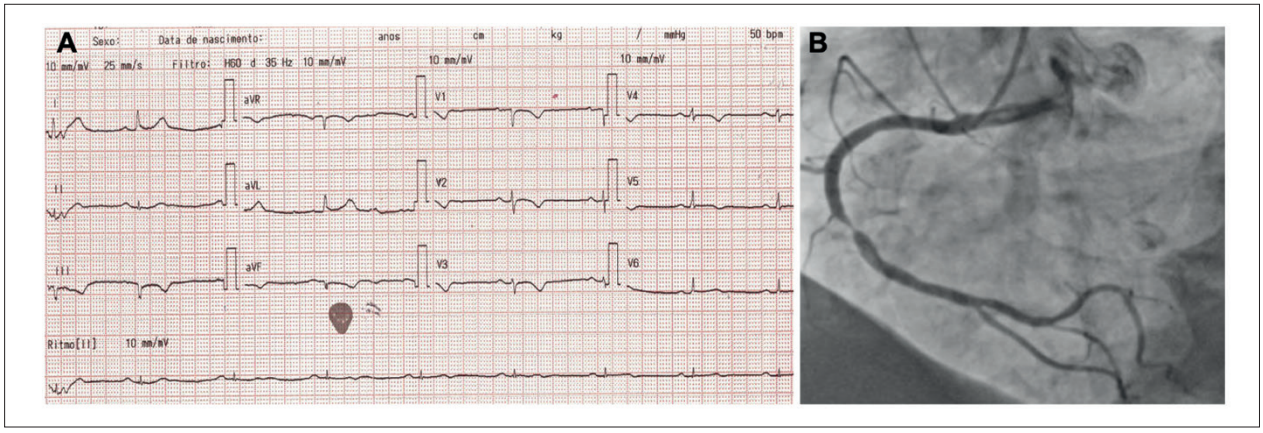

Figure 1 – *A) Admission electrocardiogram with negative T waves in leads V1 to V5 and DIII and aVF; B) Cardiac catheterization showing a subocclusive lesion in the middle third of the right coronary artery.*

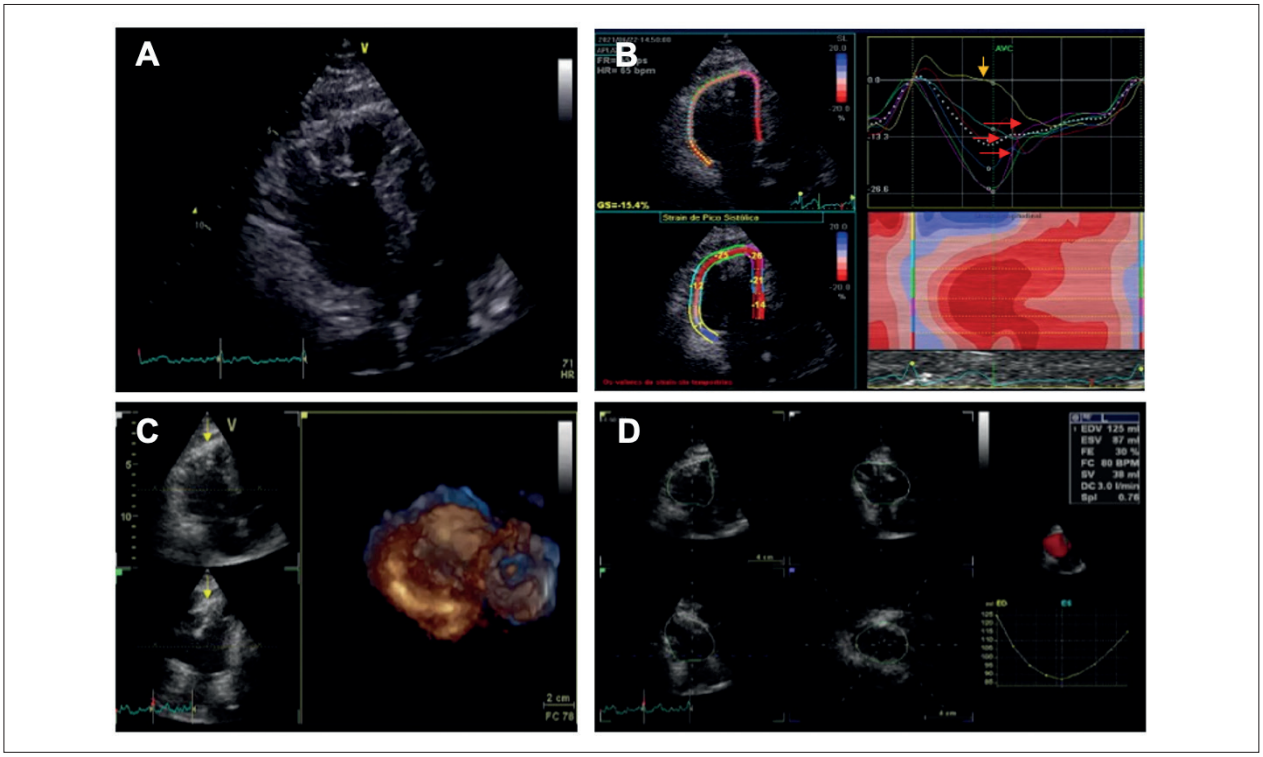

Figure 2 – *TTE showing A) Significant dilation of the right ventricle (RV), associated with increased trabeculations and images suggestive of microaneurysm in the RV lateral wall; B) Reduced RV longitudinal strain, segmental dyskinesia (yellow arrow) and high mechanical dispersion (red arrow); and C, D) three-dimensional full volume method that identified an RV ejection fraction of 30%, corresponding to significant systolic dysfunction.*

Discussion

Current literature discusses clinical indicators that raise the diagnostic suspicion of ARVC, such as (1) frequent ventricular ectopy; (2) ventricular tachycardia with superior axis LBBB morphology/multiple QRS morphologies; and (3) arrhythmogenic sudden death.[4] However, the definitive diagnosis is hindered by the disease's low prevalence and lack of specific tests, becoming even more complex when affecting elderly patients.[1,4] In this context, ARVC diagnosis is performed using the Task Force criteria (2010),[3] first listed in 1994 and revised in 2010 (Table 1), which, despite having limitations in their sensitivity, provides an efficient tool to direct diagnostic reasoning.[1] When applying the criteria, patients are submitted to structural, tissue and electrocardiographic investigation in search of major (two points) and minor (one point) findings. Patients who score four or more are diagnosed with ARVC, while those who score three are likely carriers of the disease.[1,3,4]

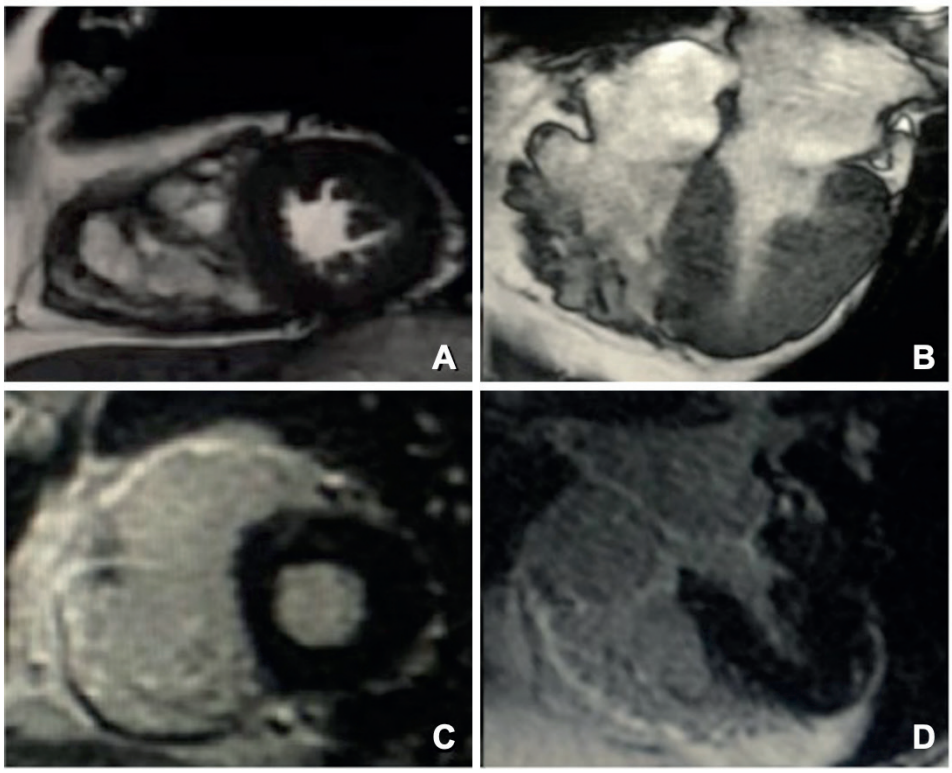

Figure 3 – *A) Short-axis systolic view; and B) four-chamber view showing RV dilation and lateral wall alterations (microaneurysms). (C and D) RV diffuse transmural delayed enhancement.*

ARVC suspicion was only listed for the patient under investigation after the disagreement between the angiographic findings and the subsequent echocardiographic evaluation. In order to explain the RV alterations, such as those found, a proximal occlusion of the right coronary artery, reaching the acute marginal branch, with RV infarction characteristics, would be necessary, which was not revealed by the patient's exams or symptoms.

Moreover, changes in the electrocardiogram on admission disagree with the coronary disease found, with inverted T waves in V1-V3 leads being the most common finding in ARVC.[4]

The RV structural and functional findings on this case's echocardiogram and cardiac magnetic resonance are typical of ARVC, with segmental alteration being a compulsory factor.

Once the diagnosis of ARVC is established, it is important to decide how to manage the patient in order to reduce the risk of sudden death. Although ICD acts positively in reducing mortality from arrhythmic causes, its implantation has been related to short- and long-term complications. In relation to this, there is a lack of prospective and randomized studies that support the routine use of the ICD prophylactically.[5] The estimation of the risk of sustained ventricular arrhythmia based on inherent characteristics of the patient and their history is an ally in management decisions.[5,6] Some situations are considered high risk, such as patients with recovered cardiac arrest or patients with previous events of sustained ventricular arrhythmia, history of arrhythmogenic syncope, significant RV and/or left ventricular systolic dysfunction. Shared decision-making between patient and physician should always be considered regarding risks, benefits and longevity itself.[6]

An American cohort with 312 patients with ARVC showed that ventricular tachycardia at presentation or its induction by electrophysiological study, male patients, inverted T waves in ≥ 3 precordial leads, and premature ventricular contraction count ≥ 1000/24h, were predictors of appropriate therapy in patients with ICD.[7] However, further studies are needed to better individualize the risk of sudden death in these situations.

The combination of pharmacological therapy through beta-blockers and antiarrhythmics are measures that minimize the use of appropriate therapy by the ICD. Also, part of the recommendation is neurohormonal blockades with angiotensin-converting enzyme inhibitors and beta-adrenergic receptor antagonists. Another recommended therapy is catheter ablation, although it has been shown not to be able to reduce the risk of sudden death and increase survival rates, being categorized as an adjuvant therapy.[5,8]

Conclusion

ARVC is a hard-to-diagnose genetic disorder often associated with adverse clinical outcomes. With advances

Table 1 – Task Force Criteria for the Diagnosis of ARVC (2010)[3]

1 – Structural changes and global or regional dysfunction
Major criteria
– Two-dimensional echocardiogram:
Regional RV aneurysm, akinesia, or dyskinesia associated with one of the following diastolic measures:
RVOT PLAX ≥ 32 mm (PLAX/BS ≥ 19 mm/m^2) or
RVOT PSAX ≥ 36 mm (PSAX/BS ≥ 21 mm/m^2) or
Change in fractional area ≤ 33%
– Cardiac Magnetic Resonance
Regional RV dyskinesia or akinesia, or RV contraction dyssynchrony associated with one of the following:
RV EDV BS ≥ 110 mL/m^2 (male) or ≥ 100 mL/m^2 (female)
RV ejection fraction ≤ 40%
Right ventriculography
RV aneurysm, akinesia, or dyskinesia
Minor criteria
– Two-dimensional echocardiogram:
RV dyskinesia, akinesia, or RV contraction dyssynchrony, and one of the following diastolic function measures:
RVOT PLAX ≥ 29 to < 32 mm (PLAX/BS ≥ 16 to < 19 mm/m^2) or
RVOT PSAX ≥ 32 to < 36 mm (PSAX/BS ≥ 18 a < 21 mm/m^2) or
Change in fractional area > 33% to ≤ 40%
– Cardiac Magnetic Resonance
Regional RV dyskinesia or akinesia, or RV contraction dyssynchrony, and one of the following:
RV EDV/BS ≥ 100 to 110 mL/m^2 (male) or ≥ 90 to 100 mL/m^2 (female)
RV ejection fraction > 40 to ≤ 45%
2 – Tissue aspects
Major criteria
Residual myocyte count < 60% by morphometric analysis (or < 50% if estimated), with RV free wall fibrous replacement in ≥ 1 sample, with or without fatty replacement tissue on endomyocardial biopsy.
Minor criteria
Residual myocyte count from 60% to 70% by morphometric analysis (or 50% to 65% if estimated), with RV free wall fibrous replacement in ≥ 1 sample, with or without fatty replacement tissue on endomyocardial biopsy.
3 – Repolarization abnormalities
Major criteria
Inverted T waves in right precordial leads (V1, V2, and V3) or extending beyond V3 in individuals > 14 years old (in the absence of RBBB-QRS ≥ 120 ms)
Minor criteria
Inverted T waves in V1 and V2 in individuals > 14 years old (in the absence of RBBB)
Inverted T waves in V1, V2, V3, and V4 in individuals > 14 years old (in the presence of RBBB)
4 – Depolarization/conduction abnormalities
Major criteria
Epsilon wave (reproducible low amplitude signals between the end of QRS and the beginning of the T wave) in the right precordial leads (V1 - V3)
Minor criteria
Late potentials on HR-ECG in ≥ 1 of 3 parameters in the absence of QRS ≥ 110 msec on 12-lead ECG:
Filtered QRS (fQRS) duration ≥ 114 msec
QRS terminal duration < 40 microV ≥ 38 ms
Terminal mean square voltage 40 ms ≤ 20 microV
Duration of the final portion of the QRS ≥ 55 ms (measured from the nadir of the S wave to the end of ventricular depolarization - including R') in V1, V2 or V3

5 – Arrhythmias
Major criteria
Unsustained or sustained VT with RBBB-like morphology and superior axis
Minor criteria
Non-sustained or sustained VT with morphology suggestive of RVOT (LBBB-type morphology and inferior or indeterminate axis) or > 500 ventricular extrasystoles/24h on 24h Holter
6 – Family history
Major criteria
ARVD/D in a first-degree relative who meets this task force 2010 criteria
Pathologically confirmed ARVD/D in a first-degree relative (autopsy or biopsy)
Identification of pathogenic mutation classified as associated or probably associated with ARVD/D in the patient under evaluation
Minor criteria
History of ARVD/D in first-degree relatives
History of ARVD/D in a first-degree relative for whom it was not possible to determine if criteria are met
Premature sudden death (< 35 years old) with suspected ARVD/D in a first-degree relative
ARVD/D confirmed pathologically or according to the criteria in a second-degree relative

ARVD/D: arrhythmogenic right ventricular heart disease/dysplasia; BSA: body surface area; CMR: cardiac magnetic resonance; ECG: electrocardiogram; EDV: end-diastolic volume; RBBB: right bundle branch block; LBBB: left bundle branch block; PLAX: long-axis parasternal window; PSAX: short-axis parasternal window; RV: right ventricular; RVOT: right ventricular outflow tract; HR-ECG: high-resolution electrocardiogram; VT: ventricular tachycardia; BS: body surface.

in complementary exams and greater knowledge about the patients' profiles, more and more cases of the disease have been discovered. Diagnosis in elderly patients makes management even more complex, requiring careful evaluation by the multidisciplinary team. Although ICD implantation is considered the most accepted therapeutic strategy in individuals with ARVC, adequate stratification of the patient's risk, as well as additional data about their clinical history, is required to analyze its indication.

Author Contributions

Conception and design of the research: Fernandes RM, Souza VQC; acquisition of data and analysis and interpretation of the data: Fernandes RM, Weber LC, Souza VQC, Guedes MB, Azevedo DFC; writing of the manuscript: Fernandes RM, Weber LC, Souza VQC, Guedes MB; critical revision of the manuscript for intellectual content: Fernandes RM, Weber LC, Guedes MB, Azevedo DFC, Rabelo MMN.

Potential Conflict of Interest

No potential conflict of interest relevant to this article was reported.

Sources of Funding

There were no external funding sources for this study.

Study Association

This study is not associated with any thesis or dissertation work.

Ethics Approval and Consent to Participate

This article does not contain any studies with human participants or animals performed by any of the authors.

References

1. Corrado D, Link MS, Calkins H. Arrhythmogenic Right Ventricular Cardiomyopathy. N Engl J Med. 2017;376(15):1489-90. doi: 10.1056/NEJMc1701400.
2. Corrado D, Basso C, Judge DP. Arrhythmogenic Cardiomyopathy. Circ Res. 2017;121(7):784-802. doi: 10.1161/CIRCRESAHA.117.309345.
3. Marcus FI, McKenna WJ, Sherrill D, Basso C, Bauce B, Bluemke DA, et al. Diagnosis of Arrhythmogenic Right Ventricular Cardiomyopathy/Dysplasia: Proposed Modification of the Task Force Criteria. Eur Heart J. 2010;31(7):806-14. doi: 10.1093/eurheartj/ehq025.
4. Elias J Neto, Tonet J, Frank R, Fontaine G. Arrhythmogenic Right Ventricular Cardiomyopathy/Dysplasia (ARVC/D) - What We Have Learned after 40 Years of the Diagnosis of This Clinical Entity. Arq Bras Cardiol. 2019;112(1):91-103. doi: 10.5935/abc.20180266.
5. Calkins H, Corrado D, Marcus F. Risk Stratification in Arrhythmogenic Right Ventricular Cardiomyopathy. Circulation. 2017;136(21):2068-82. doi: 10.1161/CIRCULATIONAHA.117.030792.
6. Towbin JA, McKenna WJ, Abrams DJ, Ackerman MJ, Calkins H, Darrieux FCC, et al. 2019 HRS Expert Consensus Statement on

Evaluation, Risk Stratification, and Management of Arrhythmogenic Cardiomyopathy. Heart Rhythm. 2019;16(11):e301-e372. doi: 10.1016/j.hrthm.2019.05.007.

7. Orgeron GM, James CA, Te Riele A, Tichnell C, Murray B, Bhonsale A, et al. Implantable Cardioverter-Defibrillator Therapy in Arrhythmogenic Right Ventricular Dysplasia/Cardiomyopathy: Predictors of Appropriate Therapy, Outcomes, and Complications. J Am Heart Assoc. 2017;6(6):e006242. doi: 10.1161/JAHA.117.006242.

8. Priori SG, Blomström-Lundqvist C, Mazzanti A, Blom N, Borggrefe M, Camm J, et al. 2015 ESC Guidelines for the Management of Patients with Ventricular Arrhythmias and the Prevention of Sudden Cardiac Death: The Task Force for the Management of Patients with Ventricular Arrhythmias and the Prevention of Sudden Cardiac Death of the European Society of Cardiology (ESC). Endorsed by: Association for European Paediatric and Congenital Cardiology (AEPC). Eur Heart J. 2015;36(41):2793-867. doi: 10.1093/eurheartj/ehv316.

18F-FDG PET/CT in Diagnosis, Therapeutic Evaluation and Definition of Management in Cardiac Sarcoidosis: Learn From This Case Report

Simone Cristina Soares Brandão,[1] Matheus de Araújo Lucena,[1] Christiane Wiefels,[2] Pedro Rodrigues da Silva,[1] Claudio Tinoco Mesquita,[3,4,5] Maria Fernanda Rezende,[4] Fabio Mastrocola[6]

Universidade Federal de Pernambuco,[1] Recife, PE – Brazil
Universidade de Ottawa,[2] Ottawa – Canada
Departamento de Radiologia, Universidade Federal Fluminense,[3] Rio de Janeiro, RJ – Brazil
Hospital Pró-Cardíaco,[4] Rio de Janeiro, RJ – Brazil
Hospital Samaritano da Barra e Vitória,[5] Rio de Janeiro, RJ – Brazil
Hospital Universitário Onofre Lopes (UFRN),[6] Natal, RN – Brazil

Introduction

Sarcoidosis is a non-caseating granulomatous inflammatory disease of unknown etiology. The presentation can range from an asymptomatic condition with nonspecific findings on chest radiography to organ failure. Any part of the body can be affected, but the most common sites are the mediastinal lymph nodes and the lungs, followed by the skin and ocular structures such as the uvea. Other systems, such as the nervous, endocrine, gastrointestinal, urinary, musculoskeletal, and cardiovascular systems, can also be affected.[1]

Cardiac sarcoidosis is a disease that is still under-researched in cardiology. It is related to cardiomyopathy conditions that can be confused with hypertrophic, infiltrative, or even ischemic cardiomyopathy, and it courses with ventricular arrhythmias and conduction disorders with possible progression to heart failure and/or sudden death. It is worth emphasizing that cardiac sarcoidosis is responsible for up to 35% of cases of complete atrioventricular block (CAVB) in patients under 60 years of age.[1] These patients benefit from the implantation of a pacemaker and implantable cardioverter defibrillator (ICD). Immunosuppressive therapy is indicated to control the inflammatory process.[2]

Positron emission tomography with computed tomography (PET/CT) using fluorine-18 fluorodeoxyglucose (^{18}F-FDG) is a hybrid imaging method that provides anatomical and molecular information of diseases in a non-invasive and objective manner. The degree of ^{18}F-FDG uptake in the regions affected by sarcoidosis reflects the inflammatory intensity of the disease.[3] In this context, ^{18}F-FDG PET/CT is able to identify early the presence and extent of intra- and extracardiac involvement, thus being able to guide and monitor the therapeutic response. Furthermore, early diagnosis of cardiac sarcoidosis is essential, since late diagnoses are related to greater cardiac damage and worse prognosis.[4]

The objective of this article is to demonstrate that presumptive diagnosis of cardiac sarcoidosis is possible, based on clinical and radiological criteria, especially with the use of ^{18}F-FDG PET/CT. Furthermore, in this report we show how ^{18}F-FDG PET/CT assists therapeutic monitoring and definition of conduct.

Case description

We describe the case of a 39-year-old male patient who was hospitalized with recurring "off-on" syncope. The 24-hour Holter showed frequent ventricular extrasystoles and intermittent episodes of CAVB, with pauses of up to 14.5 seconds. On echocardiography, the left ventricle (LV) was dilated with segmental and global dysfunction (LV ejection fraction 43%). Coronary angiography did not show obstructive coronary lesions. Cardiac magnetic resonance imaging (CMR) showed structural heart disease with a non-ischemic enhancement pattern, predominantly in the basal region of the septum, with a large quantity of fibrosis. In this context, the diagnostic hypothesis of cardiac sarcoidosis was considered as the cause of intermittent CAVB and ventricular dysfunction, and implantation of a permanent dual-chamber pacemaker with ICD was performed to treat bradyarrhythmia and prevent sudden death.

As a diagnostic complement, ^{18}F-FDG PET/CT was performed, revealing a focal increase in glycolytic metabolism throughout the entire length of the basal region of the LV (anterior, anteroseptal, inferoseptal, inferolateral, and anterolateral segments). Whole body imaging also showed pulmonary, lymph node, and bone involvement, in addition to diffuse increase in the arm muscles (Figure 1). Resting myocardial perfusion scintigraphy (Figure 2) showed abnormally low tracer concentration in the apical region (match of ^{99m}Tc-sestamibi and ^{18}F-FDG: did not show uptake of either tracer, suggesting an area of fibrosis without inflammation) and in the basal segment of the LV anteroseptal wall (mismatch of ^{99m}Tc-sestamibi and ^{18}F-FDG: no uptake of ^{99m}Tc-sestamibi and uptake of ^{18}F-FDG, suggesting an area of fibrosis with local inflammation).

Keywords

Sarcoidosis; Positron-Emission Tomography; Fluorodeoxyglucose F18

Mailing Address: Simone Cristina Soares Brandão •
Universidade Federal de Pernambuco. Av. Prof Moraes Rego, SN. CEP: 50670-901. Cidade Universitária, Recife, PE – Brazil
E-mail: sbrandaonuclearufpe@gmail.com
Manuscript received March 12, 2023; revised manuscript March 19, 2023; accepted April 4, 2023
Editor responsible for the review: Rafael Lopes

DOI: https://doi.org/10.36660/abcimg.20230029i

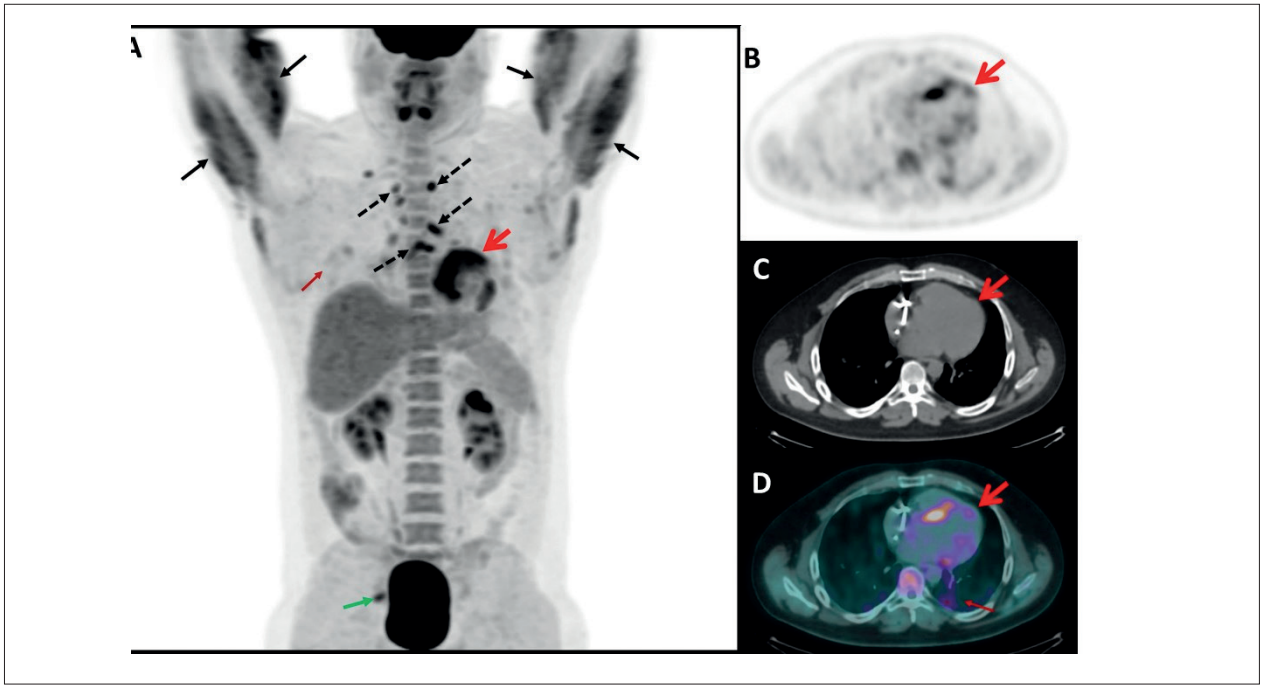

Figure 1 – *^{18}F-FDG PET/CT scan showing increased glycolytic metabolism in several mediastinal lymph nodes (black hatched arrows) with ^{18}F-FDG standardized uptake value (SUV) of up to 5.9, in small, grouped reticulonodular lung opacities (thin red arrow), with lymphatic distribution, some with foci of calcifications, sparse in both lungs (SUV of up to 3.6), in the left ventricular myocardium (thick red arrow), with heterogeneous pattern (SUV = 6.7), in the right iliac bone marrow (green arrow), next to the right sacroiliac joint (SUV = 4.6) and in the musculature of both arms (black arrows), mainly biceps and triceps, which were hypertrophied, with a heterogeneous pattern that was a little more intense in the right arm (SUV = 5.5). In A, 3-dimensional full-body maximum intensity projection of ^{18}F-FDG PET imaging; in B, coronal section of the chest from PET with ^{18}F-FDG at the cardiac level; in C, computed tomography; in D, PET/CT fusion.*

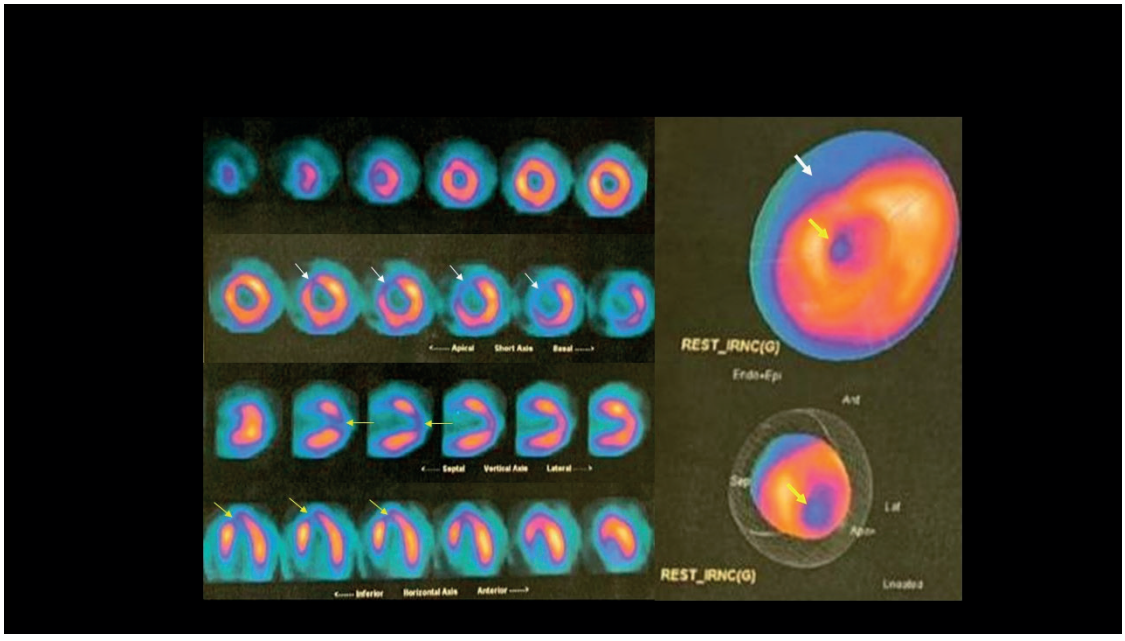

Figure 2 – *Resting myocardial perfusion scintigraphy with ^{99m}Tc-sestamibi showing abnormally low tracer concentration in the basal anteroseptal (white arrows) and apical (yellow arrows) segments of the LV, suggesting fibrosis.*

Corticosteroid therapy was initiated at a dose of 40 mg of prednisone orally for 3 months. After this period, the steroid dose was progressively reduced. The patient complained of dyspnea on routine exertion and atypical chest pain. He was completely dependent on the pacemaker (CAVB no longer intermittent). A new Holter revealed normal functioning pacemaker rhythm, frequent ventricular extrasystole, and episodes of accelerated idioventricular rhythm. A new ^{18}F-FDG PET/CT was carried out, showing persistence of cardiac and extracardiac inflammatory activity. Due to the maintenance of cardiac inflammation, methotrexate 15 mg orally once a week was added, in addition to optimization of therapy for heart failure.

To assess the therapeutic response, approximately 8 months after starting methotrexate, a new PET/CT showed complete resolution of cardiac uptake of ^{18}F-FDG and improvement in heart failure with increased LV ejection fraction, but the patient remained dependent on the pacemaker. The other regions showed persistence of inflammatory disease activity (Figure 3).

Discussion

Cardiac involvement by sarcoidosis is characterized by the presence of non-caseating granulomas in the myocardium and/or pericardium. Clinical manifestations depend on the location and intensity of the granulomatous inflammation.[1]

The diagnostic definition of cardiac sarcoidosis is based on expert consensus recommendations. Diagnosis can be histological, identifying the presence of non-caseating granuloma in the heart, or clinical, based on imaging tests.[1] Myocardial biopsy is the gold standard; however, in addition to the fact that it is an invasive procedure, its sensitivity does not exceed 30%.[5] Table 1 summarizes the criteria applied for diagnosing cardiac sarcoidosis according to the 2016 update of the Japanese Circulation Society guideline.[6] According to these criteria, this patient fulfilled the criteria for systemic sarcoidosis with cardiac involvement.

Considering the typical findings of sarcoidosis on CMR and ^{18}F-FDG PET/CT scans, associated with the lack of experience in performing myocardial biopsy in cardiology and thoracic surgery services in Brazil, the use of ^{18}F-FDG PET/CT has become popular among cardiologists.[7] A meta-analysis published in 2012, with data from 164 patients, showed that ^{18}F-FDG PET/CT has a sensitivity of 89% and specificity of 83% for diagnosis of cardiac sarcoidosis.[4]

It is, nonetheless, worth noting that the test should be performed in specialized centers, given that findings of cardiac sarcoidosis can be confused with other cardiac conditions, such as hibernating myocardium in patients with ischemic heart disease, or active myocarditis in systemic rheumatic conditions.[7] For this reason, the interpretation of the exam by an excellent professional is fundamental in order to avoid diagnostic errors.[3]

In addition to assisting diagnosis, these advanced imaging modalities play a key role in monitoring the therapeutic response, as they are capable of detecting the inflammatory state before and after the start of therapy. The use of these exams can guide safer professional decisions, such as when

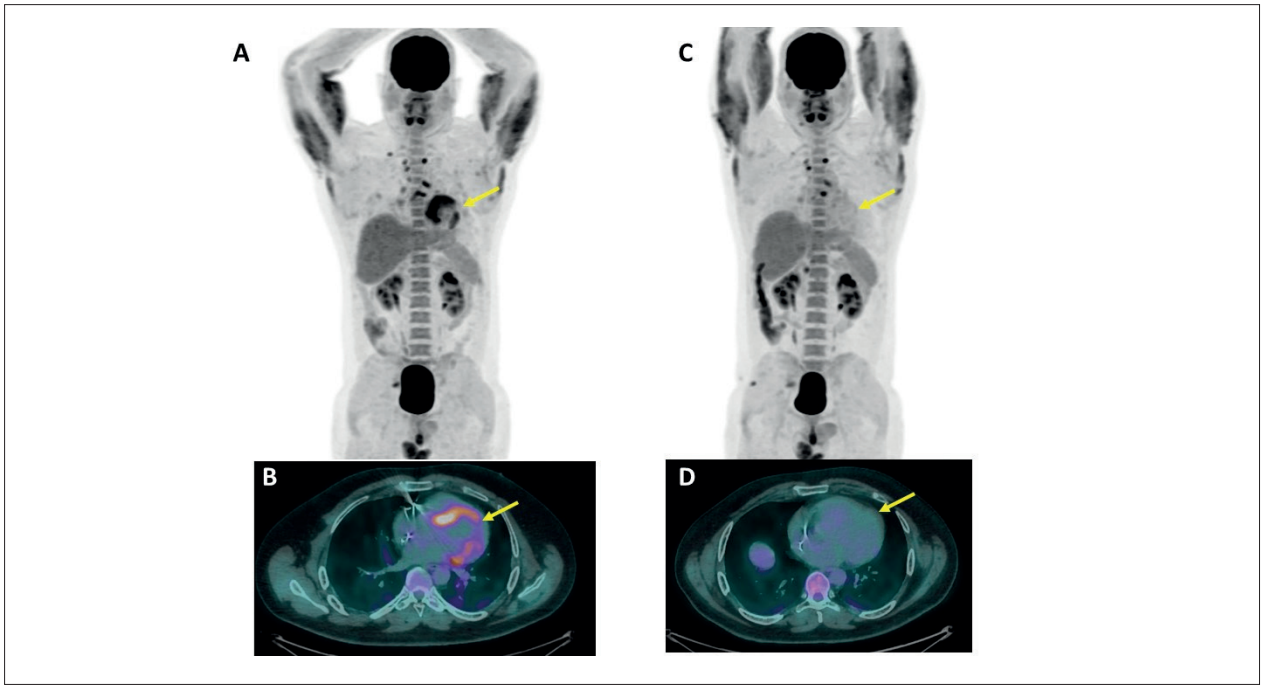

Figure 3 – *^{18}F-FDG PET/CT scans performed before (A and B) and after (C and D) initiation of methotrexate. A and C show 3-dimensional full-body maximum intensity projection images of ^{18}F-FDG PET; B and D show axial slices (PET/CT) of the chest at the heart level. About 8 months after starting methotrexate, PET images showed complete resolution of ^{18}F-FDG uptake in the left ventricular myocardium (yellow arrows). The other regions (arm muscles, mediastinal lymph nodes, lungs, and right iliac region) show persistence of ^{18}F-FDG uptake.*

Table 1 – Criteria for defining cardiac sarcoidosis according to the Japanese Circulation Society (JCS)

Japanese Circulation Society criteria for clinical diagnosis of cardiac sarcoidosis		
Criteria for clinical definition of pulmonary sarcoidosis[1]	1. Bilateral hilar lymphadenopathy 2. CT or high-resolution CT images showing thickened interstitium surrounding the bronchial vascular bundles and multiple nodular opacities along lymphatic vessels*	
Laboratory/imaging criteria characteristic of sarcoidosis and clinical findings strongly suggestive of cardiac involvement[2]	1. Bilateral hilar lymphadenopathy 2. High serum angiotensin-converting enzyme activity or elevated serum lysozyme levels 3. High serum levels of SIL-2R 4. Increased uptake of tracers for inflammation such as gallium-67 citrate on conventional scintigraphy or ^{18}F-FDG on PET/CT 5. High percentage of lymphocytes with a CD4/CD8 ratio of > 3.5 in the bronchoalveolar lavage fluid	
	Major criteria	**Minor criteria**
Criteria for clinical definition of cardiac sarcoidosis[3]	1. High-grade atrioventricular block (including CAVB) or fatal ventricular arrhythmia (for example, sustained ventricular tachycardia, and ventricular fibrillation)	1. Abnormal ECG findings: ventricular arrhythmias (nonsustained ventricular tachycardia, multifocal or frequent premature ventricular contractions), bundle branch block, axis deviation, or abnormal Q waves
	2. Basal thinning of the ventricular septum or abnormal ventricular wall anatomy (ventricular aneurysm, thinning of the middle or upper ventricular septum, regional thickening of the ventricular wall)	2. Perfusion defects on resting myocardial perfusion scintigraphy.
	3. Left ventricular contractile dysfunction (left ventricular ejection fraction less than 50%) or focal ventricular wall asynergy	
	4. Scintigraphy with gallium-67 or ^{18}F-FDG PET/CT revealing high tracer uptake in the heart	
	5. CMR with gadolinium revealing delayed contrast enhancement in the myocardium	

1. The clinical definition of pulmonary sarcoidosis depends on the presence of at least 1 of the 2 criteria listed; 2. At least 2 out of 5 laboratory/imaging criteria characteristic of sarcoidosis and clinical findings strongly suggestive of cardiac involvement; 3. The clinical definition of cardiac sarcoidosis requires the presence of 2 or more major criteria or 1 major criterion plus 2 or more minor criteria. CAVB: complete atrioventricular block; CMR: cardiac magnetic resonance imaging; CT: computed tomography; ECG: electrocardiogram. *Multiple nodular opacities along the lymphatic vessels may be found in the central and/or peripheral parts of the lobules along the pleura, interlobular septa, and bronchopulmonary arteries. Source: Terasaki et al.[6]*

to start weaning from a certain medication or when to add or withdraw certain drugs (Figure 4).[3]

It is important to emphasize that all of this patient's ^{18}F-FDG PET/CT scans were performed strictly following the preparation protocol for physiological suppression of glucose uptake by cardiomyocytes (Figure 5).[7]

^{18}F-FDG PET/CT is indicated for evaluation of inflammatory disease activity in patients with persistent symptoms or clinical worsening and evaluation of the therapeutic response.[4] Accordingly, the PET/CT scan was important in confirming cardiac sarcoidosis, in the systemic staging of the disease, in therapeutic monitoring, and in determining management.

In sarcoidosis, nonspecific chest pain, dyspnea, and fatigue are common symptoms that are generally associated with extracardiac disease.[5] In all ^{18}F-FDG PET/CT scans performed, extracardiac disease persisted. For these patients, extracardiac involvement is common; however, it is practically restricted to low-grade lung injury and almost never symptomatic involvement of other organs.[7]

Conclusion

This case report has illustrated how ^{18}F-FDG PET/CT can be useful in confirming cardiac and extra-cardiac sarcoidosis, avoiding endomyocardial biopsy and serving to evaluate therapeutic response and determine management.

Author Contributions

Conception and design of the research: Brandão SCS, Lucena MVA, Wiefels C, Mesquita CT, Rezende MF, Mastrocolla F; acquisition of data: Brandão SCS, Lucena MVA, Da Silva PHR, Mastrocolla F; analysis and interpretation of the data: Brandão SCS , Lucena MVA, Mastrocolla F; writing of the manuscript: Brandão SCS, Lucena MVA, Da Silva PHR; critical revision of the

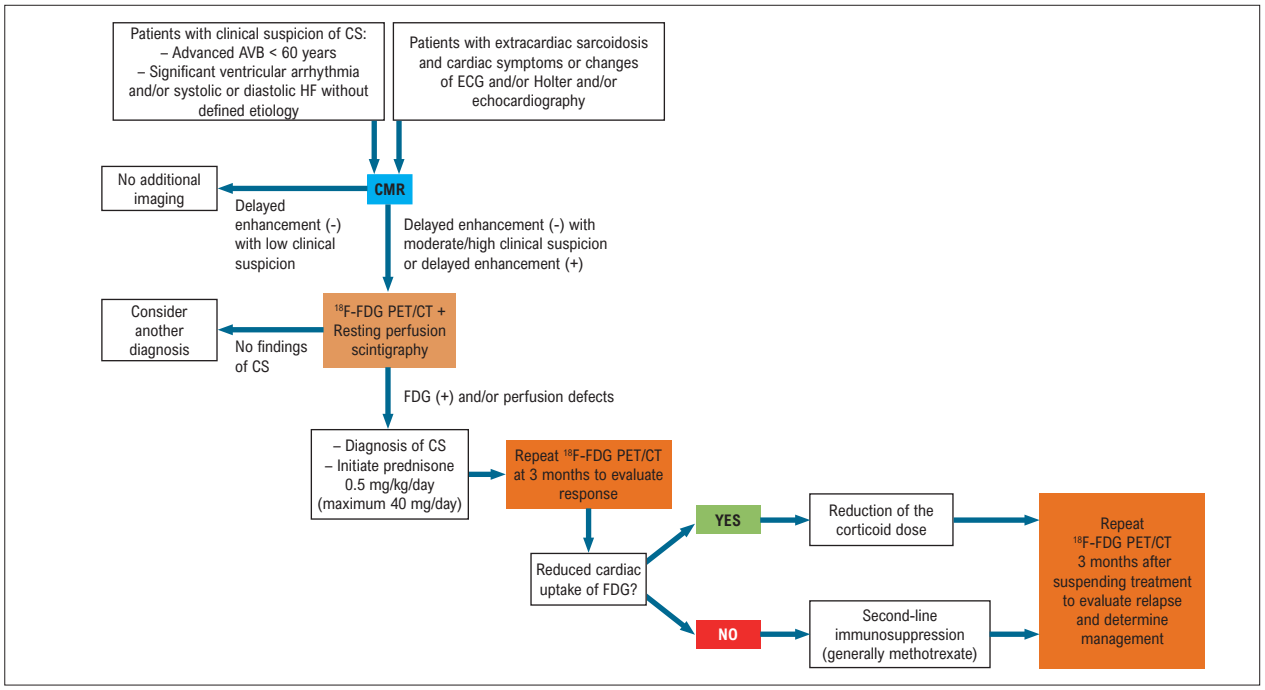

Figure 4 – *Algorithm for investigation and therapeutic monitoring of cardiac sarcoidosis according to data from the literature and the authors' experience with the use of 18F-FDG PET/CT. AVB: atrioventricular block; CMR: cardiac magnetic resonance imaging; CS: cardiac sarcoidosis; ECG: electrocardiogram; HF: heart failure; FDG: fluorodeoxyglucose.*

Figura 5 – *18F-FDG PET/CT in the investigation of cardiac sarcoidosis. Whole-body imaging is required to screen for systemic disease, and cardiac acquisition synchronized with the electrocardiogram is required to evaluate the heart in greater detail. In this figure, we summarize the preparation for the exam: 1. The day before the scan (at least 24 hours before), the diet should be low in carbohydrates and high in fat to stimulate the consumption of fatty acids by the heart muscle; thus, the diet is based on proteins and fibers and is rich in fat. 2. Fast for at least 12 hours (preferably 18 hours), except water, which can be consumed without restriction. 3. Avoid physical activity 24 hours before the scan. 4. Get a good night's sleep. 5. In the case of patients with diabetes using insulin, insulin use is not permitted on the day of the scan. 6. Serum glucose level must be below 180 mg/dL. 7. In some centers, unfractionated heparin 50 IU/kg is administered intravenously, 15 minutes before the 18F-FDG injection. Source: Kumita et al.[7]*

manuscript for intellectual content: Brandão SCS, Wiefels C, Da Silva PHR, Mesquita CT, Rezende MF, Mastrocolla F.

Potential Conflict of Interest

No potential conflict of interest relevant to this article was reported.

Sources of Funding

There were no external funding sources for this study.

Study Association

This study is not associated with any thesis or dissertation work.

Ethics Approval and Consent to Participate

This study was approved by the Ethics Committee of the Hospital das Clínicas da UFPE under the protocol number 6.222.794. All the procedures in this study were in accordance with the 1975 Helsinki Declaration, updated in 2013. Informed consent was obtained from all participants included in the study.

References

1. Birnie DH, Nery PB, Ha AC, Beanlands RS. Cardiac Sarcoidosis. J Am Coll Cardiol. 2016;68(4):411-21. doi: 10.1016/j.jacc.2016.03.605.
2. Kandolin R, Lehtonen J, Kupari M. Cardiac Sarcoidosis and Giant Cell Myocarditis as Causes of Atrioventricular Block in Young and Middle-Aged Adults. Circ Arrhythm Electrophysiol. 2011;4(3):303-9. doi: 10.1161/CIRCEP.110.959254.
3. Wiefels C, Lamai O, Kandolin R, Birnie D, Leung E, Mesquita CT, et al. The Role of ^{18}F-FDG PET/CT in Cardiac Sarcoidosis. Int J Cardiovasc Sci. 2020;33(4):389-400. doi: 10.36660/ijcs.20200033.
4. Kim SJ, Pak K, Kim K. Diagnostic Performance of F-18 FDG PET for Detection of Cardiac Sarcoidosis; A Systematic Review and Meta-Analysis. J Nucl Cardiol. 2020;27(6):2103-115. doi: 10.1007/s12350-018-01582-y.
5. Uemura A, Morimoto S, Hiramitsu S, Kato Y, Ito T, Hishida H. Histologic Diagnostic Rate of Cardiac Sarcoidosis: Evaluation of Endomyocardial Biopsies. Am Heart J. 1999;138(2 Pt 1):299-302. doi: 10.1016/s0002-8703(99)70115-8.
6. Terasaki F, Azuma A, Anzai T, Ishizaka N, Ishida Y, Isobe M, et al. JCS 2016 Guideline on Diagnosis and Treatment of Cardiac Sarcoidosis - Digest Version. Circ J. 2019;83(11):2329-88. doi: 10.1253/circj.CJ-19-0508.
7. Kumita S, Yoshinaga K, Miyagawa M, Momose M, Kiso K, Kasai T, et al. Recommendations for ^{18}F-fluorodeoxyglucose Positron Emission Tomography Imaging for Diagnosis of Cardiac Sarcoidosis-2018 Update: Japanese Society of Nuclear Cardiology recommendations. J Nucl Cardiol. 2019;26(4):1414-33. doi: 10.1007/s12350-019-01755-3.

Giant Right Coronary Artery Aneurysm with Arteriovenous Fistula

Maria Eduarda Menezes de Siqueira,[1] Mayra Isabel Dias,[1] Ana Claudia Vincezi Raudan Uski,[1] Luciano Figueiredo de Aguiar Filho[1]

Hospital Santa Catarina,[1] São Paulo, SP – Brazil

Introduction

Coronary artery aneurysm (CAA) is defined as a dilation that exceeds the normal diameter of the adjacent artery or the diameter of the patient's largest coronary artery by 1.5 times.[1] Some authors consider a giant coronary aneurysm when the diameter is > 20 mm, whereas the American Heart Association defines giant aneurysms as those > 8 mm. Giant CAA is a rare pathology with an approximate incidence of 0.02%.[2] We report a case of giant right coronary artery aneurysm with fistula to the coronary sinus, appearing as a giant "mass".

Case report

A 72-year-old female patient was admitted to our service with asthenia, dyspnea, mental confusion, and weight loss. She had a previous history of systemic arterial hypertension, diabetes mellitus, hypothyroidism, and Alzheimer's disease. She was on Aradois 50 mg/day, Syntroid 25 mcg, and a multivitamin. Upon physical examination, she had normal hemodynamic parameters (heart rate 75 bpm and blood pressure 118/81 mmHg), low oxygen saturation (80%), and temperature of 36 °C. To assist diagnosis, chest computed tomography angiography was requested, revealing findings compatible with bilateral acute pulmonary thromboembolism, in addition to right coronary artery ectasia with a voluminous rounded mass in the distal segment, of undetermined etiology. Investigation continued with angiotomography of the coronary arteries. The study was conducted on a 320-channel scanner (Aquilion One/Prism, Canon), showing significant right coronary artery ectasia (10 mm in diameter), calcified plaques that did not promote significant luminal reduction, and a large, partially thrombosed aneurysmal formation in the distal third measuring 80 × 67 mm. Communication between the aneurysm and the coronary sinus (arteriovenous fistula) was also observed (Figures 1, 2, and 3). Cardiac magnetic resonance imaging was performed, corroborating the diagnosis of CAA and demonstrating compression of the right ventricle by the voluminous mass with preserved biventricular function, in addition to the absence of myocardial fibrosis/necrosis (Figure 4). Surgical correction of the CAA was indicated; however, due to the patient's age and comorbidities, family members opted for expectant treatment. One year after diagnosis, the patient had an episode of chest pain and was hospitalized with suspected coronary syndrome. Coronary cineangiography was performed, without signs of obstructive coronary disease, and, in this study, the CAA was not characterized (Figure 5). It should be noted that cases of aneurysm filled with thrombus may not be detected by invasive coronary angiography.

Discussion

The most frequent etiology of CAA is atherosclerotic (likely etiology of the reported case). Other causes include congenital heart disease (for example, Kawasaki disease), trauma, percutaneous coronary intervention, arteritis (for example, syphilis or Takayasu arteritis), mycotic infection, and connective tissue disorders (for example, Ehlers-Danlos syndrome).[3] The most affected sites are the proximal and middle portions of the right coronary artery and the proximal portion of the anterior descending and circumflex coronary arteries.[4]

Most patients with CAA have asymptomatic clinical presentation, and detection occurs as an incidental finding during imaging tests. When symptomatic, these aneurysms may present as acute coronary syndromes or mimic other conditions, such as ascending aorta or pulmonary trunk

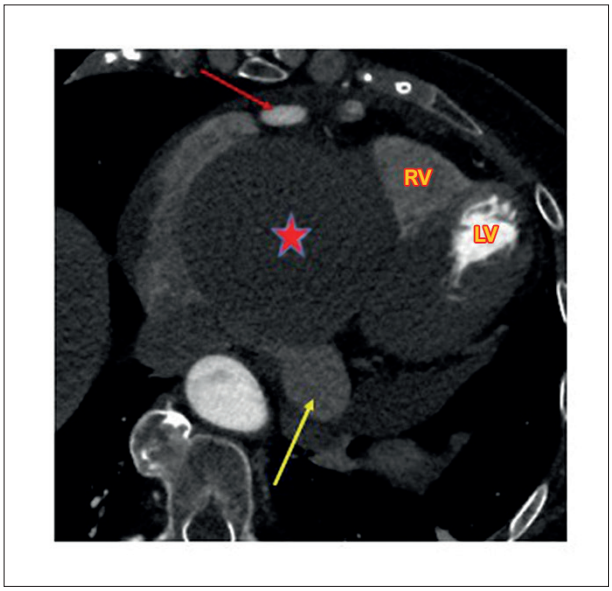

Figure 1 – *Axial view of angiotomography demonstrating the voluminous aneurysm (red star), right coronary artery ectasia (red arrow), and dilated coronary sinus communicating with the aneurysm (yellow arrow). LV: left ventricle; RV: right ventricle.*

Keywords

Coronary Vessel Anomalies; Tomography, X-Ray Computed; Ventricular Dysfunction, Right; Coronary Aneurysm

Mailing Address: Maria Eduarda Menezes de Siqueira •
UNIFESP. Rua Napoleão de Barros. Postal Code: 04080-005. São Paulo, SP – Brazil
E-mail: dadasiqueira@yahoo.com.br
Manuscript received March 9, 2023; revised manuscript April 14, 2023; accepted May 22, 2023
Editor responsible for the review: Leonardo Sara da Silva

DOI: https://doi.org/10.36660/abcimg.20230025i

Figure 2 – *Three-dimensional reconstruction of angiotomography showing dilated coronary sinus (green arrow) and giant right coronary artery aneurysm.*

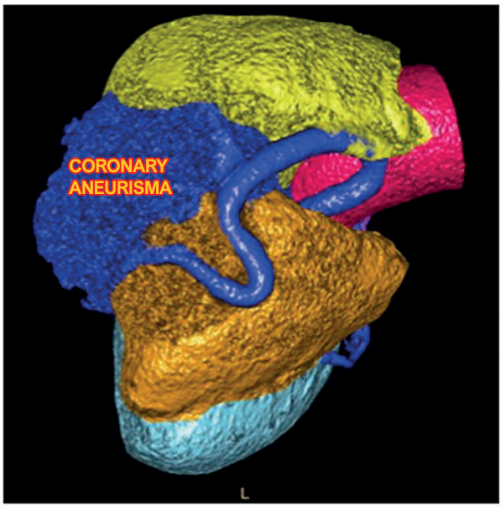

Figure 3 – *Three-dimensional reconstruction of angiotomography showing ectasia and giant right coronary artery aneurysm.*

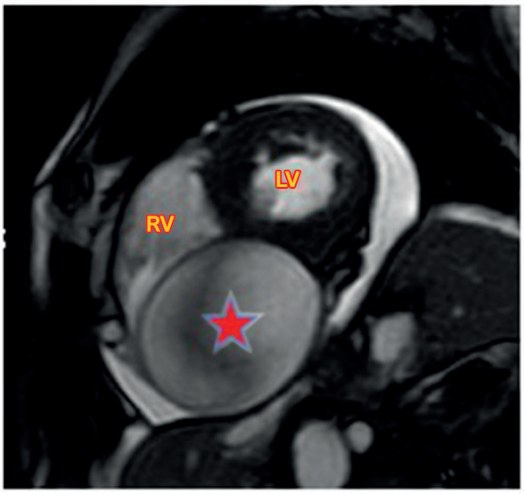

Figure 4 – *Short-axis cardiac magnetic resonance imaging showing the voluminous right coronary artery aneurysm (red star). LV: left ventricle; RV: right ventricle.*

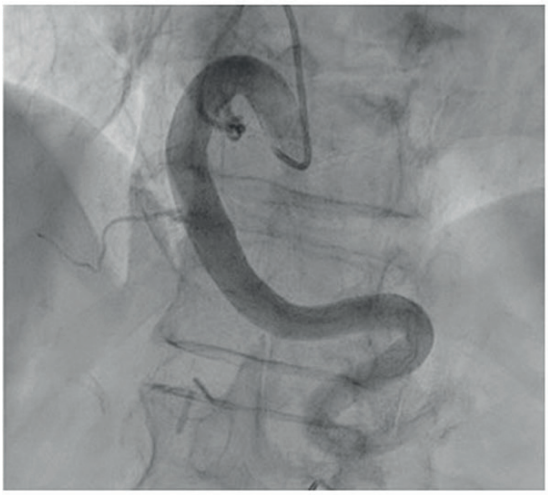

Figure 5 – *Coronary cineangiography demonstrating right coronary artery ectasia, with no evidence of aneurysm in the study.*

aneurysms, pericardial cysts, cardiac tumors, and thymomas.[5] Myocardial infarction may occur due to low-flow state ischemia, thrombosis, or distal embolization.[6] Fistulas between the aneurysm and a cardiac chamber are also possible complications depending on the size of the aneurysmal sac. The association of CAA with coronary sinus fistula is not uncommon, with some cases already described in the literature.[7] Diagnosis is made by angiotomography of the coronary arteries or by invasive angiography. Clinical management can vary from the pharmacological approach with anticoagulants and antiplatelet agents to endovascular management with stents, or even surgery with resection and graft reconstruction.[8]

Author Contributions

Conception and design of the research and writing of the manuscript: Siqueira MEM; critical revision of the manuscript for intellectual content: Dias MI, Uski ACVR, Aguiar Filho LF.

Potential Conflict of Interest

No potential conflict of interest relevant to this article was reported.

Sources of Funding

There were no external funding sources for this study.

Study Association

This study is not associated with any thesis or dissertation work.

Ethics Approval and Consent to Participate

This article does not contain any studies with human participants or animals performed by any of the authors.

References

1. Swaye PS, Fisher LD, Litwin P, Vignola PA, Judkins MP, Kemp HG, et al. Aneurysmal Coronary Artery Disease. Circulation. 1983;67(1):134-8. doi: 10.1161/01.cir.67.1.134.
2. Li D, Wu Q, Sun L, Song Y, Wang W, Pan S, et al. Surgical Treatment of Giant Coronary Artery Aneurysm. J Thorac Cardiovasc Surg. 2005;130(3):817-21. doi: 10.1016/j.jtcvs.2005.04.004.
3. Jha NK, Ouda HZ, Khan JA, Eising GP, Augustin N. Giant Right Coronary Artery Aneurysm- Case Report and Literature Review. J Cardiothorac Surg. 2009;4:18. doi: 10.1186/1749-8090-4-18.
4. Erdöl C, Celik S, Baykan M, Gökçe M, Karahan B, Bayram A. A Coronary Aneurysm Complicated by Acute Myocardial Infarction. A case report. J Cardiovasc Surg. 2001;42(1):65-7.
5. Kawsara A, Núñez Gil IJ, Alqahtani F, Moreland J, Rihal CS, Alkhouli M. Management of Coronary Artery Aneurysms. JACC Cardiovasc Interv. 2018;11(13):1211-23. doi: 10.1016/j.jcin.2018.02.041.
6. Yoshino S, Minagoe S, Yu B, Kosedo I, Yamashita M, Ishizawa M, et al. Cardiac Tamponade due to Rupture of Coronary Artery Fistula to the Coronary Sinus with Giant Aneurysm of Coronary Artery: Usefulness of Transthoracic Echocardiography. Heart Vessels. 2013;28(4):536-40. doi: 10.1007/s00380-012-0279-9.
7. Gala AB, Pope MTB, Leo M, Kelion AD, Bashir Y. Giant Right Coronary Artery Aneurysm and Fistula Into the Coronary Sinus. Rev Port Cardiol. 2021;40(6):463-464. doi: 10.1016/j.repce.2021.07.013.
8. Kawsara A, Núñez Gil IJ, Alqahtani F, Moreland J, Rihal CS, Alkhouli M. Management of Coronary Artery Aneurysms. JACC Cardiovasc Interv. 2018;11(13):1211-23. doi: 10.1016/j.jcin.2018.02.041.

Evaluation of Coronary Flow Reserve by Myocardial Scintigraphy in Left Ventricular Hypertrophy

Renata Christian Martins Felix,[1,2] Felipe Hermely Villela Pedras,[2] Odorico de Souza Lima Neto,[2] Leonardo Medeiros Vitório[2]

Instituto Nacional de Câncer,[1] Rio de Janeiro, RJ – Brazil

Clínica de Medicina Nuclear Villela Pedras,[2] Rio de Janeiro, RJ – Brazil

Introduction

The microvascular integrity of the myocardial bed can be assessed by coronary flow reserve (CFR), which is a calculation of the ratio between the absolute coronary blood flow under vasodilator stress and under resting conditions. This measurement is capable of estimating vasomotor dysfunction, and it reflects the hemodynamic effect of focal, diffuse, or small-vessel coronary disease.[1]

Currently, it is possible to measure CFR invasively using the techniques of thermodilution or intracoronary Doppler and through non-invasive methods, such as echocardiography, magnetic resonance imaging, computed tomography, or nuclear medicine.[1]

The gold standard for non-invasive assessment of CFR is positron emission tomography (PET) myocardial perfusion, which has proven to be a valuable diagnostic and prognostic marker in the context of coronary disease and non-obstructive heart diseases.[2] Radiotracers used for PET myocardial perfusion are not usually available in many medical centers worldwide, including Brazil, due to the need for complex and costly logistics of production.

CFR can also be measured by means of conventional myocardial perfusion scintigraphy using special gamma cameras with solid state detectors, known as cadmium-zinc-tellurium (CZT), which are already present in many nuclear medicine services in Brazil. The measurement of CFR using CZT has shown good agreement with PET, and it has a proven impact on prognosis and therapeutic management.[3]

We report a clinical case in which the evaluation of CFR through myocardial scintigraphy using a CZT camera proved to be useful in understanding the pathophysiology of the patient's clinical condition and in stratifying cardiovascular risk.

Keywords:

Myocardial Perfusion Imaging; Hypertrophy, Left Ventricular; Microvascular Angina; Regional Blood Flow.

Mailing Address: Renata Christian Martins Félix •
Instituto Nacional de Câncer (Inca). Praça da Cruz Vermelha, 23. Postal code: 20230-130. Centro, Rio de Janeiro, RJ – Brazil
E-mail: rcmf1973@gmail.com
Manuscript received June 2, 2023; revised manuscript August 1, 2023; accepted August 7, 2023.
Editor responsible for the review: Rafael Lopes

DOI: https://doi.org/10.36660/abcimg.20230053i

Case presentation

We report the case of a 42-year-old, White, male patient with hypertension and overweight, who complained of recurrent atypical chest pain.

He performed an exercise test that presented exclusively electrocardiographic criteria for myocardial ischemia, reaching 95% of the predicted maximum heart rate and 10 metabolic equivalents.

He was referred for myocardial perfusion scintigraphy under physical exertion, which provided evidence of mild myocardial ischemia in the anteroseptal (middle), latero-apical, and inferolateral (middle) segments, with an estimated ischemic burden of less than 5% of the myocardium.

The patient underwent coronary cineangiography, which did not reveal coronary obstructions, but identified an extensive myocardial bridge in the territory of the left anterior descending artery, with a maximum systolic constriction of 70% in the distal third, and signs of left ventricular hypertrophy.

In spite of optimized clinical therapy, the symptoms persisted.

A new myocardial perfusion scintigraphy was performed with assessment of CFR under pharmacological stress with dipyridamole, which provided evidence of pronounced myocardial ischemia of the left ventricle including segments of the apical, lateral, and inferior walls. A relative increase in radiotracer uptake was observed in the apical wall of the left ventricle on the resting images, suggestive of asymmetric ventricular hypertrophy (Figure 1).

CFR assessment (Figure 2) revealed decreased CFR in all vascular territories and reduced total CFR with a value of 0.97, applying values greater than 2.1 as a reference for normality.[4]

A subsequent echocardiographic study confirmed the presence of important mid-apical hypertrophy of the left ventricle, suggestive of Yamaguchi syndrome (Figure 3).

Discussion

More than 20% of patients with angina who undergo invasive assessment of coronary anatomy do not have significant obstructive lesions. However, in the majority of cases, it is possible to identify factors that justify the symptom, such as myocardial bridge or signs of microvascular disease.[5]

Dysfunction of coronary microcirculation has been shown to play a key role in the development and evolution of a series of cardiovascular conditions, whether in obstructive or non-obstructive atherosclerosis, as well as cardiomyopathies of diverse etiologies.[6]

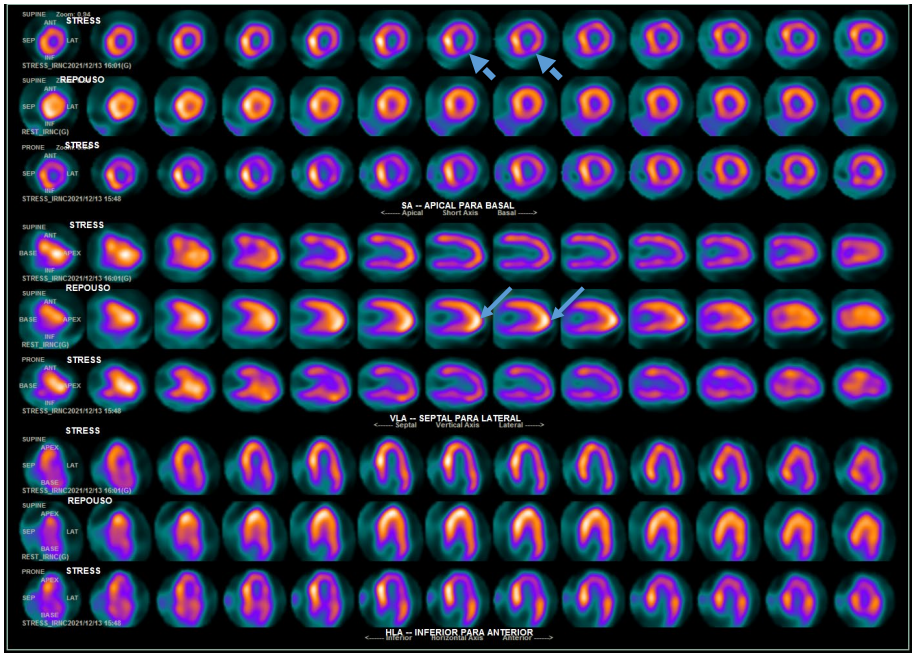

Figure 1 – *Myocardial perfusion scintigraphy. *Images in three axes: short, vertical, and horizontal, respectively. The upper and middle rows show sections in the stress and resting phase with the patient in the supine position, and the bottom row shows sections in the prone position during the stress phase. Short arrows demonstrate areas of perfusion defect in the inferior wall of the left ventricle. The long arrows indicate the relative increase in radiotracer uptake in the apical wall in resting images.*

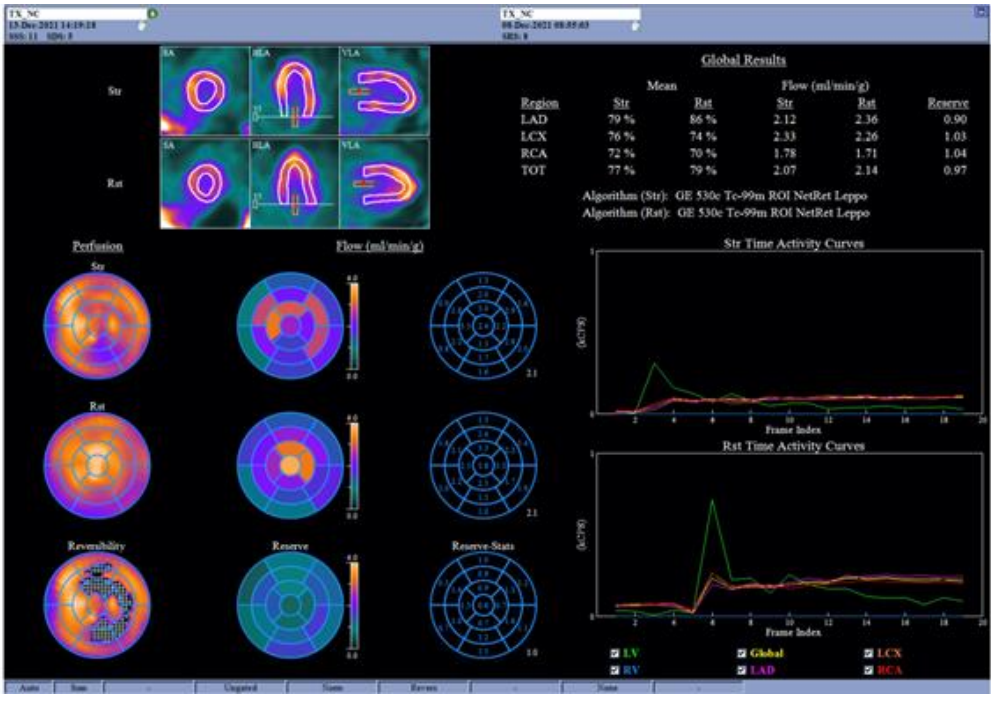

Figure 2 – *CFR assessment. * Upper right: Absolute values of myocardial blood flow under stress and at rest and flow reserve by vascular territory and global reserve. LAD: left anterior descending artery; LCX: left circumflex artery; RCA: right coronary artery; TOT: total values of the left ventricular myocardium. Bottom left: Polar maps condense myocardial perfusion under stress and at rest in the 17 myocardial segments. Reversibility highlights the area of myocardial ischemia. Bottom right: Myocardial radiotracer activity curves over time by vascular territory and globally under stress and at rest.*

Case Report

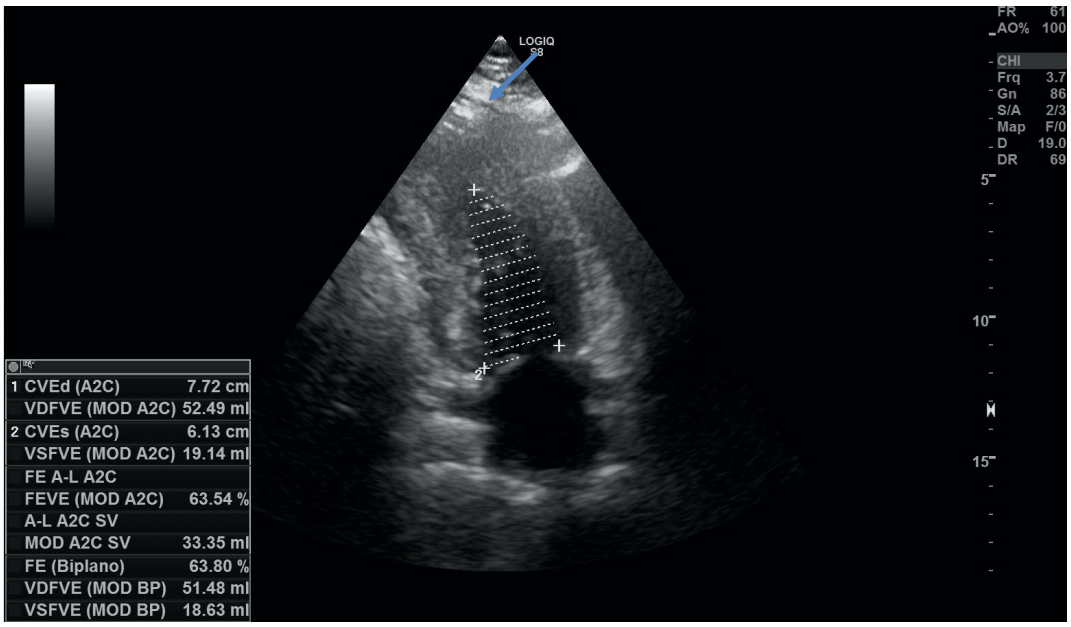

Figure 3 – *Longitudinal two-chamber echocardiogram demonstrating mid-apical left ventricular hypertrophy (arrow).*

Hypertrophic heart disease is a disease of genetic etiology characterized by thickening of the left ventricular wall. It manifests concentrically or asymmetrically, as in apical hypertrophy, also known as Yamaguchi syndrome. Although it is more prevalent among Asian patients, it can be found in up to 10% of cases of left ventricular hypertrophy in patients who are not Asian. Patients with apical hypertrophy may present atrial fibrillation, chest pain, pulmonary hypertension, or ventricular arrhythmias, in addition to an annual mortality rate of up to 4%.[7]

Although magnetic resonance has greater diagnostic sensitivity, echocardiography identifies the disease in the majority of cases, and it can determine prognostic factors, such as the presence of diastolic dysfunction or apical aneurysm.[8]

Myocardial ischemia is a recurrent finding, and it may occur with loss of myocytes and fibrosis. More than the increased demand for oxygen by the hypertrophied myocardium, it is known that structural changes in small vessels are the primary mechanism of perfusion deficit. Thus, damage to the coronary microcirculation is at the core of the ischemic substrate of hypertrophic heart disease.[6]

Studies on the assessment of flow reserve in hypertrophic heart disease have demonstrated the presence of altered CFR, even in areas without hypertrophy, and it plays an important role in prognostic evaluation as a predictor of clinical deterioration, systolic dysfunction, and death, related to the degree of alteration in coronary flow.[9]

In addition to apical ventricular hypertrophy, the patient in this case had a myocardial bridge, a congenital anomaly that determines the intramural course of the coronary epicardial artery. The clinical significance of the myocardial bridge is questionable, considering that it is a systolic compression of the vessel wall, whereas myocardial perfusion is a phenomenon that mainly occurs in diastole. However, the association with ventricular hypertrophy is a determinant additional factor for it reducing myocardial flow reserve and being the cause of angina in these cases.[10]

Evidence has demonstrated that patients with very low global CFR, less than 1.5, without obstructive coronary disease, constitute a high-risk group for cardiovascular events. Unfortunately, the strategies that can alter this clinical outcome are not clear, considering that the pathophysiological mechanisms involved are not completely known.[11]

The assessment of CFR in patients with hypertrophic heart disease, as in the case reported, as well as in other scenarios such as metabolic syndrome, cardio-oncological complications associated with chemotherapy, and heart failure with preserved ejection fraction, identifies the pathophysiological substrate that justifies the patient's clinical condition, stratifies risk, and indicates patients who may benefit from the intensification of the available clinical arsenal with the aim of modifying unfavorable prognosis.[11]

Author Contributions

Conception and design of the research; analysis and interpretation of the data; writing of the manuscript: Félix RCM; acquisition of data: Félix RCM, Pedras FHV, Lima Neto OS, Vitório LM; obtaining financing; critical revision of the manuscript for intellectual content: Pedras FHV.

Potential Conflict of Interest

Renata Christian Martins Félix, Odorico de Souza Lima Neto and Leonardo Medeiros Vitório are collaborators at Clínica Villela Pedras; and Felipe Hermely Villela Pedras is medical director at Clínica Villela Pedras.

Sources of Funding

This study was funded by por Clínica de Medicina Nuclear Villela Pedras.

Study Association

This study is not associated with any thesis or dissertation work.

Ethics Approval and Consent to Participate

This study was approved by the Ethics Committee of the Instituto Nacional de Cardiologia under the protocol number 67072022.3.000.5272. All the procedures in this study were in accordance with the 1975 Helsinki Declaration, updated in 2013. Informed consent was obtained from all participants included in the study.

References

1. Gould KL. Does Coronary Flow Trump Coronary Anatomy? JACC Cardiovasc Imaging. 2009;2(8):1009-23. doi: 10.1016/j.jcmg.2009.06.004.
2. Gould KL, Johnson NP, Bateman TM, Beanlands RS, Bengel FM, Bober R, et al. Anatomic Versus Physiologic Assessment of Coronary Artery Disease. Role of Coronary Flow Reserve, Fractional Flow Reserve, and Positron Emission Tomography Imaging in Revascularization Decision-Making. J Am Coll Cardiol. 2013;62(18):1639-53. doi: 10.1016/j.jacc.2013.07.076.
3. Petretta M, Storto G, Pellegrino T, Bonaduce D, Cuocolo A. Quantitative Assessment of Myocardial Blood Flow with SPECT. Prog Cardiovasc Dis. 2015;57(6):607-14. doi: 10.1016/j.pcad.2014.12.007.
4. Agostini D, Roule V, Nganoa C, Roth N, Baavour R, Parienti JJ, et al. First Validation of Myocardial Flow Reserve Assessed by Dynamic 99mTc-sestamibi CZT-SPECT Camera: Head to Head Comparison with 15O-Water PET and Fractional Flow Reserve in Patients with Suspected Coronary Artery Disease. The WATERDAY Study. Eur J Nucl Med Mol Imaging. 2018;45(7):1079-90. doi: 10.1007/s00259-018-3958-7.
5. Lee BK, Lim HS, Fearon WF, Yong AS, Yamada R, Tanaka S, et al. Invasive Evaluation of Patients with Angina in the Absence of Obstructive Coronary Artery Disease. Circulation. 2015;131(12):1054-60. doi: 10.1161/CIRCULATIONAHA.114.012636.
6. Del Buono MG, Montone RA, Camilli M, Carbone S, Narula J, Lavie CJ, et al. Coronary Microvascular Dysfunction Across the Spectrum of Cardiovascular Diseases: JACC State-of-the-Art Review. J Am Coll Cardiol. 2021;78(13):1352-1371. doi: 10.1016/j.jacc.2021.07.042.
7. Klarich KW, Jost CHA, Binder J, Connolly HM, Scott CG, Freeman WK, et al. Risk of Death in Long-Term Follow-Up of Patients with Apical Hypertrophic Cardiomyopathy. Am J Cardiol. 2013;111(12):1784-91. doi: 10.1016/j.amjcard.2013.02.040.
8. Hughes RK, Knott KD, Malcolmson J, Augusto JB, Mohiddin SA, Kellman P, et al. Apical Hypertrophic Cardiomyopathy: The Variant Less Known. J Am Heart Assoc. 2020;9(5):e015294. doi: 10.1161/JAHA.119.015294.
9. Cecchi F, Olivotto I, Gistri R, Lorenzoni R, Chiriatti G, Camici PG. Coronary Microvascular Dysfunction and Prognosis in Hypertrophic Cardiomyopathy. N Engl J Med. 2003;349(11):1027-35. doi: 10.1056/NEJMoa025050.
10. Tarantini G, Migliore F, Cademartiri F, Fraccaro C, Iliceto S. Left Anterior Descending Artery Myocardial Bridging: A Clinical Approach. J Am Coll Cardiol. 2016;68(25):2887-99. doi: 10.1016/j.jacc.2016.09.973.
11. Taqueti VR, Di Carli MF. Clinical Significance of Noninvasive Coronary Flow Reserve Assessment in Patients with Ischemic Heart Disease. Curr Opin Cardiol. 2016;31(6):662-9. doi: 10.1097/HCO.0000000000000339.

Cardiac Lipoma as an Incidental Finding in Cardiovascular Imaging Exam

Fábio P. Taniguchi,[1] *Marcelo G. Silas,*[1] *Patrícia M. Oliveira*[1]
Hospital do Coração,[1] *São Paulo, SP – Brazil*

Introduction

The advent of cardiac imaging has ushered in an era where incidental findings can be detected using less invasive methods, even in asymptomatic patients. The clinical presentation of cardiac masses, characterized by their varying growth rates and diverse locations within the heart, poses a formidable challenge to cardiologists. Therefore, paramount importance lies in reducing the clinical burden and costs, considering the potential of cardiac imaging to optimize the clinical pathway.[1] The most common cardiac masses in the right atrium include thrombi, vegetations, and neoplasia. Approximately 75% of primary tumors are benign, with myxomas comprising 50% of benign cases. Other benign tumors that usually may arise in the right atrium are rhabdomyomas, fibromas, fibroelastomas, and lipomas. Cardiac lipomas are rare, accounting for 2.9% to 8% of all benign cardiac tumors. They rank third in frequency after myxomas and papillary fibroelastomas. The literature suggests that 25% of cardiac lipomas are intramyocardial; 25% are extracavitary of epicardial origin, and 50% are intracavitary of subendocardial origin.[2] Lipomas are well-encapsulated and homogeneous masses composed of mature fat. Although the etiology of cardiac lipomas is unknown, they can originate from any of the three cardiac tissues: subendocardial (the most common), pericardial, or myocardial.[3]

The aim of this report is to present a case of an asymptomatic right atrial lipoma and to discuss the etiology, natural history, and optimal management strategies for right atrial lipomas.

Case presentation

A 66-year-old asymptomatic woman was diagnosed with cardiac tumor. Physical examination and laboratory test results were unremarkable. An electrocardiogram showed normal sinus rhythm. Chest X-ray was also unremarkable. Echocardiography demonstrated an echogenic image, which was homogeneous, measuring approximately 26 × 17 mm, sessile, with well-defined borders, located in the posterior wall of the right atrium (Figure 1). Magnetic resonance imaging described a homogeneous nodular image in the posterior wall of the right atrium, which was movable, with well-defined borders, measuring 2.4 × 2.2 × 1.9 cm. It showed low signal intensity on T2-weighted images, high signal intensity on T1-weighted images with fat saturation, absence of first-pass gadolinium perfusion, and absence of delayed enhancement (Figure 2). The patient was referred to cardiac surgery with cardiopulmonary bypass. After right atriotomy, a smooth, yellowish fatty mass protruding into the right atrium was noted. The 3 × 3 × 2.5-cm mass had a broad attachment to the right atrium. The tumor was resected (Figure 3); free margins of the atrium were cautiously taken (Video 1). The patient had an unremarkable recovery and was discharged from the hospital at day 4.

Pathological examination revealed proliferation of mature adipose cells forming monotonous sheets traversed by thin collagen septa in continuity with a thin capsule. Additionally, there were randomly arranged vessels of various sizes. At the periphery, there was representation of adhered endomyocardial tissue with mild interstitial edema, and the muscle fibers were focally separated by adipocytes (Figure 4).

Discussion

Cardiac lipomas are slow-growing tumors that may remain asymptomatic for years. However, they may present a wide range of clinical symptoms and signs, including arrhythmia, peripheral embolization, obstructive symptoms, and even sudden cardiac death. The manifestation of symptoms is often influenced by the size, location, and infiltration of the tumor.[4] There are no differences in the incidence of cardiac lipomas between age groups or sexes.[5]

These tumors can occur anywhere within the heart, with approximately 53.1% located in the cardiac chambers, 32.5% in the pericardium, 10.7% within the myocardium, and 3.7% involving multiple structures. Specifically, around 40% of cardiac lipomas are found in the right atrium.[5]

In a setting of 26 cases of right atrial lipomas, with 13 cases in females, 12 cases in males, and 1 case in a transgender individual, the median age of the patients was 55.5 years, ranging from 17 to 74 years. Symptoms related to right atrial lipomas were present in 21 out of 26 patients (80%). The symptoms varied significantly, with dyspnea being the most common (35%), followed by chest pain (15%) and palpitations (12%).[6]

Lipomas are characterized as soft masses of fat tissue often surrounded by a thin layer of fibrous tissue. While most cardiac lipomas are composed of mature white adipose tissue, there have been reported cases of cardiac lipomas consisting of fetal brown fat. The etiology of these mesenchymal tumors remains unknown. Genetic variations, mainly involving the HMGA2 gene, are commonly observed in extracardiac lipomas.[6,7] Multiple cardiac lipomas have been reported in patients with tuberous sclerosis, although their relationship

Keywords

Cardiovascular Surgical Procedures; Neoplasms; Lipoma

Mailing Address: Fábio Papa Taniguchi •
Hospital do Coração (HCor). R. Des. Eliseu Guilherme, 147. Postal code: 04004-030. Paraíso, São Paulo, SP – Brazil
E-mail: ftaniguchi@hcor.com.br
Manuscript received June 23, 2023; revised August 10, 2023; accepted August 22, 2023
Editor responsible for the review: Daniela do Carmo Rassi Frota

DOI: https://doi.org/10.36660/abcimg.20230059i

Contents

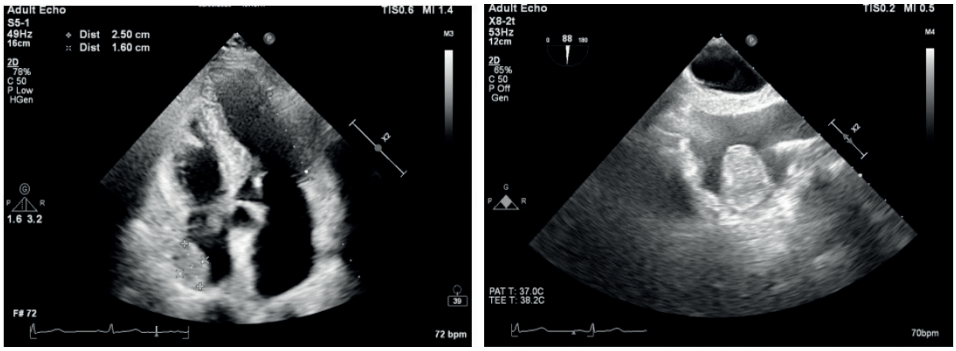

Figure 1 – *Echocardiography: echogenic, homogeneous image, measuring approximately 26 x 17 mm, sessile, and with well-defined borders, located in the posterior wall of the right atrium*

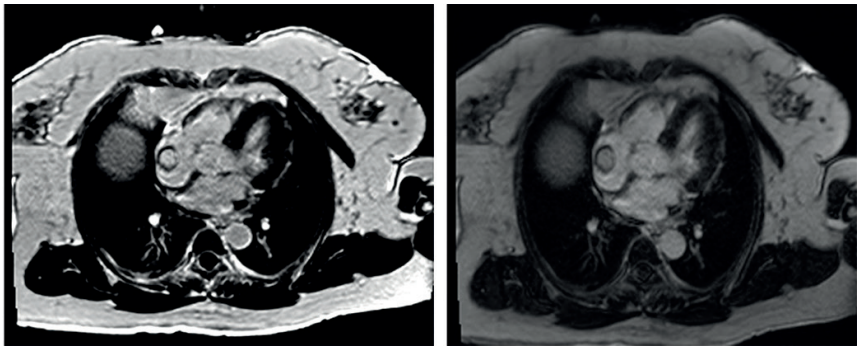

Figure 2 – *Magnetic resonance image showing low signal intensity on T2-weighted images, high signal intensity on T1-weighted images with fat saturation, absence of first-pass gadolinium perfusion, and absence of delayed enhancement.*

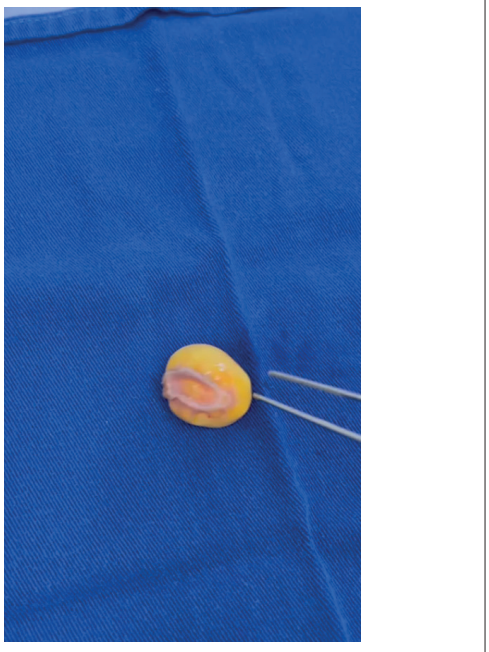

Video 1 – *Link: http://abcimaging.org/supplementary-material/2023/3603/2023-0059_CC_video_1.mp4*

Figure 3 – *Gross macrospcopy of the tumor. Left: upper view of the tumor revealing smooth, yellowish fatty mass; right: bottom view, resected pediculous attachment to the atrium wall.*

has yet to be fully established. There is currently no evidence suggesting that cardiac lipomas can undergo malignant transformation. However, it is possible for mature lipomas and well-differentiated liposarcomas to coexist within the same heart.[8] Cardiac liposarcoma is another rare entity with an unfavorable prognosis that is predominantly localized in the right atrium.

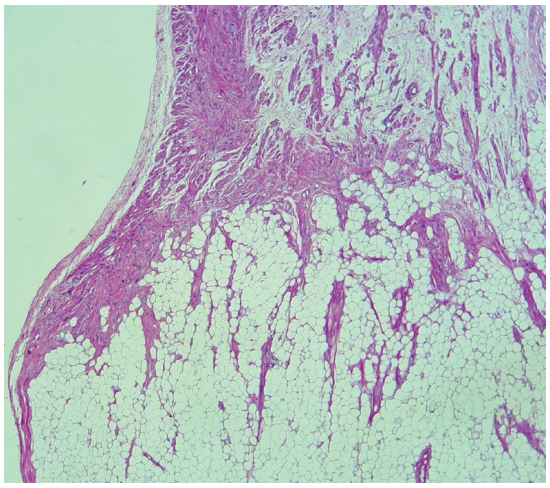

Figure 4 – *Tumor cells demonstraded by mature adipose cells.*

Accurate diagnosis and comprehensive evaluation of cardiac lipomas are heavily reliant on the utilization of multimodality imaging methods. Among these, transthoracic echocardiography emerges as a cost-effective and easily accessible approach that avoids exposure to radiation or ionizing contrast agents. Meanwhile, transesophageal echocardiography assumes significance in the assessment of atrial lesions or mobile valvular lesions, offering superior visualization of mass morphology and its anatomical relationships. Complementary to these techniques, cardiac computed tomography plays a vital role in providing a detailed assessment of calcified lesions and extracardiac anatomy, in addition to the opportunity to highlight irregular mass margins and invasions. Lastly, cardiac magnetic resonance imaging demonstrates exceptional prowess in accurately distinguishing between thrombus and tumor entities, thereby bolstering the diagnostic accuracy in this intricate domain.[1,4,6]

The management of asymptomatic patients with cardiac lipomas is a subject of debate. Radical resection of the lipoma is the optimal method of treatment in symptomatic patients. Conservative management may be implemented for asymptomatic cardiac lipomas, and prophylactic resection should also be considered.

Author Contributions

Conception and design of the research, analysis and interpretation of the data, statistical analysis, writing of the manuscript: Taniguchi FP; acquisition of data and critical revision of the manuscript for intellectual content: Taniguchi FP, Silas MG, Oliveira PM.

Potential Conflict of Interest

No potential conflict of interest relevant to this article was reported.

Sources of Funding

There were no external funding sources for this study.

Study Association

This study is not associated with any thesis or dissertation work.

Ethics Approval and Consent to Participate

This article does not contain any studies with human participants or animals performed by any of the authors.

References

1. Quah KHK, Foo JS, Koh CH. Approach to Cardiac Masses Using Multimodal Cardiac Imaging. Curr Probl Cardiol. 2023;48(8):101731. doi: 10.1016/j.cpcardiol.2023.101731.
2. Valenti V, Zia MI, Uretsky S, Wolff SD. Intra-Myocardial Left Ventricular Lipoma Associated with Non-Compaction Cardiomyopathy. Eur Heart J Cardiovasc Imaging. 2012;13(11):963. doi: 10.1093/ehjci/jes110.
3. Naseerullah FS, Javaiya H, Murthy A. Cardiac Lipoma: An Uncharacteristically Large Intra-Atrial Mass Causing Symptoms. Case Rep Cardiol. 2018;2018:3531982. doi: 10.1155/2018/3531982.
4. Bardakci H, Altintas G, Unal U, Kervan U, Arda K, Birincioglu L. Giant Cardiac Lipoma: Report of a Case. J Card Surg. 2008;23(3):254-6. doi: 10.1111/j.1540-8191.2007.00519.x.
5. Shu S, Wang J, Zheng C. From Pathogenesis to Treatment, a Systemic Review of Cardiac Lipoma. J Cardiothorac Surg. 2021;16(1):1. doi: 10.1186/s13019-020-01379-6.
6. Bajdechi M, Onciul S, Costache V, Brici S, Gurghean A. Right Atrial Lipoma: A Case Report and Literature Review. Exp Ther Med. 2022;24(5):697. doi: 10.3892/etm.2022.11633.
7. Nishio J. Contributions of Cytogenetics and Molecular Cytogenetics to the Diagnosis of Adipocytic Tumors. J Biomed Biotechnol. 2011;2011:524067. doi: 10.1155/2011/524067.
8. Kong F, Zhang W, Guo Q. Multiple Well-Differentiated Cardiac Liposarcoma with a Concomitant Myocardial Lipoma: A Case Report. Mol Clin Oncol. 2018;9(6):617-21. doi: 10.3892/mco.2018.1741.

Cardiac Metastasis and Krukenberg Tumor: A Case Report

Jessyca Gonçalves Cruz,[1] Ana Gardenia Liberato Ponte Farias,[1] João David Leitão de Lucena,[1] Christiane Bezerra Rocha Liberato,[1] Ana Carolina Brito de Alcantara,[1] Mauricio Costa Lima[1]

Universidade Federal do Ceará Hospital Universitário Walter Cantídio, Cardiologia/Ecocardiografia,[1] Fortaleza, CE – Brazil

Introduction

Primary cardiac tumors are rare, affecting between 0.0017% and 0.28% of the population.[1] Secondary or metastatic tumors, on the other hand, are 40 to 100 times more frequent than primary tumors.[2] The primary sites that most often metastasize to the heart are the lungs, breast, malignant melanoma, and hematological tumors. Cardiac metastasis secondary to ovarian tumors is infrequent and, in the cases described, mainly affects the pericardium, with no intracavitary lesions described.[3] Metastatic neoplasms can reach the heart by these routes: hematogenous, direct extension, lymphatic vessels, and through the pulmonary veins and vena cava.[4,5]

The term "Krukenberg tumor" is used clinically to designate a metastatic carcinoma of mucin-secreting signet ring cells in the dense fibroblastic stroma of the ovary.[5,7] It mainly affects premenopausal women, at a mean age of diagnosis of 45 years, with 70% of cases in the stomach as the most common primary site, followed by the colon, appendix, and breast.[5,6] A history of carcinoma prior to the diagnosis of Krukenberg is obtained in only 20% of cases, and the primary site is often unknown.[7] The mortality rate is high, and survival is 14 months on average after diagnosis.[6,7]

This case report describes the case of a patient with a secondary Krukenberg tumor and significant cardiac metastatic involvement, presenting multiple intracavitary tumors assessed by transesophageal echocardiography (TEE), demonstrating the importance of careful assessment of tumor lesions by echocardiographers.

Case report

A 45-year-old woman sought medical attention due to diffuse abdominal discomfort which had started about 9 months earlier. Physical examination revealed a palpable mass in the right iliac fossa. She underwent an outpatient abdominal ultrasound, which revealed an expansive solid-cystic formation presumably in the right ovary. The patient was admitted for surgical treatment in August 2022.

Keywords

Neoplasm Metastasis; Brenner Tumor; Krukenberg Tumor.

Mailing Address: Jessyca Gonçalves Cruz •
Universidade de Fortaleza. Av. Washington Soares, 1321. Postal code: 60811-905. Edson Queiroz, Fortaleza, CE – Brazil
E-mail: jessycagcruz@hotmail.com
Manuscript received May 30, 2023; revised September 1, 2023; accepted September 4, 2023
Editor responsible for the review: Marco Stephan Lofrano Alves

DOI: https://doi.org/10.36660/abcimg.20230051i

During her admission, the patient had a sudden episode of dyspnea, raising the hypothesis of a pulmonary embolism. The patient was tachycardic and tachypneic, with a heart rate of around 105 bpm, an estimated respiratory rate of 25 bpm, and peripheral oxygen saturation close to 95% on oxygen supplementation via a nasal catheter. No hemodynamic instability or other alterations were seen on the cardiopulmonary physical examination. The extremities were perfused, with no clinical signs of peripheral venous thrombosis. The electrocardiogram showed tachycardic sinus rhythm, with no other alterations.

A transthoracic echocardiogram (TTE) was requested. It was urgently conducted in bed, with acoustic windows that were difficult to see through, but multiple intracavitary mobile lesions could already be seen. Except for a slight increase in the left atrium, the other cavities were normal in size. The valves were morphologically normal, with only mild mitral and tricuspid regurgitation. Her biventricular function was preserved, with an estimated left ventricular ejection fraction of 60% on a two-dimensional scan, with an unfavorable apical acoustic window for using the Simpson Rule. No signs of pulmonary hypertension were seen. We opted for immediate TEE, which showed multiple mobile echogenic lesions, loose inside the cavities, homogeneous, with well-defined contours and varying dimensions inside both atria (Figures 1A and 1B) moving into the ventricles through the mitral and tricuspid valves. Approximately 6 masses were found inside the right atrium, the largest of which came from the inferior vena cava and measured 7.1 × 0.3 cm (Figures 2 and 4). Inside the left atrium, the masses were smaller, multiple and mobile, around 12 in total, and their diameters were difficult to measure. They appeared to originate in the right atrium through a patent foramen ovale (PFO), as one of the masses passed from the right atrium to the left atrium through the PFO during the examination (Figures 3A and 3B). No implants were seen in the topography of the pericardium, which presented its usual appearance, and no pericardial or pleural effusions were seen.

The investigation of the abdominal mass was followed up with a contrast-enhanced abdominal CT scan, which showed a large heterogeneous solid-cystic mass measuring 29.1 × 25.6 × 20.7 cm, and dilatation and filling of the right gonadal vein and inferior vena cava with soft tissue density, extending into the right atrium. A biopsy of the right ovary was performed, revealing the presence of small, isolated cells, with vacuolized cytoplasm like a signet ring, sparse in the middle of the stroma. Upper gastrointestinal endoscopy was also performed and showed no gastric lesions. Cardiac MRI was conducted, describing intracardiac tumor lesions as solid tubular expansive formations, extending from the inferior vena cava to the right atrium and right ventricle, reaching the pulmonary artery, with discrete perfusion of the

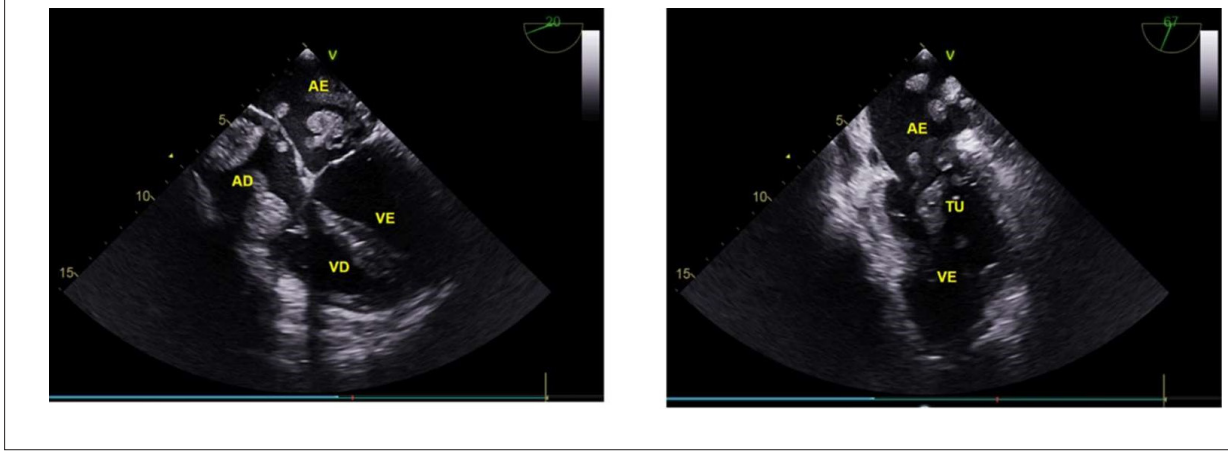

Figure 1A and 1B – *TEE images showing the tumors in the heart cavities. In Figure 1A, taken at 20º, we observe the tumors in both atria, with the mass passing through the interatrial septum. Figure 1B, taken at 67º, shows the tumors in the left chambers, passing through the mitral valve.*

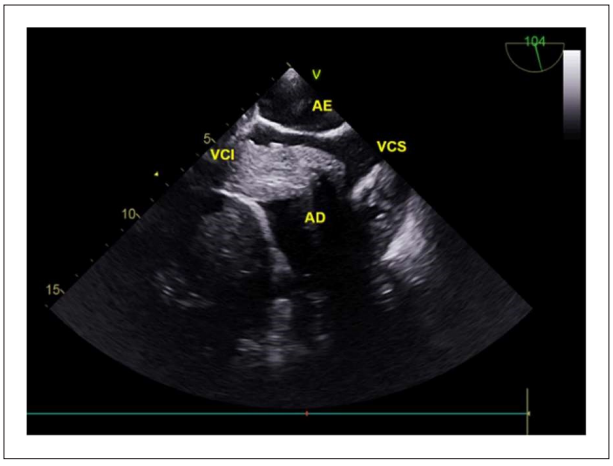

Figure 2 – *Image of a bicaval section, taken at 104º, showing the largest tumor inside the right atrium, originating in the inferior vena cava.*

lesion in the first pass and uniform late enhancement after contrast injection, compatible with tumor implants.

Clinical cardiology, cardiac surgery, clinical oncology, general surgery, surgical oncology, and palliative care teams assessed the patient jointly. The main diagnostic hypothesis, based on the clinical-imaging cardiac and abdominal symptoms, and the histopathology of the ovary, showing a spindle cell neoplasm with signet ring cytoplasm, which would be Krukenberg tumor, a secondary tumor with no established primary site, associated to multiple cardiac metastases. Biopsies of the heart tumors and invasive procedures to investigate the primary site related to the ovary neoplasm were discouraged by the attending teams, in agreement with the patient and her family, due to the risk of the procedures and the low prospect of resectability of the lesions. So, palliative care prevailed, with no curative proposal. The patient was clinically treated with full anticoagulation and her symptoms improved. She was discharged from hospital and is currently asymptomatic, being followed up as an outpatient by the palliative care and general surgery teams.

Discussion

Metastatic disease is the most common cardiac neoplasm in adults, with a reported incidence of 0.7% to 3.5% in the general population, and 9.1% in patients with established advanced neoplasia.[8,1] The increased incidence is due, partly at least, to advances in diagnostic imaging and improved therapeutic interventions in cancer patients. The primary sites that metastasize most frequently to the heart are lung, breast, malignant melanoma, and hematological tumors, probably due to their high prevalence and aggressive nature.[1] Malignant metastatic disease can reach the heart in various ways, including direct extension (lung carcinoma), via the hematogenous route (melanoma and hematological neoplasms), via the lymphatic route (breast carcinoma), and venous extension (renal carcinoma).[4]

The clinical picture of cardiac metastasis is often unspecific, depending mainly on the location of the tumor and the degree of involvement, and it can be asymptomatic, with diagnosis only after autopsy.[8] Percardial metastases, which account for more than 60% of cardiac metastases, can cause pericarditis or effusion, resulting in corresponding clinical signs and symptoms.[8,4] Myocardial metastases account for around a third of cases and can evolve with arrhythmia and chest pain, in addition to contractile dysfunction and a clinical picture of heart failure.[9] Endocardial involvement is rare, described in 3% to 5% of cases, and can evolve with obstruction and/or embolization. Paraneoplastic phenomena, such as thromboembolic events, can also occur.[8]

The first-line test for the initial assessment of cardiac metastatic lesions is echocardiography, which is a widely available, noninvasive procedure which identifies the presence of masses, and their respective characteristics, location, and relationship with adjacent structures.[3]

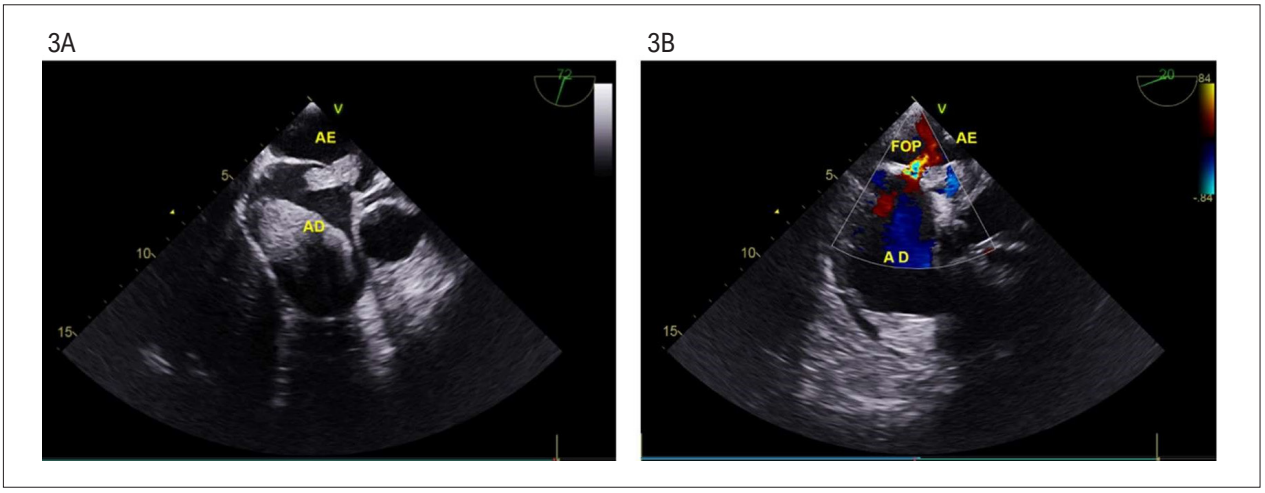

Figures 3A and 3B – *Images of the interatrial septum. Figure 3A reveals a tumor lesion passing through the PFO. Figure 3B, showing right-to-left flow using color Doppler.*

Cardiac resonance imaging and computed tomography act as complementary imaging techniques, providing more detailed anatomical images and information on the tumor's vascularization and local invasion.[10]

The treatment of cardiac metastases depends on the clinical presentation and is initially aimed at controlling symptoms and complications, such as pericardial tamponade, arrhythmias, and symptoms of heart failure. Other forms of treatment, such as tumor resection, chemotherapy, and radiotherapy, must be individually adapted to each patient.

Currently, no protocol for investigating cardiac metastases in patients with malignant neoplasms is established. However, for screening purposes, some authors suggest performing an echocardiogram on patients with lung and liver cancer who have cardiac arrhythmias. The prognosis of malignant cardiac tumors secondary to metastases is poor, given that patients present with advanced cardiac metastases at the time of diagnosis.[11]

This report illustrates a case of extensive cardiac metastatic involvement, originating in the inferior vena cava, with multiple intracavitary mobile tumors affecting all 4 heart chambers, associated with the presence of a secondary ovarian tumor, with no defined primary etiology.

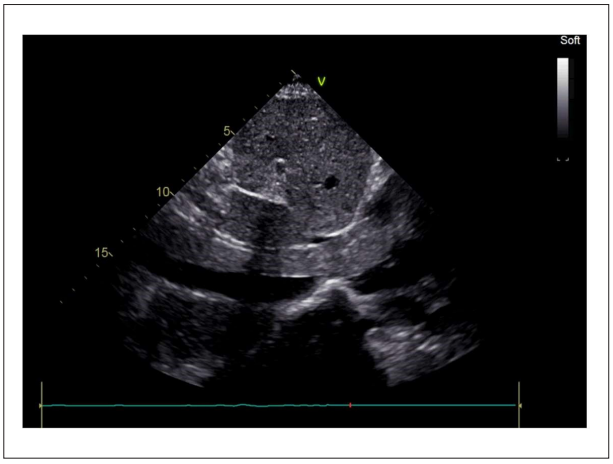

Figure 4 – *Image of the inferior vena cava in a subcostal window on TTE, filled with an extensive tumor lesion, up to its entrance into the right atrium.*

Conclusion

In cases of advanced neoplasms, a detailed assessment of the cardiac structures (pericardium, epicardium, myocardium, and endocardium) should be performed in the search for metastases. Echocardiography, in its various forms, enables early diagnosis of cardiac involvement.

Author Contributions

Conception and design of the research, acquisition of data: Cruz JG, Lucena JDL

Cruz JG, Lucena JDL; analysis and interpretation of the data, writing of the manuscript: Cruz JG; critical revision of the manuscript for intellectual content: Cruz JG, Lucena JDL, Farias AGLP, Liberato CBR, Alcantara ACB, Lima MC.

Potential Conflict of Interest

No potential conflict of interest relevant to this article was reported.

Sources of Funding

There were no external funding sources for this study.

Study Association

This study is not associated with any thesis or dissertation work.

Ethics Approval and Consent to Participate

This article does not contain any studies with human participants or animals performed by any of the authors.

References

1. Goldberg AD, Blankstein R, Padera RF. Tumors Metastatic to the Heart. Circulation. 2013;128(16):1790-4. doi: 10.1161/CIRCULATIONAHA.112.000790.
2. Morosin M, Azzu A, Capoccia M, Rosendahl U. Extensive Cardiac Infiltrative Melanoma. J Card Surg. 2019;34(9):858-9. doi: 10.1111/jocs.14184.
3. Baba Y, Ishikawa S, Ikeda K, Honda S, Miyanari N, Iyama K, et al. A Patient with 43 Synchronous Early Gastric Carcinomas with a Krukenberg Tumor and Pericardial Metastasis. Gastric Cancer. 2007;10(2):135-9. doi: 10.1007/s10120-007-0416-9.
4. Kavanagh MM, Janjanin S, Prgomet D. Cardiac Metastases and a Sudden Death as a Complication of Advanced Stage of Head and Neck Squamous Cell Carcinoma. Coll Antropol. 2012;36 Suppl 2:19-21.
5. Lionetti R, De Luca M, Raffone A, Travaglino A, Coppellotti A, Peltrini R, et al. Clinics and Pathology of Krukenberg Tumor: A Systematic Review and Meta-Analysis. Minerva Obstet Gynecol. 2022;74(4):356-63. doi: 10.23736/S2724-606X.21.04797-7.
6. Xie H, Erickson BJ, Sheedy SP, Yin J, Hubbard JM. The Diagnosis and Outcome of Krukenberg Tumors. J Gastrointest Oncol. 2021;12(2):226-36. doi: 10.21037/jgo-20-364.
7. Zulfiqar M, Koen J, Nougaret S, Bolan C, van Buren W, McGettigan M, et al. Krukenberg Tumors: Update on Imaging and Clinical Features. AJR Am J Roentgenol. 2020;215(4):1020-9. doi: 10.2214/AJR.19.22184.
8. Maleszewski JJ, Bois MC, Bois JP, Young PM, Stulak JM, Klarich KW. Neoplasia and the Heart: Pathological Review of Effects with Clinical and Radiological Correlation. J Am Coll Cardiol. 2018;72(2):202-27. doi: 10.1016/j.jacc.2018.05.026.
9. Srinivas SK, Subramanyam K, Ramalingam R, Bhat S, Kalpana SR, Manjunath CN. A Rare Case of Left Ventricular Outflow Tract Mass. Echocardiography. 2013;30(9):E274-7. doi: 10.1111/echo.12294.
10. Crean AM, Juli C. Diagnosis of Metastatic Melanoma to the Heart with an Intrinsic Contrast Approach Using Melanin Inversion Recovery Imaging. J Comput Assist Tomogr. 2007;31(6):924-30. doi: 10.1097/RCT.0b013e31804b213b.
11. Nova-Camacho LM, Gomez-Dorronsoro M, Guarch R, Cordoba A, Cevallos MI, Panizo-Santos A. Cardiac Metastasis from Solid Cancers: A 35-Year Single-Center Autopsy Study. Arch Pathol Lab Med. 2023;147(2):177-84. doi: 10.5858/arpa.2021-0418-OA.

Initial Experience of Intracardiac Echocardiography-Guided Left Atrial Appendage Occlusion: Report of Six Cases

Fabricio Sarmento Vassallo,[1,2] Henrique Teixeira Giestas Serpa,[2] Betina Reseck Walker,[1] Vinícius Fraga Mauro,[1] Carlos Volponi Lovatto,[1,2] Eduardo Serpa,[1] Lucas Corsino dos Santos,[1] Hermes Carloni,[1] Aloyr Simões,[1] Edevaldo da Silva,[1] Gracielly Barros,[1] Renato Giestas Serpa[1]

Hospital Santa Rita de Cássia,[1] Vitória, ES – Brazil

Hospital Santa Casa de Misericordia de Vitória,[2] Vitória, ES – Brazil

Introduction

In recent decades, the incidence of atrial fibrillation (AF) has increased exponentially worldwide.[1,2] This comorbidity is directly related to cardioembolic events, and oral anticoagulation is considered the gold standard treatment for its prevention. Although oral anticoagulation is effective in preventing ischemic stroke, warfarin is contraindicated in 14% to 44% of patients at risk for cardioembolic stroke; nevertheless, even in eligible patients, only 54% are anticoagulated. Currently, direct-acting oral anticoagulants (DOAC) are preferable as preventive therapy for ischemic stroke; however, the discontinuation rates of these drugs reported in clinical trials, mainly due to intolerance or side effects, vary from 23% to 35%. In patients with a history of hemorrhagic stroke, uncontrolled non-intracranial bleeding, and end-stage chronic kidney disease or dialysis, the use of DOAC is relatively or absolutely contraindicated.

In cases of non-valvular AF, when the aforementioned contraindications to DOAC use are present, left atrial appendage occlusion (LAAO) has shown to be effective as a therapeutic alternative.[3] This procedure has been guided and performed using transesophageal echocardiography, which is considered the gold standard. However, services that have incorporated intracardiac echocardiography as an auxiliary tool during catheter ablation for the treatment of AF went on to use this method as a safe and effective alternative to transesophageal echocardiography in LAAO procedures. [3-5]

Case reports

Between July 2022 and March 2023, 6 patients underwent intracardiac echocardiography-guided LAAO therapy along with catheter ablation for AF. The mean age of patients was 74 ± 8 years, and 4 (66.7%) were male. The mean CHA_2DS_2VASC score was 5.2 ± 1.4, and the mean HASBLED score was 3.2 ± 1.8. The individual demographic data of the patients as well as the indications for LAAO are displayed in Table 1. The ablation procedures were conducted with electroanatomical mapping and a ViewflexTM intracardiac echocardiography catheter (Abbott, USA), as shown in Figure 1A. We performed measurements of the left atrial appendage (LAA) with intracardiac echocardiography in the left atrium after transseptal puncture with pre- and post-ablation measurements, which showed no differences. Measurements were taken in the left interatrial septum, the left superior pulmonary vein, in the ostium of the left inferior pulmonary vein, and in the mitral annulus inferior to the LAA. The mean procedure times for ablation and LAAO were 72.8 ± 13.7 minutes and 24.7 ± 13.8 minutes, respectively. The contrast volume used was 39.2 ± 24.6 ml. Data from the echocardiography and procedures are displayed in Tables 2 and 3. The procedures were considered successful, and 1 patient had a right femoral artery pseudoaneurysm with conservative treatment.

Discussion

In patients with non-valvular AF, ischemic stroke, in addition to being a feared complication with catastrophic consequences, can be prevented with the use of DOAC. Nonetheless, there are patients who have limitations to the DOAC, as well as patients who, even when using them, have cardioembolic events. For these reasons, LAAO has become an efficient mechanical alternative for preventing ischemic stroke.

Currently, transesophageal echocardiography and fluoroscopy are frequently used to guide LAAO. The main advantage of intracardiac echocardiography-guided LAAO would be avoiding general anesthesia in cases where this procedure is performed alone, in addition to being performed by the interventionist, keeping in mind that it is widely used in AF ablations. Even though the images produced by intracardiac echocardiography have excellent quality and clarity, in some cases, the evaluation of some structures may be limited, especially in enlarged left atria, as in patients with AF. This imaging limitation can generally be overcome by placing the intracardiac echocardiography catheter directly into the left atrium, which is not a limitation, considering that transseptal puncture is a step in this procedure.

Keywords

Atrial Fibrillation; Atrial Appendage; Embolic Stroke; Anticoagulants.

Mailing Address: Fabricio Sarmento Vassallo •
Hospital Santa Rita de Cássia. Rua Marechal Campos, 1579. Postal code: 29043-260. Santa Cecília, Vitória, ES – Brazil
E-mail: fsvassallo@cardiol.br
Manuscript received June 23, 2023; revised September 4, 2023; accepted September 11, 2023
Editor responsible for the review: Marco Stephan Lofrano Alves

DOI: https://doi.org/10.36660/abcimg.20230062i

Table 1 – Demographic data of study patients. CKF: chronic kidney failure; DM: diabetes mellitus; LAA: left atrial appendage; SAH: systemic arterial hypertension; AF: atrial fibrillation; DOAC: direct-acting oral anticoagulants.

Demographic data	Patient 1	Patient 2	Patient 3	Patient 4	Patient 5	Patient 6
Age (years)	79	82	76	80	73	55
Sex	M	F	M	M	M	F
Indication for occlusion	Major bleeding	CKF + major bleeding	Major bleeding	Ischemic stroke with DOAC use	Major bleeding	Cardioembolic event + LAA thrombus
SAH	Yes	Yes	Yes	Yes	Yes	Yes
DM	No	Yes	Yes	Yes	No	No
Vascular disease	Yes	Yes	Yes	Yes	Yes	Yes
Type of AF	Persistent	Persistent	Paroxysmal	Persistent	Persistent	Paroxysmal

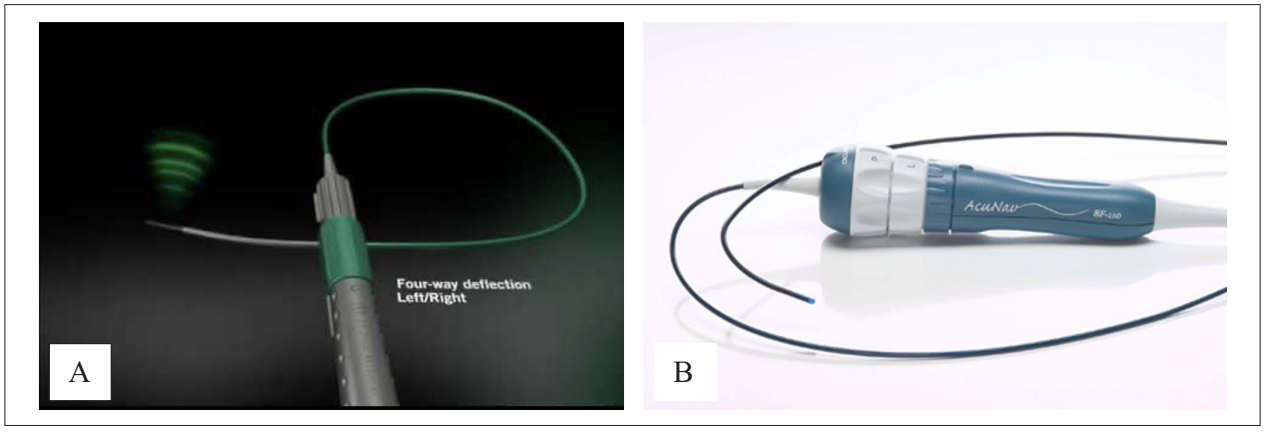

Figure 1 – *Models of intracardiac echocardiography catheters. A) Viewflex catheter (ABBOTT™); B) Acunav catheter (Biosense Webster™).*

Table 2 – Pre-procedure echocardiographic data of study patients. LA: left atrial; LVEF: left ventricular ejection fraction.

Pre-procedure echocardiographic data	Patient 1	Patient 2	Patient 3	Patient 4	Patient 5	Patient 6
LA diameter (mm)	39	54	39	41.7	42	42
LVEF (%)	59	55	71	67	66	62

The intracardiac echocardiography probe in the left superior pulmonary vein provides a long-axis view of the LAA that is similar to the 0° view on transesophageal echocardiography. With the probe 1 cm proximal to the ostium of the left pulmonary veins, tilted posteriorly (also called retroflexion), a view similar to 45° on transesophageal echocardiography can be obtained, showing the left superior pulmonary vein, the ostium of the LAA, the circumflex artery, and the mitral valve. This view, known as "home view," is preferred during the procedure (Figures 2 and 3). Another important projection is known as "supramitral" (or inferior) view of the LAA similar to the 135° view on transesophageal echocardiography.[6]

Available clinical studies have shown that intracardiac echocardiography-guided LAAO appears to be non-inferior to transesophageal echocardiography in terms of procedural success, periprocedural complications, and embolic events.[6,7] A recent meta-analysis, which did not include any prospective randomized studies, with more than 1000 patients analyzed, confirmed that the success rates of the procedures are similar, with a tendency toward a lower rate of procedure-related complications and a lower contrast volume used in patients who received intracardiac echocardiography-guided LAAO compared to transesophageal echocardiography.[7] Given that intracardiac echocardiography is a monoplanar imaging technique, we recommend that, prior to the procedure, transesophageal echocardiography or computed tomography angiography of the left atrium and LAA should be

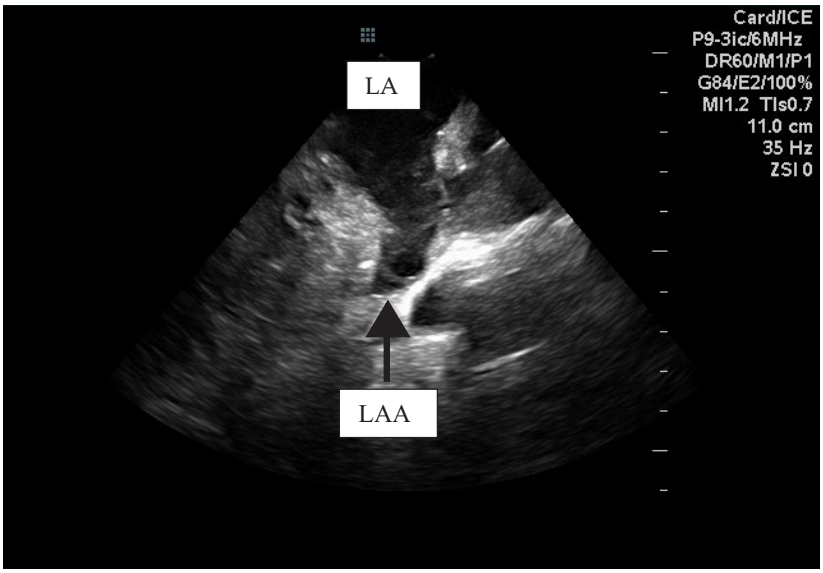

Figure 2 – *LAA visualized with an intracardiac echocardiogram probe in the "home view" position, which is positioned on the left side of the interatrial septum (LA). LAA: left atrial appendage; LA: left atrium.*

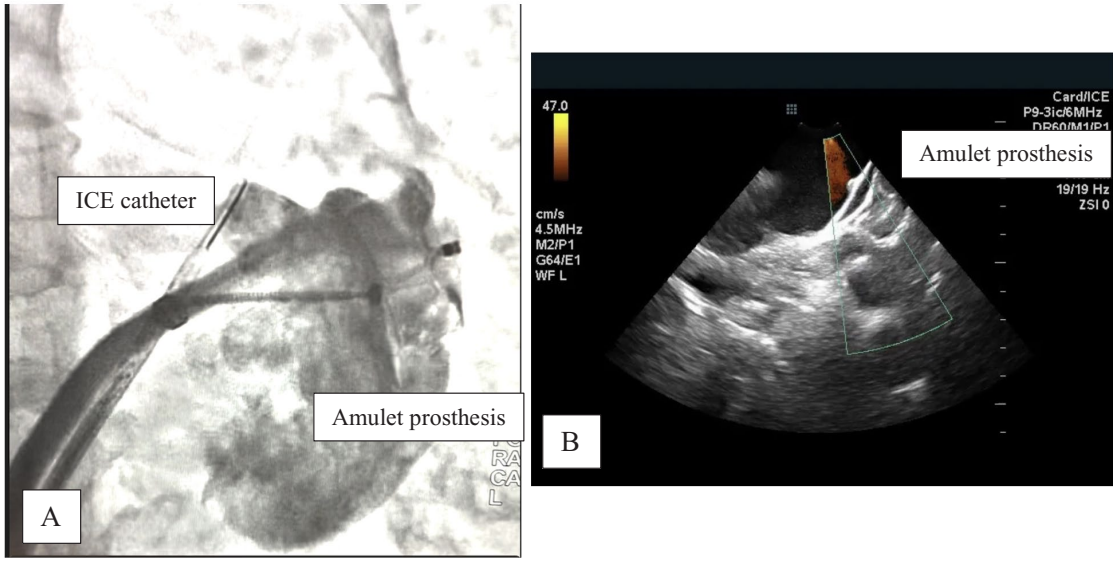

Figure 3 – *A: ICE catheter viewed under fluoroscopy in the left "home view" position for final assessment of the LAAO prosthesis before release. B: Final position of the AmuletTM prosthesis after release and Doppler analysis to evaluate periprosthetic leakage. ICE: intracardiac echocardiogram.*

performed to rule out the presence of thrombi and to obtain adequate measurement of these structures that will be used to guide the intervention.

In summary, intracardiac echocardiography-guided LAAO shows results and follow-up similar to transesophageal echocardiography. Due to the large volume of LAAO procedures worldwide, new techniques to better integrate this procedure into the standard laboratory routine are important. Intracardiac echocardiography guidance simplifies the procedure in many cases, avoiding general anesthesia, reducing patient discomfort, and improving and optimizing room usage time. Taken together, the results of several observational studies support the adoption of intracardiac echocardiography-guided LAAO; nonetheless, operators need to master the technique by going through the learning curve necessary to improve and use this complex technique. Our initial experience with use of intracardiac echocardiography as a guide in this procedure was positive,

Table 3 – Procedure data of study patients.

Procedure data	Patient 1	Patient 2	Patient 3	Patient 4	Patient 5	Patient 6
Prosthesis used	Amulet	Amulet	Watchman	Amulet	Amulet	Amulet
Prosthesis diameter	28	28	27	28	25	31
X-ray time (min)	2.4	4.5	4.1	4.4	2.9	5.9
Occlusion time	22	28	23	23	25	27
Contrast volume ml	60	0	35	40	60	40
Hospitalization time	1	3	1	1	1	2
Major complication	Femoral artery pseudoaneurysm	No	No	No	No	No
Minor complication	No	Hematoma	No	No	Hematoma	No

obtaining initial success in all cases, without major acute complications during the procedure or subsequent months. We believe that this is a technique that can be adopted as an option for transesophageal echocardiography in centers with experienced operators.

Author Contributions

Conception and design of the research: Vassallo FS, Serpa HTG, Serpa E; acquisition of data: Vassallo FS, Serpa HTG, Santos LC, Serpa E, Walker BR, Silva E; analysis and interpretation of the data: Vassallo FS, Simões A, Mauro VF; statistical analysis: Vassallo FS; Writing of the manuscript: Vassallo FS, Serpa HTG; critical revision of the manuscript for intellectual content: Vassallo FS, Santos LC, Lovatto CV, Serpa E, Walker BR, Simões A, Carloni H, Mauro VF, Barros G, Silva E, Serpa RG.

Potential Conflict of Interest

Receipt of fees for the left current appendage occlusion procedure by the companies Abbott and Boston.

Sources of Funding

There were no external funding sources for this study.

Study Association

This study is not associated with any thesis or dissertation work.

Ethics Approval and Consent to Participate

This article does not contain any studies with human participants or animals performed by any of the authors.

References

1. Lippi G, Sanchis-Gomar F, Cervellin G. Global Epidemiology of Atrial Fibrillation: An Increasing Epidemic and Public Health Challenge. Int J Stroke. 2021;16(2):217-21. doi: 10.1177/1747493019897870.
2. Wang L, Ze F, Li J, Mi L, Han B, Niu H, et al. Trends of Global Burden of Atrial Fibrillation/Flutter from Global Burden of Disease Study 2017. Heart. 2021;107(11):881-7. doi: 10.1136/heartjnl-2020-317656.
3. Holmes DR Jr, Alkhouli M, Reddy V. Left Atrial Appendage Occlusion for The Unmet Clinical Needs of Stroke Prevention in Nonvalvular Atrial Fibrillation. Mayo Clin Proc. 2019;94(5):864-74. doi: 10.1016/j.mayocp.2018.09.025.
4. Berti S, Pastormerlo LE, Korsholm K, Saw J, Alkhouli M, Costa MP, et al. Intracardiac Echocardiography for Guidance of Transcatheter Left Atrial Appendage Occlusion: An Expert Consensus Document. Catheter Cardiovasc Interv. 2021;98(4):815-25. doi: 10.1002/ccd.29791.
5. Korsholm K, Jensen JM, Nielsen-Kudsk JE. Intracardiac Echocardiography from the Left Atrium for Procedural Guidance of Transcatheter Left Atrial Appendage Occlusion. JACC Cardiovasc Interv. 2017;10(21):2198-206. doi: 10.1016/j.jcin.2017.06.057.
6. Berti S, Pastormerlo LE, Santoro G, Brscic E, Montorfano M, Vignali L, et al. Intracardiac versus Transesophageal Echocardiographic Guidance for Left Atrial Appendage Occlusion: The LAAO Italian Multicenter Registry. JACC Cardiovasc Interv. 2018;11(11):1086-92. doi: 10.1016/j.jcin.2018.05.008.
7. Ribeiro JM, Teixeira R, Puga L, Costa M, Gonçalves L. Comparison of Intracardiac and Transoesophageal Echocardiography for Guidance of Percutaneous Left Atrial Appendage Occlusion: A Meta-Analysis. Echocardiography. 2019;36(7):1330-7. doi: 10.1111/echo.14415.